"Functional characterisation and validation of an *in vitro* model of Catecholaminergic Polymorphic Ventricular Tachycardia type 1"

João Bigares

Submitted in accordance with the requirements for the Degree of Doctor of Philosophy

School of Medicine

September 2015

DECLARATION

This work has not been submitted in substance for any other degree or award at this or any other university or place of learning, nor is being submitted concurrently in candidature for any degree or other award.

Signed …… (candidate) Date ……

STATEMENT 1

This thesis is being submitted in partial fulfillment of the requirements for the degree of PhD.

Signed …… (candidate) Date ……

STATEMENT 2

This thesis is the result of my own independent work/investigation, except where otherwise stated.

Other sources are acknowledged by explicit references. The views expressed are my own.

Signed …… (candidate) Date ……

STATEMENT 3

I hereby give consent for my thesis, if accepted, to be available online in the University's Open Access repository and for inter-library loan, and for the title and summary to be made available to outside organisations.

Signed …… (candidate) Date ……

STATEMENT 4: PREVIOUSLY APPROVED BAR ON ACCESS

I hereby give consent for my thesis, if accepted, to be available online in the University's Open Access repository and for inter-library loans **after expiry of a bar on access previously approved by the Academic Standards & Quality Committee.**

Signed …… (candidate) Date ……

Acknowledgements

This project would not be possible without the help of others. Therefore, here I leave my sincere thank you.

I would like to thank firstly to my supervisors Professor Alan Williams, Professor Paul Kemp and Professor Gary Baxter for the unconditional support and many lessons learned during these years.

To Professor Nick Allen for all the support with stem cell culture.

To Professor Chris Denning group from University of Nottingham, for also making this project possible, by providing hiPSC CM and for the cell culture support. A very special thanks to Dr. Elena Matsa and Dr. Divya Rajamohan for all the teaching with hiPSC derived CM cell culture.

To Dr. David Edwards, thank you for all the mentoring and support with cell culture and writing review. Also many thanks for the best trout in Wales.

Many thanks to my lab colleagues who were always willing to help over these years: Dr. Mark Bannister, Dr. Lowri Thomas, Dr. Chlóe Maxwell, Dr. Saptarshi Mukherjee, Dr. Bevan Cumbes, Dr. Christopher George, Dr. Joanne Euden, Dr. Monika Seidel and Jahn Firth.

A very special thanks to Dr. Sam Mason for all the help with the patch clamp technique and to Dr. Cedric Viero for helping with Ca^{2+} fluorescence imaging.

To Sarah, my partner, for all the support and patience, during these last writing up months.

My best friends, Robin Olden, João Casqueira, António Ribeiro Alves, Nuno Gomes and Sandra Monteiro. They were always there when I needed them.

This thesis is dedicated to

my parents and my brother

always by my side,

to my daughter

for our time, that I have missed

The rewards of research

Only . . . by way of experiment, can we hope to attain a comprehension of the "wisdome of the body and the understanding of the heart," and thereby to the mastery of disease and pain, which will enable us to relieve the burden of mankind.

—Ernest H. Starling (1866–1927)

SUMMARY

In the UK alone 28 000 sudden cardiac deaths a year are found to be unrelated to structural heart problems, likely having ion channel malfunction and arrhythmia as an underlying cause. With the discovery of human induced pluripotent stem cells (hiPSC), a new field has emerged, allowing the creation of personalised cellular models of disease that can be studied *in vitro*. In this study we aim to functionally characterize and validate an *in vitro* model of Catecholaminergic Polymorphic Ventricular Tachycardia type 1 (CPVT1), an adrenergically elicited arrhythmic condition caused by a mutation in the cardiac ryanodine receptor (S2246L). The cardiac ryanodine receptor (RyR2) is an intracellular ion channel that releases Ca^{2+} stores essential to cardiac contraction during EC-coupling. Inherited defects in the RyR2 can result in an intracellular calcium leak during diastole that may lead to arrhythmia. The most frequent arrhythmic events at a cellular level in CPVT cardiomyocytes (CM) are delayed afterdepolarizations (DADs) although early afterdepolarizations (EADs) and triggered activity (TA) may also occur. With the need of obtaining a human cell based disease model to establish *in vitro* valid assays for CPVT study and drug screening, a standardized quantitative approach is ideal. Nonetheless, because the quantitative definition of these arrhythmic endpoints is subjective by nature, most studies using hiPSC CPVT derived CM have assessed these cells only from a qualitative point of view. Using whole cell patch clamp in the ruptured membrane modality and Ca^{2+} fluorescence imaging, this study aimed to provide a quantitative characterization of arrhythmic endpoints in a CPVT hiPSC model. Pharmacological rescue was carried out using flecainide, propafenone, dantrolene (10µM for all drugs) and propranolol (1µM) in the presence of isoprenaline. Our results show that the average response of hiPSC CPVT CM to recapitulate disease is heterogeneous and therefore not a consistent *in vitro* model of disease.

GLOSSARY

3D – Three dimensions

AM - Acetoxymethyl ester

AMP - Adenosine Monophosphate

AP – Action Potential

APD – Action Potential Duration

ARVD - Arrhythmogenic Right Ventricular Dysplasia

BC – Beating Cluster

BMCs – Bone Marrow derived stem Cells

CaM – Calmodulin

CaMII - Ca^{2+}/calmodulin-dependent serine–threonine protein kinase II

cAMP - Cyclic Adenosine Monophosphate

CASQ2 – Calsequestrin

CAVB – Cardio AtrioVentricular Block

CHO – Chinese Hamster Ovary

CICR – Calcium Induced Calcium Release

CM – Cardiomyocyte

CPC – Cardio Progenitor Cell

CPVT – Catecholaminergic Ventricular Polymorphic Tachycardia

DAD – Delayed After Depolarisation

DAPI - 4′,6-diamidino-2-phenylindole

DCM – Dilated CardioMyopathy

DNA – DesoxyriboNucleic Acid

EAD – Early After Depolarization

EB – Embrioid Body

ECG – Electrocardiogram

EMA – European Medicines Agency

ESC – Embrionic Stem Cells

F1 – First Generation

FA - Friedreich's Ataxia

FDA – Food and Drugs Administration

GMT - Gata4, Mefc2 and Tbx5

HCM – Hypertrophic CardioMyopathy

HEK – Human Embryonic Kidney

hERG – human Eter-a-Go-go channel

hESC – human Embrionic Stem Cells

HF – Heart Failure

HF – Heart Failure

hiPSC – human induced Pluripotent Stem Cells

HLHS – Hypoplastic Left Heart Syndrome

hPSC – human Pluripotent Stem Cells (includes hiPSC and hESC)

HRP – Horse Radish Peroxidase

IC – Current Clamp

ICC – Immunocytochemistry

ICD – Implantable Cardiac Defibrillator

IP_3 - Inositol Triphosphate Receptor

ITN – Inter Transient Noise

JCN - Junctin

KO – Knock Out

LCSD – Left Cardiac Sympathetic Denervation

LTCC – L-Type Calcium Channel

LVAD – Left Ventricle Assisting Device

LVEF – Left Ventricular Ejection Fraction

MDP – Maximum Diastolic Potentials

MEA – Multi Electrode Array

MEA – Multi Electrode Array

microRNA – micro RiboNucleic Acid

MLC – Myosin Light Chain

mRNA – messenger Ribonucleic Acid

NCX – Sodium-Calcium Exchanger

NTD – N-Terminal Domain

OCT4 - octamer-binding transcription factor 4

OSKM - Oct3/4 , Sox2, Klf4 and c-Myc

PAGE – PolyAcrylamide Gel Electrophoresis

PBS – Phosphate Buffered Saline

PCR – Polymerase Chain Reaction

PD – Population Doubling

PFA – Paraformaldehyde

PLA-2 – Phospholipase-2

PLB – Phospholamban

PP1 – Protein Phosphatase 1

PP2 - Protein Phosphatase 2

PTD – Post Transduction

RIPA – Radio ImmunoPrecipitation Buffer

RMP – Resting Membrane Potential

RPM – Rotations Per Minute

RyR2 – Ryanodine Receptor type 2

SALVO - (Synchronization, Amplitude, Length and Variability of Oscillation)

SCN5A – Sodium Channel 5A

SDS – Sodium Dodecyl Sulphate

SERCA2A – Sarcoplasmic reticulum Ca-ATPase

siRNA – small interference RiboNucleic Acid

SOICR – Store Overload Induced Calcium Release

SR – Sarcoplasma Reticulum

SSEA1 - stage-specific embryonic antigen 1

SSEA4 - stage-specific embryonic antigen 4

TA – Triggered Arrhythmia

TdP – Torsade de Pointes

TM – Transmembrane segments

TRA1-60 - tumor rejection antigen 1–60

TDN - Triadin

VF – Ventricular Fibrilation

VPB – Ventricular Premature Beat

VT – Ventricular Tachycardia

WB – Western Blot

CONTENTS

LIST OF FIGURES

Chapter 1; Introduction

Chapter 2; General materials and methods

Chapter 3; hiPSC derived CM Ca^{2+} handling protein detection and imaging

Chapter 4; hiPSC derived CM functional characterisation

Chapter 5; hiPSC derived CM *in vitro* CPVT1 model of disease

LIST OF TABLES

Chapter 2; General materials and methods

Chapter 4; hiPSC derived CM functional characterisation

Chapter 1

Introduction

1.1 Sudden arrhythmic cardiac death – the unsolved mystery

Among death causes in developed countries, sudden cardiac death (SCD) is still the leading cause of mortality. It is defined as an unexpected death that occurs in a short period of time, due to the onset of cardiac related symptoms (Kauferstein et al.,2013). In the UK alone, about 60 000 sudden cardiac deaths occur every year (Papadakis et al.,2009) and in USA circa 300 000 deaths occur (Kannel et al.,1987) reporting no structural cause for about 40% of these cases.

There are several potential causes for sudden cardiac death. Sudden death fatalities can be related to anatomical or structural disease, such as valvulopathies (mitral valve prolapse, aortic valve stenosis), inflammatory disease (myocarditis, amyloidosis, sarcoydosis), vascular disease (myocardial infarctation, coronary spasm or anomalies, aortic rupture), cardiomyopathy (dilated and hypertrophic cardiomyopathy, myotonic dystrophy, arrhythmogenic right ventricular cardiomyopathy), arrhythmic syndromes (long QT, short QT, Catecholaminergic Polymorphic Ventricular Tachycardia, Brugada syndrome, Wolf Parkinson's White Syndrome) or even trauma (*commotio cordis*).

From the above mentioned causes, vascular related, namely ischaemic heart disease is responsible for the majority of events. Although most SCD causes can be identified on a *post mortem* exam, a proportion of cases do not present any structural, anatomical toxicological or pathological underlying findings that could justify a cardiac arrest. These cases are considered as sudden arrhythmic cardiac deaths (SACD) and most SACD happen in young people, children and young infants that die suddenly and unexpectedly sometimes during their sleep. The definition of SACD is sudden unexpected death from age 4 to 64 years, with no previous cardiac disease history, last seen alive within 12h of being found dead and without identifiable *post mortem* cause.

The predominant aetiology for SACD involves inherited cardiac disease, namely genetic mutations that are translated into functional defects in ion channels and receptors (channelopathies) that affect the cardiac action potential and hence its electrical activity. Channelopathies are likely responsible for about half of SACD (Behr et al.,2008).

Molecular autopsies should always be performed in SACD, but due to several factors it still isn't a routine practice in developed countries. One of the reasons why genetic screening (in living or dead subjects) for inherited cardiac is not always performed is

that the mutated genes have a highly variable degree of penetrance. This means that a known mutation doesn't always cause disease. Therefore, a set of factors, such as clinical history, family records and genotyping, have to be considered for a more accurate diagnosis. In some cases a functional test is needed, with a pharmacological challenge using ß-agonists, such as adrenaline, during monitored exercise to elicit a potential arrhythmic event.

Due to the above mentioned factors, SACD is still difficult to diagnose and predict even if genotyping is available. From all diagnosed patients with channelopathies, circa 30% are refractory to treatment. There is currently a huge need to find channelopathy models of disease that allow a more efficient study of mechanisms of disease and drug screening.

1.2 Catecholaminergic Polymorphic Ventricular Tachycardia (CPVT)

This inherited arrhythmogenic channelopathy is an example of abnormal regulation of intracellular Ca^{2+}. A mutation in the gene coding for the cardiac Ryanodine Receptor (RyR2) in the sarcoplasmic reticulum (SR) can cause CPVT1. It can also be caused by a mutation in the gene coding for the SR intra-luminal protein, calsequestrin (CASQ2), causing CPVT2. Arrhythmia, syncope and death can be elicited by strong emotions or stress via ß-agonist (catecholaminergic) stimulation.

Two other forms of CPVT have been described but without having RyR gene mutations as an underlying cause. CPVT3 is related with loss of function of Kir 2.1, a channel responsible for an inward potassium rectifying current (I_{K1}) and was described by Postma et al.,(2002) and Tester et al.,(2006). The other form of disease, CPVT4 is associated with an abnormal ankyrin-B structural protein, in which impairment of I_{NCX} and IP_3 receptors can lead to arrhythmia (Mohler et al.,2004).

1.2.1 Background and recent history

The earliest reference to this clinical entity was made by Reid et al., 1975, describing a bi-directional tachycardia in the ECG trace upon physical effort or emotional stress (both related to ß-adrenergic stimulation). A few years later, Coumel et al.,1978 named this condition CPVT for the first time. The next major publication happened in 1995 authored by Leenhardt et al. with a series of clinical cases presented. Later, a group from Finland (Swan et al.,1999) reported that a mutation in chromosome lq42-q43 occurring in 2 large Finnish families with a history of SACD was related to malignant polymorphic ventricular tachycardia. Only in 2001, advances in molecular genetics, allowed Priori et al. and Laitinen et al., to associate RyR2 autosomal dominant mutations with CPVT1. This type of CPVT accounts for 70% of all CPVT patients (Cerrone et al.,2004) with 155 different mutations already known (http://www.triad.fsm.it/cardmoc/). In the same year, Lahat et al. also correlated abnormalities in the calsequestrin protein (CASQ2) with CPVT2. In this case disease was caused by an autosomal recessive mutation, found in a family of a Bedouin tribe in chromosome 1p13-21.These findings show that lack of functional CASQ2 in autosomal recessive mutations is not lethal.

Given the fact that there are still a significant number of CPVT patients that are negative for the known abnormal proteins mentioned above, the involvement of other genes was obvious, as we now know in the case of CPVT3 and CPVT4.

Healthy paediatric patients, account for most CPVT cases and it has been described that by the age of 40, 80% of patients will have presented cardiac symptoms, with a mortality rate of 30-50% (Liu et al.,2008). In their first or second decade of life, most patients will present their first cardiac episode and clinical diagnosis is always challenging, as most patients present a normal echocardiogram and ECG (Electro cardiogram). In the absence of genetic diagnosis or family history, exercise stress tests may be performed to achieve a diagnosis. During the stress exercise diagnostic tests, when heart rate increases to 90-110 beats per minute, episodes of ventricular tachycardia (VT) are frequently recorded in the ECG with a typical bidirectional shape which is the hallmark of the disease.

The use of mice as animal models of disease has been extremely valuable to understand possible CPVT mechanisms of disease. Several knock-in models have been made for different CPVT1 mutations (Jiang et al.,2002; Cerrone et al.,2005; Liu et al.,2006; Kannankeril et al.,2006; Lehnart et al.,2008; Sedej et al.,2010; Kobayashi et al.,2010; Bai et al.,2013; Denegri et al.,2014) as well for CPVT2 (Knollmann et al.,2006; Song et al.,2007; Rizzi et al.,2008). Mice models are also used to study drug effect and potential new treatments, such as flecainide (Liu et al.,2010) a drug which already has clinical use, derived from translational research.

1.2.2 The cardiac ryanodine receptor - RyR2

The RyR channel was first identified in 1985 when isolated from the skeletal muscle by Fleischer et al., who reported that a plant alkaloid from *Ryania speciosa* usually used as an insecticide, could lead to irreversible muscle contractures. Another isoform named RyR2 was later isolated from the canine cardiac muscle by Meissner and Henderson in 1987. The skeletal muscle predominant isoform, RyR1 is activated directly by Ca^{2+} via the LTCC (L-Type Calcium Channel), releasing SR Ca^{2+} stores during muscle contraction and a third isoform RyR3 is found in the brain and nervous tissue mainly. Although a conservative domain of 70% of the protein composition is shared between the three RyR isoforms, all three isoforms have been found in smooth muscle and the brain, with not completely elucidated physiological roles. Similar permeation properties, with large conductance for divalent and monovalent cations, and relatively low Ca^{2+} selectivity are shared by all three isoforms (Fill & Copello, 2002).

RyR2 is the biggest membrane protein in the human body. The monomer contains 4967 amino acids encoded by one of the largest genes in the human genome containing 105 exons. This large protein is present in the sarcoplasmic reticulum of the cardiomyocyte and has a transmembrane and a cytosolic domain.

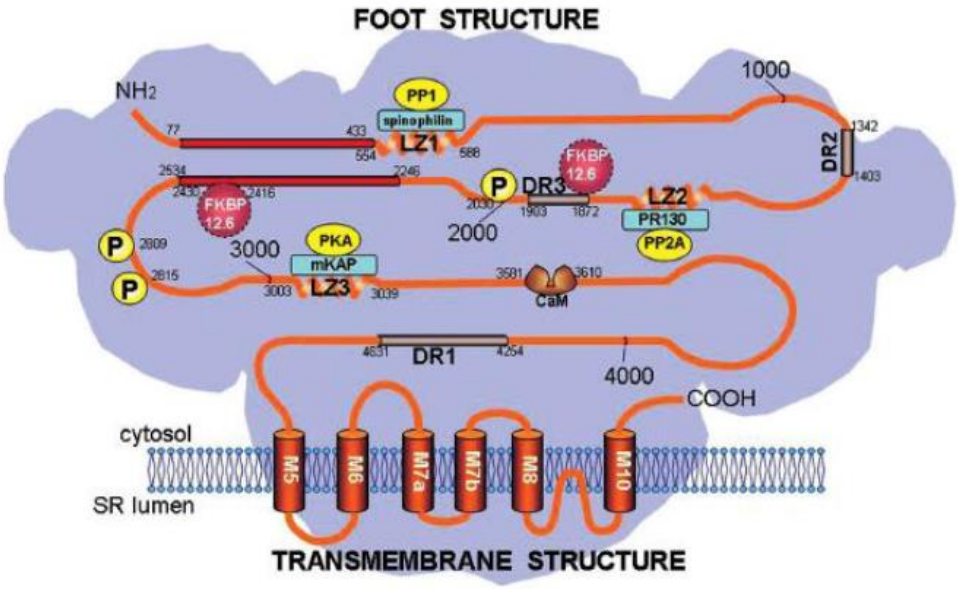

Figure 1.1– RyR2 protein structure *– RyR2 satellite proteins are shown around the primary polypeptide chain. Junctin (JCN) and triadin (TDN) should bind to luminal interluminal region where they anchor CASQ. The three main divergent regions are indicated as DR1, DR2 and DR3. On the cytosolic region, FKBP 12.6, phosphatase 1, calmodulin and phosphatase 2A are shown to bind (Yano et al.,2008).*

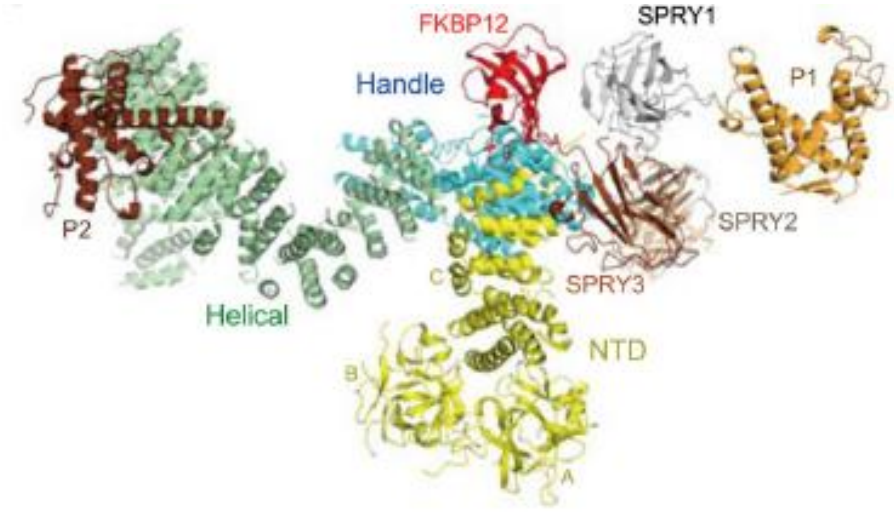

Figure 1.2– Structure and cytoplasmic domain organization of the rabbit RyR1 *– Cytoplasmic view of spatial arrangement of the cytoplasmic domains preceding the Central domain within one RyR1 protomer (Yan et al.,2015).*

1.2.3 RyR2 pharmacology

Several drugs can be used to study RyR2 function. However none have been used as potential therapeutical agents for CPVT. For purely classification purposes it is considered that agonists will trigger Ca^{2+} release from the SR and antagonists will block SR Ca^{2+} release. The mechanisms of action can range from altering channel gating to direct block of the RyR2 pore via physical obstruction. Finally a third possible mechanism of action may occur by enhancing RyR2 subunits interaction. Although these agents do not have current therapeutic use, they can be studied and profiled for new drug discovery based on their mechanisms of action. Known RyR2 agonists are: methylxanthines such as caffeine, digoxin, suramin, 4-CMC (4-Chloro-m-cresol), tacrolimus, halothane, isofluorane and imperatoxin A (IpTxa), a toxin from the scorpion *Pandinus imperator*. Pharmacological RyR2 antagonists are ryanodine (at 10μM and above), ruthenium red, dantrolene, tetracaine and procaine (West & Williams.,2007).

1.2.4 RyR2 Mutations

Most of the RyR2 mutations able to cause CPVT1 are missense mutations (in which one single base pair is abnormal) and occur in three hot-spot regions: the N-terminal region, the central domain and the C-terminal domain including the pore-forming region. These three regions are well conserved among the RyR gene family and are involved in the regulation of RyR channels. Recently Medeiros-Domingos et al.,2009 confirmed these 3 hot-spots as key for CPVT mutations in a patient cohort study in which 105 exons were screened. Although missense mutations are more frequent in these mentioned hot-spots, some large deletions and rearrangements have been reported in domains I and II (Medeiros-Domingos et al.,2009; Marjamaa et al.,2011). It should be routine to screen for mutations outside the most frequent hot-spots and exons as these can occur as previously reported.

As with other channelopathies, mutation penetrance is highly variable, from 25 to 100%. In some cases, CPVT1 genotyped members of the same family, have suffered sudden death as a first symptom, despite not presenting any arrhythmia during stress exercise tests (Bauce et al.,2002).

1.3 Ca^{2+} handling and mechanisms of disease

1.3.1 Cardiac EC-coupling

Cardiac myocytes (CM) are unique cells that present complex functional molecular mechanisms essential to their function. The cardiac muscle and chambers need to expand and contract in order to propel oxygenated blood to all the tissues and cells in the body. Cardiac Excitation- Contraction coupling is the process that allows the heart to function and it starts by an electrical sequence of events terminating with the mechanical contraction of the cell. Excitation begins when a depolarisation of the cardiac cell membrane (with an average resting membrane potential – RMP of -80 mV) occurs leading to an action potential (AP). This depolarisation, starts via the $I_{(Na)}$, with an inward Na^+ current reaching 30-50mV, activating $I(_{to})$ and subsequent repolarization process. Activation of inward Ca^{2+} $I_{(L\text{-}Ca)}$ causes a plateau that is more prolonged in ventricular cells compared to atrial CM. Inactivation of $I_{(L\text{-}Ca)}$ is then followed by repolarisation through the outward K^+ current, $I_{(Ks),}$ $I_{(Kr)}$ and inward rectifier K^+ current $I_{(K1).}$ All of these events mark and represent the different phases of the cardiac AP (0-4).

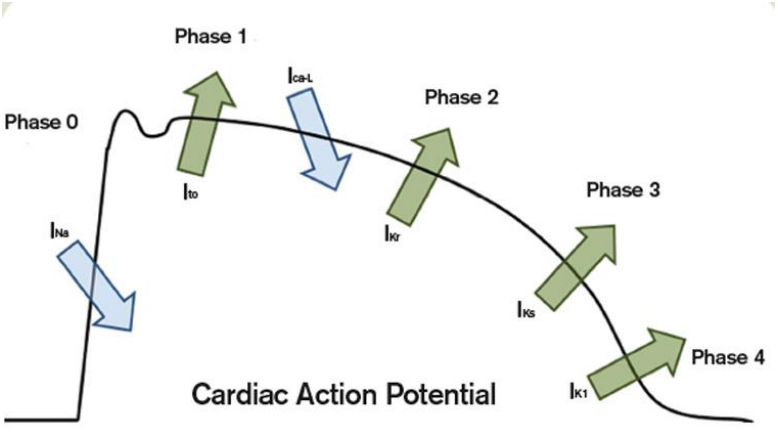

Figure 1.3 – The ventricular cardiac action potential *- different phases and involved electrical currents (Morita et al.,2008).*

During the $I_{(L\text{-}Ca)}$ activity, Ca^{2+} concentration increases in the cytosol, activating RyR2 channels to release more Ca^{2+} from the SR. RyR2 are large ion channels located in the SR, one of the CM organelles responsible for storing intracellular Ca^{2+} (figure 1.4). Stimulated by Ca^{2+} influx via LTCC, RyR2 opens, creating a Ca^{2+}transient, allowing these ions to bind to the CM contractile machinery, namely to troponin C present in the myofibers. This process, by which cytosolic Ca^{2+} influx from the extra-cellular space

triggers Ca^{2+} release from the SR via activation of RyR2, is referred to as Calcium-Induced Calcium-Release or CICR, (Fabiato, 1983). After a systole, Ca^{2+} is then removed from the CM cytosol via four possible mechanisms: SR Ca^{2+}ATPase (SERCA2A), NCX, sarcolemmal Ca^{2+}ATPase, and mitochondrial Ca^{2+} transporter. NCX function is of particular relevance in triggering possible arrhythmogenic events in CPVT.

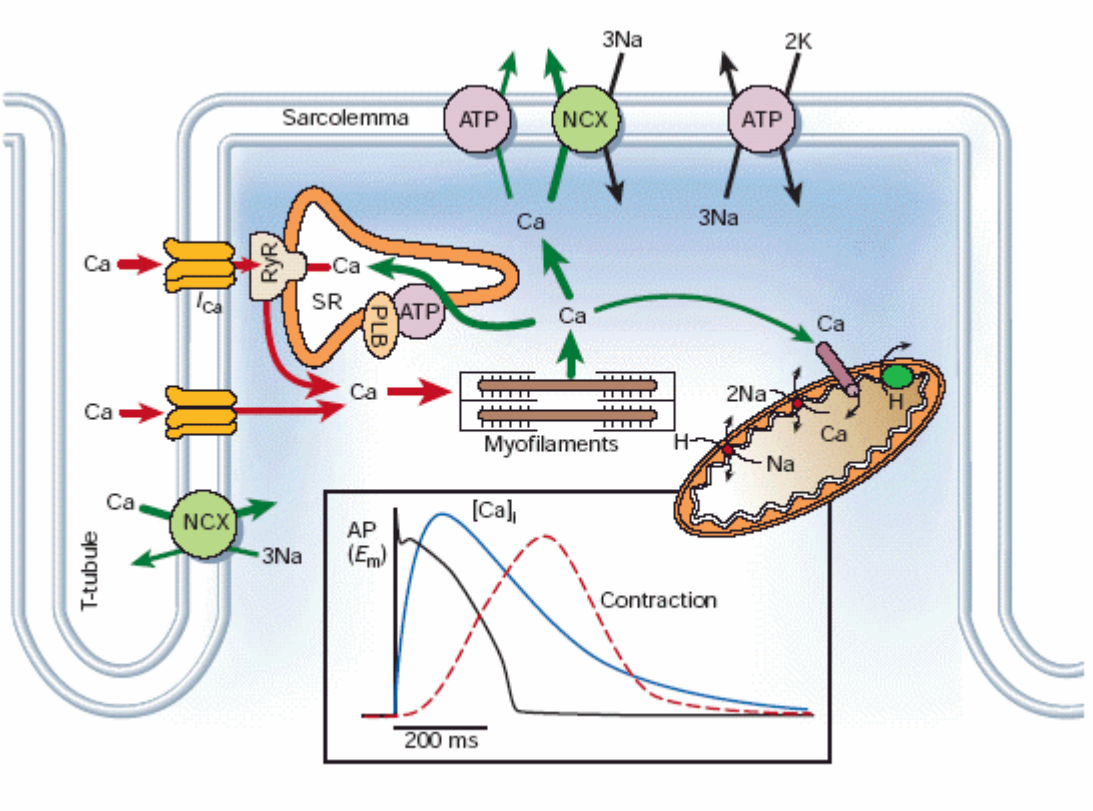

Figure 1.4 – Ca^{2+} transport in ventricular myocytes *- time course of an action potential, Ca^{2+} transient and contraction, measured in a rabbit ventricular myocyte at 37ºC. Ca^{2+} occurs via L-type Ca^{2+} channel, induces Ca^{2+} release from SR via RyR2 to allow myofilament contraction. Ca^{2+} is then released into cytosolic space to be extruded via Ca-ATPase, NCX and mitochondrial calcium pump (Bers, 2002).*

In ventricular CM the AP plateau is more prominent and hence the APD is longer than in atrial cells. This plateau also allows the contracted cell to relax before the next beat (and Ca^{2+} transient) preventing permanent contraction of the heart, that would clearly prevent the re-filling of the cardiac chambers and impair cardiac function.

1.3.2 ß-Adrenergic stimulation

One of the most important cardiac control mechanisms, is clearly the chain of events triggered by sympathetic ß-adrenergic stimulation and the classical cardiac physiological response of inotropy, lusitropy and chronotropy.

All sympathetic nerve endings in the heart have ß-adrenergic receptors and there are four main mechanisms underlying the cardiac inotropic, lusitropic and chronotropic properties: 1) decreased myofilament Ca^{2+} sensitivity due to troponin I phosphorylation, 2) increased $I_{(L\text{-}Ca)}$, 3) enhanced SERCA2A (Sarcoplasmic Reticulum Ca-ATPase) rate via PLB (Phospholamban) phosphorylation and 4) altered RyR2 gating.

Endogenous ß-adrenergic agonists or synthetic analogous such as isoprenaline cause the above effects by stimulating adenylyl cyclase, activating binding protein G_s and elevating cAMP-dependent PKA (Protein Kinase A), which in its turn phosphorylates several other key proteins in the process. In the presence of ß-receptor agonists, more calcium enters the cell at each cycle, causing the SR to build bigger Ca^{2+} stores.

Experiments made in mice ventricular CM demonstrated that PLB is a key protein in the inotropic and lusitropic ß-adrenergic mediated effects. Transgenic PLB KO (Knock Out) mice had CM with a significant decrease in both effects when compared to wild type mice CM (Li et al., 2000). The same authors also reported that, although significantly reduced, there was still an inotropic effect in PLB KO CM. This could be due to a large increase in $I_{(L\text{-}Ca)}$ which progressively increases Ca^{2+} stores in the SR in the absence of PLB.

Another important characteristic of most mammalian CM (excluding rat and mouse) is the positive force-frequency relationship that describes the increase of calcium transient amplitude (and hence force in Newtons) with an increase in rate. Several authors have demonstrated this CM property in different species including human adult CM (Pieske et al.,1999). There are three factors suggested as possible underlying causes for this property: 1) increased $I_{(L\text{-}Ca)}$ 2) increase in cytosolic diastolic Ca^{2+} and 3) increased SR load available for release as a consequence of the previous two factors. In addition, due to an increased rate of depolarization a subsequent increase in intracellular Na^{+} concentration reduces NCX (Sodium-Calcium Exchanger) Ca^{2+} extrusion and hence more calcium is available in the cytosol and SR (Boyett et al.,1987).

1.3.3 SOICR – Store Overload Induced Calcium Release

In CPVT1 or CPVT2 a ventricular diastolic Ca^{2+} leak is the basic event that can predispose to after-depolarisation and arrhythmia. This is the most widely accepted arrhythmic mechanism for the above mentioned channelopathies, resulting from either a dysfunctional RyR2 or CASQ2 protein, in which an abnormal action potential may follow an initial after-depolarization. Events of this type are described as triggered activity, as they can generate an extra systole in cardiac regions other than the pacemaker tissue.

During systole, Ca^{2+} concentration rises rapidly from approximately 100nM to 1µM, favouring binding to troponin C and leading to sarcomere contraction. The majority of this Ca^{2+} does not come from the extracellular space but from the SR, although it's a small influx of Ca^{2+} via the LTCC (I_{Ca}) that triggers RyR2 opening and a huge release of SR Ca^{2+} via CICR. During diastole, Ca^{2+} is removed from the CM cytosol via four possible mechanisms: SR Ca^{2+}ATPase (SERCA2A) (70%), NCX (28%), sarcolemmal Ca^{2+}ATPase (1%) and mitochondrial Ca^{2+} transporter (1%). These percentages can differ from species to species and while the above average values are from rabbit ventricle, in the rat heart SERCA2A can be responsible for up to 92% of Ca^{2+} re-uptake (Bers, 2000). These proteins and their regulatory pathways play a key role in one of the main suggested mechanisms of arrhythmogenesis related to the dramatic increase of cytosolic Ca^{2+}.

Diastolic SR Ca^{2+} release can occur in the absence of depolarization through a mechanism described as spontaneous Ca^{2+} release (Fabiato et al.,1992) and this event is facilitated by a SR Ca^{2+} overload (Lakatta et al.,1992). Diastolic spontaneous SR Ca^{2+} release events have been described as SOICR (Store Overload Induced Calcium Release) (Jiang et al.,2004;2005) and can be triggered by digitalis intoxication, ß-adrenergic stimulation, elevated extracellular Ca^{2+} and fast pacing, such as in the case of CPVT (Lakatta et al.,1993).

Stimulation of the ß-adrenergic receptor, leads to phosphorylation of several proteins, as a consequence of an increase of cAMP and subsequent PKA activation, contributing to SOICR. Proteins such as the LTCC and phospholamban (PLB) will favour SR Ca^{2+} uptake when phosphorylated by increasing cytosolic Ca^{2+} influx and by reducing SERCA inhibition, respectively.

Cardioglycosides such as digoxin and digitoxin inhibit Na^+/K^+ ATPase. This effect leads to cytosolic Na^+ concentration increase and inhibition of NCX. By causing NCX inhibition, more cytosolic Ca^{2+} is available for SR Ca^{2+} uptake, leading to SR Ca^{2+} overload and consequently SOICR.

Evidence suggests that spontaneous Ca^{2+} release will occur when SR Ca^{2+} reaches an excessive critical load (Diaz et al.,1997) and hence that Ca^{2+} concentration from the inside of the SR (luminal side) is the main trigger for Ca^{2+} release during SOICR.
Some authors suggest that luminal Ca^{2+} activates RyR2 by passing from the SR via the channel pore and activates Ca^{2+} release by from the cytosolic side. This mechanism, also known as the "feed-through" hypothesis (Tripathy et al.,1996), is challenged by single channel experiments in which RyR2 Ca^{2+} release is activated by cytosolic Ca^{2+} in the absence of luminal Ca^{2+} (Ching & Williams & Sitsapesan, 2000) leading these authors to suggest that luminal Ca^{2+} activation has a different site than the cytosolic activation site.
Moderate changes in RyR2 activity are regulated by the SR Ca^{2+} content, probably as the result of RyR2 regulation by SR luminal Ca^{2+} (Trafford et al.,2000), a mechanism known as "SR autoregulation".

1.3.4 Afterdepolarizations and Triggered Arrhythmia

As a consequence of ß-stimulation, SOICR can occur leading to an increase of cytosolic Ca^{2+} that can alter the sarcolemmal membrane potential by activating NCX. The activation of this electrogenic exchanger will cause a transient inward current by increasing the cytosolic Na^+ concentration, while removing Ca^{2+} to the extracelluar space at the ratio of 1 (Ca^{2+}) : 3 (Na^+). If the membrane depolarization occurs after an action potential has ended, this event is called a delayed after-depolarization (DAD) (Marban et al.,1986). If this DAD reaches an amplitude sufficient to activate the sodium channels it can initiate $I_{(Na)}$ and trigger a full arrhythmic action potential – triggered activity (TA). It has been estimated that the release of at least 50 to 70% of the SR Ca^{2+} load is necessary to create a DAD with enough amplitude to generate TA (Schlotthauer & Bers, 2000).

Another possible arrhythmic electrogenic event is an early after-depolarization (EAD). These depolarising events may take place before the action potential has terminated,

frequently during phase 2 and 3 of the AP. Both $I_{(L\text{-}Ca)}$ and $I_{(Na)}$ seem to be the main currents involved in EAD arrhythmogenic activity (Volders et al.,2000). Other authors have also suggested that $I_{(NCX)}$ can play a role in EAD genesis (Priori et al.,1990).

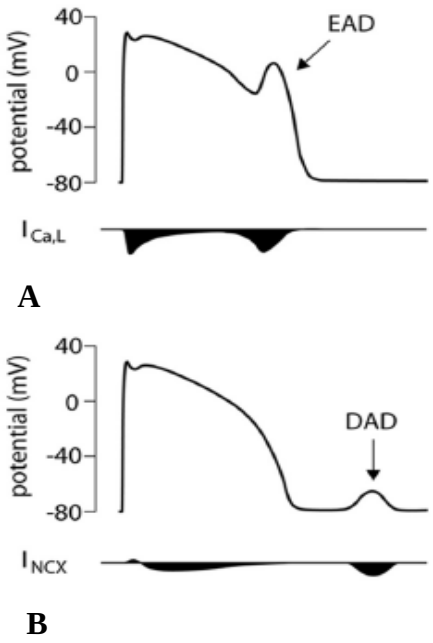

Figure 1.5 – DAD and EAD *- Cardiac AP arrhythmogenic events and respective differences in AP time and involved electrical currents. EAD events (A) occur before repolarization completion and are caused mainly by* $I_{(L\text{-}Ca)}$ *, while DAD events (B) are mainly caused by* $I_{(NCX)}$ *and only occur after complete repolarization between two consecutive APs (Hoekstra et al.,2012).*

1.4 Current clinical diagnosis and therapy

1.4.1 Clinical diagnosis

Most CPVT early symptoms happen in children, presenting syncope episodes, related to exercise or strong emotions. A polymorphic ventricular tachycardia observed on the ECG, is typically present in most cases. The heart is usually structurally normal and a lower resting heart rate has been reported, especially for boys with RyR2 mutations (Hayashi et al.,2009). A typical CPVT patient usually has a normal ECG but the arrhythmia is usually reproduced in an exercise stress test or with isoprenaline administration. Using a Holter monitor, ECG traces for 24h can be obtained and usually a polymorphic ventricular tachycardia is recorded when heart rate thresholds around 120-130 beats per minute.

Figure 1.6 – CPVT ECG trace - *Classical CPVT patient ECG trace, from a twelve-lead machine during exercise stress test, showing typical bidirectional ventricular tachycardia characterised by 180º alternating QRS axis on a beat to beat basis, presenting a right bundle branch block pattern suggesting a left ventricular origin (Leenhardt et al.,2011)*

The trace will initially present ventricular premature beats (VPBs) and progress to bidirectional ventricular tachycardia (VT). If exercise or isoprenaline stimulation

persists, VT increases in frequency and number and can lead to syncope that in some cases can progress to ventricular fibrillation and death.
Although ventricular tachycardia is most prevalent in CPVT, atrial arrhythmia including atrial fibrillation can be observed in stress tests and has been described in adult patients (Kazemian et al., 2011).

1.4.2 Current therapeutic approaches

Understanding the pathophysiology of CPVT1 is a critical step to direct pharmacological treatment. Drugs that can target and help prevent SOICR caused by RyR2 modulation and prevention of SR Ca^{2+} overload, would be ideal choices but medicine still lacks specific molecules for this purpose.
There are some drugs available with some clinical efficacy such as ß-blockers and LTCC inhibitors. Although ß-blockers can reduce heart rate and hence reduce phosphorylation favouring SERCA2A inhibition and LTCC blockers reduce Ca^{2+} influx, RyR2 inhibition itself seems an obvious promising therapeutic target as mono or combined therapy.
Flecainide and other Na^{+} channel blockers such as propafenone, are old drugs with a few good results and renewed clinical interest, when added to ß-blockers in refractory cases to first line pharmacological treatment (Watanabe et al.,2009).
Preliminary pre-clinical reports, in mice and rabbit models as well as CPVT human induced pluripotent stem cells (hiPSC) derived CM, indicate that dantrolene is a possible candidate to undergo clinical trials in CPVT patients refractory to other drug classes.

Other alternatives involve medical device implantation such as an implantable cardioverter defibrillator (ICD) to prevent VF. This device may be indicated in patients refractory to pharmacological treatment that may reach 20 to 30% of CPVT cases (Zipes et al.,2006). Surgical procedures such as left cardiac sympathetic denervation (LCSD) can also be indicated. A report recently presented by de Ferrari et al.,(2015) from an observational study from 1988 to 2014, in 63 CPVT patients, reveals that LCSD seems very promising. However the procedure still lacks quantitative clinical trial data.

1.5 Models of cardiac disease

The study of cardiac disease and the great medical advances achieved in the past, would not have been possible if it wasn't for the use of cardiac models either at a full organ or cellular and molecular level. Cardiovascular disease is the leading cause of morbidity and mortality worldwide, with estimated 17 million deaths per year (Laslett et al.,2012).

In drug discovery and development, cardiac toxicity is a huge burden. In the past 30 years alone, about 20 different compounds have been commercialised and withdrawn from the market, due to unexpected cardiovascular events. Toxicity at the ion channel level is known to cause LQT, Torsade des Pointes, syncope and death. It is estimated that each of these discarded compounds has cost about 1.5 billion US dollars in research and development (Quigley et al.,2011).

Regulatory authorities such as the FDA and EMA have set new rules for preclinical testing regarding cardiac toxicity and including animal and cell base models in which specific ion channels are overexpressed in order to try and predict adverse cardiac events.

Despite an obvious need of human cardiac cell models, access to live human cardiac tissue is restricted. Lack of viable cardiac tissue from human donors is a problem due to ethical, legal and physiological reasons. Human CM are also difficult to isolate and maintain in culture, with only a few days of viability. In some institutions, foetal cardiac tissue can be obtained from pregnancy interruptions, more frequently than adult cardiac tissue.

For these reasons different mammalian species have been used for research, from mice, rat, rabbits, guinea pig, even carnivores such as ferrets and dogs and occasionally non-human primates. Although huge advances in cardiac physiology, and pathophysiology have been achieved by using other mammalian species, the inter-species differences are still a great limitation for a better understanding of human CM.

Animal models can be used for whole organism research or to obtain primary single CM for cell level experiments.

Heterologous mammalian cell models (transfected with ion channels) such as HEK293 or CHO immortal lines are also frequently used due to their robustness minimal culture demands.

Immortalised cardiac cell lines such as H9c2, derived from an embryonic rat ventricle have also been used for more than three decades (Kimes & Brandt, 1976). Another immortalised cardiac cell line has been isolated from a mouse atrial tumor (HL-1). HL-1 cells have been extensively studied for ion channel and calcium handling physiology research (Claycomb et al.,1998).

1.6 Pluripotent stem cells

More recently a new *in vitro* cardiac cell model has become available from the stem cell emergent field. Stem cell derived CM are now a reality and can be used for the same purposes as primary cells, with the advantage of being human cells and coming from a stable cell line. The main disadvantages are that these cells still have foetal features, culture requires intensive labour and are much more sensitive to cell culture routine procedures than other cell lines (HEK, CHO, etc.).

Despite these disadvantages, the potential derived from this technique is immense and future research will likely improve and overcome these disadvantages.

Stem cells are cells with the capacity of differentiation into any type of tissue in the body and can be classified regarding their potential of differentiation.

Regarding their potential of differentiation stem cells can be: totipotent (differentiate into all tissues including trofoectoblast – placenta), pluripotent (differentiate into all tissues except trofoectoblast) and multipotent (can only differentiate into an organ cell lineage with different sub-types) (Tanabe et al.,2014).

For mainly ethical reasons human totipotent stem cells are not used extensively in research since in theory they could give origin to a complete human being. Pluripotent stem cells are nowadays the focus of intense research since these can originate any cell or tissue except for the placenta embryonic precursor (trofoectoblast), offering additional advantages over multipotent stem cells.

The first report of these cells was made regarding mouse embryonic stem cells (mESC) obtained from the inner part of a day 8 embryo or blastocyst (Evans et al.,1981). But if research with mouse ESC was not controversial, the same was not true when human embryonic stem cells (hESC) started being studied. Research with these cells met great public opinion resistance, mainly for religious and ethical reasons.

Still, significant advances were made regarding hESC differentiation in to different tissues and in 1994, Maltsev et al. reported for the first time a functional study using hESC derived CM characterising it's action potential and isolated currents. These authors confirmed the presence of $I_{(Na)}$, $I_{(to)}$ $I_{(L\text{-}Ca),}$ $I_{(K)}$ and $I_{(K1)}$ in hESC derived CM.

Due to the inherent ethical problems in using human embryos to obtain hESC, some countries halted almost all research with these cells but kept work with multipotent stem cells such as cardioprogenitor cells, blood chord cells and mesenchymal stem cells.

The presence of cardioprogenitor cells (CPCs) in mammalian hearts challenge the view that the heart is terminally differentiated, as *in vitro* studies show that CPCs can differentiate in to different CM sub-types, endothelial and smooth muscle cells (Beltrami et al.,2003). These cells have been used in several trials for cardiac regeneration as they can be harvested from a patient atrial biopsy, expanded *in vitro* and then injected into the cardiac affected areas. Despite the regenerative potential, no major outcomes came from such trials (Messina et al., 2004). These multipotent stem cells have the advantage of being harvested from adult hearts and hence being more mature cells than hESC.

Researching the genetic basis of pluripotentcy, a new type of pluripotent stem cells was created more recently by Yamanaka et al. in 2006 revolutionising the stem cell field and opening the door for new possible applications in stem cell technology. The creation of induced pluripotent stem cells (iPS) by reprogramming somatic cells back into a pluripotent stage resolved the ethical issues that hESC presented and heralded the beginning of personalised cell models.

These iPS are equally immortal as hESC, as able to be maintained indefinitely in culture and hold the potential to differentiate into any type of tissue including CM. With the advantage of maintaining most of the original somatic cell genome, they allow the possibility of developing *in vitro* models of disease as well opening the field of individual drug screening.

1.6.1 Human induced pluripotent stem cells – hiPSC

1.6.1.1 Historical background

The idea that some cells hold totipotency goes back to 1895, when Hans Dreish succeeded for the first time in cloning an animal, namely a sea urchin (Gilbert, 2010). His experiment revealed that a single cell from an embryo had the potential to create an entire organism. Decades would pass with the field still quiescent. In 1952, the first nuclear transfer from a late stage embryo into a frog enucleated egg was made, growing to a full adult as a result (Briggs and King, 1952). Science would have to wait another decade until the first adult somatic cell nuclei from an adult frog enterocyte was transferred into an unfertilized frog egg, still creating tadpoles (Gurdon, 1962). This last experiment reported by John Gurdon was pivotal in showing that the adult cell nuclear material had all the genes to originate a tadpole. This event was dependant on external factors to unlock that potential. Finally, the culmination of embryonic transfer and cloning reached a peak when in 1997, Wilmut et al. successfully cloned a mammal from an adult epithelial cell, transferred into an unfertilized oocyte.
These reports provided evidence that adult terminally differentiated somatic cells have the potential to re-differentiate into other cell-types and that oocytes hold the factors to unravel that potential.

1.6.1.2 Induced Pluripotency

With the discovery of mESC in 1981 (Evans et al.) pluripotency was confirmed as a cellular property without resorting to unfertilized oocytes. It was obvious that mESC contained in their genome, the active 'factors' allowing them to produce different types of tissues.
Although cell fate conversion by defined ectopic factors was a known fact to science, (Davis et al.,1987; Laiosa et al.,2006; Cobaleda et al.,2007) it was only in 2006 that Takahashi et al. working under Shynia Yamanaka's supervision, achieved success in identifying the factors able to make cells retrocess, in the Wadson differentiation scale.

From among 24 identified factors that could maintain pluripotency of ESC, Yamanaka's team found that expression of four proteins was essential and sufficient to reprogram cells: Oct3/4, Sox2, Klf4 and c-Myc (OSKM). These reprogrammed cells via viral delivery of the OSKM factor genes, had similar features to ESC regarding expression

and epigenetic profiles. More importantly they were pluripotent and able to differentiate into teratomas and the three germinal layers. These cells were then denominated 'induced pluripotent stem cells' (iPS).

The creation of fully reprogrammed iPS cells was not completely achieved initially as iPS cells didn't manage to originate a viable chimeric mouse after being inserted into an oocyte. Researchers used other factors such as Nanog and Oct3/4 locus as a reporter system instead of Fbx15 (previously unsuccessful). The result was the first generation of iPS chimeric mice (Okita et al.,2007). One other factor, c-Myc (a known oncogene) was not used in this experiment, allowing oncogenesis reduction on F1. (Nakagawa et al.,2008).

Less than a year from the first iPS report in mice, human iPS (hiPSC) were produced with the same success (Takahashi et al.,2007). In the same year, Yu et al. published a new efficient pluripotent combination of defined factors to create hiPSC using Oct3/4, Nanog, Sox2 and LIN28.

1.6.1.3 iPS cell generation and pathways

Despite the important step achieved with the discovery of iPS, pluripotency induction was very low and typically less than 1% of reprogrammed cells that received OSKM combination, become iPS cells (Takahashi et al.,2006). However, a new report mentions significant improvement of pluripotency induction, achieving 20% success of pluripotency induction with the same OSKM factors (Tanabe et al.,2013).

One of the best pluripotency surface markers is TRA-1-60. Within 7 days of transduction, more than 20% of transduced cells (normally fibroblasts) are TRA-1-60 positive. Despite this, 15 days post-transduction, the majority of TRA-1-60 positive cells frequently become negative for this marker. This observation suggests that maturation rather than initiation is the biggest obstacle during the reprogramming process. Promotion of additional factors to be expressed, such as LIN28 (Tanabe et al.,2013) and LIN41 (Worringer et al.,2014) can also increase pluripotency efficiency.

Histone modifications and DNA methylation play a very important role in the reprogramming process and have been targets of intense research. Histones regulate gene expression and therefore help to maintain stable cell lines. At a very early stage of the reprogramming process, up to 48h after transduction, Oct3/4, Sox2 and Klf4 bind to

close chromatin sites of promoters resistant to DNase digestion. After the binding, these heterochromatic regions are opened. This way Oct3/4, Sox2 and Klf4 function as initiators, opening the epigenetic barriers and increasing the reprogramming transcription factors accessibility (Soufi et al.,2012). Some histone deacetylase inhibitors have been reported to increase iPS generation, such as valproic acid, trichostatin A and sodium butyrate (Huangfu et al.,2008; Mali et al.,2010)

Promoters of ESC responsible genes, such as Nanog and Oct3/4 are known to suffer demethylation during the reprograming process (Takahashi et al.,2007). The reduction of DNA methylation levels by a methyl-transferase inhibitor (Aza-C) promotes reprogramming efficiency (Mikkelsen et al., 2008).

These findings show the complexity of the reprogramming process and iPS induction protocols will surely become much more efficient when most of the pathways are unravelled and used to create reliable and more stable iPS cell lines in the future.

1.7 hiPSC derived CM

Following cell reprogramming and creation of hiPSC, (Takahashi et al., 2007) differentiation of these cells into CM was an obvious sequential step (Zhang et al., 2009). A new opportunity emerged to study human CM. Although our knowledge of cardiac physiology is vast and detailed as a result of decades of research, human CM are by far the most relevant and yet less studied CM from all mammalian models.

When hiPSC technology was initially developed, the first expected clinical applications were, as in the case of human embryonic stem cells (hESC), to use them in regenerative medicine. Unlike hESC, the problem of immune response and rejection of allogenic cell therapy could be overcome. These cells (hiPSC) can be made from other postnatal somatic adult cells of a patient and hence allow autologous cytotherapy with minimum rejection probabilities. Another frequent problem with hESC cell therapy was the development of teratomas (Nussbaum et al., 2007) that in several clinical trials had to be surgically removed. Despite being embryonic benign tumors and having a low metastatic potential, their growth could reach life threatening proportions in a vital organ like the heart or brain.

After some initial expectations, it was clear that, as is the case for hESC, hiPSC, could also be responsible for teratoma formation (Liu et al., 2013).

Although several research groups still work in the cardiac regeneration field using hESC and hiPSC, a new field has emerged using the latter. Disease modelling allied to

the potential perspective of personalised medicine and individual pathophysiology study was a real possibility. By creating *in vitro* models of disease, using hiPSC became obvious and a new field was born.

The problems that cardiac researchers faced for decades due to lack of human cardiac tissue, seemed to have a new hope with this technology. The main advantage was having a bigger translational potential and creating more bench to bedside knowledge.

Inherited cardiac disease such as cardiac channelopathies, always have been a particular challenge to study, since animal models aren't ideal for several reasons. Faster repolarization rates, different body/heart size ratio, different expression levels of ion channels and individual specific evolutionary adaptations, are responsible for significant inter-species differences.

New and more efficient hiPSC CM differentiation protocols have been reported, reaching in some cases near 100% beating cluster terminal differentiation (Burridge et al., 2012). After 5 years of their discovery, hiPSC derived CM started being researched intensively as these cells have several advantages over hESC and primary cells for ethical, physiological and economical reasons.

1.7.1 Drug discovery and toxicology screening

During the reprogramming process, target cells (usually fibroblasts) maintain their basic genome mostly unchanged, even when undergoing other tissue terminal differentiation such as becoming CM. As a result, these newly differentiated cells can be used as *in vitro* models of inherited disease. The main advantage that hiPSC present is the possibility of collecting information regarding a particular inherited disease in a specific patient, something that was impossible to achieve until this technology was discovered.

Cardiac toxicology is a major problem in some patients undergoing chemotherapy for cancer treatment, namely with anthracycline derivative drugs such as doxorubicin (Bernstein et al.,2014). If a patient already presents a degree of cardiac disease such as HF, clinicians may decide to hold the use of anti-cancer drugs to prevent further cardiac damage. This could decrease life expectancy as the patient may not benefit for the anti-cancer drug. By creating hiPSC derived CM from candidates for chemotherapy, personalised predictive toxicity screening could be performed. This information would

help in making a better clinical decision, by detecting abnormalities in the cardiac AP (Zhang et al.,2014).

Besides personalised cardiac toxicity screening, hiPSC derived CM can also be a powerful tool to screen for drug efficacy in patients needing any cardiac treatment. By allowing drug selection with less adverse events and optimal response, significant advantages could be obtained for the patient. But this area is still an unexplored field, and research has been focused mostly in inherited cardiac disease (Liang et al.,2013).

Specific hiPSC derived CM from patients with inherited cardiac disease, may have a major role in new drug discovery. Drug companies have now available different models of hiPSC derived CM that allow screening of new chemical entities that can result in potential new drugs.

As is the case with hESC, the major drawback that hiPSC derived CM have is that they retain an immature CM phenotype. These pluripotent derived CM present immature sarcomeric architecture characterized by the absence of H zones, I bands and M lines. They also present spontaneous contraction due to the high presence of pace-maker currents; immature sarcoplasmic reticulum and more round/irregular shape than the classical rod shape (Yang et al., 2014).

Several approaches have been developed in attempts to mature hiPSC derived CM. These can range from plating them in 3D platforms to enhance contractile function, promoting CM elongation, orientation, alignment and conduction velocity (Zhang et al.,2013). Plating hiPSC CM in continually electrically stimulated platforms has also been attempted (Mihic et al.,2014). However, a successful maturation process will likely have to involve multiple components such as the inclusion of hormonal and pharmacological factors to the protocols described above.

Despite these cells immaturity, physiological characterization confirms that they possess several functional cardiac receptors. Response to ß-adrenergic and muscarinic agonists and antagonists, anti-arrhythmic drugs and ion channel modulators are reported (Fatima et al.,2011; Kujala et al.,2012; Novak et al.,2015). Cardiac chronotropic, lusitropic and inotropic responses have been documented for hiPSC CM (Matsa et al.,2012), demonstrating that these cells can be very useful in screening new potential cardiac drugs.

1.8 Recent work and context of this project

The main objective of this project is to characterise and assess the validation of a CPVT1 *in vitro* model of disease using hiPSC derived CM. Several authors have published data regarding similar models of disease for the same channelopathy (Jung et al.,2012; Fatima et al.,2011; Itzhaki et al.,2012) as well for CPVT2 (Novak et al.,2012).

Most reports present a strong suggestion of disease recapitulation and good pharmacological response, but a systematic standardised functional study hasn't been reported yet. Each publication relates to a different mutation and possibly phenotype. Hence, it is difficult to assess those differences with such diverse experimental protocols. If we need to determine if this technology really has translational potential and can be used as a model of disease, different mutations should follow similar protocols to elicit arrhythmia and drug rescue.

Most publications rely on spontaneous data, assuming that observed arrhythmic events are better seen without external pacing. Using spontaneous beating cells can be a problem since single cells can have their own pacing frequency. On the other hand, by controlling the pacing we may also bypass these cells nature and artificially correct possible arrhythmogenic behaviour.

A common feature of the data presented in most of these publications, is that, although they present DADs percentages, there is no quantitative information regarding these arrhythmic traces, namely regarding frequency, amplitude and/or duration, making it more difficult to quantify DAD-based drug response.

Ca^{2+} handling is also a major component of CM physiology. Basic pharmacological characterisation and protein detection was reported in most studies regarding hiPSC CPVT CM, but there is still a need to provide a deeper characterisation of these cells Ca^{2+} transients. Functional study of Ca^{2+} handling during pacing and ß-agonist stimulation is essential in order to mimic exercise and strong emotions. These are pivotal in CPVT pathophysiology.

In 2011 the first report of a CPVT1 hiPSC derived CM was published by Fatima et al. This report characterised a mutation localized in the FKBP1.2 binding domain of the RyR2 protein (p.F2483I). Cells were differentiated in co-culture with a murine visceral endoderm-like cell line. Immunocytochemistry and protein expression (PCR) profiles were made, demonstrating a similar profile between control and CPVT cells with

immature characteristics. Functional data were only presented regarding spontaneous activity. Mutant cells presented negative chronotropy compared with control cells when perfused with isoprenaline and 34% presented DADs in the presence of a ß-agonist. No details on the DADs duration or these events presence in control cells, were provided. No quantitative data regarding the DAD were provided.

Although DADs are the arrhythmic hallmark of CPVT, other events may occur. Kujala et al.,2012 demonstrated that EADs can also be present in hiPSC CPVT CM for the P2328S mutation. Patch-clamp recordings were only made in spontaneously beating cells and a quantitative definition for EADs and DADs was given (≥3% amplitude of the previous AP). A qualitative assessment of calcium transients was presented in terms of variations in amplitude and rhythm.

Similar qualitative assessment of Ca^{2+} transients is also reported by Jung et al.,(2012). Amplitude and rhythm are presented, although paced at different frequencies. These authors demonstrated for the first time, hiPSC CPVT CM potential for new drug discovery, reporting that dantrolene could rescue arrhythmic DADs and restored normal Ca^{2+} spark properties. Electrophysiology data were obtained with partial pacing of hiPSC CM at 1Hz. This publication presented a more systematic approach for electrophysiology recordings than other authors. No definition of a DAD or quantitative data for DADs is provided.

Itzhaki et al.,(2012) reported the use of flecainide (10µM) with apparently good response to abolish disease phenotype in hiPSC CPVT CM with RyR2 heterozygous point mutation M4109R. Patch-clamp recordings were obtained from both spontaneously beating and quiescent cells (paced at 1Hz). Percentage of cells presenting DADs, and quantification of DAD magnitude (amplitude) is presented: 13.0±8.2mV for mutant cells and circa 5.7±3.9mV for control CM. No data regarding DAD duration is mentioned and no quantitative definition of DADs is provided.

Zhang et al.,(2013) reports a very detailed study on Ca^{2+} handling using CPVT derived hiPSC CM from a patient carrying the RyR2 F2483I mutation. These authors presented mainly voltage-clamp data, using the patch clamp technique to determine $I_{(L\text{-}Ca)}$ and $I_{(NCX)}$. No current clamp data or action potential characterisation is reported. Only spontaneous beating cells were used and this report is the only one to suggest that based on functional Ca^{2+} experiments, hiPSC CPVT cells present an adult CM phenotype.

Support for the drug screening and therapeutic strategy optimization of CPVT hiPSC derived CM comes from Di Pasquale et al.,(2013). These authors used CM with RyR2 mutation p.Glu2311Asp and tested a novel anti-arrhythmic chemical entity, KN-93. This molecule acted as an inhibitor of CaMKII to reduce DADs in hiPSC CPVT CM. Evoked (0.5Hz) and spontaneous AP were recorded. Despite the authors suggestion of KN-93 efficacy, no quantitative data is presented regarding number of DADs, amplitude or duration, and no definition of DAD is given. Results are reported as significant relating to n=7 hiPSC CPVT CM cells.

While Ca^{2+} handling and AP functional characterisation are given in these cited reports demonstrating the CM phenotype of these cells, the lack of systematic definition and quantitative data regarding DADs is obvious. Such definition should be a critical point to report validation of a CPVT *in vitro* model of disease. Despite this, all authors suggest very clearly that disease phenotype recapitulation is demonstrated in their experiments.

1.9 Aims and hypothesis of this study

The CPVT hiPSC derived CM used in this project were obtained from a patient that had undergone cardiac surgery for ICD implantation. This 5 year old patient presented a RyR2 genotyped mutation, c.6737C>T (Ser2246Leu) and the resultant ryanodine receptor malfunction is known to cause a classical bidirectional ventricular tachycardia, leading to arrhythmia.
In channelopathies such as CPVT preclinical research plays a vital role in trying to discover new basic mechanisms of disease, drug toxicity testing and new drug discovery. A potential for personalised treatment is also in sight if mutant hiPSC CM can be validated as a good model of disease.

To my knowledge no reports have been published regarding the use of hiPSC derived CM with this mutation. A robust characterisation has been made by different groups regarding different mutations, mainly from a functional CM perspective. A consistent systematic approach to model CPVT *in vitro* using patch-clamp and Ca^{2+} imaging is a gap in this field of research. Such experiments will help to clarify how good the disease modelling potential of this technology is.

The main aim of this project is to assess if hiPSC CPVT derived CM can recapitulate the disease *in vitro* and if so, if the observed arrhythmic phenotype can be rescued or reduced with pharmacological treatment. For this objective it is necessary to proceed to a basic physiological characterisation of these mutant cells and their controls.

The following hypotheses were formulated regarding functional characterisation:
1 – hiPSC CPVT CM and hiPSC Control CM (BT-1) express basic cardiomyocyte markers (Troponin C) and Ca^{2+} handling proteins (RyR2, CASQ2, PLB, SERCA)

2 - hiPSC CPVT CM and hiPSC Control CM (BT-1) present a typical CM AP and that the three CM sub-types are present in a cell population.

3- hiPSC CPVT CM and hiPSC Control CM (BT-1) present basic cardiomyocyte physiological and pharmacological responses, namely increased pacing and ß-adrenergic response (to isoprenaline and propranolol) demonstrated by the expected inotropic, lusitropic and chronotropic properties.

4 - hiPSC CPVT CM and hiPSC Control CM (BT-1) present basic cardiomyocyte Ca^{2+} handling pharmacological responses, namely to caffeine, ryanodine and nifedipine.

The following hypotheses were formulated regarding disease modelling:

1 – hiPSC CPVT CM will present a higher arrhythmic response (having higher DADs incidence as a hallmark) than hiPSC Control CM (BT-1) from a qualitative and quantitative point of view when stimulated by increased pacing or ß-agonist stimulation.

2 – hiPSC CPVT CM will present higher Ca^{2+} handling arrhythmic behaviour (having higher incidence of abnormal calcium transients) than hiPSC Control CM (BT-1) from a qualitative and quantitative point of view when stimulated by increased pacing or ß-agonist stimulation.

3 - hiPSC CPVT CM arrhythmic behaviour (namely DADs frequency, amplitude and duration) can be rescued or improved when treated with anti-arrhythmic drugs in the presence of isoprenaline.

4 – hiPSC CPVT CM arrhythmic behaviour (abnormal Ca^{2+} transients and respective parameters) can be rescued or improved when treated with anti-arrhythmic drugs in the presence of isoprenaline.

The previous hypotheses were tested using different techniques, namely western blot, immunocytochemistry, patch-clamp and Ca^{2+} imaging.

Although spontaneous AP recordings were also obtained, one of the main objectives regarding patch-clamp experiments is to study these cells as a potential *in vitro* model of disease, using a systematic protocol of evoked action potentials for different conditions. Studies of this nature have not yet been reported in the literature.

Another novel objective is to present a more objective and quantitative analysis of spontaneous and stimulated Ca^{2+} transients from hiPSC CPVT CM. By using a specialised software, SALVO, a more detailed analysis of Ca^{2+} handling properties of these cells may be obtained.

1.10 Future applications and scientific impact

Disease modelling plays a pivotal role in medical research to study new mechanisms of disease, find new treatments, drug testing and for the development of personalised treatment with optimal efficacy and safety.

With all the challenges that each new technology faces, disease modelling with hiPSC derived CM has had a significant impact in the field. It has brought new information regarding mechanism of disease (Itzhaki et al., 2012; Ma et al., 2015), new possible drug treatments (Jung et al.,2012) and innovative therapeutic approaches (Matsa et al.,2014). In less than a decade, the cardiac pluripotent stem cell differentiation field has seen great advances, (Burridge et al.,2012; 2014).

Already based on this technology, there is at least one report that demonstrates the bench to bedside translational potential of these cells. In this case, a clinical decision of increasing the pacing frequency of an ICD, in a LQT patient with a complex phenotype, was made based on data obtained from personalised hiPSC CM (Terrenoire et al.,2013).

Therefore despite a recognized immature phenotype of hiPSC derived CM, these cells are already providing valuable information that in some cases has already saved lives (Terrenoire et al.,2013).

Researchers are placing increased effort in creating a more mature phenotype of these cells. There is a need to establish an optimal maturation stage, ideal culture substrate and stimulation factors (Rao et al.,2013).

The real potential of these cells may be better understood and unlocked when effective robust differentiation and maturation protocols to produce hiPSC CM are obtained.

But if a true translational application of this technology is to have a significant impact in the clinical setting a specialized group initiative, such as a consortium, should be created. Testing different mutations with the same experimental protocols to characterise and recapitulate a disease *in vitro*, would help to achieve uniformity and consistency in the data obtained. In this way innovative diagnostic and therapeutic guidelines could possibly be achieved for CPVT.

Chapter 2

General materials and methods

2.1 Cell culture and differentiation of hiPSC CM

The main objective of this current report is to characterise and validate a CPVT1 *in vitro* model of disease. For this purpose, CM differentiated from both a control hiPSC BT1 cell line and a CPVT hiPSC cell line were used.

All hiPSC were obtained from reprogrammed adult somatic fibroblasts, made at the University of Nottingham, by the Prof. Chris Denning group. For more details on fibroblast reprogramming and CPVT hiPSC characterisation please refer to Appendix I.

For this project, the adopted CM differentiation protocol was the Burridge protocol (Burridge et al., 2011) chosen because it presents high efficiency in producing beating clusters of cells as EBs.

In this project cell culture of both hiPSC CPVT and BT1 CM was carried out in Cardiff University to proceed with CM differentiation. However as this process was very challenging and due to low CM differentiation efficiency, most hiPSC CMs were generously provided by Notthingham University.

2.1.1 Burridge Protocol

2.1.1.1 Cell Maintenance

The original Burridge protocol uses a conditioned media to feed hiPSC. MEF (Mouse Embryoic Fibroblast) conditioned media was used to feed all hiPSC daily, adding 2ng/ml FGF2 before changing the media. Conditioned media was obtained by feeding a layer of **4.5 x10**^{6} MEFs in a T75 gelatin 0.1% coated flask over 24h.

The media obtained was frozen and could be kept for 6 months at -40°C. This media was then used to feed hiPSC.

All pre-conditioned media was made of basal DMEM F12, 15% KSR (Knock-Out Serum Replacement), 1% NEAA (Non Essential Amino Acids), 1% P/S (Penicillin/Streptomycin) and 100μM β-Mercaptoethanol.

However the use of MEF conditioned media presents some disadvantages, namely batch variability, irregular supply and more frequent infections. In this project it also presented lower efficiency in differentiating CMs from hiPSC.

In order to increase hiPSC quality and eliminate the use of undefined media from our cultures we add the mTeSR1 media from Stem Cell Technologies. mTeSR1 is a defined, feeder-free maintenance medium for hESCs and hiPSCs designed to maintain pluripotency of all cultured cells.

Both hiPSC and control cells from a healthy subject (confirmed CPVT1 mutation free) were expanded and split every 3 days and plated at **1.25 x10**^{6} cells in Geltrex® (Invitrogen) coated T25 flasks. Each T25 flask was coated with 5ml of the Geltrex® suspension (0.25ml Geltrex® in 49.5ml DMEM) and incubated at 37°C for 1h.

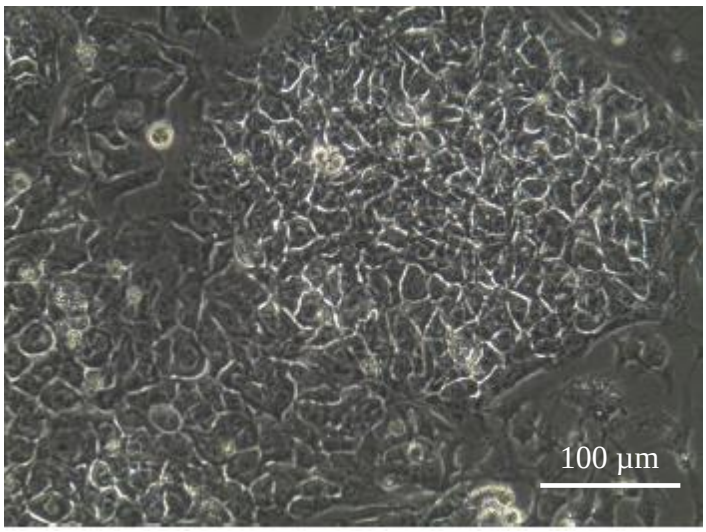

Figure 2.1– Colony of hiPSC CPVT *- Morphology of a confluent colony of hiPSC CPVT ready for splitting. Image obtained using inverted microscope (20x magnification).*

Splitting hiPSC was carried out at 80-100% confluence. Maintenance media was removed and PBS was used to wash culture flasks before adding 1ml TryplE enzyme (Invitrogen) and incubating for 1 minute at 37°C. PBS wash was important to avoid enzymatic inhibition from residual media. TryplE was blocked with addition of 5ml maintenance media. Cells were aspirated and spun in a 15ml falcon tube at 1000 RPM for 3 minutes, and counted. All media used were filtered to avoid pathogen contamination.

2.1.1.2 Differentiation protocol

The basal media for all the Burridge protocol is RPMI 1640 and this protocol involves three main steps with different media composition.

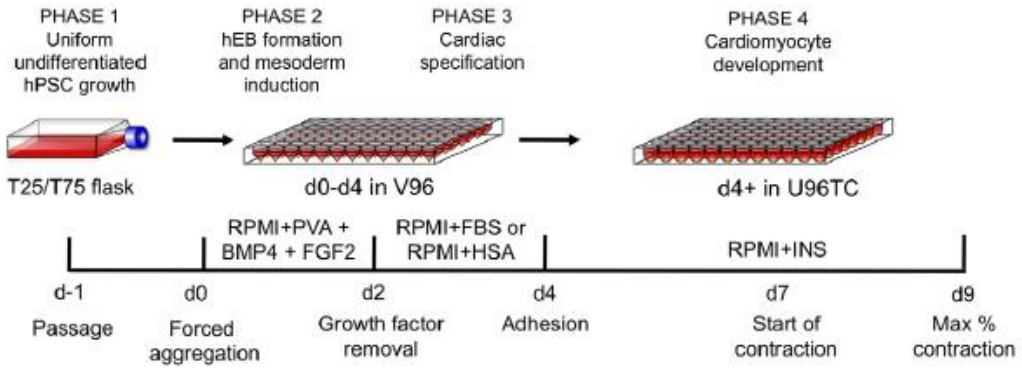

Figure 2.2 – Timeline diagram of hiPSC derived CM differentiation protocol *(Burridge et al.,2011)*

CPVT hiPSC and BT1 hiPSC were split and re-suspended on day 0 media (RPMI-PVA). The number of cells used for a V-bottom 96 well plate depended on the size of EBs desired, but it is recommended that $5x10^3$ cells per well are used as a minimum and not more than $10x10^3$ to prevent undernourishment of cells at the EB core.

Day 0-2 media contains RPMI 1640, PVA (poly vinyl alcohol), lipids, ITS, BMP4, FGF2 and 1-Thioglycerol (Table 2.1). BMP4 and FGF2 factors should always be added fresh from frozen aliquots. Cells remain in a suspension in the media and using a multi-channel pipette, 100µL are placed in each well of a V-bottom 96 well plate (figure 2.2).

On day 2, 95µL of the old media is removed and replaced with 100 µL fresh RPMI – FBS, containing RPMI, FBS and 1-Thioglycerol. At this stage solid embryoid bodies (EBs) should be observed.

On day 4 the media is changed and the EBs are transferred to a U-bottom 96 well plate. The old media is aspirated with multichannel pipette set to 90µL and 100µL fresh RPMI-ITS is added after to each well. This media contains ITS, lipids and 1-Thioglycerol and can subsequently be used to feed differentiated beating clusters.

To transfer EBs a multichannel pipette is set to 115µL and holding it at an oblique angle and in a continuous movement, 60µL are aspirated and flushed to detach the EB (figure 2.3). The pipette is then positioned vertically and the full content of the aspirated well,

is dropped to a U bottom 96 well plate normally containing the detached EB. The EBs should be cohesive and solid enough at this stage to survive the turbulence produced.

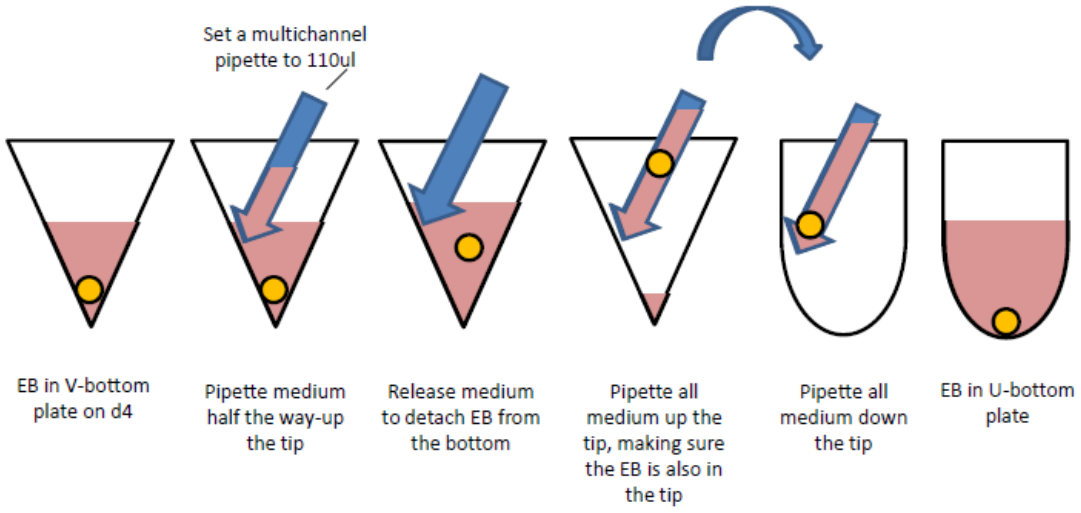

Figure 2.3 - Embryoid body transfer at day 4 *- Burridge protocol pictogram. Passage from V-bottom 96 well plate to U-bottom 96 well plate.*

At day 8 some beating clusters should be seen,and spontaneous contractibility may be considered the main macroscopic differentiation endpoint.

These beating clusters can then be plated on other plates or cover slips depending on the experiment to be done or if they are to be maintained as a beating cluster.

Differentiated cells appear to maintain their contractile phenotype longer if in culture as EBs, and not so stable if disaggregated, but no accurate studies have been found in the literature regarding this issue.

If EBs are maintained in the U-bottom 96 well, there is a tendency for fibroblast overgrowth to be observed whichcan cover the EB and hence reduce physical space for contractibility.

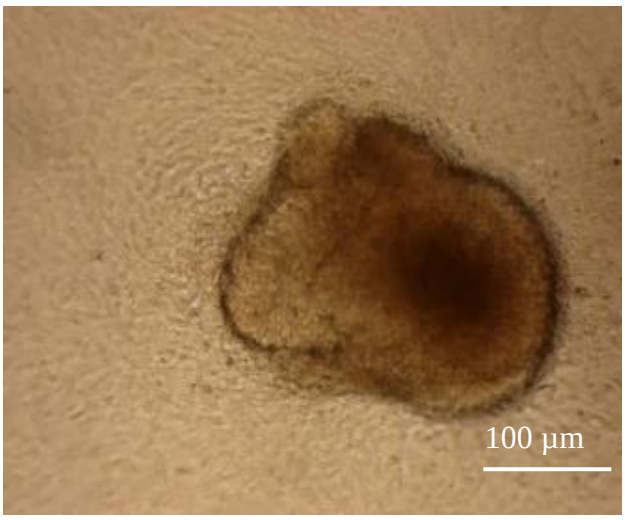

Figure 2.4 - Beating cluster hiPSC CPVT CM *- EB from hiPSC CPVT CM in a 6cm plate after transplanted from 96 well plate. Abundancy of fibroblasts is seen growing around the EB. Image obtained using an inverted microscope (10x magnification).*

However if transferred to a larger area plate (i.e. 6 well plate), although fibroblast growth is still a potential problem, to preserve contractility the EBs can more easily be physically detached and transferred to another plate.

Differentiated hiPSC CM were fed every 4-5 days with fresh RPMI-ITS media.

Medium	Component	Stock. Conc.	Working conc.	Volume/Mass per 100ml	Product number
RPMI-PVA-ITS (d0-2)	RPMI 1640	1x	1x	98ml	Invitrogen; 21875034
	PVA	powder	4mg/ml	400mg	SIGMA; P8136
	Allow to dissolve at 4°C for at least 72h. Store at 4°C for several months. Filter sterilise before use.				
	1-thioglycerol	11.5M	400uM	3.5ul	SIGMA; M6145
	Lipids	100x	1x	1ml	Invitrogen; 11905-031
	ITS	100x	1x	1ml	Invitrogen; 51500-056
	BMP4	10ug/ml	20ng/ml	200ul	R&D Systems; 314-BP-050
	FGF2	4ug/ml	6ng/ml	150ul	Peprotech; 100-18
	Use fresh				
RPMI-FBS (d2-4)	RPMI 1640	1x	1x	80ml	Invitrogen; 21875034
	1-thioglycerol	11.5M	400uM	3.5ul	SIGMA; M6145
	FBS	N/A	20%	20ml	PAA; A15-101
	Use fresh.				
RPMI-ITS (d4-9)	RPMI 1640	1x	1x	98ml	Invitrogen; 21875034
	1-thioglycerol	11.5M	400uM	3.5ul	SIGMA; M6145
	Lipids	100x	1x	1ml	Invitrogen; 11905-031
	ITS	100x	1x	1ml	Invitrogen; 51500-056
	Use fresh.				

Table 2.1 – Cardiac differentiation protocol for hPSC *– Protocol used to induce hPSC differentiation into CM. (Burridge et al.,2011)*

2.1.2 hiPSC cell lines

The Burridge protocol has shown excellent results in differentiating several hiPSC cell lines (Burridge et al.,2011) withconsistent high percentages of beating clusters and although several publications and our collaborator's experience confirm this fact, this efficiency was not always seen in this project. In order to gain experience and acquire skills with this protocol, hESC H9 were also used, since these were readily available and produced good results. All subsequent experiments were made with cells provided from our collaborators from Nottingham University.

2.1.3 EB disaggregation and plating

In order to study the differentiated hiPSC derived CM, beating clusters had to be disaggregated enzymatically and plated on cover slips as single cells.

For patch clamp experiments 13mm cover slips previously coated with 0.1% gelatine incubated at 37 $^{\circ}$C for 30 minutes were used. The same coating and incubation times using glass bottom Mattek dishes, were used for all Ca^{2+} imaging experiments..

The disaggregation protocol of Maltsev et al., 1997 was used. This protocol uses a three-step gentle dissociation process using collagenase B as the active enzyme. This protocol uses three different buffers with specific composition (table 2.2). Each buffer is made and frozen in 0.5ml aliquots, being stored for 6 months at -40ºC.

Before starting the disaggregation process 20µl/ml of 1M glucose were added to each thawed buffer aliquot (i.e. 20µL in 1 ml aliquots).

For the first step, EBs were dissected from the original wells/flasks collected in a P200 tip and transferred to 0.5ml of buffer 1. A maximum number of 6-8 EBs per eppendorf is recommended and these were incubated at room temp for 30 minutes in buffer 1.

The second step involves collecting the EBs in a P200 tip and transfer to 0.5ml of buffer 2. Incubate at 37°C for 30-45 minutes in buffer 2 (depends on size of beaters).
For step 3, EBs were collected in a P200 tip and transferred to 0.5ml of buffer 3 incubated at room temp for 60 minutes.

As soon as the buffer 3 incubation period ends and clumps are collected in a P200 tip, these were transferred to a desired volume of RPMI-ITS media.

At this point the EBs need to be pressure dissociated and by pipetting up and down 5-6 times with either a P1000 or P200 a single cell suspension should be obtained.
Harsh pipetting may also damage the cells and experience needs to be gained with this step.

Once dissociated, cells were plated in gelatine coated Mattek dishes, allowing 24h for the cells to attach undisturbed.
A ratio of 1/2 beater per dish should be plated in 150µL RPMI-ITS, dropped carefully onto the centre of the slide, and carefully add 200µL RPMI-ITS after 24 hours.

Component	Supplier	Product number	Buffer 1 (low Ca^{2+})		Buffer 2 (enzyme)		Buffer 3 (recovery)	
			100ml	Conc.	100ml	Conc.	100ml	Conc.
NaCl	SIGMA	S5886	12ml	120mM	12ml	120mM	-	-
KCl	SIGMA	P5405	540µl	5.4mM	540µl	5.4mM	8.5ml	85mM
$MgSO_4$	SIGMA	M2643	500µl	5mM	500µl	5mM	500µl	5mM
Na pyruvate	SIGMA	P5280	500µl	5mM	500µl	5mM	500µl	5mM
Taurine	SIGMA	T8691	20ml	20mM	20ml	20mM	20ml	20mM
HEPES	SIGMA	H3784	1ml	10mM	1ml	10mM	-	-
EGTA	SIGMA	E0396	-	-	-	-	100ul	1mM
Creatine	Fluka	27890	-	-	-	-	5ml	5mM
$CaCl_2$	SIGMA	C5080	-	-	30µl	30µM	-	-
K_2HPO_4	SIGMA	P3786	-	-	-	-	3ml	30mM
Na_2ATP	SIGMA	A6419	-	-	-	-	101mg	2mM
Collagenase B	Roche	1088807	-	-	100mg	1mg/ml	-	-
pH (NaOH)	-	-	6.9		6.9		7.2	

Table 2.2 – Disaggregation buffer composition *- method used for hPSC derived EB (Maltsev et al., 1997)*

2.1.4 Cardiac differentiation efficiency

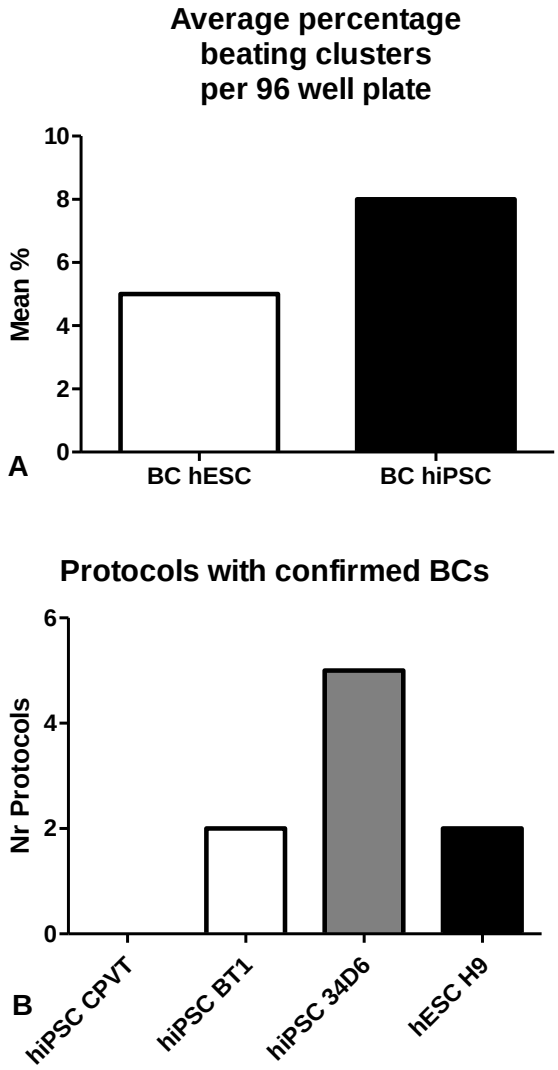

Figure 2.5 – Cardiac differentiation efficiency in the current project *– Average percentage EB per 96-well plate for both hESC and hiPSC (A). Total number of protocols in which at least one beating cluster was produced (B).*

2.2 ICC and Protein detection

2.2.1 Western Blot (WB)

2.2.1.1 Protein analysis by SDS-PAGE

Sodium dodecyl sulphate polyacrylamide gel electrophoresis (SDS-PAGE) is used for the separation of proteins according to their Molecular Weight (MW). This method is used for several different purposes such as to identify a protein, determine protein size and abundance, find the number of proteins present and find the purity of a sample.

The proteins in a sample will have a number of variables including length, shape, weight and charge. For SDS-PAGE to work correctly the proteins must be put in their native state, i.e. primary structure. SDS is an anionic detergent that disrupts the hydrogen bonds and Van der Waal's interactions in proteins and breaks down cell membranes. This destroys the proteins secondary, tertiary and quaternary structures causing them to become linear. SDS also gives the protein a uniform negative charge making the protein travel to the positive pole in an electrical field.

After protein separation, specific protein identification can be obtained using antibodies with the WB technique. Primary antibodies will bind to the target protein, a secondary antibody will then bind to the primary based on species similarity. This secondary antibody carries a molecule capable of light emission (HRP) and when stimulated, detection can be achieved as a photographic record.

2.2.1.2 SDS-PAGE Running Gel Preparation

The running gel preparation includes several steps and several aspects must be taken in consideration:

- Prepare running buffer
- After assembling the gel case, add running buffer inside and wash wells with pipette.
- On first well use a control or a ladder, (20-40 µL for Biorad)
- Deposit protein sample in sequential wells
- Run gel at 90V first half hour and then when reached half way, increase voltage to 130V. Stop when bromophenol blue line hits the bottom.
- After running the gel, wash glass support and membrane in distilled water
- Cut and detach membrane

Required solutions:

- 10 x electrophoresis running buffer (SDS) 1L : 30.3g Tris base + 144g Glycine + 10g SDS in distilled water.

- 5x sample buffer : 1.19ml 1M Tris-HCl pH 6.8 + 1g SDS + 1ml B-mercaptoethanol + 3.96g glycerol + 1ml 0.2% bromophenol blue (filtered) + water to make 10 ml

- 10 x TBS-Tween: (1L) 60.57 g Tris base + 87.66 g NaCl (pH 7.4 HCl) + 10ml Tween 20

Gel parts:

Bottom gel: 4x Tris-HCl 1.5M pH 8.8 (100 ml) 18.2g Tris base; pH 8.8 with HCl.

Top gel (Stacking): 4x Tris-HCl 0.5M pH 6.8 (100 ml) 6.05g Tris base; pH 6.8 with HCl.

	15%	10%	5%	3.5% (stacking)
Acrylamide	7.5 ml	5 ml	2.5 ml	583 µl
Tris (1.5M)	5 ml	5 ml	5 ml	1.25 ml (0.5M)
SDS (5g-50ml)	160 µl	160 µl	160 µl	50 µl
APS (10%)	160 µl	160 µl	160 µl	50 µl
TEMED	20 µl	20 µl	20 µl	8.3 µl
Water	7.16 ml	9.66 ml	12.16 ml	4.73 ml

Table 2.3 – SDS – PAGE Running gel composition. *Acrylamide percentage according to target protein molecular weight.*

Acrylamide concentration will depend on the molecular size of the protein to be detected. In this study 15% acrylamide concentration was used for small proteins such as CASQ and PLB and 5% acrylamide concentration was used for SERCA2A, ATPase and RyR2 detection.

2.2.1.3 Cell lysis

Protein extraction from cell pellets (minimum $1x10^6$ cells per pellet) was achieved by solubilisation for 30 minutes at 4ºC using RIPA modified buffer (150 mM NaCl, 1% Triton, 50 mM TRIS; pH 7.4 (HCl)) with protease inhibition cocktail (1:100) (Sigma P-8340). Cells used in these experiments were hiPSC CPVT, hiPSC CPVT CM and primary guinea pig CM. The pellet was centrifuged for 5 minutes at 7000 rpm (MiniSpin® Eppendorf), separating the supernatant which was used for WB. BCA Protein Assay kit (Thermo Scientific, ref.: 23227) was used to assess protein supernatant concentration. Samples containing at least 100µg of protein were stored at -80 ºC and used when necessary.

2.2.1.4 Sample Preparation

Each sample, adjusted to contain approximately 35µg of protein, was mixed with SDS sample buffer and bromophenol blue in order to achieve a volume no greater than 60µL. Individual samples were inserted into individual wells of prepared running SDS gel. A guinea pig *(Cavia porcellus)* heart lysate was used as control in the first well and a Biorad control ladder (20-40 µL) inserted in the second well.

2.2.1.5 Protein Transferring

When electrophoresis was completed, the gel was washed in distilled water, and iBlot ® Dry Blotting System (Life Technologies) was used to transfer proteins to a nitrocellulose membrane, following the manufacturer's instructions as shown in figure 2.6. A P3 program was used and the transfer process took 13 minutes at 20V. Proteins transfer to the cathode direction. When the transfer was complete the sample part of the nitrocellulose membrane was cut out as necessary for the protein detection process.

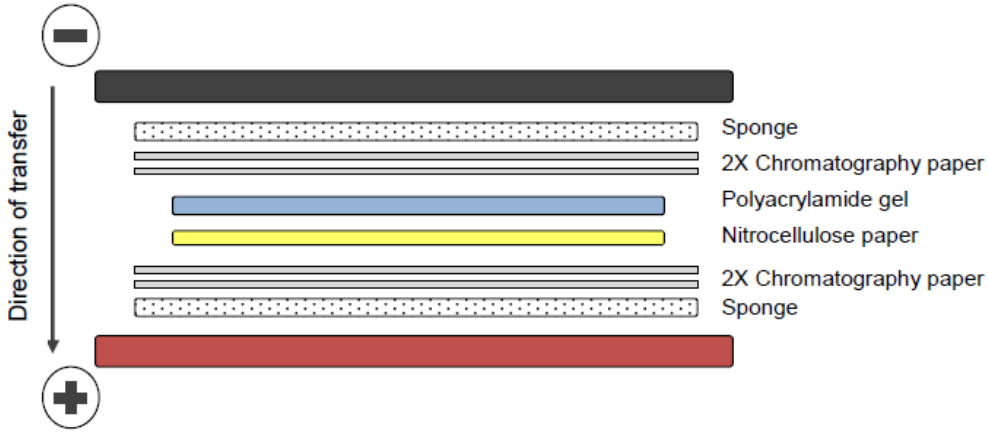

Figure 2.6 – iBlot ® Electroblotting layout *– layout used to transfer SDS-PAGE separated proteins into nitrocellulose membrane. Proteins are transferred in the cathode direction.*

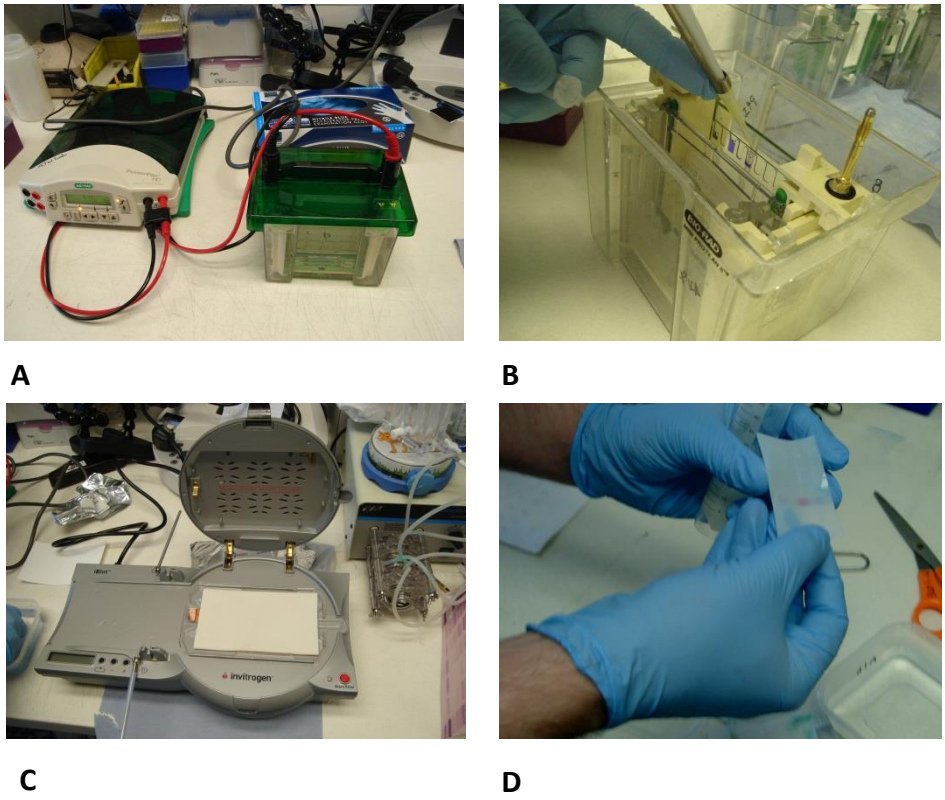

Fig 2.7 – SDS-PAGE and WB *– Electrophoresis machine and gasket used in SDS – PAGE experiments (A), sample insertion in SDS-PAGE gel wells (B), iBlot machine used for protein transfer from SDS-PAGE gel to nitrocellulose membrane (C) and nitrocellulose membrane with transferred proteins (D).*

2.2.1.6 Antibody detection

After the protein transfer step to a nitrocellulose membrane, protein identification using antibodies was performed. A blocking protein step was carried out to reduce unspecific protein binding using a TBS-Tween solution with 50mg/ml of powdered milk for 60 minutes at room temperature on an automatic shaking platform . The sample membrane was then washed in TBS-Tween for 5 minutes in constant movement. Primary antibody incubation was carried out for 2h at room temperature or overnight (16h) at 4ºC in TBS-Tween with powdered milk at 50mg/ml. After primary antibody incubation, the sample membrane was washed 3 times for 5 minutes in TBS-Tween using a shaking platform. Secondary antibody (HRP-conjugated) was incubated at room temperature for 45 minutes and the sample membrane was once again washed 3 times for 5 minutes in TBS-Tween.

For radiographic protein detection, a chemiluminescence kit from GE (Amersham ECL Prime Western Blotting Detection Reagent) was used according to the manufacturer's instructions. The membrane was placed on a plastic surface with the protein side up and the mixed detection solution was added to the membrane with incubation for 1 minute. Excess solution was removed and the membrane was covered with transparent plastic.

In a dark room, the membrane was placed in an X-ray film cassette with the protein side up and a sheet of X-ray autoradiography film was placed on the top of the membrane. Reaction times depended on result ranging from 15 seconds to 1 minute. The film was then removed for development in an automatic developing system (X-Radiograph Imaging system, Compact X4).

2.2.1.6.1 Antibodies

Primary antibodies included: Anti-RyR2 ARP106/1 'in house' rabbit polyclonal (used at 1:1000) (West et al.,2002), Anti-SERCA2A mouse monoclonal (Affinity BioReagents - used at 1:1000 dilution), Anti-PLB mouse polyclonal (Badrilla - used at 1:5000 dilution), Anti-CASQ rabbit polyclonal (Affinity BioReagents - used at 1:5000 dilution)

Secondary antibodies included: Anti-mouse secondary, HRP conjugate (Invitrogen), used at 1:5000 and Anti-rabbit secondary, HRP conjugate (Sigma), used at 1:10000 dilution.

Used antibodiy dilutions were provided by personal communication from Dr. Mark Bannister and Dr. Lowri Thomas.

2.2.2 ICC – Immunocytochemistry

2.2.2.1 Fixation and permeabilization

Cells used in patch clamp experiments were also used for ICC. After patch clamp experiment termination hiPSC CM were fixed with PFA (paraformaldehyde 4%) for 15 minutes at room temperature. Cover-slips were rinsed three times with PBS and then permeabilized with Triton X-100 (0.2%) for 1 hour at room temperature.

2.2.2.2 Primary antibody incubation

Samples were blocked with 5% non-fat dry milk in 0.2% Triton X-100 solution for 2 hours at room temperature on a rotator. Cover slips were rinsed with PBS twice and primary antibody was added to 0.1% Triton + 1% BSA (bovine serum albumin) and incubated overnight at 4ºC. Cover-slips were washed twice in PBS with 0.2% Tween 20.

2.2.2.3 Secondary antibody incubation

A secondary antibody was added in the same solution as the first antibody. Cells were incubated at room temperature in a dark room for 1.5 hours. Cover slips were washed with PBS twice and nuclei were stained using Hoescht for 5 minutes at room temperature. Finally one drop of antifade agent (ProLong® Gold – Life Technologies) was added to each slide.

2.2.2.4 Imaging

All preparations were imaged with a confocal fluorescence microscope (SP5; Leica Microsystems, Wetzlar Germany). An oil immersion lens with magnification of 63x was used. Light source was argon laser at fluorescent wavelength of 488nm.

2.2.2.5 Antibodies

Primary antibodies included: Anti-RyR2 ARP106/1 'in house' rabbit polyclonal (used at 1:1000) (West et al.,2002), Anti-Troponin I mouse polyclonal (Sigma - used at 1:1000 dilution),

Secondary antibodies included: Anti-rabbit secondary, Alexa 488 conjugate (Invitrogen), used at 1:5000 and Anti-mouse secondary, Alexa 488 conjugate (Sigma), used at 1:5000 dilution.

Antibody dilutions were provided by personal communication from Dr. Mark Bannister and Dr. Lowri Thomas.

2.3 Electrophysiology - Patch clamp technique

In order to study the electrophysiological properties of hiPSC derived CM, the whole cell patch clamp technique, was used.

This technique is a powerful tool to assess the hiPSC derived CM AP. The main objective was to obtain action potential recordings under specific experimental conditions using pharmacological intervention and electrical stimulation to record not only spontaneous action potentials but also evoked activity.

2.3.1 Stage set-up

Cover slips with plated cells, were transferred manually to 35mm glass bottomed culture dishes containing a superfusion insert (Automate PCP-1; Digitimer Ltd.,Welwyn Garden City, UK) (figure 2.8)

Figure 2.8 – Superfusion insert for patch clamp *– superfusion insert used in drug perfusion trial attached to 35mm petri dishes (Falcon 351008 easy grip petri dishes 35x10mm). This insert was attached to the petri dishes with Lubricant Grease (Dow Corning valve lubricant & sealant).*

The prepared glass bottomed culture dishes were mounted on the stage of an inverted microscope (CKX-41; Olympus, Tokyo, Japan) (figure 2.9)

Patch pipettes were made from "Kwik-Fill" borosilicate glass capillaries (World Precision Instruments (1B150F – 4). Pipettes were pulled in a Micropipette Puller (Sutter instruments Co. Model P-97).

Figure 2.9 – Patch clamp stage set up *– patch clamp rig and inverted microscope used in electrophysiology experiments for this project.*

2.3.2 Solutions and drugs

The HEPES based extracellular perfusate (modified Tyrode's) for current-clamp recordings consisted of (in mmol/L): 140 NaCl, 5.4 KCl, 1.8 $CaCl_2$, 1 $MgCl_2$, 10 glucose, 10 HEPES and pH was adjusted to 7.4 with NaOH. All reagents used from (Sigma)

The intracellular solution consisted of (in mmol/L): 130 KCl, 1 $MgCl_2$, 10 HEPES, 5 EGTA and KOH was used to set pH to 7.2. All reagents used were obtained from Sigma. Intracellular pipette solution was frozen in aliquots and stored at -20 ºC for up to 6 months.

Drugs and working concentrations used in patch clamp experiments were respectively: isoprenaline (1µM), flecainide (10 µM), dantrolene (10 µM), propranolol (1µM), propafenone (10 µM). All drugs used were obtained from Sigma.

Stock aliquots for all drugs were made and frozen at -20 ºC for up to 6 months.

Isoprenaline aliquots were made with ascorbic acid (Sigma) prepared in the ratio of 10:1 of ascorbic acid to isoprenaline to reduce oxidation of isoprenaline (Clements et al.,1980).

2.3.3 Patch clamp recordings

Recordings were made using a CV-7 headstage and MultiClamp 700B amplifier (Axon Instruments, Sunnyvale, CA, USA) controlled by Multiclamp software (Molecular Devices, Sunnyvale, CA).

Current clamp (IC) recordings were digitized and acquired using a Digidata 1322a card and pClamp 10.3 software (Copyright © 2012 Molecular Devices, LLC). AP were sampled at 10 kHz and filtered at 5 kHz using the low pass (eight pole Bessel) filter.

Data analysis obtained from patch clamp experiments was extracted using Clampfit 10.3 (Copyright © 2012 Molecular Devices, LLC).

2.3.3.1 Recording conditions

Recordings were obtained at 25ºC from both hiPSC CPVT CM and hiPSC BT1 CM.

Pipette bath resistance was between 2 and 5 MΩ. Pipette access resistance to cells was between 4 and 10 MΩ.

Spontaneously beating cells were defined as cells presenting spontaneous activity in a Gap free protocol (no current or voltage clamp injected) that records native cell resting membrane potential.

Quiescent cells were defined as cells not presenting spontaneous activity in a Gap free protocol. They did present evoked APs which were obtained in Current Clamp mode by injecting a single pulse of 500pA with 3ms duration. Cells RMP was clamped at -80mV to standardise evoked AP.

Evoked APs were obtained from both spontaneous and quiescent cells.

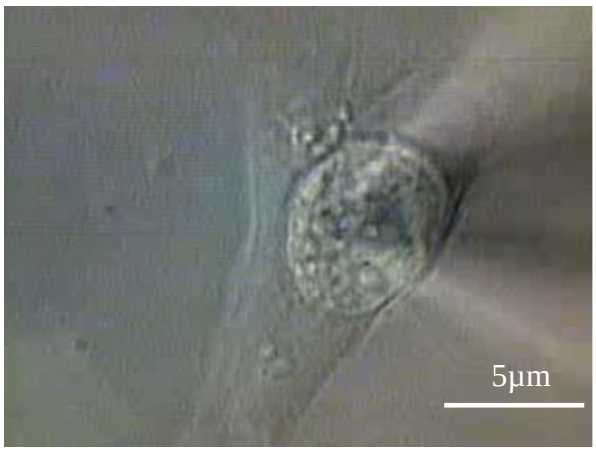

Figure 2.10 – Image of hiPSC CPVT CM- *hiPSC CPVT CM being patch clamped. Triangular shade on the right side corresponds to glass micropipette.*

2.3.3.2 Protocol sequence

In order to try and reproduce disease *in vitro*, a sequence of recording protocols were designed using evoked action potentials.

The sequence for patch-clamp experiments involved 4 protocols. The purpose of this experimental sequence was to try and trigger any arrhythmic activity with isoprenaline perfusion and then observe if anti-arrhythmic drugs could rescue any presented pro-arrhythmic events such as DADs.

The first recording was a Gap-free protocol perfused with Tyrode's to record spontaneous activity or the cell RMP (if quiescent) with 60 seconds duration. The first Gap-free protocol was followed by 3 current-clamp protocols in which a minimum of 50 evoked AP were recorded per cell. Experiments with paced cells were made at 0.5Hz and 1Hz.

The first protocol for evoked activity was done with cells perfused with Tyrode's solution only, the second with isoprenaline (1µM) in Tyrode's and the third with one of the used antiarrythmic drugs in the presence of isoprenaline (1µM).

2.3.3.3 Data extraction

All the data used in Chapter 4 and Chapter 5 was obtained from the same experiments following the previous mentioned perfusion sequence. In Chapter 4, isoprenaline perfusion data is a sum from isoprenaline prefusion of the different drug trial. This was done in order to assess the effect of isoprenaline on more cells, as it was difficult to obtain a high number of cells that endured the full duration of the protocol when patched.

DAD measurement was done manually using Clampfit 10.3 since no specific software was available to adequately measure these events.

2.4 Ca^{2+} fluorescence imaging

2.4.1 Confocal microscopy

A confocal microscope (SP5; Leica Microsystems) was used for all Ca^{2+} imaging experiments. Confocal microscopes allow tri-dimensional (x,y,t) visualization of the analysed cell upon light stimulation (usually a laser). A Ca^{2+} sensitive fluorophore indicator can then allow indirect visualisation of intracellular Ca^{2+} distribution.

2.4.2 hiPSC CM loading and plating

The microscope stage allows the use of Mattek dishes with a bottom glass cover slip, (Mattek dishes - uncoated 35mm glass diameter 14mm, P35G-1.5-14-C) which were used in all experiments.

EB disaggregation (please see protocol in chapter 3) allowed plating hiPSC CM in dishes previously coated with gelatin 0.1%. Gelatin 0.1% (500µl per dish) was incubated 30 minutes at 37ºC and excess removed before plating cells.

Fluo-4 AM (Life Technologies) was used to load cells in every Mattek dish. The working concentration of Fluo-4 AM was 5µM. Pluronic® F-127 (20% Solution in DMSO- Invitrogen P-3000MP) was used to dissolve one frozen vial of Fluo-4 (50 µg).

Before loading the cells, 5µL of stock mixture of Fluo-4 and Pluronic was added to 1ml of Tyrode's. RPMI-ITS was removed from the Mattek dish and 1ml of Tyrode's containing Fluo-4 was used to incubate cells at room temperature in the dark for 20 minutes.

After loading, loading solution was removed and cells were washed with Tyrode's three times. Cells were then left with 1ml Tyrode's in the Mattek dish to rest for 20 minutes at room temperature for de-esterification of the Fluo-4 AM.

Mattek dishes with loaded cells were then used for confocal imaging experiments.

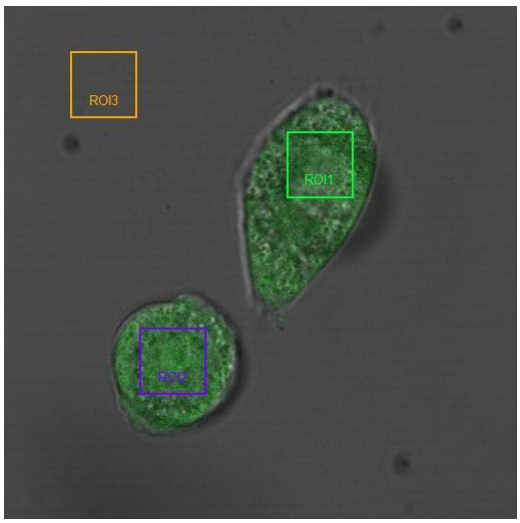

Figure 2.11 – FLUO-4 loaded hiPSC CPVT CM and regions of interest (ROIs) *– Cell pleomorphism observed (63x magnification oil immersion lens). Image extracted with Leica LAS software.*

2.4.3 Perfusion chamber and external stimulator

The use of a perfusion insert chamber with platinum electrodes (model RC-37FS – Warner instruments – figure 2.12) allowed not only continuous perfusion of solutions but also field electrical stimulation to elicit CM contraction at different pacing frequencies.

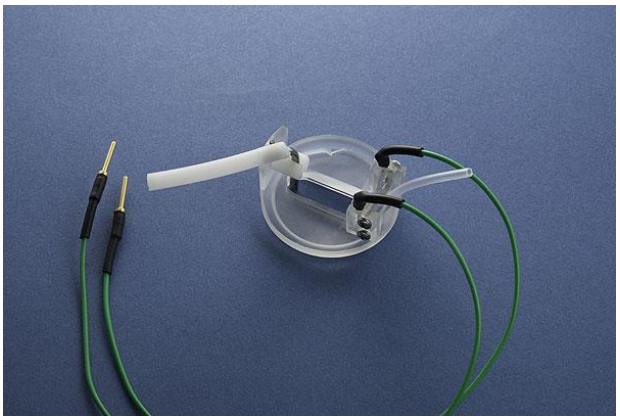

Figure 2.12 – Perfusion and stimulation chamber used in Ca^{2+} imaging experiments *- Perfusion insert with electric field stimulation for cell culture dishes. Suitable for Mattek 35mm dishes. This commercial insert, model RC-37FS is designed for applications requiring field stimulation and incorporates a pair of platinum electrodes.*

In order to stimulate cells, a specific tailor, made electrical stimulator was used (built by R.A.P. Montgomery). hiPSC CM were stimulated with bipolar pulses of 10-30Volts for 5ms. Pacing frequencies were 0.5, 1, 1.5 and 2Hz.

2.4.4 Perfusion drugs and solutions

The HEPES based extracellular perfusate (modified Tyrode's) used as perfusion media in all recordings, consisted of (in mmol/L): 140 NaCl, 5.4 KCl, 1.8 $CaCl_2$, 1 $MgCl_2$, 10 glucose, 10 HEPES and pH was adjusted to 7.4 with NaOH. All reagents used, were obtained from Sigma.

Perfusion was always carried out with drugs dissolved in modified Tyrode's (as previously described). Drugs used were isoprenaline (1µM) propranolol (1µM), nifedipine (1µM), flecainide (10µM), dantrolene (10µM), ryanodine (10µM) and caffeine (10mM).

All drugs were acquired from Sigma.

Stock concentration aliquots were made for isoprenaline, propranolol, dantrolene flecainide and ryanodine and frozen at -80ºC until used.

10 mM caffeine was made fresh from solid every time required.

2.4.4.1 Perfusion protocol

The perfusion protocol for hiPSC CPVT CM and BT1 CM characterisation (Chapter 4) consisted of two recordings of 90 seconds. One in Tyrode's perfusion and another with Tyrode's in the presence of isoprenaline 1µM. Isoprenaline perfusion started 30 seconds after initiating recording (figure 2.13)

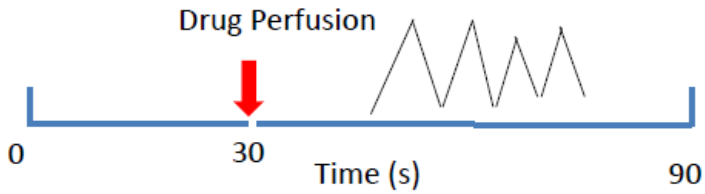

Figure 2.13 - Ca^{2+} imaging drug perfusion diagram *– Drug perfusion was initiated 30 seconds after start recordings. Maximum length recording was 90 seconds.*

In pacing experiments, stimulation would also be initiated 30 seconds after the start of recording.

For drug rescue experiments (Chapter 5) three different recording files were made in sequence, with a 2 minute Tyrode's washout period in between different perfusates:

1 – Tyrode's only, 2 – Tyrode's in the presence of isoprenline, 3 – Tyrode's with drug in the presence of isoprenaline.

Caffeine (10mM) was always added at the end of experiments. No other experiments were made after caffeine perfusion.

2.4.5 Recordings

For experimental purposes spontaneous cells were considered as cells beating with no external pacing. Stimulated cells could be both quiescent and spontaneously active cells that responded to external pacing.

Data used in Chapter 4 is a sum from all isoprenaline perfusion experiments, including data from Chapter 5.

2.4.5.1 hiPSC culture

Experiments were performed in hiPSC CM 5 days after disaggregation and plating down on Mattek dishes. Experiments were made with hiPSC CM between 5-30 days in culture after disaggregation. Studied hiPSC single cells never had more than 2 months post differentiation (as EBs or single cells). Feeding media while cells were on Mattek dishes was RPMI-ITS as per the protocol.

2.4.5.2 Data acquisition

Fluo-4 Ca^{2+}-dependent signals were visualized as 100-μm^2 ROIs. Only one ROI per hiPSC CM was analysed, selected so as to be away from the area of the nucleus to avoid excessive fluorescence. A 63× oil immersion objective using argon laser excitation (488 nm) at 20% strength was used.

Cells were maintained at 37 °C throughout experiments. Images were recorded every 100ms at a 512 × 512–pixel resolution.

External pacing stimulation experiments were recorded as 90 second files. External stimulation was initiated 30 seconds after the start of recording. Frequencies of 0.5Hz, 1Hz, 1.5Hz and 2Hz were studied in the presence or absence of isoprenaline.

For spontaneous activity recordings, similar conditions were used but without external stimulation. Drug perfusion was started at 30 seconds after the start of recording. A 2 minute Tyrode's wash out period was given in between recordings.

2.4.6 Data analysis - SALVO

Data analysis was done using SALVO (Synchronization, Amplitude, Length and Variability of Oscillation) software. This program allows decoding the spatiotemporal patterning of Ca^{2+} oscillations within individual cells and across multicellular populations (Lewis et al.,2014). This specialized software outputs thirty parameters that describe Ca^{2+} signal organization.

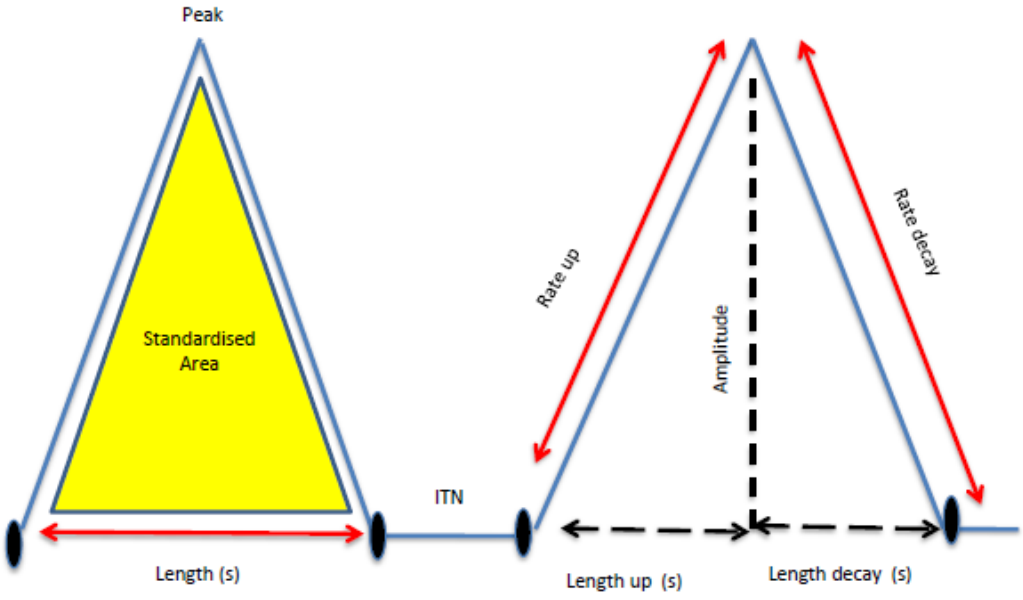

Figure 2.14* – Ca^{2+} *transient parameters - *Schematic showing some of the Ca^{2+} transient kinetic parameters monitored in this project.*

For Ca^{2+} transient characterisation (Chapter 4) the following parameters were analysed: peak regularity, inter transient noise (ITN), height (amplitude), length (duration), standardised area, rate (Hz), rate up, length up, rate decay and length decay.

For Ca^{2+} transient study and validation of *in vitro* disease modelling (Chapter 5) the following parameters were analysed: peak regularity, ITN (total), height (amplitude), standardised area, rate (Hz) and rate decay.

Peaks and valleys used to analyse data in SALVO were taken from full length (90 seconds) traces.

SALVO output parameters definition, used in this study:

Peak regularity *Standard deviation of the distance between the transient peaks.* If the ROI is perfectly regular, with each transient peak occurring exactly the same space apart, this will return zero.

ITN (total) *Intertransient noise*. Sum of the absolute point to point difference in intensity of the sections of the trace between transients. In non-oscillating ROIs, this covers the entire trace. Calculated between start and stop.

Height (Amplitude) *Average height of the ROI's transients.* Averaged across all transients in the ROI. Height of a single transient is calculated as the difference between the maximum peak point and the valley at the start of the transient, divided by the start valley (all using intensity values.

Length (Duration) *Average length of the ROI's transients.* Averaged across all transients in the ROI. Length of a transient is calculated as the difference between the ending valley and the starting valley (time in seconds).

Standardised Area *Average standardised area of the ROI's transients.* Averaged across all transients in the ROI. Standardised area of a transient is calculated using the trapezoid method to find the area under the curve and bounded by the start and finish valleys and the maximum peak point, divided by the intensity of the starting valley.

Rate (Hz) *Rate of oscillation of ROI in Hz.* Transients per second. Calculated by the number of transients in the ROI divided by the length of the ROI.

Rate up *Average rate of increase to peak of transient.* Averaged across all transients in the ROI. Rate up for a transient is calculated by the difference between the intensity of the first peak point and the first valley point of a transient, divided by the time between the two points**.**

Length up *Average time to increase to peak of transient.* Averaged across all transients in the ROI. Length up for a transient is calculated by the difference between the time of the first peak point and the first valley point of a transient.

Rate decay *Average rate of decrease back to baseline of transient.* Averaged across all transients in the ROI. Rate decay for a transient is calculated by the difference between the intensity of the ending valley point and the first peak point of a transient, divided by the time between the two points.

Length decay *Average time to decrease back to baseline of transient.* Averaged across all transients in the ROI. Length decay for a transient is calculated by the difference between the time of the ending valley point and the first peak point of a transient.

2.4.6.1 Data analysis and presentation

Data obtained from SALVO were organised in tables using Microsoft Excel. Graphs produced from data obtained from SALVO analysis were made using Graphpad Prism version 5.00 for Windows, GraphPad Software, La Jolla, CA, USA.

When no units are mentioned in presented graphs arbitrary units (AU) were used.

2.5 Statistical analysis

Analysis of data obtained from patch clamp experiments was performed in Microsoft Excel and GraphPad Prism version 5.00 (GraphPad Software, La Jolla, CA, USA).

Normal distribution of data sets was obtained with the D'Agostino-Pearson algorithm, and normally distributed data columns were analysed with two-tailed Student's paired or unpaired *t*-test if data sets were paired or unpaired respectively. Mann-Whitney tests were used for data sets that were not normally distributed.

When comparing multiple columns a repeated measures ANOVA with a Bonferroni Post test was used. If the data sets were not normally distributed, a Friedman statistical test was used, with a Dunn's Post Test.

Data is presented as mean ± standard error (SE) with 95% confidence interval. Statistical significance was considered for p value ≤ 0.05 (*, $p \leq 0.05$, **,$p \leq 0.01$, ***, $p \leq 0.001$).

Chapter 3

hiPSC derived CM Ca^{2+} handling protein detection and imaging

3.1 Introduction

3.1.1 Cardiac Ca^{2+} handling proteins

The mammalian CM is a cell with unique features and a protein expression profile necessary to facilitate the normal function of the heart. EC-coupling is the mechanism that allows the CM to contract. It starts as an electrical phenomenon leading to mechanical contraction. The rapid depolarization of the cell due to a Na^{+} influx activates LTCC and subsequent Ca^{2+} influx, triggering Ca^{2+} release from the SR via RyR2. Troponin T is then stimulated by Ca^{2+} and myofibres contract, leading to CM contraction.

In addition to LTCC and RyR2, other proteins play pivotal roles in maintaining Ca^{2+} homeostasis, including SERCA2A (by re-uptaking cytosolic Ca^{2+}) and PLB (by stopping SERCA2A inhibition when phosphorylated). Other proteins, such as CASQ2 bind to Ca^{2+}, storing this ion inside the SR, while TDN and JCN have an accessory role close to RyR2 in the SR.

Protein expression and detection techniques were used in this project in order to determine a preliminary Ca^{2+} handling profile for control and mutant hiPSC CM. WB and ICC were used in both cell types.

Other methods can measure indirect protein expression but were not used in this project. Collection of mRNA from beating clusters could determine if these cells had the capacity to express these proteins but would fail to determine if they had been expressed and if they were located in the appropriate sub-cellular space.

3.1.2 hPSC - Human pluripotent stem cells

Several publications report protein detection in hPSC, (for both hESC and hiPSC) using WB and ICC. One of the first publications to present detection of cardiac marker proteins using ICC was by He et al., 2003. Detection of hERG, HCN4 (responsible for the "funny" current) and LTCC was reported in hESC derived CM.

Absence of CASQ2 and PLB in hESC was reported by Binah et al., 2007. These authors found that although NCX, SERCA2A and α-actinin were detected by WB, neither CASQ2 nor PLB was found to be expressed in hESC CM.

In 2010, Asp et al., used ICC to report, not only cardiac markers but some ion channel expression and location such as hERG, HCN4 and LTCC.

Similar findings to those reported for hESC derived CM were found in the literature regarding hiPSC CM. Zhang et al., 2009 used ICC to detect sarcomeric organisation in hiPSC, namely α-actinin, myosin light chain (MLC) and troponin C. Gupta et al., 2010 used ICC and detected both troponin C and α-actinin as CM differentiation markers in a study comparing hESC and hiPSC protein expression profiles.

Although some authors report protein detection of CM markers, no publications were found with detailed and extensive results for protein expression using specifically WB. Gupta et al., 2010 present an extensive study regarding hiPSC and hESC CM mRNA expression but not confirmation that coded proteins are present in the cells.

3.1.3 hiPSC CPVT CM

Protein detection and profiling has been reported by other authors in hiPSC CPVT CM. Ca^{2+} handling protein detection with WB was not a technique of choice for the majority of CPVT CM reports. ICC was presented by most authors to characterise not only hiPSC derived CM but especially to characterise hiPSC for pluripotency markers. Kujala et al., 2012 report the use of ICC in CPVT CM, detecting troponin T and α-actinin (as CM markers). Detection of connexin 43 as a functional syncytial marker was also reported. Pluripotency profile with ICC for Nanog, Oct 4, TRA1-60 and SSEA4, was reported in hiPSC characterisation.

Two other authors, Itzhaki et al., 2012 and Fatima et al., 2011 detected the same pluripotency markers in hiPSC (namely Nanog, Oct4, TRA1-60 and SSEA4) with ICC, as well as CM markers, such as α-actinin and RyR2.

In the current project, SDS-PAGE followed by WB was used to detect CASQ2, SERCA2A, RyR2 and PLB. These were considered the most relevant proteins in CM Ca^{2+} handling and samples were obtained from CPVT patient fibroblasts, CPVT hiPSC and CPVT EBs at day 4 (d4) and EBs post differentiation day 15.

A small study of ICC was also used to detect the presence of Troponin I and RyR2 in hiPSC CPVT CM in order to evaluate if these cells presented a classical differentiation CM marker and to detect RyR2 presence and distribution.

3.2 Methods

For methods details, please refer to Chapter 2, section 2.2 (ICC and protein detection).

3.3 Results

The detection of Ca^{2+} handling proteins within hiPSC CM is important to understand their Ca^{2+} handling capacity. Establishing when these proteins are expressed during the cardiac developmental process is also essential to the characterisation of both BT1 and CPVT derived CM as these are pivotal to physiological cardiac responses such as positive inotropy and lusitropy. Due to the foetal nature of hiPSC derived CM, a protein detection and localisation study was undertaken.

Immunocytochemistry (ICC) was used to observe RyR2 and Troponin I distribution and location using specific primary antibodies that bind to target protein. Primary antibodies can then be targeted by a secondary labelled antibody enabling visualization of sub-cellular proteins distribution. This technique was applied in both CPVT and BT1 hiPSC CM previously used in patch clamp experiments (figure 3.1). Control CM stained positive for Troponin I and presented some binucleated cells. ICC was not repeated in mutant cells due to time constraints. For the same reason ICC for CASQ, PLB and SERCA2A were not performed. RyR2 positive staining was observed in both hiPSC BT1 and CPVT CM with similar distribution in the cytosol and perinuclear region.

The Western Blot (WB) technique was used for SERCA2A (figure 3.3), RyR2 (figure 3.2), CASQ (figure 3.5) and PLB (figure 3.4) detection as it's suitable to separate and detect minimal presence of proteins, given that the amount of available tissue was limited. The absence of CASQ, SERCA2A and PLB detection in WB experiments for lysates of different cells and differentiation stages, suggests that these cells could still be immature. RyR2 could not be detected by WB in EBs day 15 post differentiation due to small sample of available EBs. These results suggest that these cells did not present the expected Ca^{2+} handling protein profile of adult CMs.

3.3.1 Immunocytochemistry

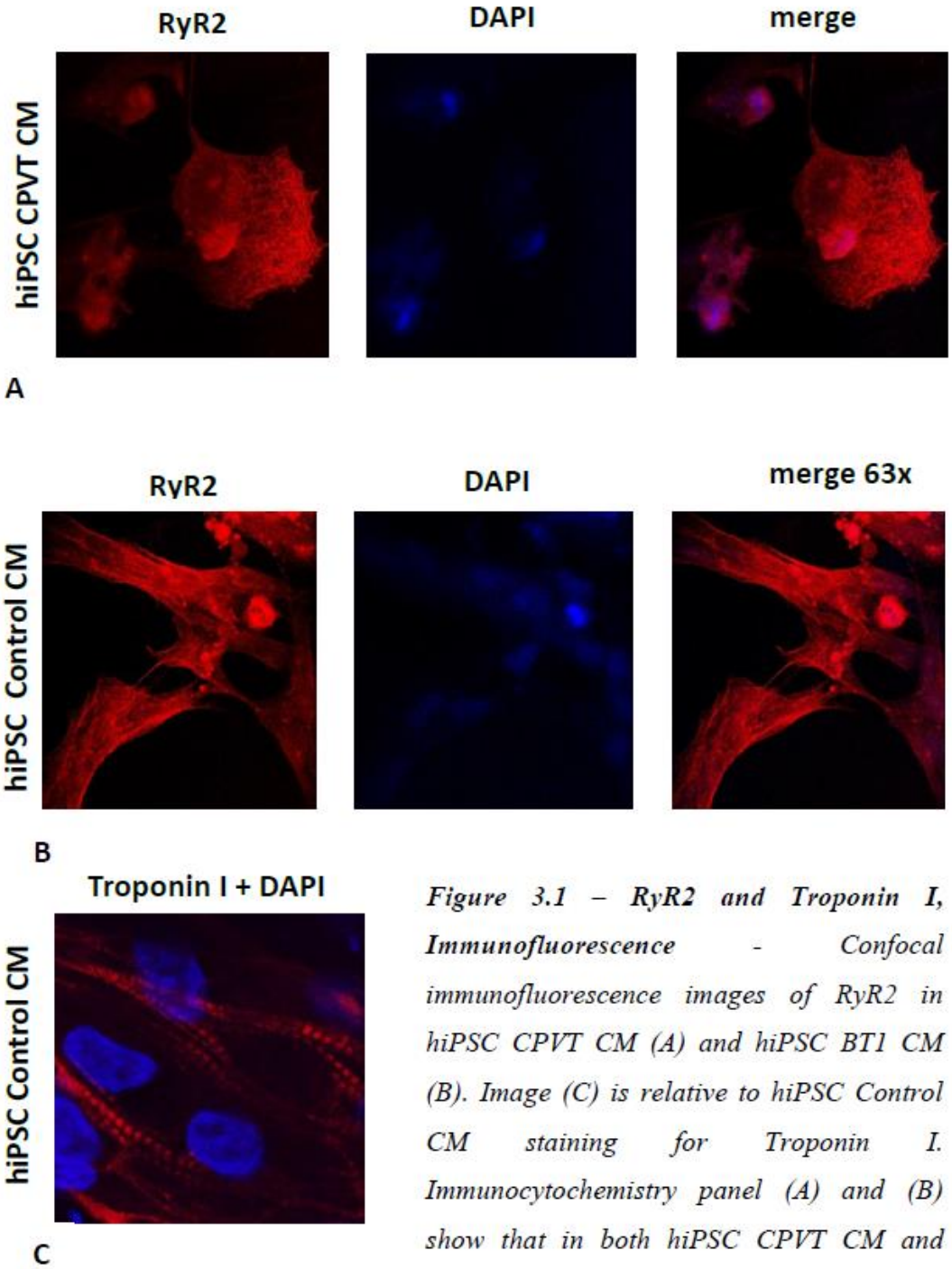

*Figure 3.1 – **RyR2 and Troponin I, Immunofluorescence** - Confocal immunofluorescence images of RyR2 in hiPSC CPVT CM (A) and hiPSC BT1 CM (B). Image (C) is relative to hiPSC Control CM staining for Troponin I. Immunocytochemistry panel (A) and (B) show that in both hiPSC CPVT CM and hiPSC BT1 CM, RyR2 seems to be similarly distributed in the perinuclear region and cytosol. Image (C) presents striations and positive staining for Troponin I in control hiPSC CM, as well double nuclei in one of the cells.*

3.3.2 Western blot protein detection

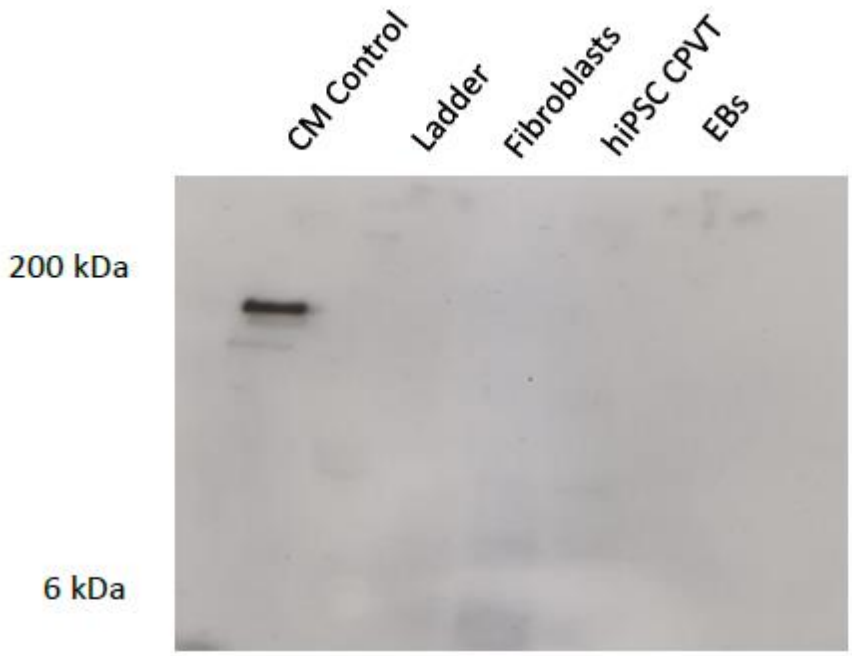

Figure 3.2 – Western Blot, SDS-PAGE for RyR2 – *Representative blot from RyR2 detection with SDS – PAGE and HRP chemiluminescence. Samples obtained from fibroblasts from a CPVT patient, hiPSC CPVT and EBs d4. Control well was dubious for RyR2 detection as blot was not close to expected MW. Possibly only RyR2 proteolysis products containing the epitope were present, explaining the less than expected MW of the proteins detected. No RyR2 (or proteolysis products) were detected in any of the samples, as expected. The quantity of material was not enough to proceed with detection of EBs d15.*

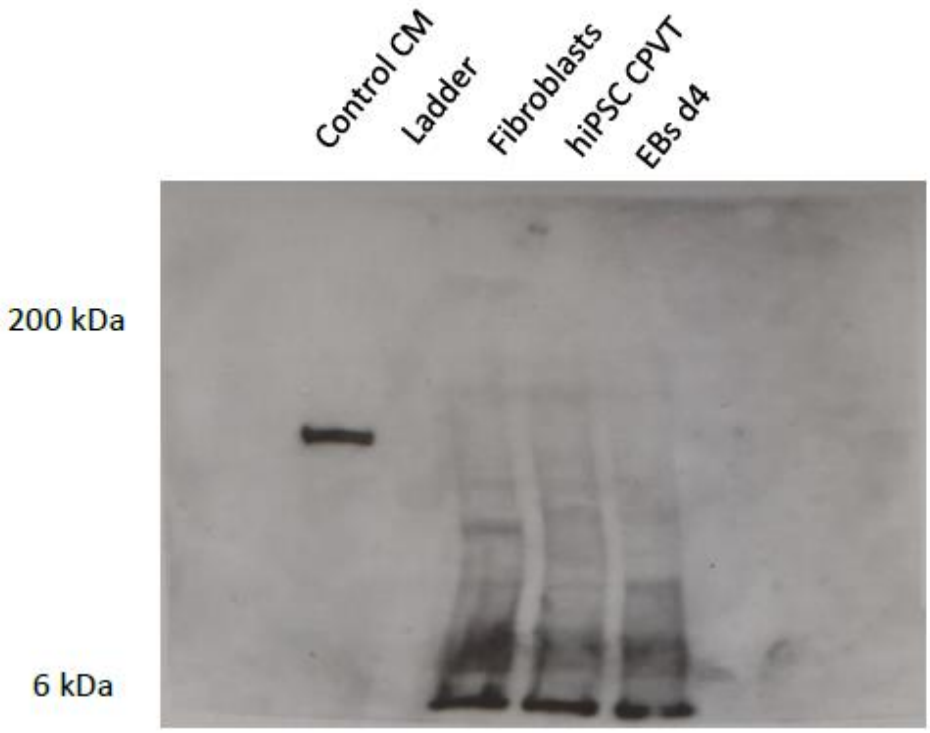

Figure 3.3 – Western Blot, SDS-PAGE for SERCA2A ATPase – *Representative blots from SERCA2A ATPase detection with SDS – PAGE and HRP chemiluminescence. Samples obtained from fibroblasts from a CPVT patient, hiPSC CPVT and EBs d4. This blot does not present a positive detection of SERCA2A in CPVT patient fibroblasts, CPVT hiPSC and EBs d4. It may however present positive SERCA2A proteolysis products close to the 6kDa range. The quantity of material was not enough to proceed with detection of EBs d15. Guinea pig control lysate also presented positive detection of SERCA2A ATPase.*

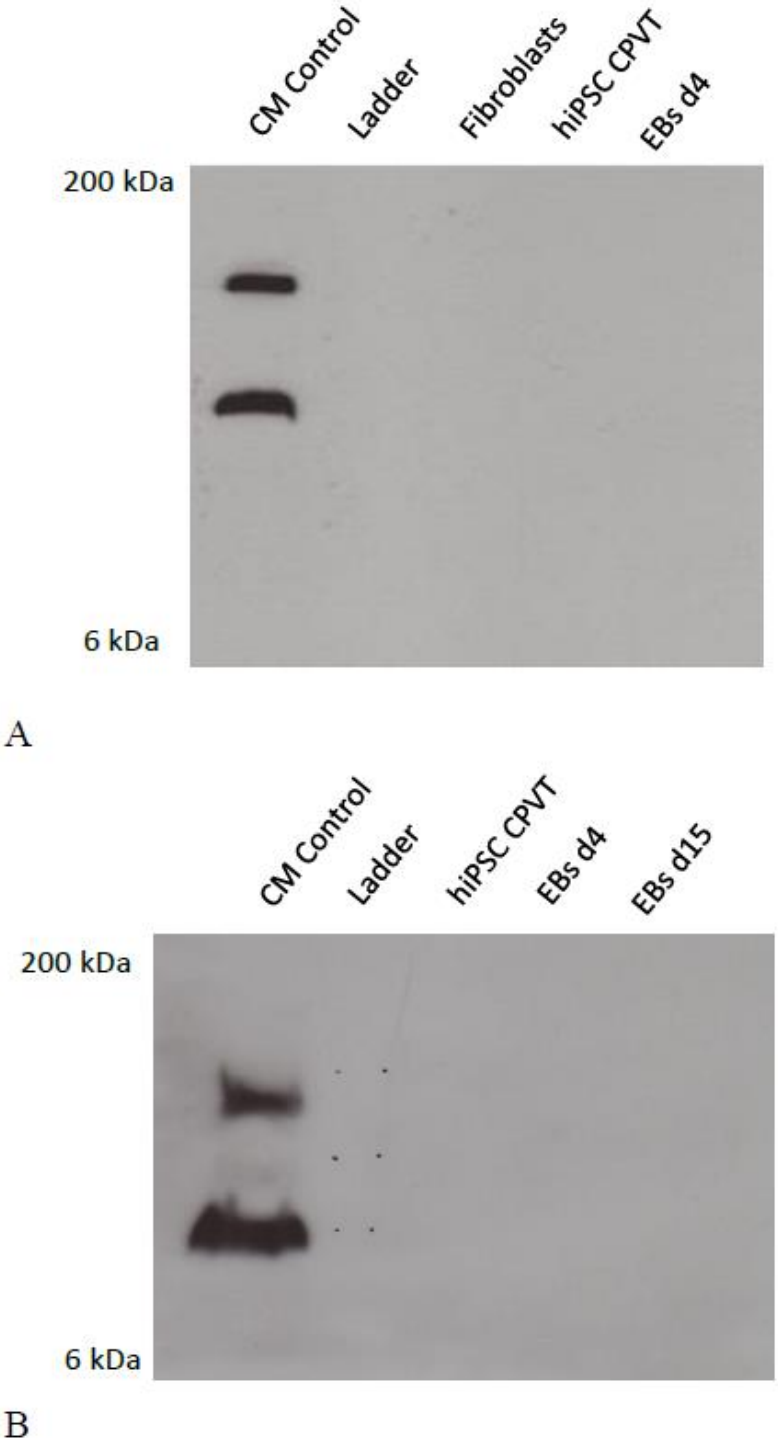

Figure 3.4 – Western Blot, SDS-PAGE for PLB – *Representative blots from PLB detection with SDS – PAGE and HRP chemiluminescence in two different experiments (A and B). Samples obtained from fibroblasts from a CPVT patient, hiPSC CPVT CM and EB d4 (A) and CPVT CM, EBs d4 and EBs d15 (B). Control well was positive for PLB detection (monomer and pentamer) in both experiments, but no PLB was detected in CPVT patient fibroblasts or CPVT hiPSC. Lysates from d4 EBs and d15 EBs were also negative for PLB detection.*

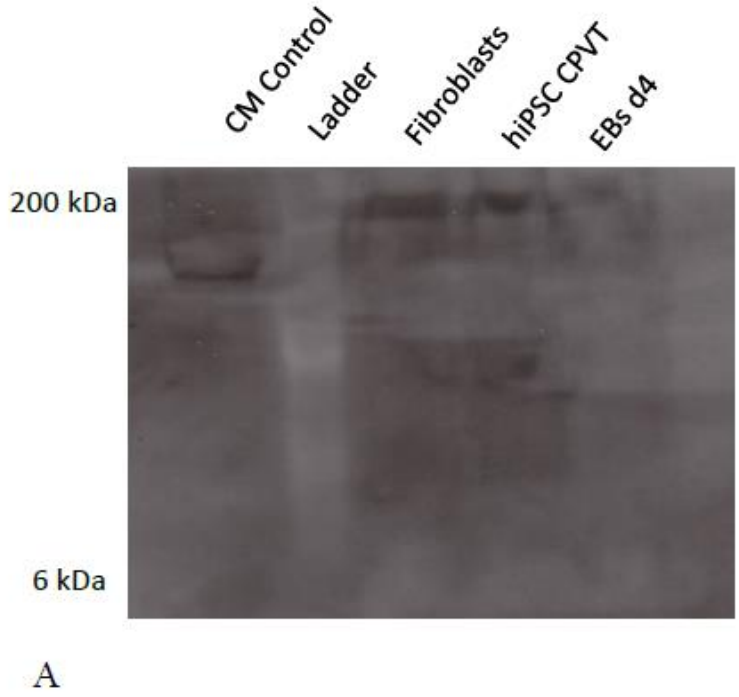

A

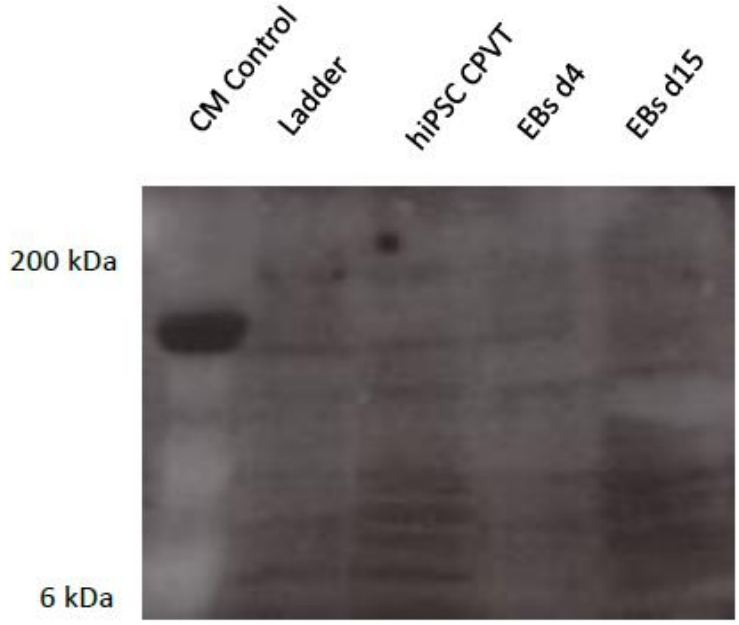

B

Figure 3.5 – Western Blot, SDS-PAGE for CASQ – *Representative blots from CASQ detection with SDS – PAGE and HRP chemiluminescence in two different experiments (A and B). Samples from fibroblasts from a CPVT patient, hiPSC CPVT CM and EBs d4 (A) and CPVT CM, EBs d4 and EBs d15 (B). Control well seems to be positive for CASQ detection although more marked in (B). No CASQ was detected in CPVT patient fibroblasts or CPVT hiPSC. Lysates from d4 EBs and d15 EBs were also negative for CASQ detection.*

3.4 Discussion

By using ICC and WB techniques, a preliminary Ca^{2+} handling protein profile was established for hiPSC CPVT CM with the mutation studied in the current project.

Repeating WB similar experiments in more mature hiPSC CPVT CM (3-4 months EB maturation) could help to determine if the absence of SERCA2A, CASQ, PLB and RyR2 was related to CM immaturity or to a trafficking defect. This last possibility would not be expected in this CPVT mutation. WB repetition was limited due to lack of abundant sample protein due to the difficulty in obtaining hiPSC CM from both control and mutant cells.

Jung et al., 2012 report that in CPVT CM matured by 2 months no CASQ2 or PLB were detected by WB, but in more mature cells with 3-4 months post terminal cardiac differentiation these authors found expression and detection of RyR2, CASQ2, PLB, TDN and JCN. In the same report, ICC revealed RyR2 with similar distribution on cytosol and perinuclear region, co-localised with myofilaments in CPVT CM. Using this last technique Jung et al., revealed that cluster density for RyR2 was similar in both mutant and control CM, suggesting that the particular mutation of CPVT CM was not a trafficking defect.

Other authors, Di Pasquale et at., 2013 detected RyR2 expression by WB in both control and CPVT CM (1-3 months post differentiation) beating clusters using human foetal CM as controls which supports the suggestion that older, more mature, EBs may express RyR2 that seems to be absent in hiPSC CM with less than 1 month post-differentiation.

In this project, both control and CPVT hiPSC CM, used in ICC experiments were more mature (1-2 months post differentiation) than the ones used in WB (1 month differentiation). This fact could explain why staining was positive for RyR2 in both CPVT and BT1 CM. Troponin I was also present in striations in control hiPSC CM (1-2 months post differentiation), indicating that cardiogenesis maturity is marked in this batch of cells. A mature cardiac feature is also evident in this image (figure 3.1C), in which a cell presents two nuclei, a typical characteristic of adult CM.

Detection of SERCA2A ATPase was negative for all the screened cell types. However, this protein detection was expected in early embryonic stages in most cell types. It is possible than some SERCA2A proteolytic fragments of the protein full length were

present and separated with SDS-PAGE (figure 3.3). Additional experiments could determine the presence of this protein in d15 EBs, but due to time constraints and lack of lysate sample this experiment could not be repeated.

According to published results for the detection of Ca^{2+} handling proteins by WB and in accordance with results obtained in this project, a study with more mature hiPSC CM could confirm if cardiogenesis and Ca^{2+} handling associated protein expression increases with maturation.

Ideally, ICC should be done to detect the presence and distribution of other proteins screened with WB (CASQ, SERCA2A and PLB). Due to time constraints such experiments could not be done.

3.5 Conclusion

The Ca^{2+} handling protein profile of hiPSC CM used in the reported experiments is more suggestive of a foetal CM for these cells. Essential Ca^{2+} handling proteins, namely CASQ, SERCA2A and PLB seem to be absent from early stage maturation hiPSC CPVT EBs. PLB and CASQ2 absence is characteristic of immature CM as these proteins are pivotal in classical cardiac response, such as positive inotropy and lusitropy. RyR2 detection could not be assessed in differentiated cells (EB day 15), due to the low number of cells available. Sensitivity of the protocol used for WB can also be related with the negative results in the selected proteins detection. New experiments with higher protein concentration present in the lysates, could determine if this was the case. However, small amounts of available material limited the sample size used for this set of experiments. Although RyR2 was not obviously detected with WB, ICC indicated expression of RyR2. A maturation time point study for detection of post differentiated hiPSC CM would aid in the understanding of differentiation and maturation of hiPSC CM. If hiPSC are to be used to recapitulate disease *in vitro*, they should ideally have a completely functional CICR and EC-coupling.

Chapter 4

hiPSC derived CM functional characterisation

4.1 Introduction

The cardiac muscle cell is unique from a physiological point of view, regarding its AP and Ca^{2+} handling properties. Excitation-Contraction (EC) - coupling is the process that starts with the electrical event of depolarization of the CM and that culminates in mechanical activity with the contraction of the cell. The initial electrical depolarization via I_{Na} will sequentially activate $I_{L\text{-}Ca}$ creating a Ca^{2+} ion influx into the cell sarcoplasm. In CM this influx will trigger CICR (Calcium Induced Calcium Release) by opening the ryanodine type 2 receptor (RyR2). This receptor is imbedded in the sarcoplasmic reticulum (SR), allowing Ca^{2+} stores in the SR to be released into the sarcoplasm, triggering contraction of myofibers by troponin C.. During the relaxation phase, SR Ca^{2+} release is terminated, and the released Ca^{2+} is recycled into the SR by the SR Ca^{2+}-ATPase (SERCA) or extruded from the cell by the Na^{+}/Ca^{2+}exchanger (NCX). These events will effectively lower the cytosolic Ca^{2+} concentration and allow Ca^{2+} dissociation from the myofilaments and muscle relaxation.

The advent of hiPSC technology, coupled with advances in cardiac differentiation protocols, has provided a potential, more accessible model of the human cardiac muscle cell. Some published studies (Itzhaki et al., 2010; Matsa et al., 2011; Malan et al., 2011; Jung et al., 2012; Fatima et al., 2012) suggest a very promising use for these cells as *in vitro* models of disease. In these publications, functional assessment and experimental methodological heterogeneity raise some questions regarding these cell's physiology. Hence these cells need to be properly characterised before rigorous and accurate translational applications can be made.

All mutant cells in this project were hiPSC derived CM from a CPVT1 patient. This patient carried the RyR2 mutation S2246L in the central domain of the receptor. CM were made from a healthy subject and used as control (BT1 CM). AP characterisation for both control and CPVT hiPSC derived CM was performed using the patch clamp technique.

The study of CM Ca^{2+} handling physiology is also pivotal to do a functional characterisation of these cells. Three of the main defining properties of adult CM (positive inotropy, chronotropy and lusitropy in the presence of ß-agonists) should be present if hiPSC CM are to be compared to adult human CM. Current existing reports for both beating clusters (Dolnikov et al., 2005; Binah et al., 2007) or single cells

(Mummery et al., 2003; Liu et al., 2009; Fu et al., 2010) present inconsistent methodology and divergent results.

In this project Ca^{2+} imaging of single CM, was used to characterise functional Ca^{2+} handling in both mutant and control CM.

E-C coupling has been well documented in several adult mammalian species, including in human CM. However, there are still diverging reports regarding some of the proteins involved and the physiological characterisation of hiPSC CM. Therefore, before testing CPVT hiPSC derived CM as an *in vitro* model of disease, it was essential to characterise the cells used in this study. This characterisation should allow a better understanding of the physiology and maturity stage of these cells, playing a pivotal role in their use, by determining their functional profile.

4.2 Electrophysiology characterisation

The first functional characterisation of spontaneously contracting hiPSC derived CM was reported in 2009 by Zhang et al. Since then hiPSC derived CM, similar to hESC derived CM, have been demonstrated (Gupta et al., 2010). Basic parameters of the CM AP such as RMP, amplitude, time to peak, APD50 and APD90, have been recorded from several hiPSC derived CM cell lines, with very similar results (table 4.1). This similarity was also verified for individual currents such as $I_{(Na)}$, $I_{(K)}$, $I_{(to)}$, $I_{(Ca,L)}$ that have been well characterised by several authors for both hESC (Jian Qiang-He et al., 2003; Kehat et al., 2001) and hiPSC derived CM (Honda et al., 2011; Ma et al.,2011).

The cardiac AP is the basic electrophysiological signature of the cardiac muscle cell. It is the resulting sum of the coordinated ion channel currents, namely $I_{(Na)}$, $I_{(Ca,L)}$, $I_{(K)}$ and $I_{(to)}$. It is also the primary event in the E-C coupling process that starts with an electrical event and ends in a mechanical contraction of the cardiac cell. The RMP of an adult human CM is approximately -80mV in ventricular and atrial cells, while pace-maker cells tend to have a resting membrane potential of about -50 mV. Several authors (Zhang et al., 2009; Ma et al., 2011; Lahti et al., 2012) report that most hiPSC derived CM have a less negative RMP than the adult cells, suggesting a more foetal-like phenotype.

The AP characterisation and shape, allows the classification of these cells in to three different main sub-types: nodal-like, atrial-like and ventricular-like.

Cell type	BPM	APD_{90} (ms)	dv/dt_{max} (V/s)	APA (mV)	MDP/RMP (mV)	Exp. conditions	References
iPSC-CM V IMR90C4	43.8 ± 2.7	320.1 ± 17	40.5 ± 4.6	87.7 ± 2.6	−63.5 ± 1.7	37°C, me LJP: corr.	Zhang et al., 2009
iPSC-CM V ForeskinC1	44.2 ± 3.5	312.5 ± 11.2	27.2 ± 3.7	87.9 ± 2.4	−63.3 ± 1.5	37°C, me LJP: corr.	Zhang et al., 2009
iPSC-CM V	68.2 ± 2.7	381.3 ± 35.3	9 ± 0.2	107.8 ± 2.1	−63.5 ± 2.1	35°C, wc LJP:nk	Moretti et al., 2010
iPSC-CM V	72 ± 1.2	314.4 ± 17.6	26.8 ± 6.3	113.2 ± 2.4	−63.4 ± 1.3	36°C, pp LJP: nk	Lahti et al., 2012
iPSC-CM V	35.5 ± 2.1	414.7 ± 21.8	27.8 ± 4.8	101.5 ± 2.5	−75.6 ± 1.2	35–37°C pp, LJP: nk	Ma et al., 2011
iPSC-CM V	28 ± 5	495 ± 36	9.5 ± 1.8	109 ± 3	−57 ± 1	32°C, wc LJP: nk	Itzhaki et al., 2011a
iPSC-CM* ns	60	173.5 ± 12.2	115.7 ± 18.4	106 ± 3.2	−72.4 ± 0.9	37°C, pp LJP: corr	Davis et al., 2012
hESC-CM V	47.1 ± 23.3	247.2 ± 66.7	13.2 ± 6.2	85.4 ± 9.3	−53.9 ± 8.6	37°C, me LJP: nk	He et al., 2003
hESC-CM V		285.8 ± 52.6	11.4 ± 2.8	86.8 ± 52.6	−62.3 ± 8.6	rt, wc LJP: nk	Zhang et al., 2011
VM*	50	213 ± 7	215 ± 33	106.7 ± 1.4	−81.8 ± 3.3	37°C, wc LJP: nk	Magyar et al., 2000
VM endo*	60	330 ± 16	234 ± 28	105 ± 2	−87.1 ± 1	37°C, wc LJP: nk	Drouin et al., 1998
VM epi*	60	351 ± 14	228 ± 11	104 ± 2	−86 ± 1	37°C, wc LJP: nk	Drouin et al., 1998

*iPS-CM V, iPS-CM of ventricular-like phenotype; iPS-CM ns, not specified to action potential type; VM, native human ventricular myocyte; endo, endocardial; epi, epicardial; BPM, beats per minute; APD_{90}, action potential duration at 90% of repolarization; dV/dt_{max}, maximal upstroke velocity; APA, action potential amplitude; MDP, maximum diastolic potential; RMP, resting membrane potential; *, non spontaneous beating cells; hESC-CM V, hESC-CM of ventricular-like phenotype; me, micro electrode; wc, whole cell patch-clamp configuration; ljp: corr, corrected for liquid junction potential; ljp:nk, not known if corrected for liquid junction potential; rt, room temperature.*

Table 4.1 - AP parameter characteristics in hiPSC and human ventricular cardiomyocytes *(Hoekstra et al., 2012.*

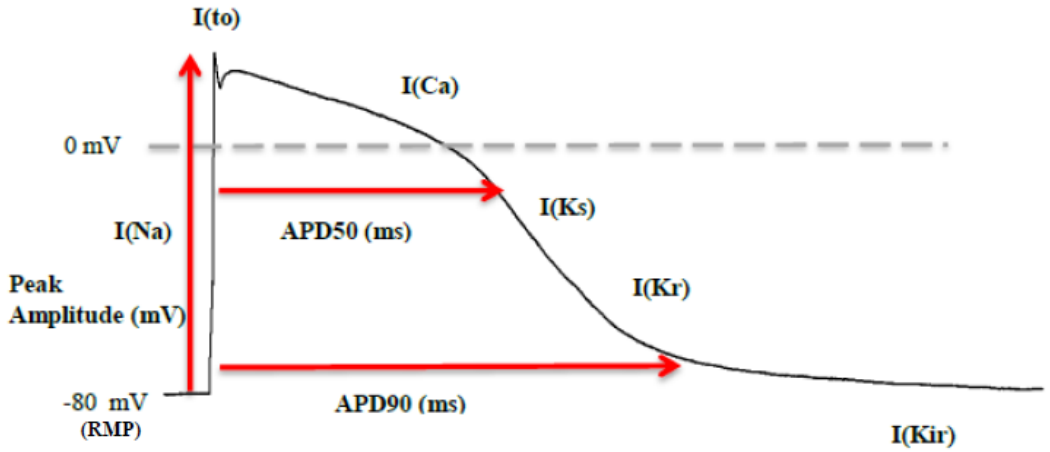

Figure 4.1 –Human ventricular cardiac AP *- Example trace of a cardiac ventricular AP from and adult human CM with electrophysiology parameters diagram and involved electrical currents.*

The ß-adrenergic response of these cells is essential to functionally characterise CM physiology. Pace-maker cardiac cells should have a positive chronotropic response to

isoprenaline. This effect in pace-maker cells will then control atrial and ventricular CM. These last two CM sub-types are quiescent in the adult heart and contraction is controlled by the pace-maker CM.
In contrast to what is seen in adult CM, positive chronotropy can also be observed in both atrial and ventricular-like hiPSC derived CM (Zhang et al., 2009). This observation is possibly due to the foetal nature of these cells. Positive chronotropy is nonetheless a marker of ß-adrenergic response and is relevant to functional characterisation in hiPSC derived CM.

Chen et al.,(1979); report that the ß-adrenergic chronotropic response of the foetal mammalian heart increases in the third gestational period due to 3 possible factors: 1) receptor density increase, 2) receptor affinity increase and 3) maturation of other molecules and coupling mechanisms. This can explain why in different studies with different maturation times and cell lines, different chronotropic responses have been observed.

In the present study, a detailed characterisation of individual currents was not performed. Functional properties of I_{Na}, I_{to}, $I_{Ca,L}$ and I_K have been well established in the literature for hESC (Maltsev et al.,1994) and hiPSC derived CM (Honda et al., 2011; Ma et al., 2011). The focus of this project was the AP due to the fact that the arrhythmic hallmark of CPVT (DAD) is obtained from the full AP trace.

4.2.1 Methods

For more detailed methods used for electrophysiology, please refer to section 2.3 from Chapter 2.

For this project, both control BT-1 hiPSC and hiPSC CPVT derived CM were patch clamped in the whole-cell mode. Perforated patch was not performed because despite several attempts and recordings, whole cell access wasn't obtained consistently.

Spontaneous activity recordings were obtained using a Gap Free mode protocol. In this protocol no current or voltage is injected into the cell. The reading is recorded as presented by the CM and the RMP is not clamped.

Induced AP were obtained from both quiescent and spontaneous CM, by pacing hiPSC at 0.5Hz and 1Hz, using a 3ms step protocol in Current Clamp mode injecting a single pulse of 500pA. Before obtaining any recordings, RMP was clamped at circa -80mV.

By lowering the resting membrane potential of these cells close to -80mV, a more physiological and standardised RMP was obtained. Inhibition of the funny current $I_{(f)}$ was achieved, preventing spontaneous activity driven by this current.

An average of five consecutive AP within the second half of a minimum of a one minute recording was used for AP analysis. Isoprenaline perfusion (1µM) was made one minute after normal Tyrode's perfusion as a washout procedure.

4.2.2 Results

The objective of the work presented in this chapter, was to characterise hiPSC derived CM AP electrophysiology for both spontaneous and evoked activity models. This was achieved by using the patch clamp technique in both CM cell lines (CPVT and BT-1) in order to define AP parameters and ß-agonist response. Using AP electrophysiology data the predominant CM sub-type can also be suggested. This last classification is relevant, since CPVT is based in ventricular tachycardia episodes. Several parameters were obtained from AP recordings, but particular relevance was given to RMP, APD50, APD90, peak and amplitude. A study of force-frequency relation is also presented since in adult human CM a positive force-frequency relation is observed.

4.2.2.1 Spontaneous APs

The majority of current hiPSC derived CM differentiation protocols are based on the embryoid body technique. This technique has spontaneous contractile activity of the beating cluster as a terminal differentiation endpoint. This is both the benefit and the curse of hiPSC derived CM as ideally, only pace-maker cells should have spontaneous contractility. Atrial and ventricular cells should be quiescent. Because spontaneous beating CMs are visually contracting, they can be easily selected for analysis. Ideally analysed CM should be quiescent with a ventricular phenotype as spontaneously active cells may give false positives for certain pro-arrhythmic events. An ideal differentiation protocol would produce different subtypes of CM according to required needs but such a protocol is still not currently available.

Comparison of the responses of hiPSC CPVT CM and control BT1 cells to isoprenaline perfusion did not reveal any significant changes (figure 4.2A, C) for RMP and AP peak. A significantly lower RMP in Tyrode's was observed in CPVT CM, when compared to BT1 CM (figure 4.2A). BT1 CM have a RMP of approximately -60 mV, still far from the physiological -80mV of adult human CM. A significantly higher (10%) AP peak was observed in CPVT CM comparing to BT1 CM in Tyrode's (figure 4.2C).

A significant lower RMP was observed in spontaneous BT1 CM compared with spontaneous CPVT CM (figure 4.3A). Spontaneous beating CPVT CM and BT1 CM also presented a significantly lower RMP compared with the same cells if quiescent (figure 4.3A).

It was found that BT1 CM had a significantly higher beating rate, when perfused in Tyrode's only, compared with CPVT CM (figure 4.4C). A positive chronotropic effect (figure 4.4D) was observed only in CPVT CM with 23% BPM average increase.

Regarding APD, the main finding was that in Tyrode's, both APD50 (figure 4.5A) and APD90 (figure 4.5C) were longer for hiPSC CPVT CM compared with control CM.

Our results show that isoprenaline has a positive chronotropic effect in the studied CPVT CM, contrary to what other authors have found for in CPVT CM with different mutations.

The number of cells with spontaneous contractile activity was higher than the percentage of quiescent cells, in CPVT CM compared to control BT1 CM (figure 4.7). A similar comparison was not found in published literature.

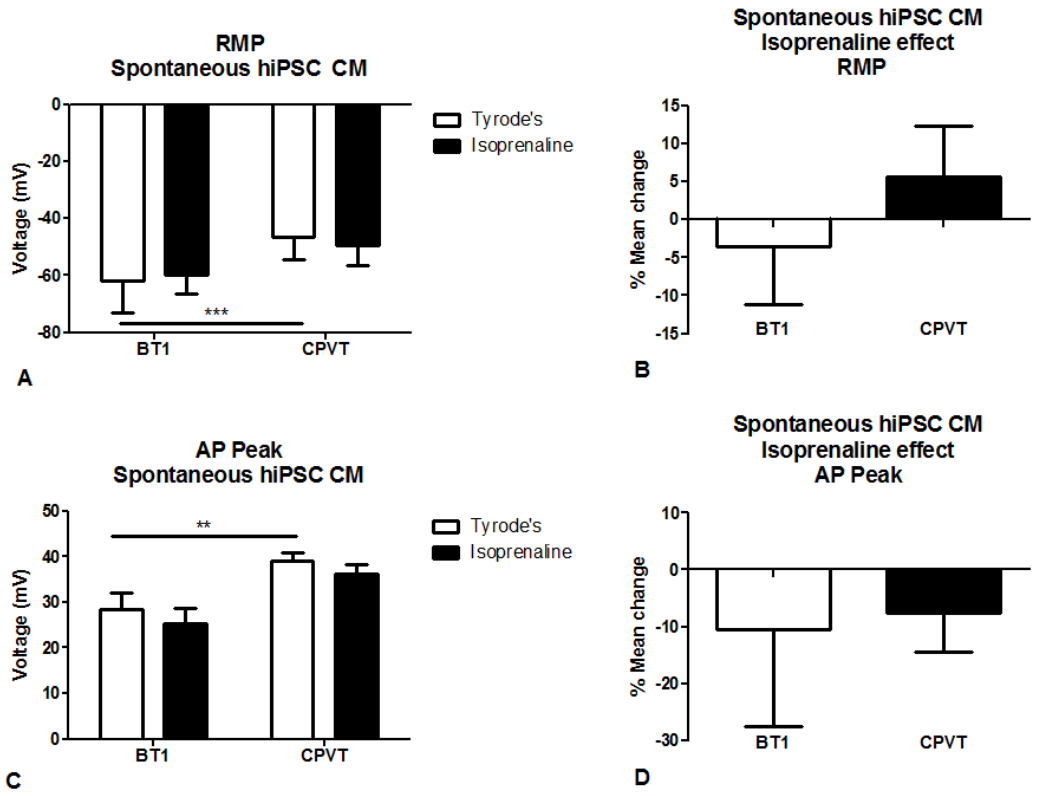

Figure 4.2 - Spontaneous beating, AP parameter comparison, RMP and AP peak *- hiPSC CPVT CM (n=21 from 5 batches) and hiPSC control BT1 CM (n=10 from 3 batches) in Tyrode's and in the presence of isoprenaline (1µM). AP peak (A) and RMP (C), with respective percentage mean difference for isoprenaline effect on RMP (B) and AP Peak (D).*

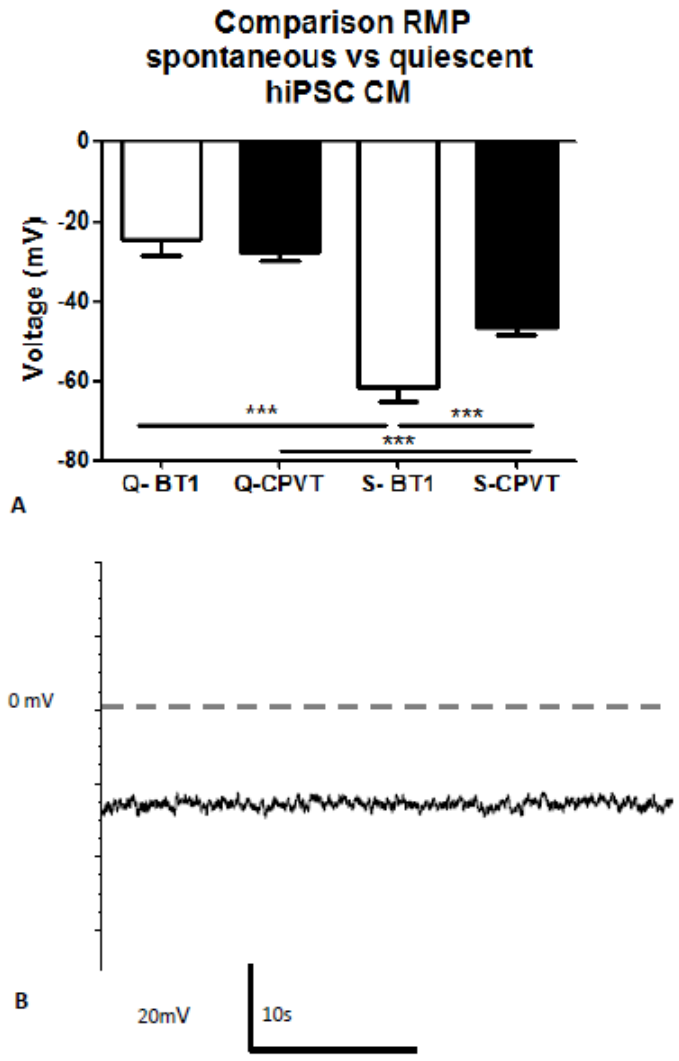

Figure 4.3 – Average RMP from Gap Free protocols in hiPSC CM - *figure showing average RMP obtained using Gap Free protocol in quiescent (Q-BT1 and Q-CPVT) and spontaneous (S-BT1 and S-CPVT) hiPSC CM. Example trace of RMP in a quiescent hiPSC BT1 CM (B). In this study quiescent cells were defined as not presenting any AP during Gap Free recordings but when evoked, presented an AP.*

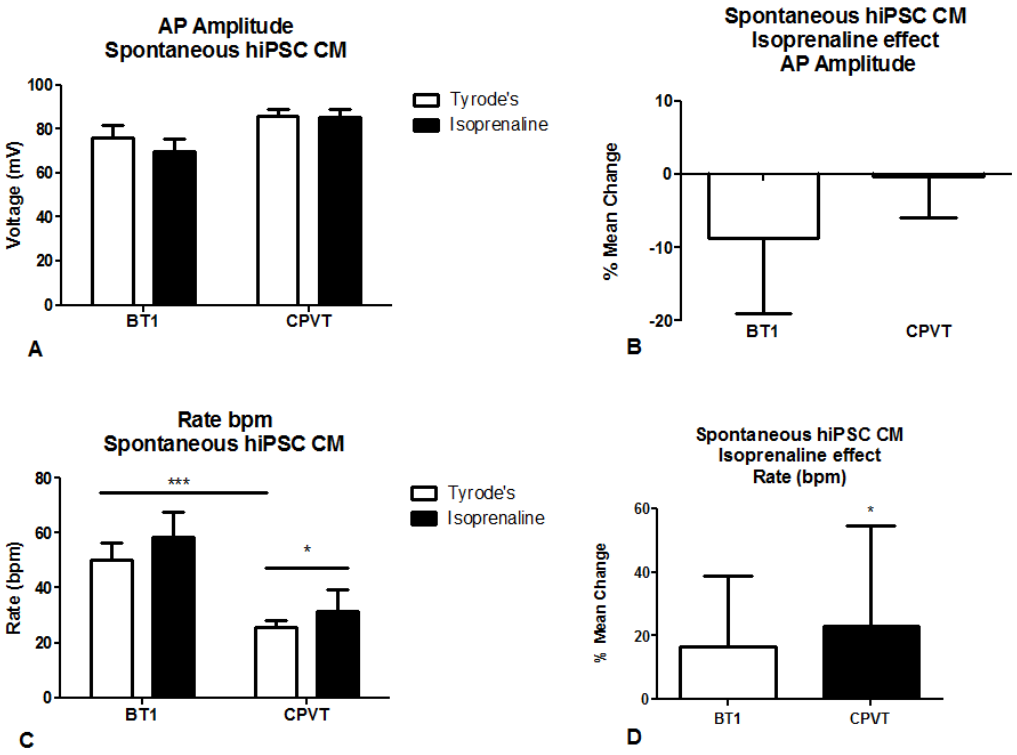

Figure 4.4 - Spontaneous AP rate and amplitude *- comparison between hiPSC CPVT CM (n=21) and hiPSC control BT1 CM (n=10) in Tyrode's and in the presence of isoprenaline (1µM) for AP Amplitude (A) and Beating rate in bpm-beats per minute (C), presenting respective percentage mean difference for isoprenaline effect on AP amplitude (B) and beating rate (D).*

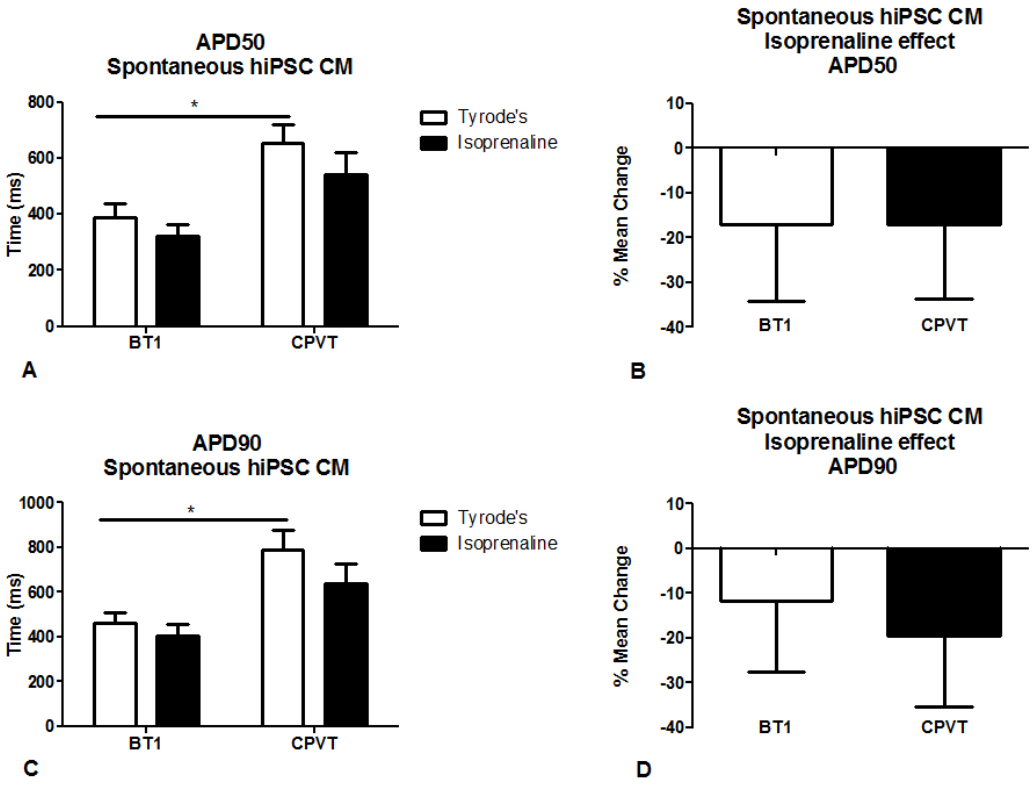

Figure 4.5 - Spontaneous AP parameter - APD50 and APD90 *- comparison between hiPSC CPVT CM (n=21) and hiPSC control BT1 CM (n=10) in Tyrode's and in the presence of isoprenaline (1µM) for APD50 (A) and APD90 (C), presenting respective percentage mean difference for isoprenaline perfusion on APD50 (B) and APD90 (D).*

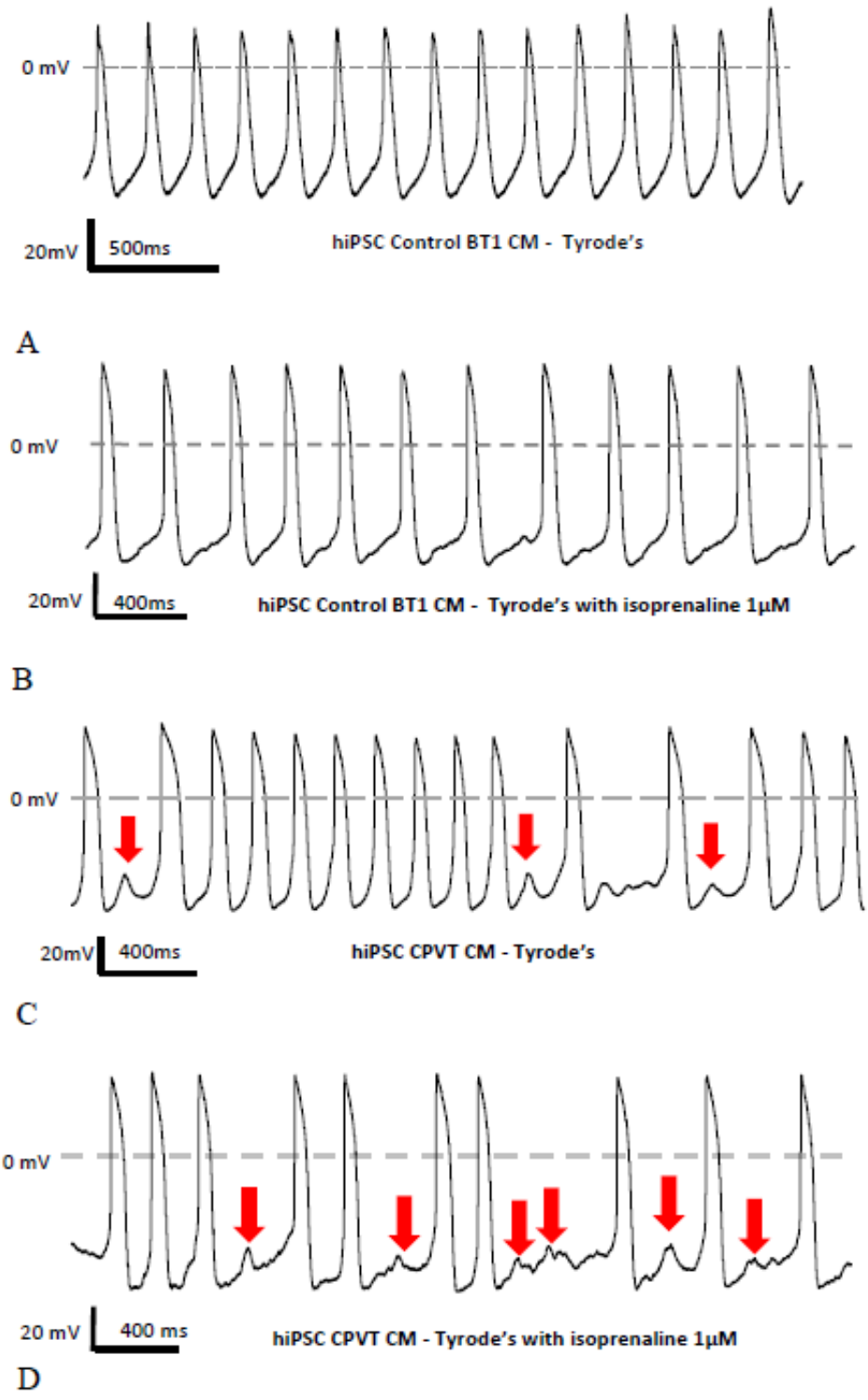

Figure 4.6 – Spontaneous AP traces with isoprenaline perfusion*- representative traces of both BT1 CM (A) and CPVT CM (C) for spontaneous recorded activity in Tyrode's solution and with isoprenaline 1µM perfusion (B and D respectively for BT1 CM and CPVT CM). Red arrows indicate spontaneous inter AP events. These events were considered as DADs. In CPVT CM, isoprenaline perfusion increased DADs frequency (figure 4.6D). This response is expected for disease phenotype recapitulation.*

4.2.2.2 Evoked AP

Not all hiPSC derived CM showed spontaneous activity after disaggregation. This work found that the vast majority become quiescent after 5 days in culture (figure 4.7). In order to better characterise these cells and study their AP signature when paced, an induced activity study was performed, since this allows a better control of experimental conditions. Beating rate can vary depending on temperature, time in culture and other idiosyncratic factors, hence the need to pace these cells.

In this study, APs were evoked in both CPVT and control BT1 CM at 0.5Hz and 1Hz. The objective was to observe the cell's response to different pacing rates in the presence and absence of isoprenaline. The patch clamp seal would not last long in frequencies higher than 1Hz.

Both quiescent and spontaneously beating cells were used in the pacing experiments. Spontaneously beating cells, displayed spontaneous AP, but responded to pacing when clamped had RMP and evoked AP.

A study of the electrophysiological profile of hiPSC derived CM evoked AP was undertaken. This included the response to ß-adrenergic stimulation with 1 µM isoprenaline perfusion, similar to the one presented for spontaneously beating cells. A frequency- response study was also made to better understand the physiological profile of these cells and determine if they present a CM expected response. For this last study both cells lines were paced at 0.5, 1, 1.5, 2 and 3 Hz.

For cells paced at 0.5Hz in Tyrode's, similar average AP peak values were observed while AP peak presented a significant decrease under the effect of isoprenaline in BT1 CM. In CPVT CM the AP peak difference was higher, with a significant 15% decrease from baseline value in Tyrode's (figure 4.9C). However despite this decrease, AP amplitude shows only 4% average decrease for both cell lines in response to ß-agonist stimulation (figure 4.9E).

When compared, APD50 and APD90 in CPVT CM present significantly longer APD than BT1 CM cells. The isoprenaline effect on APD is statistically significant in both cell types, presenting an average percentage decrease of 10% for both parameters in BT1 CM and 20% in CPVT CM (figure 4.10).

In 1Hz paced experiments, the main relevant finding is that perfusion with isoprenaline produced a 10% reduction in AP amplitude (figure 4.11F) for CPVT CM. None of the differences for APD50 and APD 90 were found to be statistically significant.

A new description is for the first time presented regarding hiPSC CM morphology, grouping them in 3 main types: lemon/fibroblast type, irregular and round shape (figure 4.14 and 4.15).

According to the selected criteria, the vast majority of studied hiPSC CM had VM features (figure 4.16). This finding was different that what has been reported in previous publications, what is probably related to the chosen criteria to group CM sub-types.

No significant observations could be made regarding the force-frequency study presented (figure 4.18).

More recordings were obtained at 0.5Hz suggesting that this can be an optimal pacing frequency in evoked AP experiments. More objective and less variable measurements were obtained with evoked AP when compared to spontaneous AP. This study was essential to characterise hiPSC CPVT as a potential model of disease with obvious advantages and less biases of evoked versus spontaneous AP.

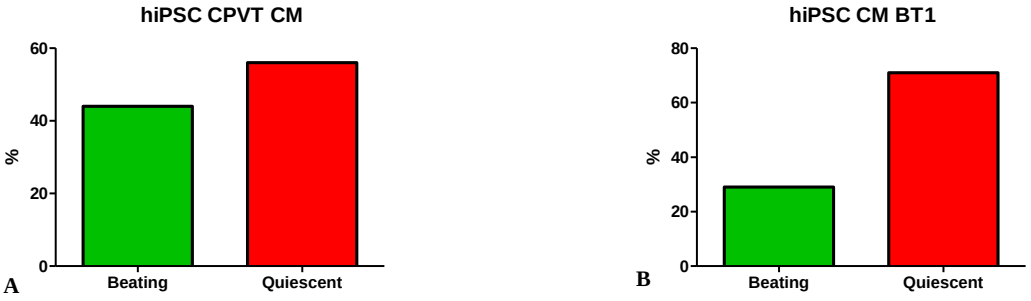

Figure 4.7 – Percentages of spontaneous contracting and quiescent CM *- data from GAP free mode, protocol recordings. Cells disaggregated from beating clusters plated as single cells for more than 5 days. Graphs (A) and (B) obtained from traces of hiPSC CPVT CM (n=61) and hiPSC BT1 CM (n=27) respectively.*

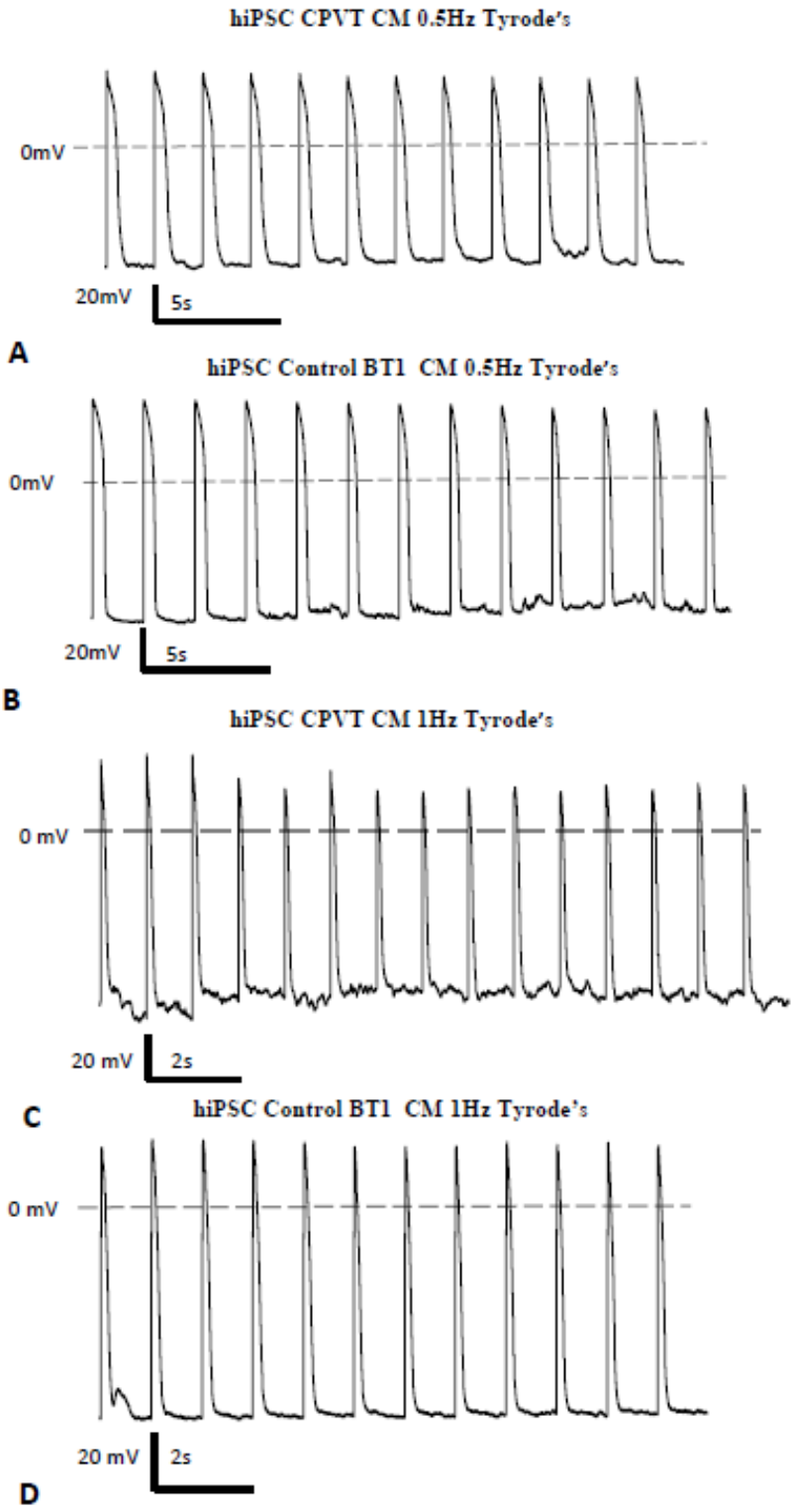

Figure 4.8 -Induced AP sequence at 0.5Hz and 1Hz *– AP example traces of hiPSC derived CPVT CM and hiPSC BT1 CM in Tyrode's paced at 0.5Hz (A, B) and 1Hz (C, D) respectively.*

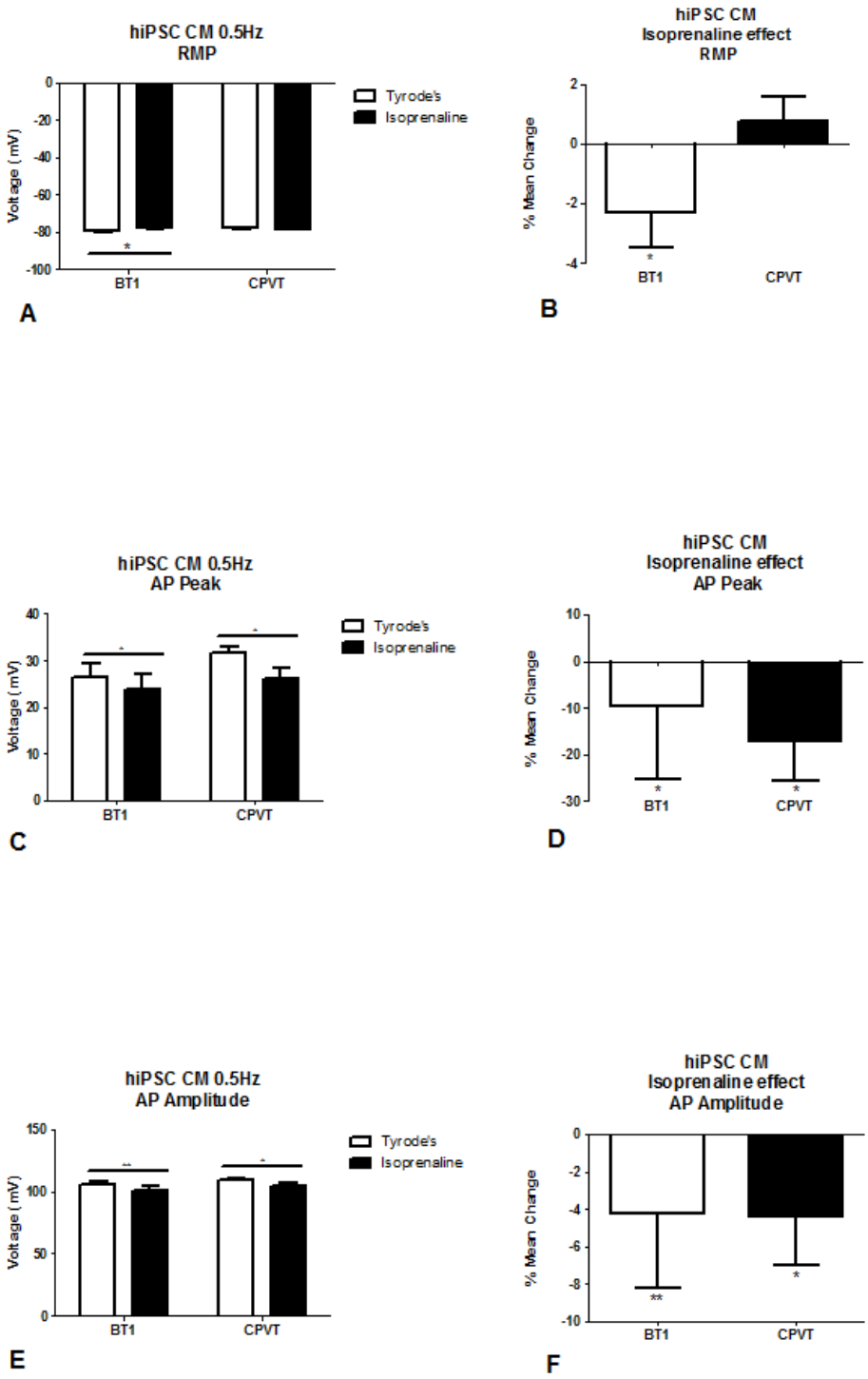

Figure 4.9 – Evoked AP parameters at 0.5Hz – RMP, Amplitude and Peak *- data obtained from parameters and mean percentage difference of isoprenaline effect (1µM) for RMP (A and B), AP Peak (C and D) and AP Amplitude (E and F) respectively. hiPSC BT1 CM (n=31) and hiPSC CPVT CM (n=48).*

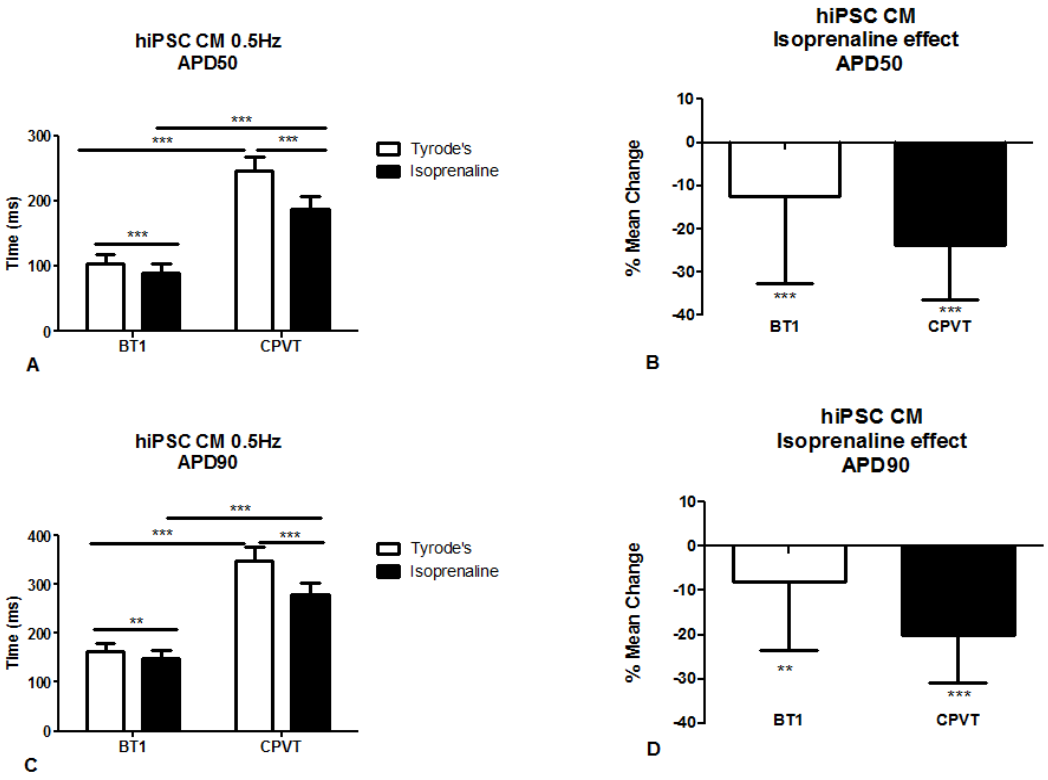

Figure 4.10 – Evoked AP parameters at 0.5Hz – APD50 and APD90 - *data obtained from parameters and mean percentage difference of isoprenaline effect (1µM) for APD50 (A and B) and APD90 (C and D) respectively. hiPSC BT1 CM (n=31) and hiPSC CPVT CM (n=48).*

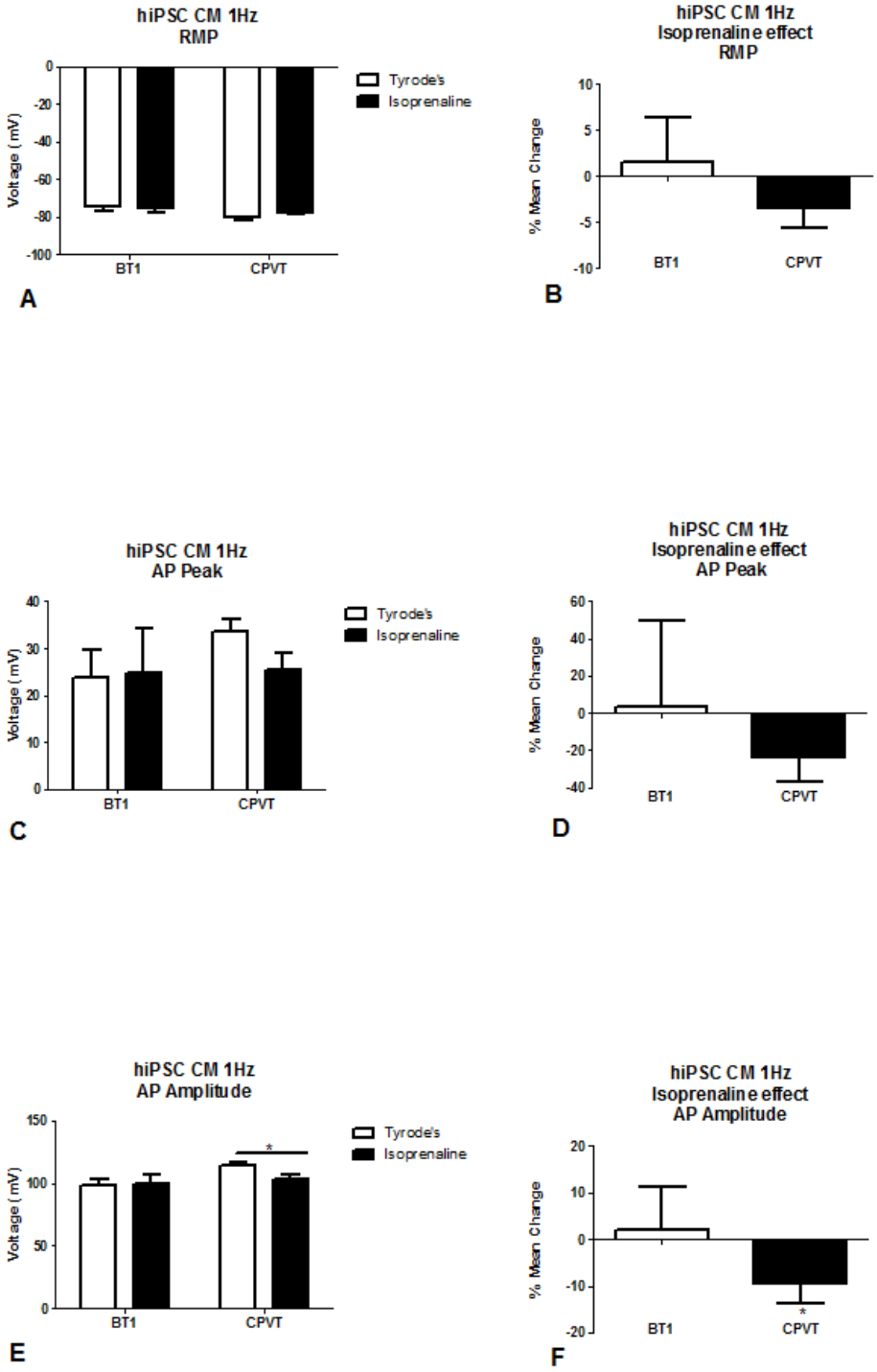

Figure 4.11 – Evoked AP parameters at 1Hz – RMP, Amplitude and Peak - *aata obtained from parameters and mean percentage difference of isoprenaline effect (1µM) for RMP (A and B), AP Peak (C and D) and AP Amplitude (E and F) respectively. hiPSC BT1 CM (n=8) and hiPSC CPVT CM (n=14).*

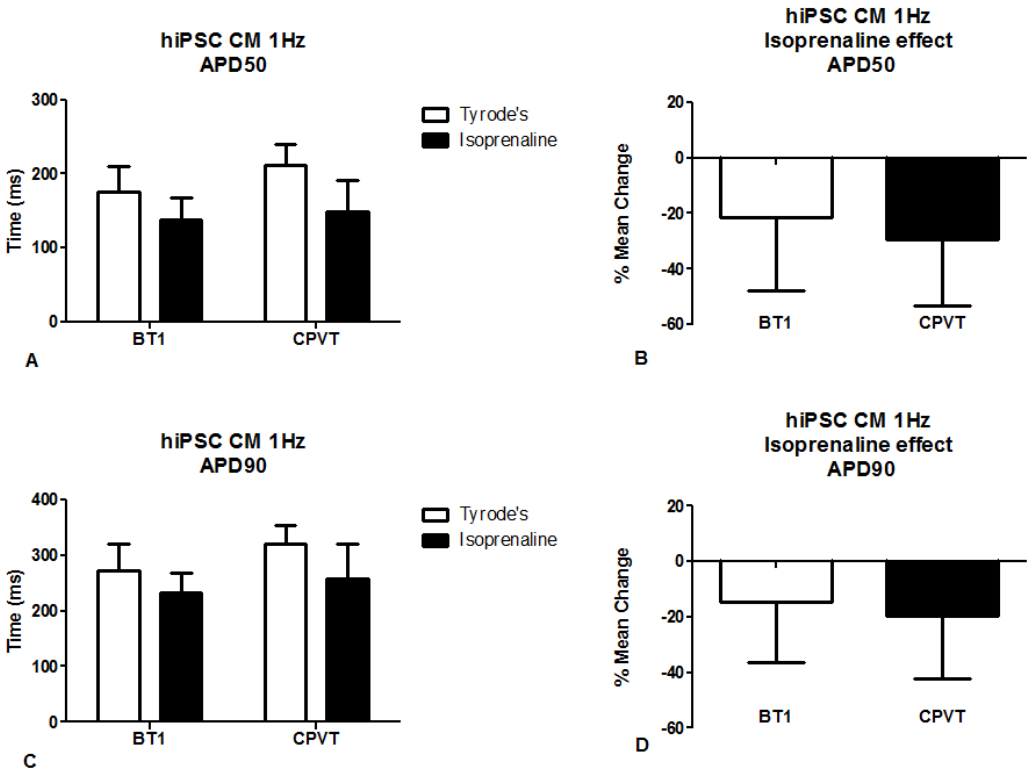

Figure 4.12 – Evoked AP Parameters at 1Hz – APD50 and APD90 -*. Graphs obtained from parameters and mean percentage difference of isoprenaline effect (1µM) for APD50 (A and B) and APD90 (C and D) respectively. hiPSC BT1 CM (n=8) and hiPSC CPVT CM (n=14).*

4.2.2.3 Cell morphology and behaviour

In addition to electrophysiological characterisation, cell morphology, size and contractile behaviour are also important criteria on which to evaluate hiPSC as CM models. Spontaneous contractility is an innate characteristic of hPSC derived CM made by the embryoid body method. However, cell behaviour changes over time, especially after disaggregation of beating clusters into single cells. Lack of contractility in a cluster is considered as indicative of poor CM viability. In agreement with this, when non-beating clusters were disaggregated, no evoked APs were obtained from patched cells and no individual AP currents were isolated (data not shown).

A known feature of hPSC derived CM morphology is their lack of normal mammalian rod shape. These cells present a variety of sizes and shapes independent of their spontaneous activity or AP signature. In this study we found that their shape can be round, "lemon like" or irregular with three or more angles. In order to compare these cells with primary CM we need to determine a cell size indicator. Cell membrane area was a good candidate to assess morphological similarities between hPSC CM and adult human CM. A good way to determine cell membrane area is via determination of cell capacitance. Capacitance value was obtained after achieving whole cell access and displayed by pClamp10.3 software. Capacitance (C) is a measure of the ability of a cell to store a charge (Q-Coulombs) when a voltage change (ΔV) occurs across the two ends of the cell:

$$Q = C\,\Delta V$$

Capacitance is proportional to the area and inversely proportional to the distance separating the two ends of the cell. Membrane capacitance is usually expressed in PicoFarads (pF).

In this study it was observed that the average capacitance of CM for both cell lines is between 15 and 20pF (figure 4.13).

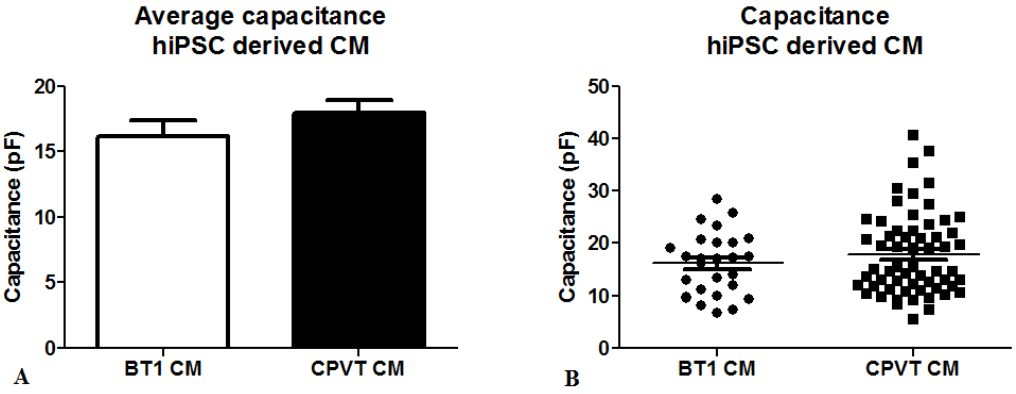

Figure 4.13 – hiPSC CM capacitance *– Average capacitance of hiPSC CPVT CM (n=61) and hiPSC control BT1 CM (n=27) shown as bar graphs (A) and vertical scatter plots (B).*

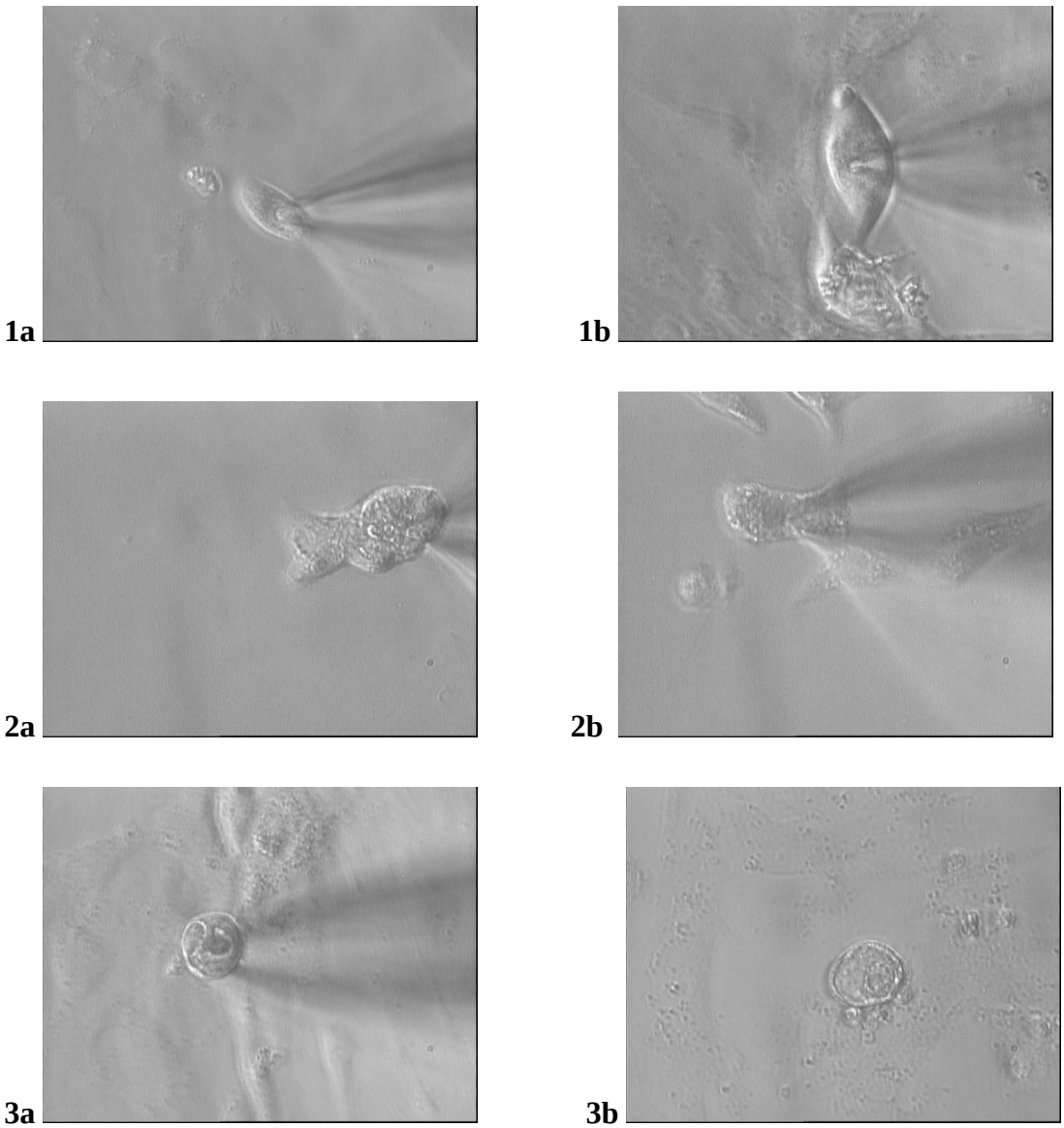

Figure 4.14 – hiPSC CM morphology - *Different morphology and shape of hiPSC CM during patch clamp experiments). These cell shapes can be grouped into 3 main categories: lemon/fibroblast type, due to their fusiform shape similar to fibroblast shape (1a, 1b), irregular (2a, 2b) or round shape (3a, 3b). Presented morphology categories were seen in both BT1 CM and CPVT CM.*

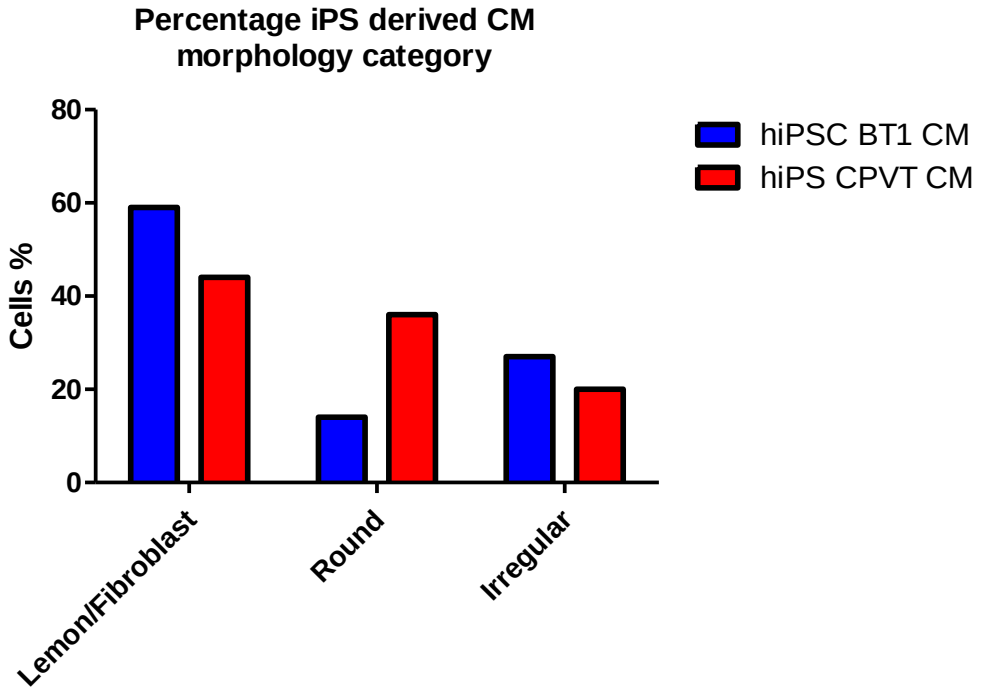

Figure 4.15 – hiPSC CM category morphology percentage – *Comparative percentages of the three different morphologies for control BT1 CM (n=22) and CPVT CM (n=25).*

No studies have been found in the literature reporting percentage of different morphology categories for hiPSC CPVT CM. No relationship was found between cell shape and AP sub-type.

4.2.2.4 Cardiomyocyte sub-types

A major challenge to the study of hiPSC derived CM is undoubtedly the characterisation of the different sub-types of these cells. In the case of primary cells it is relatively easy to separate these cells anatomically and then classify them according to their AP. There is a consensus concerning the basic electrophysiological characteristics of ventricular (VM), atrial (AM) or pace-maker (PM) primary cardiomyocytes. However, these criteria are difficult to apply to the AP analysis of hiPSC derived CM.

In a mixed population of hPSC CM, it is not easy to determine which cells are from a particular sub-type especially due to the intrinsic heterogeneity of these cells regarding shape and size. Some authors suggest visual selection using anti-ventricular myosin heavy chain antibodies marked with a fluorescent tag (Jung et al., 2012). Other authors suggest selection by cell size (i.e. above 45 pF) when patched, assuming that bigger cells are more likely to be ventricular myocytes (Honda et al., 2001).

A more recent publication suggests that hiPSC derived CM have a *sui generis* AP and it depends on cell maturation confluence not displaying classical chamber specificity AP signature (Du et al.,2015). This view has however been challenged by other authors.

Since an ideal classification system wasn't found to separate the three different CM sub-types, in this study, the APD90/50 ratio was chosen for sub-type classification (i.e. Matsa et al., 2011). If the APD90/50 ratio is ≤ 1.4 a cell was considered to have a ventricular myocyte AP. If the ratio was between 1.4 and 1.7 the AP was classified as pace-maker and if the result was ≥1.7 the AP signature was considered as an atrial cardiomyocyte.

In this project, sub-types of two different data sets from experimental patch-clamp protocols are presented. One from spontaneous beating cells obtained from gap-free protocols and the other data set obtained from APs obtained from evoked recordings at 0.5Hz pacing frequency.

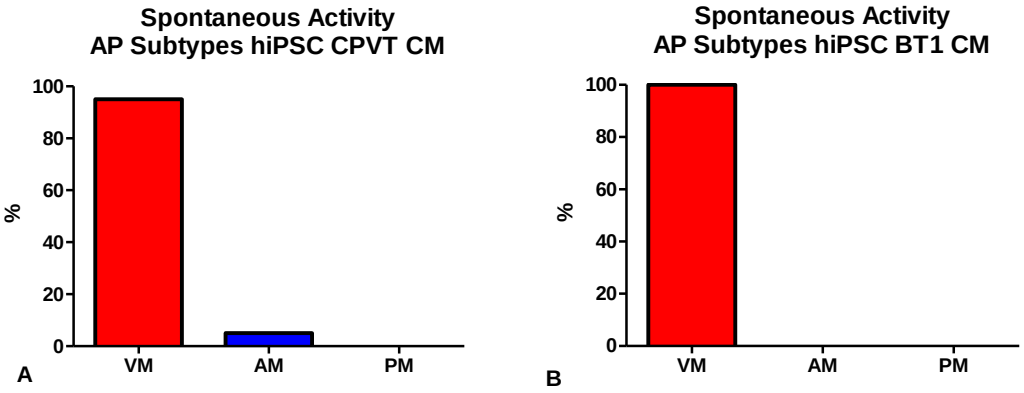

Figure 4.16 – AP sub-types for spontaneous activity - *Data in percentage for hiPSC CPVT CM (A, n=21) and Control hiPSC BT1 CM (B, n=10). VM=Ventricular CM, AM=Atrial AM and PM=Pace-maker CM.*

Ratio APD50/90 analysis was also made for evoked AP and in this case the percentage of AP sub-types is quite different. As previously mentioned, all spontaneous AP analysis involves a higher degree of subjectivity, as it's difficult to define precisely when the AP starts and ends. In evoked AP analysis it is easier to determine the depolarization start point and the end point of repolarization.

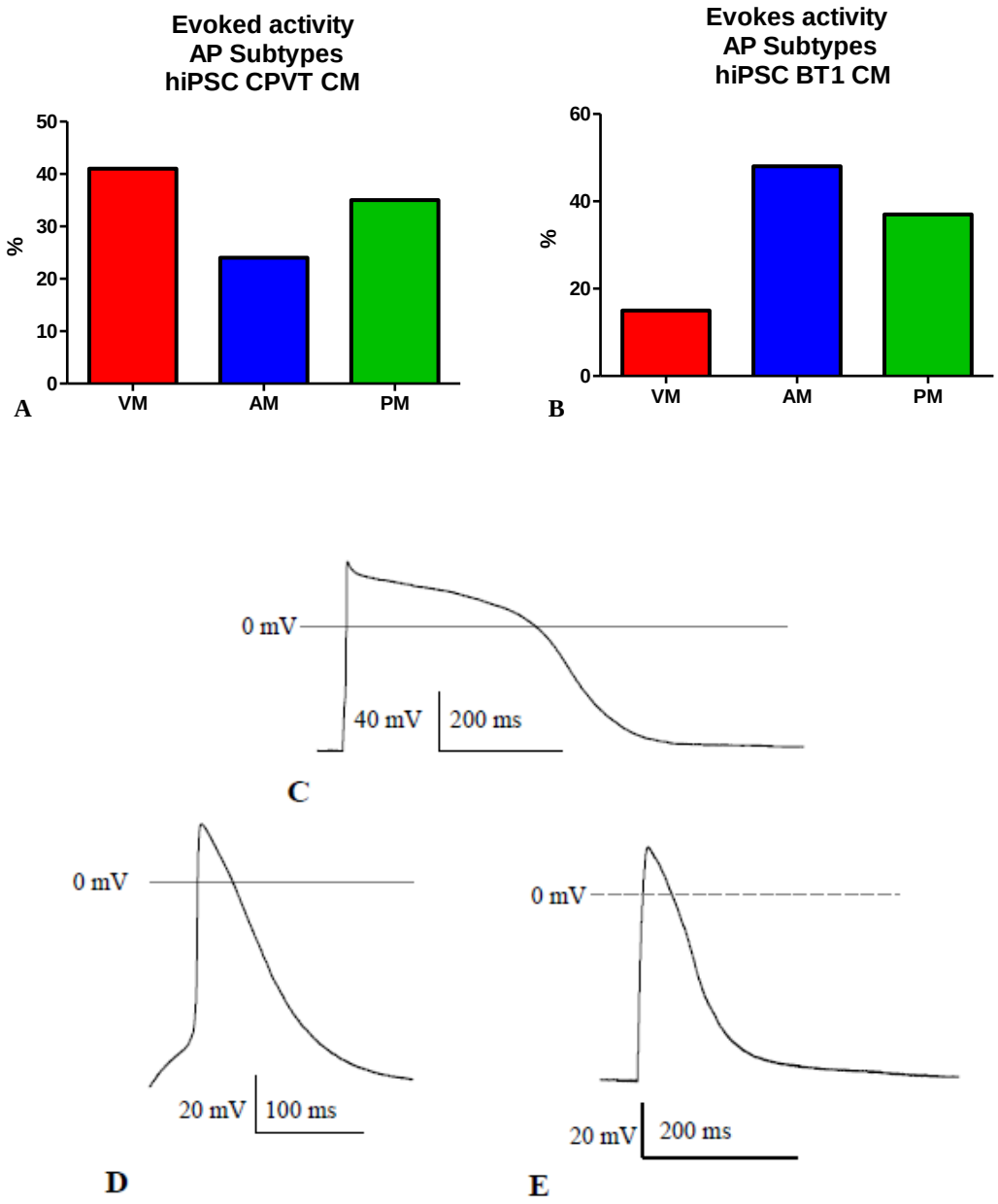

Figure 4.17 –AP sub-types from evoked activity *– Evoked AP sub-type for hiPSC CPVT CM (n=51) (A) and hiPSC Control BT1 CM (n=27) (B) from evoked AP at 0.5Hz. Data obtained from cells perfused with Tyrode's solution only. VM=Ventricular CM, AM=Atrial AM and PM=Pace-maker CM. Representative traces of ventricular like (C), pace-maker like (D) and atrial like (E) hiPSC derived CM. In control BT1 CM cell line, a higher percentage of atrial like CM was observed (figure 4.17B). In CPVT CM cells, a higher percentage of ventricular like CM is present (figure 4.17A).*

4.2.2.5 AP rate of adaptation

A fundamental property of cardiac myocytes is the ability to adapt to an increase in heart rate with a decrease in APD (He et al., 2003; Blazeski et al., 2012). Rate adaptation is present in atrial and ventricular cardiomyocytes, and it can be impaired in certain disease states. Shortening of APD with rate has also been observed in embryonic human ventricular muscle (7 to 12 weeks) (Jezek et al.,1982). Therefore, it remained important to determine if embryonic-like APs exhibited appropriate rates of adaptation. Single cells were studied with the patch clamp technique in the whole cell mode and membrane rupture modality with RMP clamped at -80 mV. Paced cells were both from spontaneously beating and quiescent populations with different AP sub-types. Cells were paced at five different rates, and steady state APs were then recorded and analysed.

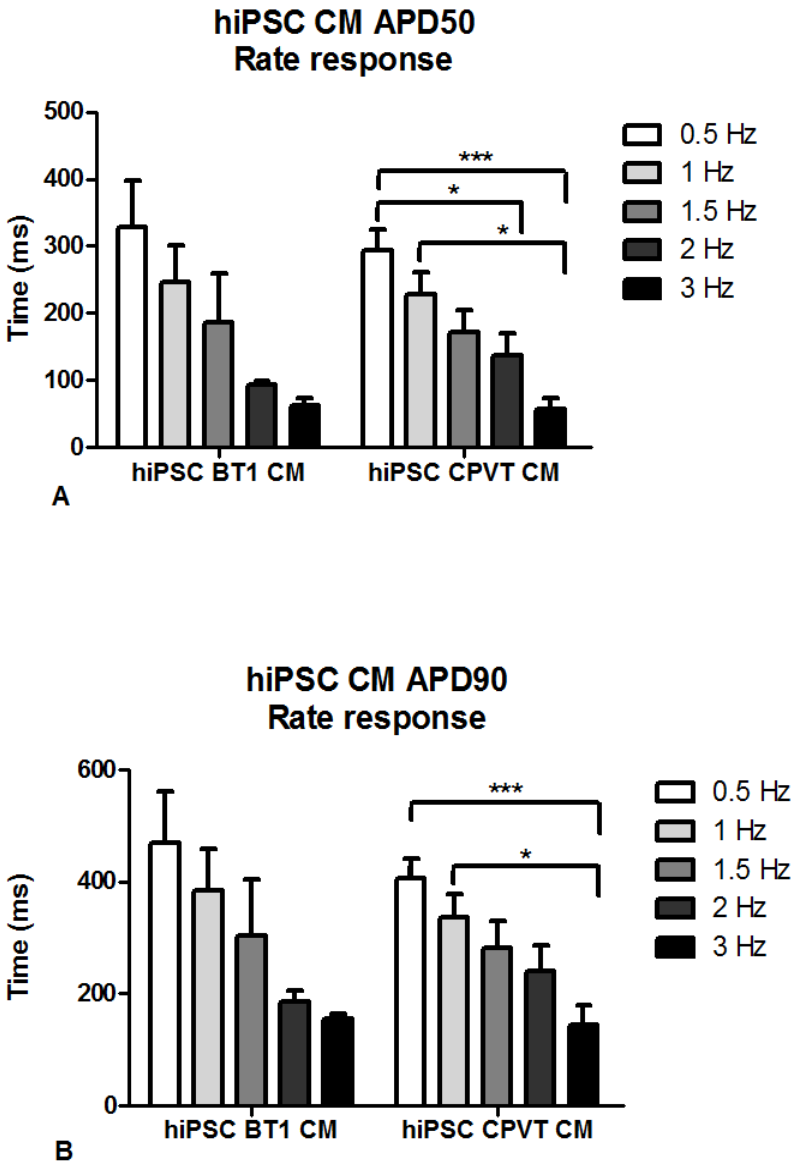

Figure 4.18 –hiPSC CM rate-response *- Rate response for APD50 (A) and APD90 (B) of hiPSC BT1 CM (n=6) and hiPSC CPVT CM (n=10) in Tyrode's for different pacing frequencies from 0.5Hz to 3Hz. A trend for APD50 and APD90 reduction is observed when pacing rate increases from 0.5Hz to 3Hz.*

4.2.2.6 Discussion for electrophysiology based characterisation

The electrophysiological characterisation of CPVT hiPSC derived CM, and control CM was essential to help understand the developmental stage of these cells before using them as *in vitro models* of disease. The spontaneous beating nature of these cells can help us to better understand the developmental processes of the human CM. This finding is however a challenge to overcome if these cells are to be used as a model of adult cardiac cells. Human adult cardiac atrial and ventricular cells do not present spontaneous activity. For this reason both spontaneous and evoked APs were analysed in this project for both mutant and control cell lines.

Data variability was observed between CM with spontaneous activity and quiescent cells. APs of spontaneously contracting cells will present less accurate and objective measurements as they will be more prone to subjective assessment of where an AP starts and ends. Spontaneous beating CM can present highly variable basal beating rates. This can influence some parameters such as AP duration (APD) as reported by He et al., 2003 and Zhang et al., 2009.

For these reasons it was decided to study spontaneous and evoked AP.

Spontaneous activity

A higher percentage in number of cells with spontaneous contractile activity compared with quiescent cells, was observed in CPVT CM compared to control BT1 CM (45% versus 30%) (figure 4.7). This observation suggests that CPVT CM may have mechanisms that predispose to higher contractibility, possibly related to the RyR2 mutation. Publications regarding the proportion of spontaneous individual beating cells used to model CPVT CM were not found in the literature. This may be due to the fact that previous publications focused mainly on cells with spontaneous activity and did not analyse quiescent cells.

As for isoprenaline stimulation, a significant positive chronotropic effect was observed in CPVT CM (figure 4.2), unlike the negative chronotropic response that some authors report for mutant cells. Two authors that studied hiPSC CPVT CM (Fatima et al., 2011; Novak et al., 2012) have presented data indicating a very marked chronotropic response to ß-adrenergic stimulation in control hiPSC CM and a negative chronotropic effect in CPVT hiPSC CM.

In one of the studies, Novak et al., reported similar frequency (in bpm), for control and CPVT CM in Tyrode's. Contrasting with those results, cells studied in this project show that BT1 CM present a significantly higher beating rate compared with CPVT CM (figure 4.2), when perfused in Tyrode's only. This difference could be explained by the fact that different CPVT mutations can display a different phenotype, not excluding other potential simultaneous mutations in other ion channel and receptors. Control cell lines can also present variability that could underlie different responses.

Measurement of RMP is also very important as this parameter can be a criteria for phenotypical maturity. Ideally this parameter should only be obtained from quiescent cells in a GAP free protocol before stimulation; since there is significant variability if the cells are contracting, as demonstrated in this project. Several authors reported RMP values when analysing spontaneously contracting CM (Kujala et al., 2012; Jung et al., 2012; Novak et al., 2011).

Author	Disease	hiPSC Control CM	hiPSC CPVT CM
Novak et al.,2011	CPVT-2	-55mV	-56mV
Jung et al., 2012	CPVT-1	-73mV	-73mV
Kujala et al., 2012	CPVT-1	-68 mV	-67 mV
Current project -contracting-	CPVT-1	-61 ± 4 mV	-46 ± 2 mV
Current project -quiescent-	CPVT-1	-25 ± 4 mV	-28 ± 2 mV

Table 4.2 – Summary of RMP comparative values *- data reported in the literature (approximate values taken from graphs) and in this project for hiPSC CPVT CM and respective controls.*

Observed RMP values from quiescent control and mutant CM, presented in this report, have a similar trend (figure. 4.3). These values correspond to less negative average RMP than the ones obtained from contracting cells. Values reported by some authors (table 4.2) in which values range from -60 to -75mV, are not obtained from quiescent cells.

A less negative RMP is more characteristic of a fetal like CM, since adult CM have RMP close to -80 mV. Measuring RMP from contracting CM can therefore bias the fact that these cells are indeed foetal and not even close to mature CM as seen in table 4.2.

The fact that average APD50 and 90 in spontaneous contracting CPVT cells in Tyrode's are significantly longer compared to BT1 CM in the same perfusion media (figure 4.5) suggests that mutant cells may have an abnormal repolarization mechanism. This abnormal mechanism can be potentially related to an increased Ca^{2+} in the cytosol due to RyR2 calcium leak in CPVT CM. Novak et al., (2012) also report significantly longer APD50 in mutant cells compared to control, although in a model of CPVT2, suggesting similar mechanisms of disease may be involved in both CPVT1 and CPVT2.

A trend for APD50 and APD90 shortening was observed in both CPVT CM and control spontaneously contracting cells, when perfused with isoprenaline (figure 4.5).

Evoked activity

No examples of evoked AP parameters paced at 0.5Hz from hiPSC CPVT cells were found in the literature and hence this may be the first report of such data.

AP peak values for control and CPVT CM paced at 0.5Hz were similar, although the percentage decrease upon isoprenaline addition was more marked in mutant cells (figure 4.9). AP amplitude decrease was minimal in both cell types for ß-agonist perfusion. This difference could be due to the fact that AP amplitude values are more consistent with fewer extreme values when averaging data.

Repolarization duration measured in APD50 and APD90 for cells paced at 0.5Hz, confirmed that CPVT CM present a significant longer value for these parameters (figure 4.10). Mutant cells present a higher number of ventricular like CM and this could also contribute to APD50 increase since this CM sub-type has the biggest value for this parameter. Isoprenaline stimulation caused a significant APD shortening in both cell lines as expected in a mammalian CM (figure 4.10). Mutant cells presented twice the average percentage decrease in both parameters. This could be possibly due to a compensatory mechanism of CPVT CM due to a likely Ca^{2+} leak.

To compare AP parameters with a higher and more physiological frequency these same experiments were repeated pacing cells at 1Hz. Most results were not significant, but total number of analysed cells at this rate was small and this may have contributed to the absence of an effect.

Cell morphology and size

Previously published data for capacitance of primary CM from rabbit, rat or ferret is in the range of 130 to 300 pF (Satoh et al. 1996; Barth et al. 1992). These are very different values from those observed in CM for the current report (figure 4.13). It seems to be a trend for hiPSC derived CM to have a much smaller average area than that of mammalian ventricular CM. This fact could be suggestive of embryonic immaturity that these cells can present. A smaller surface can also reduce the number of ion channels present in the cell membrane, which in turn can influence the AP maturity.

Since Maltsev et al., 1994 first investigated hESC CM electrophysiology, no publications were found in the literature reporting different morphology and shape for hPSC CM. The same is the case for hiPSC CPVT CM. In this project, hiPSC derived CM have for the first time been grouped into three main morphological categories: lemon/fibroblast (1) (due to their fusiform shape similar to fibroblast shape) irregular (2) or round (3). CPVT CM presented a larger percentage of lemon/fibroblast cells, followed by round shape and lastly irregular cells demonstrating the morphological heterogeneity of these cells (figure 4.14).

CM sub-types

This topic is clearly one of the most diverse and controversial found in the literature as there is no consensus on which criteria are better to classify CM into their sub-types.
Several authors including Maltsev et al., 1993; He et al., 2003; Ma et al., 2011 and Matsa et al., 2012; have mentioned three different sub-types in hESC and hiPSC, but Di Pasquale et al., 2013 and Zhu et al., 2010 classified hPSC CM in two subtypes, nodal (i.e. cells from the AV node) and working like (i.e. atrial and ventricular chamber). Di Pasquale et al., 2013 classified nodal-like cells which were distinguishable because of their pronounced phase 4 depolarization preceding the onset of the AP, and working myocardial cells, which presented the typical plateau phase, and therefore had the longest AP duration.

Zhu et al., 2010 mentions that working-type hESC CM express high-conductance gap junction proteins (connexins-40 and 43), and they exhibit greater proliferative activity and more rapid electrical propagation than their nodal counterparts as observed in primary mice CM (Christoffels et al., 2004).

In this project, the difference seen between spontaneous and evoked AP sub-types can be due to the fact that evoked AP were clamped at -80mV. This procedure was adopted to allow depolarization from a more physiological RMP. Clamping the RMP will change APD times, which in turn is the main parameter used for AP sub-type classification in this study. In spontaneous cell experiments, the number of cells or sample size is small, and this may also reduce the probability of finding cells from other subtypes. Interestingly the percentage of PM CM in evoked AP experiments was very similar in both cell lines for this set of experiments.

Some authors even suggest that each beating cluster differentiates only into one specific sub-type (Zhang et al., 2009) while others mention a mixed cell population with a tendency for VM-like predominance over the other two types (Ma et al., 2011; Jung et al., 2012). What seems clear is that some cells may fall outside the criteria chosen to categorize them and a different classification approach may be necessary to determine sub-types for hiPSC derived CMs to generate more consensus within cardiac research groups.

AP rate response

AP duration decrease is a functional response to increased beating frequency in CM (Jezek et al.,1982). He et al., (2003) reported APD rate adaptation of hESC derived CM for the first time. No reports of rate of adaptation have been found in the literature for hiPSC CPVT CM and respective controls as part of their physiological characterisation. In this project a trend was observed in APD50 and APD90 to be consistently shorter with an increased pacing frequency (figure 4.18). Statistical significance of the observed trend was only present at some CPVT CM pacing rates.

4.3 Ca^{2+} imaging based characterisation

4.3.1 Ca^{2+} handling physiology

In order to contract the cardiac cell depends not only on ion channel electrical activity but also on the orchestrated Ca^{2+} movement into the cell from the extracellular media via L-type calcium channels imbedded in the sarcolemma. Ca^{2+} in turn initiates CICR by opening RyR2 channels located in the SR membrane. The subsequent rise in intracellular Ca^{2+} facilitates myofibre contraction. The cardiac cell relaxes when intracellular Ca^{2+} is returned to resting levels.

If Ca^{2+} was not removed from the sarcoplasm it would cause permanent contraction of the myofibers preventing diastole and re-filling of the heart. Different mechanisms are in place to remove cytosolic Ca^{2+} and initiate relaxation of the cell. Cytosolic calcium can either be re-sequestered into the SR, via the SERCA2A (Ca-ATPase) pump or be removed from the CM via the NCX that extrudes Ca^{2+} into the extra-cellular media in exchange for Na^{+} or via the sarcolemmal Ca-ATPase pump that actively removes intracellular Ca^{2+} from the cell.

SERCA2A (Ca^{2+}-ATPase) pump activity is regulated by PLB; that when phosphorylated, is unable to inhibit SERCA pump activity. Once in the SR, Ca^{2+} is usually bound and buffered by calsequestrin (CASQ). This protein binds approximately 35 to 40 Ca^{2+} ions (Mitchell et al., 1988). Two other small proteins, triadin (TDN) and junctin (JCN) also interact with RyR2 and CASQ. These are usually attached to the junctional face membrane in the terminal cisternae of the SR (Zhang et al., 1997). The functions of junctin, triadin and CSQ in SR signalling have been extensively explored in transgenic animals. TDN, JCN and CSQ-null animals survive, but their longevity and ability to tolerate cardiac stress is compromised (Altschafl et al., 2011).

Ca^{2+} imaging studies of ß-adrenergic response are particularly relevant in validating functional properties of hiPSC derived CM. It is essential to study the inotropic, chronotropic and lusitropic intrinsic response of these cells. The visualisation of calcium transients using calcium-sensitive fluorescent dyes offers a unique insight into fundamental intracellular Ca^{2+} handling mechanisms. This study is especially relevant to the characterisation and study of new CM models such as hiPSC derived CM.

The mutant cells used in this project are derived from a patient with CPVT. Since CPVT is caused by a diastolic Ca^{2+} leak it is essential to use calcium imaging to establish spacio-temporal dynamics and the basal Ca^{2+}profile of these cells.

4.3.2 Previous publications

Most publications regarding hPSC derived CM present Ca^{2+} handling data from hESC derived CM spontaneous activity of beating clusters (Dolnikov et al., 2006) or single cells (Liu et al., 2007; Satin et al., 2008).

Since their discovery in 2006, hiPSC derived CM have also been the focus of Ca^{2+} handling research.

Itzhaki et al., (2011) confirm that, as in the case of hESC CM, hiPSC CM present a functional, but foetal Ca^{2+} handling phenotype. These cells presented functional SERCA-sequestering and RyR2 mediated Ca^{2+} stores, while CICR was dependent on L-type Ca^{2+} channels. In response to caffeine stimulation these cells demonstrate SR Ca^{2+} release and Ca^{2+} transient amplitude was reduced with ryanodine perfusion. The SERCA Ca^{2+} -ATPase was blocked with thapsigargin, producing a complete abolition of Ca^{2+} transients. As reported for hESC CM, functional IP_3 receptors were also detected in these hiPSC CM.

In the same year (Lee et al., 2011) published a comparison of Ca^{2+} handling in hESC and hiPSC CM using 20 day old post differentiated CM. These authors reported smaller Ca^{2+} transients and a better caffeine response in hiPSC than hESC CM. Ryanodine perfusion only reduced Ca^{2+} transients in hESC CM and no effect was seen in hiPSC CM. In this study a more immature SR and Ca^{2+} handling phenotype was observed in hiPSC CM. Consistent with this, hiPSC CM presented lower levels of expression of SERCA, JCN, TDN and RyR2 compared with hESC CM.

The potential of hPSC derived CM as models to understand mechanisms of disease and cardiac physiology were also recently highlighted by Chen et al., 2015. In a published report, transgenic-induced upregulation of PLB restored an inotropic response to ß-adrenergic stimulation in both hESC and hiPSC derived CM. These cells initially had a positive chronotropic response but no inotropy was seen when perfused with isoprenaline. PLB gene transfer, via adenoviral vector, restored Ca^{2+}handling in these immature cells, proving that the embryonic phenotype can be upgraded and matured.

Despite an abundance of data regarding hiPSC derived CM Ca^{2+} handling in the literature, there is still a need for more in depth studies regarding hiPSC CPVT CM. The spontaneous beating nature of hiPSC derived CM makes obvious the need of studying both spontaneous and stimulated activity in order to standardise experiments and allow a potential translational use of these cells in tachycardia related disease and to simulate cardiac arrhythmic behaviour.

4.3.3 CPVT1 derived CM

One of the main potential uses of hiPSC CM is as *in vitro* models of disease. Publications using CM made from hiPSC from patients carrying inherited cardiac channelopathies are now available. Several publications have studied Ca^{2+} handling properties of hiPSC CPVT1 CM in order to try and validate these cells as models of disease.

One of the first CPVT hiPSC CM models was reported by Fatima et al., 2011 and a brief characterisation of Ca^{2+} handling was made. Higher amplitude and longer duration Ca^{2+} transients were seen in mutant cells compared with control CM. Control cells were a mixed population of hESC and hiPSC derived CM but a 100% positive chronotropic effect was observed upon ß-adrenergic stimulation in these cells, while 57% of CPVT1 hiPSC had a negative chronotropic response.

In a model of CPVT2 caused by a genetically inherited abnormal CASQ2, Novak et al., 2012 demonstrated that control cells presented both positive inotropic and lusitropic effects when exposed to the ß-agonist isoprenaline (1µM), while mutant cells did not. In this study 100% of control cells had a positive chronotropic response compared with only approximately 50% of the CPVT2 cells.

Zhang et al., 2013 reported an extensive study using CPVT1 hiPSC CM concluding that both control and mutant CM had an adult CICR phenotype. It was found that CPVT1 hiPSC CM had smaller Ca^{2+} stores (due to Ca^{2+} leak) than control cells. Mutant cells also had lower levels of NCX expression and were caffeine responsive.

In 2013, Di Pasquale et al., also reported an adult-like regulation of Ca^{2+} handling in CPVT1 derived CM.

4.4 Methods

For more detailed information on Ca^{2+} imaging methods, please refer to section 2.4 of Chapter 2.

In these experiments, FLUO-4 AM® (fluo-4 acetoxymethyl) from Invitrogen was used as a Ca^{2+} sensitive fluorescent indicator at 5µM. Local and global Ca^{2+} signals were recorded from hiPSC derived CM, using laser scanning confocal microscopy (SP5; Leica Microsystems).

Disaggregated single cells, were incubated for 20 minutes at room temperature in modified Tyrode's and FLUO-4 5µM. Ca^{2+} dependent signals, were visualized with a 63x oil immersion objective, using argon laser excitation at 488nm. Experiments were carried out at 37 ºC A perfusion chamber with two electrodes was used to pace cells externally at 10-30V.

For experimental purposes spontaneous cells were considered as cells beating with no external pacing. Stimulated cells were considered to be both quiescent and spontaneously active cells that responded to external pacing.

4.5 Results - hiPSC derived CM Ca^{2+} transient characterisation

In this study, single cell fluorescent Ca^{2+} imaging was used to characterise ß-adrenergic responses and functional Ca^{2+} handling in both mutant and control CM. A more detailed Ca^{2+} transient profile analysis for hiPSC derived CM was undertaken for the first time, using SALVO software.

Inotropic, chronotropic and lusitropic positive responses are classical characteristics of adult CM and therefore studied cells should display these features if meant to be used as *in vitro* models of disease.Ca^{2+} transients from spontaneous and paced hiPSC CM were studied.

Spontaneous activity

In spontaneous beating cells, a significant amplitude decrease was observed in BT1 and CPVT cells in response to isoprenaline (figure 4.19C, D). Only BT1 CM presented a positive chronotropic effect, while CPVT CM did not presented an expected positive response (figure 4.21). The lusitropic effect can be assessed by determining the rate decay of a transient. No significant response was seen in basal rate decay or with isoprenaline perfusion for both mutant or control cells (figure 4.22).

Stimulation 0.5Hz

BT1 CM presented a negative inotropic response following an amplitude transient decrease when perfused with isoprenaline. No effect was observed in CPVT CM (figure 4.24C and D). BT1 CM rate, significantly increased with isoprenaline perfusion, superseding the imposed rate of stimulation. A positive chronotropic effect was therefore observed in control CM. No significant change in rate was seen on isoprenaline perfusion of CPVT CM (figure 4.26A). No lusitropic effect was observed in both BT1 CM or mutant cells, as no significant changes were observed in rate decay (figure 4.27C).

Stimulation 1Hz

When paced at 1Hz, no inotropic effect was observed in either cell type (figure 4.29C).A small positive chronotropic effect was observed in CPVT CM while an opposite response was observed in control CM (figure 4.31A).

No significant change in the rate of response decay was seen during isoprenaline perfusion for either mutant or control cells (figure 4.32C).

In summary, a lack of consistency in the responses to isoprenaline perfusion was observed in either spontaneously beating or paced cells at 0.5Hz and 1Hz. These results suggested a lack of mature or adult CM Ca^{2+} handling profile.

4.5.1 Spontaneous Ca^{2+} transients

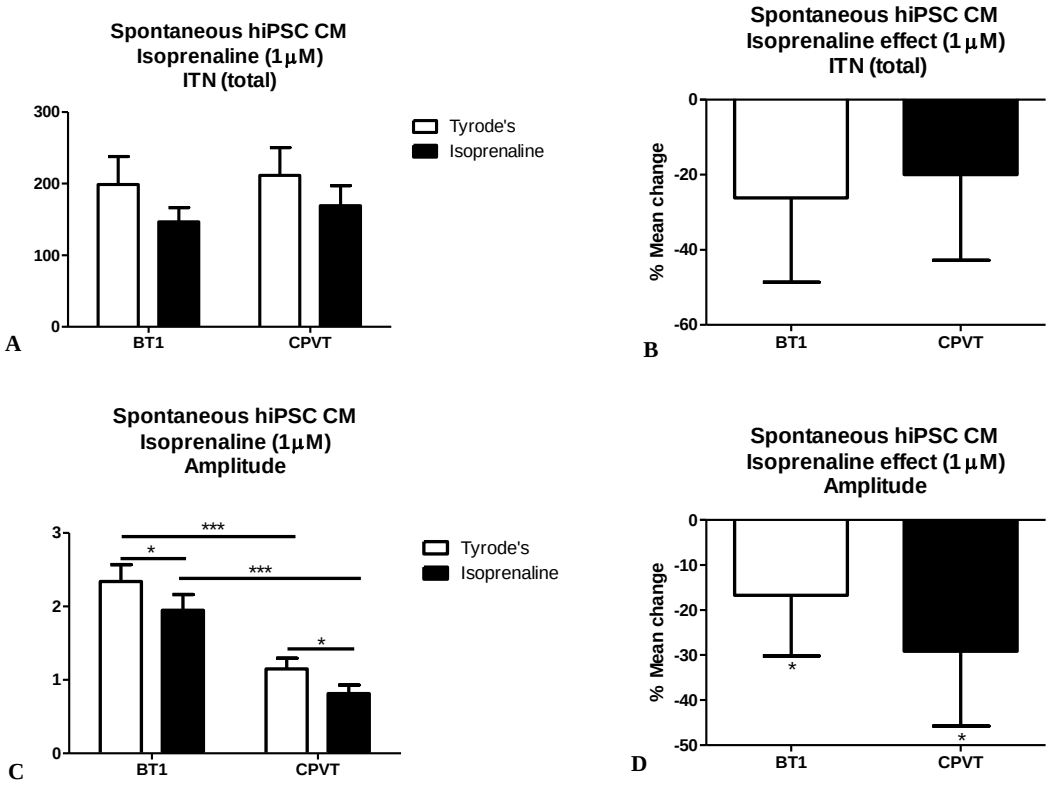

Figure 4.19 – Spontaneous Ca^{2+} transient parameters, ITN (A) and Amplitude (C) *with respective isoprenaline (1μM) effect (B and D) in mean percentage change, for hiPSC BT1 CM (n=32) and hiPSC CPVT CM (n=20). From figure 4.19A it is clear that both mutant and control cells have similar values of ITN in Tyrode's. However, there is a significant difference in amplitude between BT1 and CPVT cells and a significant decrease in amplitude in response to isoprenaline in both types of cell (figure 4.19C, D).*

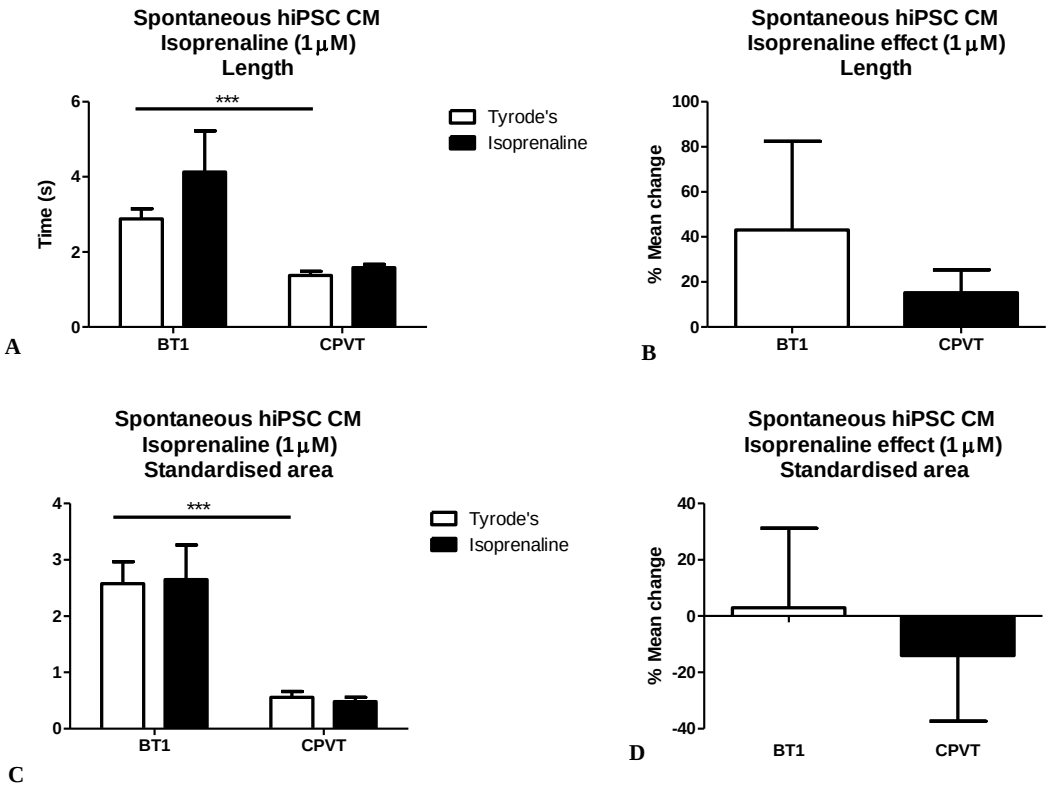

Figure 4.20 – Spontaneous Ca^{2+} transient parameters, Length (A) and Standardised area (C) *with respective isoprenaline (1μM) effect (B and D) in mean percentage change, for hiPSC BT1 CM (n=32) and hiPSC CPVT CM (n=20). A significant statistical difference was found between BT1 CM compared with CPVT CM in Tyrode's for both parameters. CPVT CM present a much smaller value compared with BT1 CM (figure 4.20A and 4.20C).*

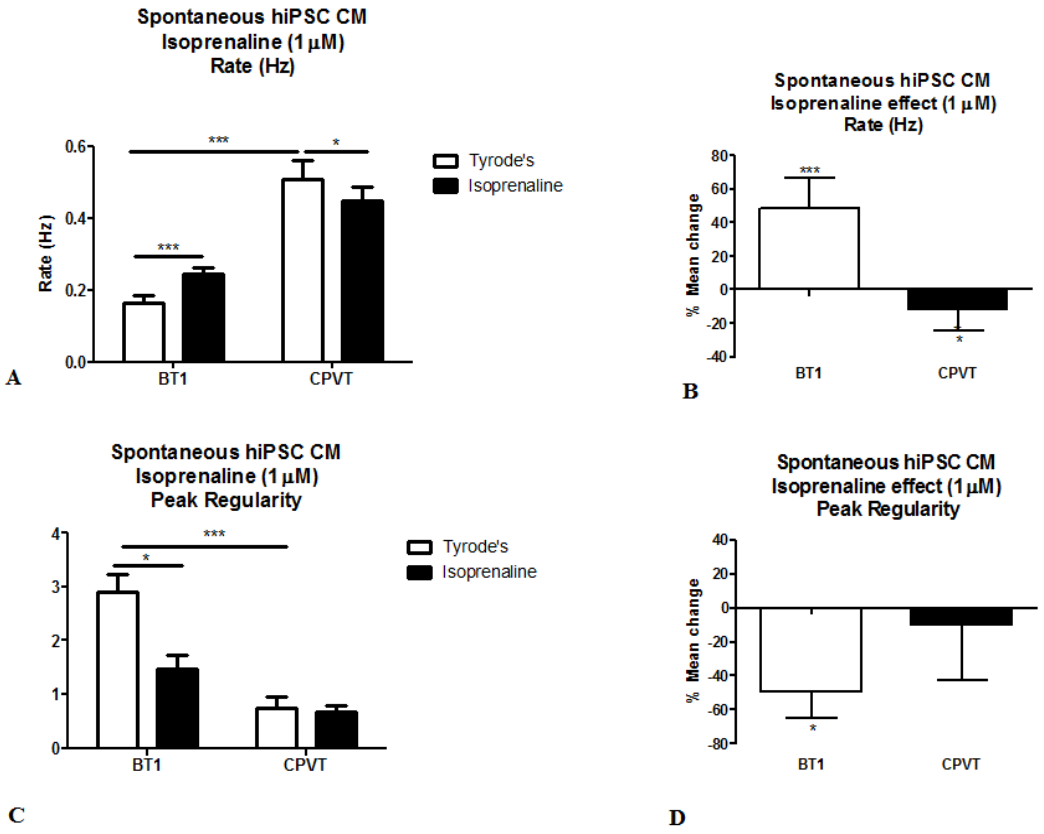

Figure 4.21 – Spontaneous Ca^{2+} transient parameters, Rate (Hz) (A) and Peak regularity *(C) with respective isoprenaline (1µM) effect (B and D) in mean percentage change, for hiPSC BT1 CM (n=32) and hiPSC CPVT CM (n=20). Basal beating rate is significantly higher in CPVT CM compared with control CM (figure 4.21A). Although a positive chronotropic response would be expected with ß-agonist perfusion, this was only observed in BT1 CM. A significant decrease in beating rate was observed in CPVT CM, demonstrating a negative chronotropic response of these cells (figure 4.21B). Peak regularity is a rhythmicity parameter in which a near zero value corresponds to a perfectly rhythmic sequence of transients. Data presented in figure 4.21C shows that BT1 CM have significantly higher peak regularity than CPVT CM. Isoprenaline perfusion reduces this parameter significantly by almost 50%, improving the rhythmicity of the control cells. No significant response is seen in mutant cells.*

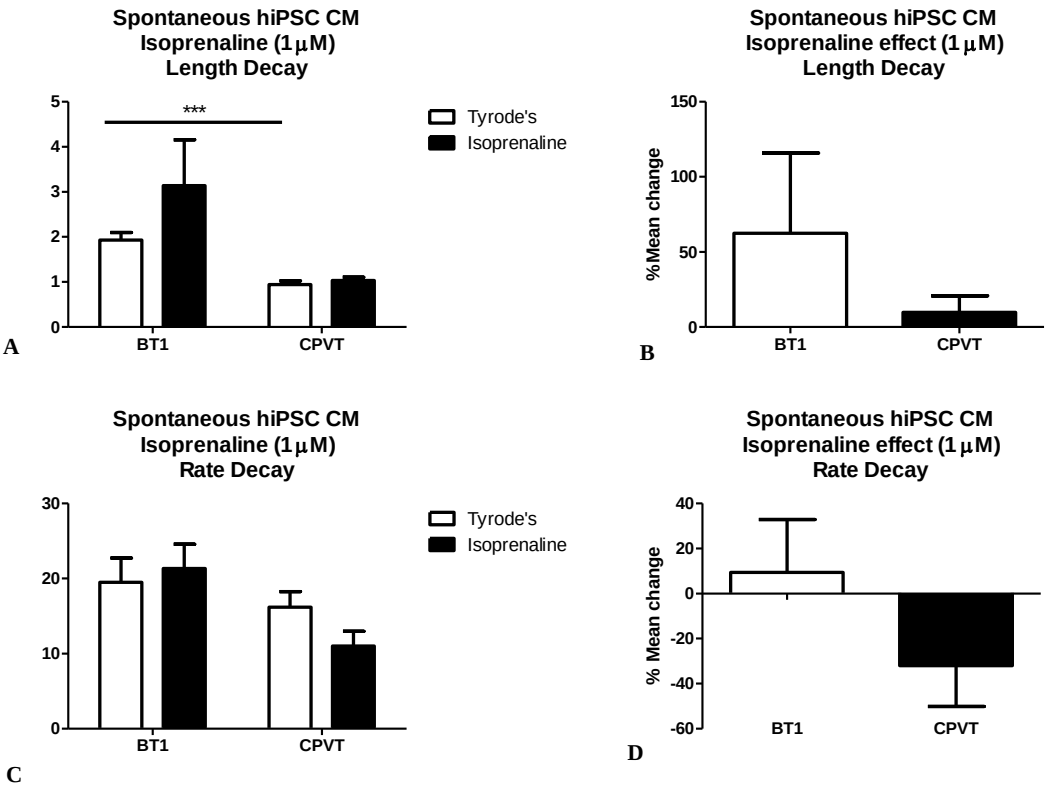

Figure 4.22 – Spontaneous Ca^{2+} transient parameters, Length decay (A) and Rate decay (C) *with respective isoprenaline (1μM) effect (B and D) in mean percentage change, for hiPSC BT1 CM (n=32) and hiPSC CPVT CM (n=20). A statistical significant difference was present in length decay, comparing BT1 CM with CPVT CM in Tyrode's. CPVT CM presented a smaller length decay value (figure 4.22A).*

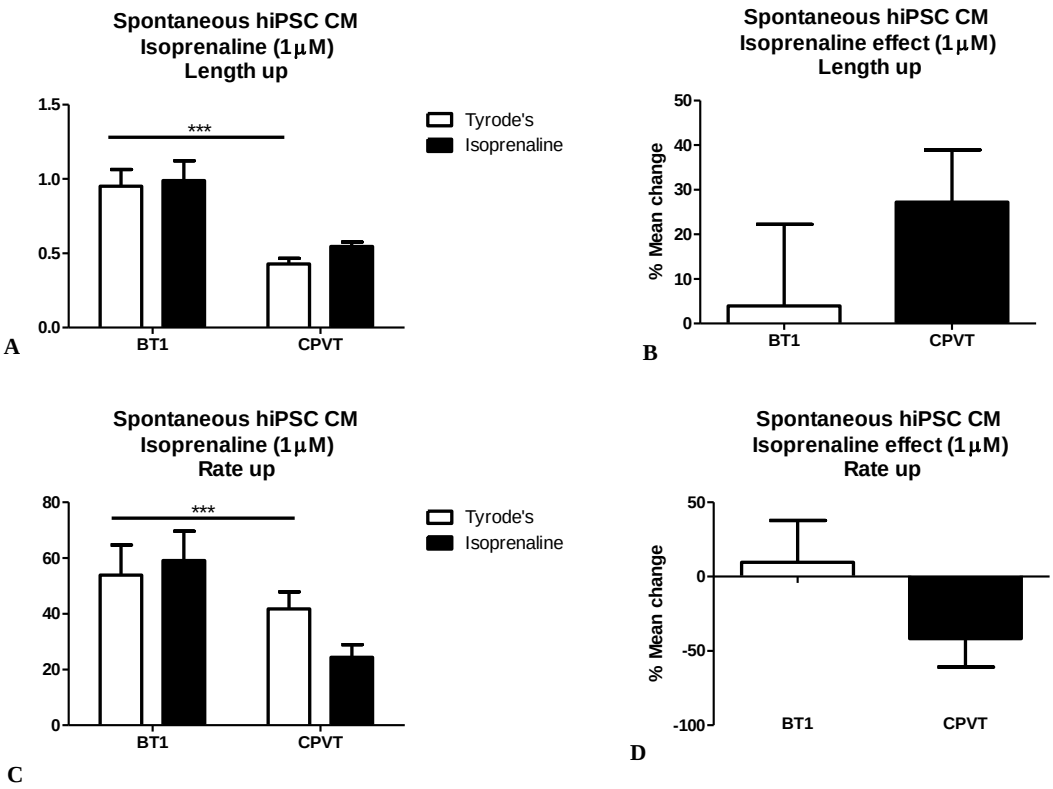

Figure 4.23 – Spontaneous Ca^{2+} transient parameters, Length up (A) and Rate up (C) *with respective isoprenaline (1µM) effect (B and D) in mean percentage change, for hiPSC BT1 CM (n=32) and hiPSC CPVT CM (n=20). A statistical significant difference was present in length up and rate up, comparing BT1 CM with CPVT CM in Tyrode's. CPVT CM presented a smaller length up and rate up value than BT1 CM (figure 4.23A and 4.23C).*

4.5.2 Stimulated Ca^{2+} transients

4.5.2.1 Stimulation 0.5 Hz

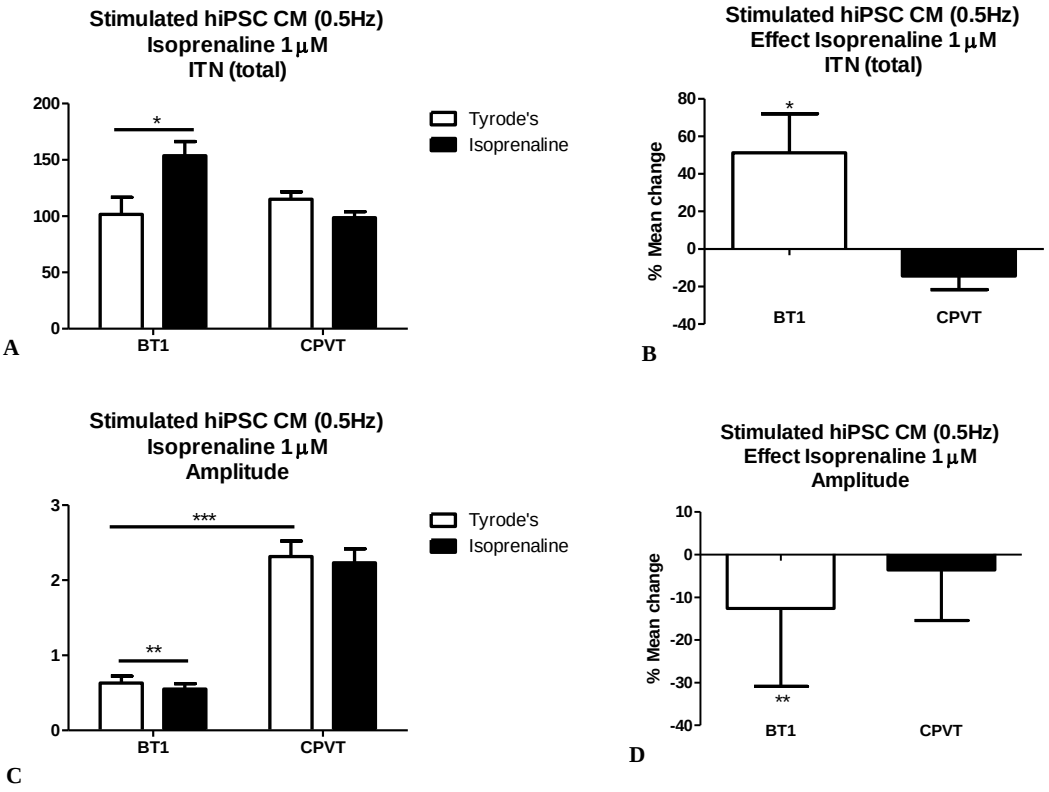

Figure 4.24 – Stimulated Ca^{2+} transient parameters (0.5Hz), ITN (A) and Amplitude (C) *with respective isoprenaline (1μM) effect (B and D) in mean percentage change, for hiPSC BT1 CM (n=18) and hiPSC CPVT CM (n=48). Isoprenaline perfusion caused a significant increase in ITN in BT1 CM while no significant effect was observed in CPVT CM (figure 4.24A).Amplitude of the average Ca^{2+} transients in Tyrode's was significantly higher in CPVT CM when compared with BT1 CM (figure 4.24C). A significant percentage decrease was observed in BT1 CM amplitude when perfused with isoprenaline that could be translated in to a negative inotropic effect. No effect of isoprenaline was observed in CPVT CM (figure 4.24C and D).*

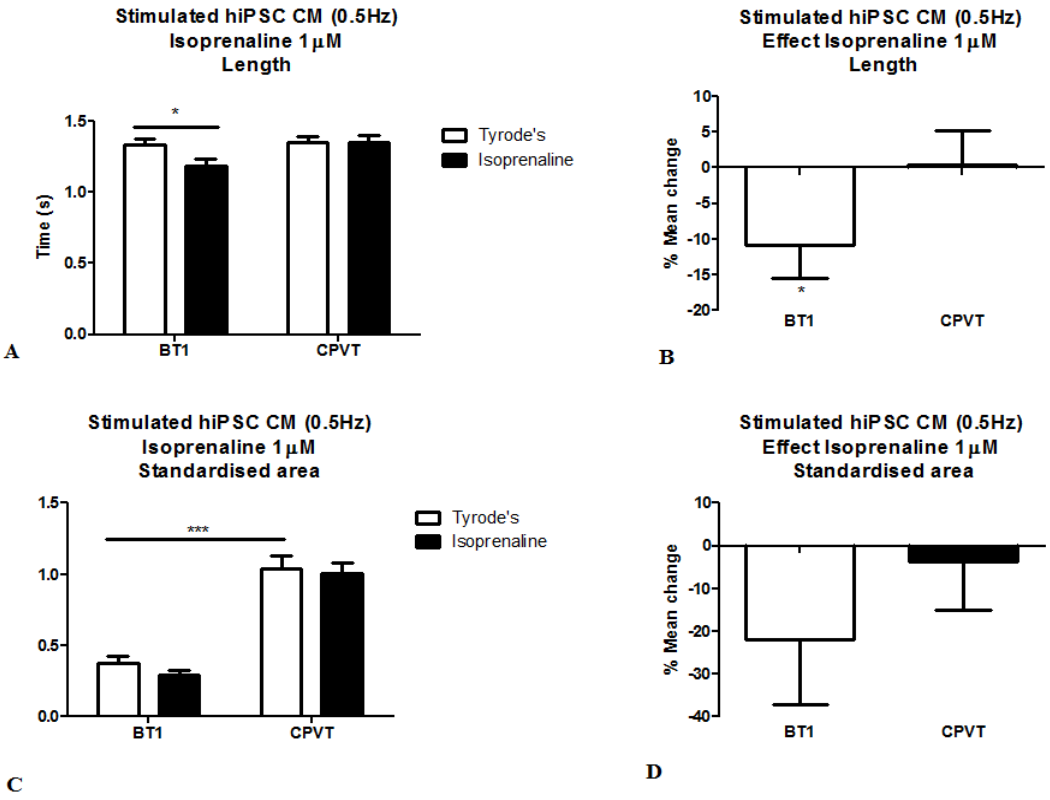

Figure 4.25 – Stimulated Ca^{2+} transient parameters (0.5Hz), Length (A) and Standardised area (C) *with respective isoprenaline (1µM) effect (B and D) in mean percentage change, for hiPSC BT1 CM (n=18) and hiPSC CPVT CM (n=48). A significant decrease in Ca^{2+} transient length in BT1 CM cells upon isoprenaline perfusion was observed (figure 4.25A). CPVT CM present a significant higher value for standardised area compared with BT1 CM in Tyrode's (figure 4.25C)*

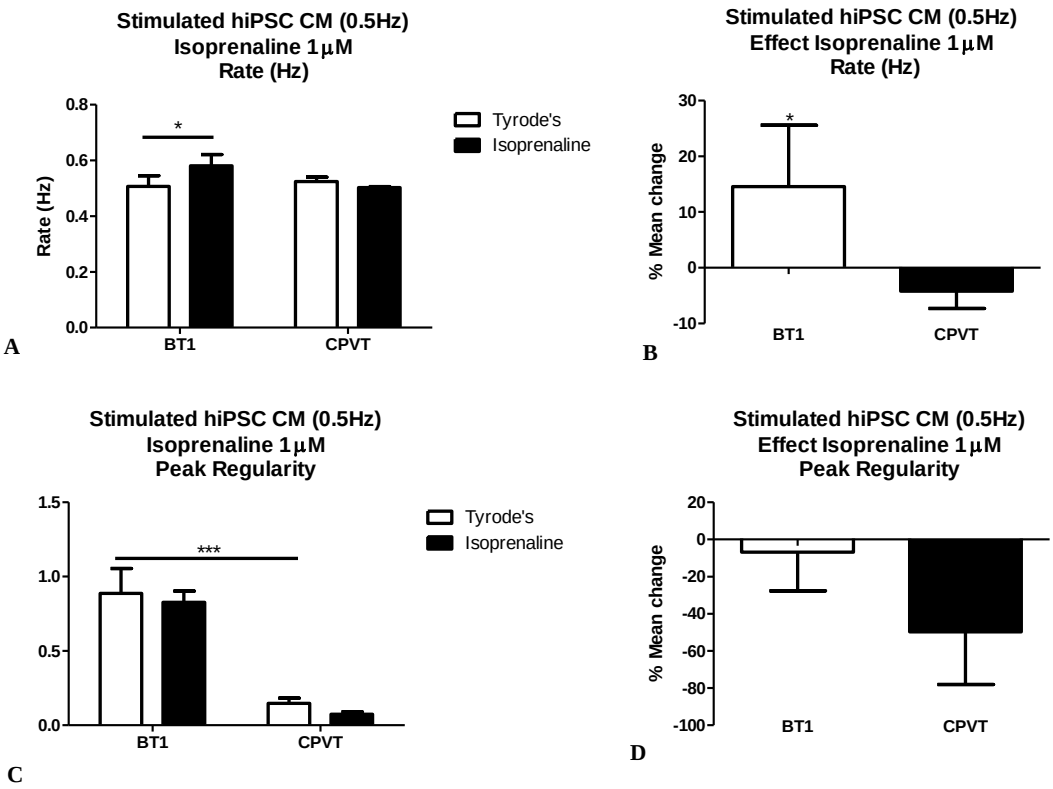

Figure 4.26 – Stimulated Ca^{2+} transient parameters (0.5Hz), Rate (Hz) (A) and Peak regularity *(C) with respective isoprenaline (1µM) effect (B and D) in mean percentage change, for hiPSC BT1 CM (n=18) and hiPSC CPVT CM (n=48). Rate response to 0.5Hz stimulation should be the same as the applied stimulation even when perfused with isoprenaline. CPVT CM and BT1 CM presented an expected 0.5Hz stimulation rate in Tyrode's. However, BT1 CM rate, significantly increased by 15% with isoprenaline perfusion. No significant change in rate was seen on isoprenaline perfusion of CPVT CM (figure 4.26A). Peak regularity value was significantly smaller in CPVT CM compared with BT1 CM in Tyrode's (figure 4.26C).*

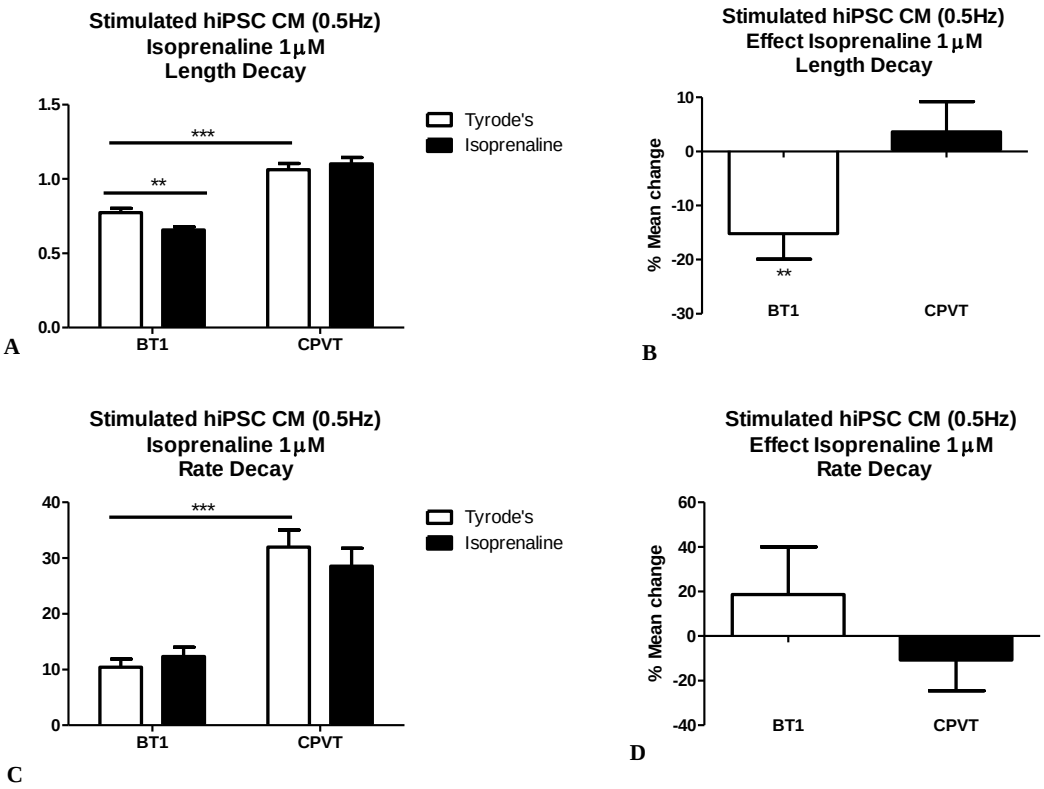

Figure 4.27 – Stimulated Ca^{2+} transient parameters (0.5Hz), Length decay (A) and Rate decay (C) *with respective isoprenaline (1µM) effect (B and D) in mean percentage change, for hiPSC BT1 CM (n=18) and hiPSC CPVT CM (n=48). A significant decrease in length decay is seen in BT1 CM cells upon isoprenaline perfusion. Length decay basal value is significantly higherin CPVT CM compared with BT1 CM (figure 4.27A). Rate decay is significantly smaller in BT1 CM compared with mutant cells in Tyrode's (figure 4.27C).*

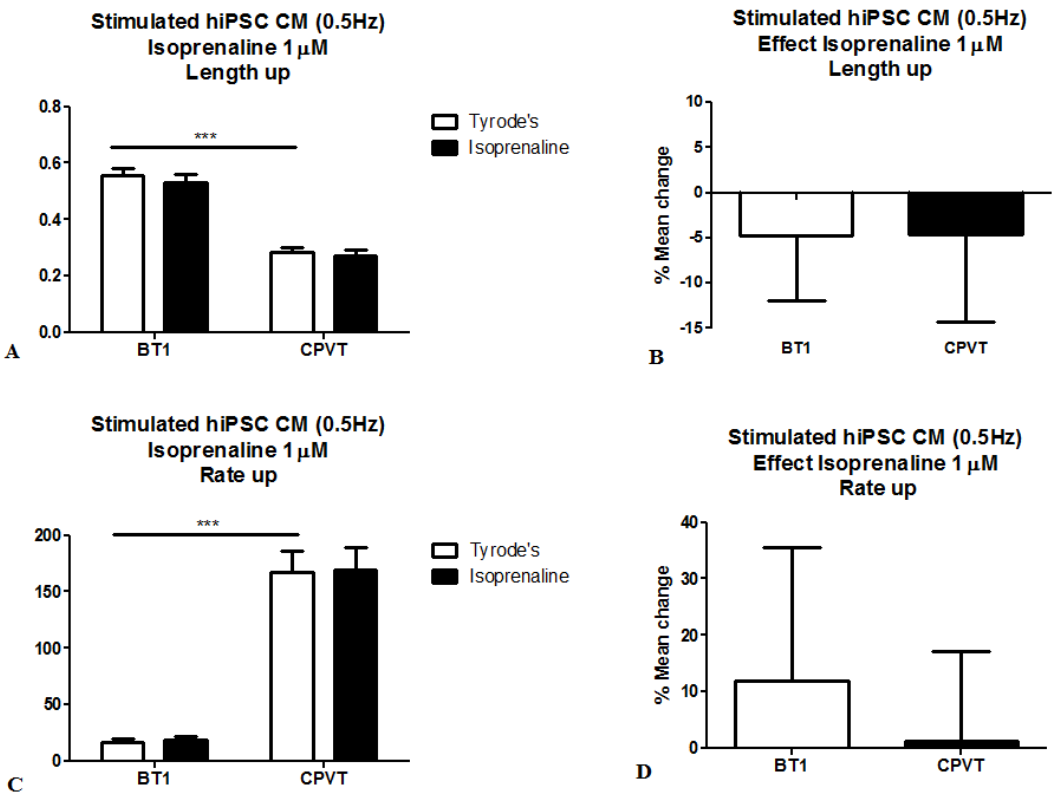

Figure 4.28 – Stimulated Ca^{2+} transient parameters (0.5Hz), Length up (A) and Rate up (C) *with respective isoprenaline (1µM) effect (B and D) in mean percentage change, for hiPSC BT1 CM (n=18) and hiPSC CPVT CM (n=48). A significant smaller value was observed for length up in CPVT CM compared with control CM in Tyrode's (figure 4.28A). Rate up presents a significantly higher value compared with BT1 CM in Tyrode's (figure 4.28C).*

4.5.2.2 - Stimulation 1Hz

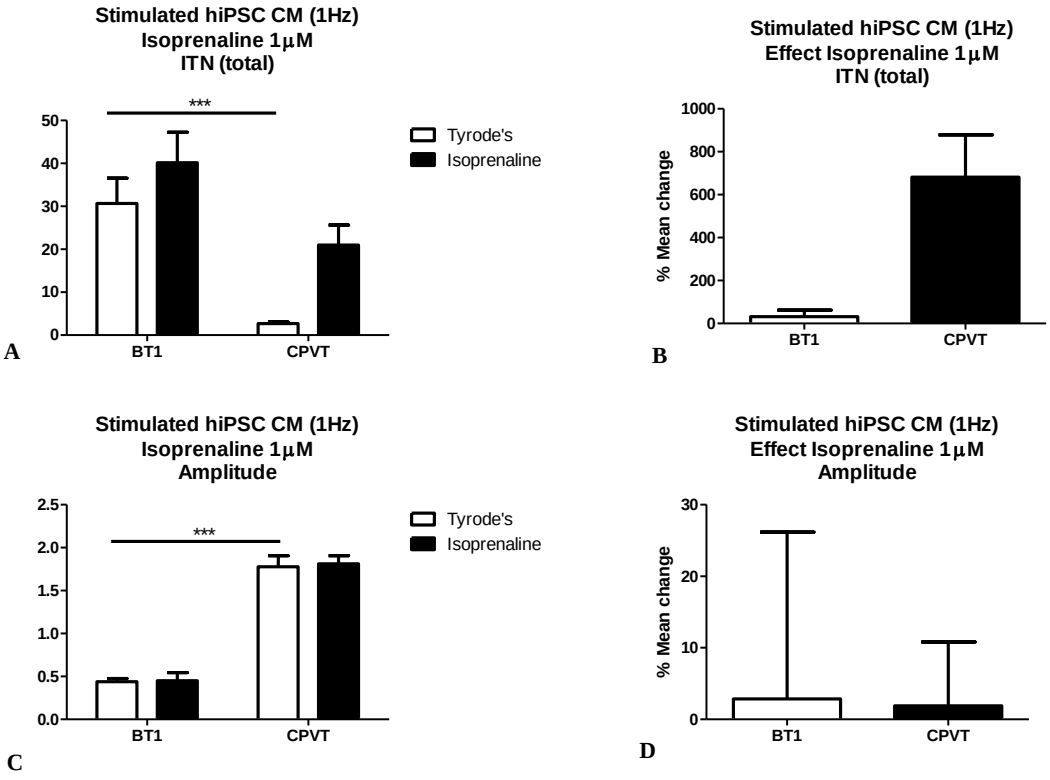

Figure 4.29 - Stimulated Ca^{2+} transient parameters (1Hz), ITN (A) and Amplitude (C) *with respective isoprenaline (1µM) effect (B and D) in mean percentage change, for hiPSC BT1 CM (n=18) and hiPSC CPVT CM (n=40). A significant smaller value was observed for ITN in CPVT CM compared with BT1 CM in Tyrode's (figure 4.29A). BT1 CM presented a significant smaller amplitude average value compared with CPVT CM in Tyrode's (figure 4.29C)*

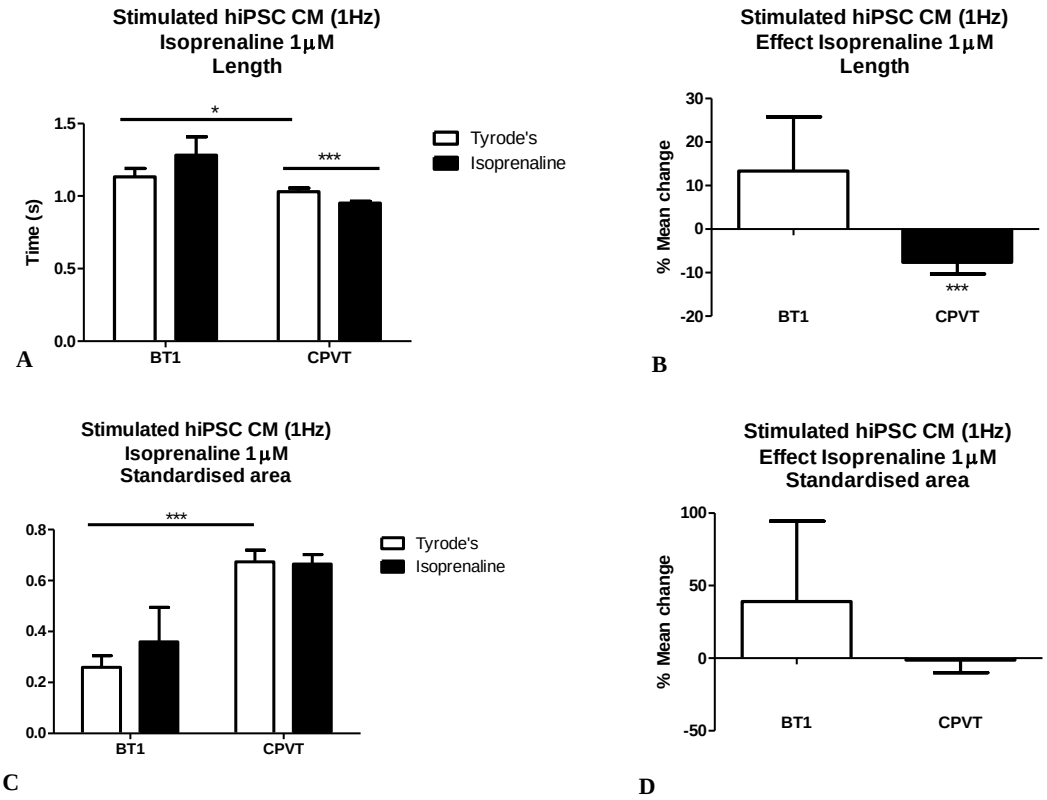

Figure 4.30 – Stimulated Ca^{2+} transient parameters (1Hz), Length (A) and Standardised area (C) *with respective isoprenaline (1µM) effect (B and D) in mean percentage change, for hiPSC BT1 CM (n=18) and hiPSC CPVT CM (n=40). A significant decrease in average transient length in CPVT CM cells upon isoprenaline perfusion was observed. Basal length value is significantly smaller in CPVT CM comparing with BT1 CM (figure 4.30A). BT1 CM standardised area value is significantly smaller in BT1 CM compared with mutant cells in Tyrode's (figure 4.30C).*

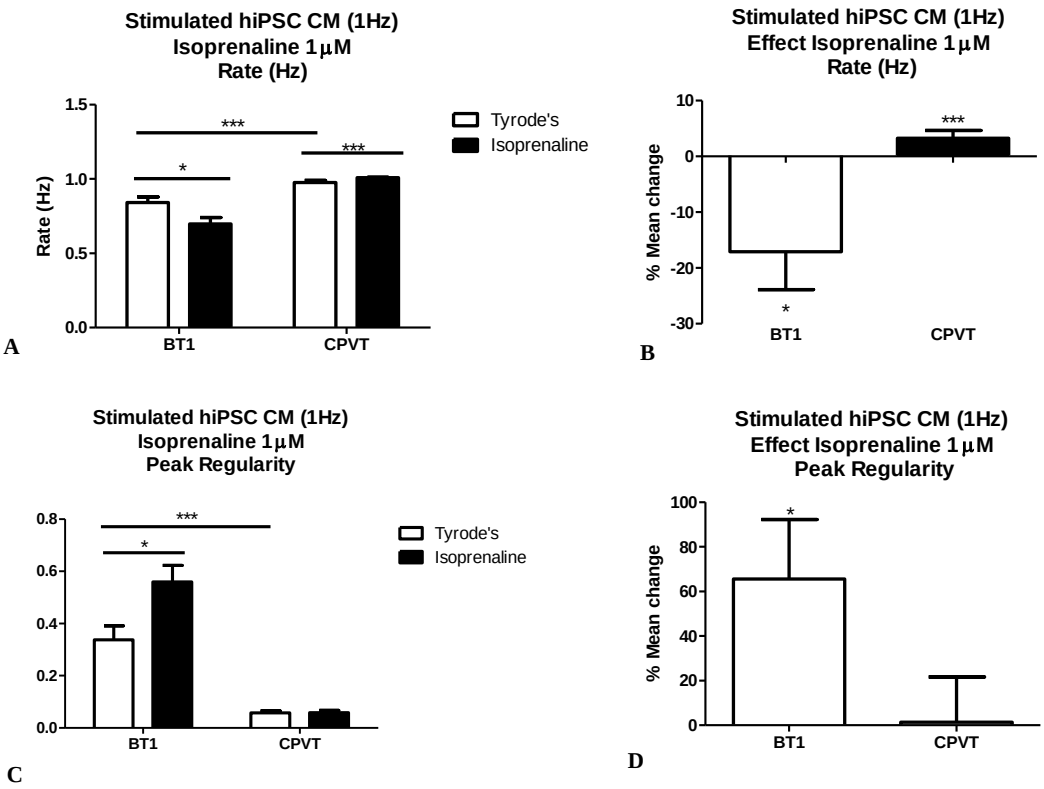

Figure 4.31 – Stimulated Ca^{2+} transient parameters (1Hz), Rate (Hz) (A) and Peak regularity (C) *with respective isoprenaline (1µM) effect (B and D) in mean percentage change, for hiPSC BT1 CM (n=18) and hiPSC CPVT CM (n=40). Beating rate should be 1Hz exactly, since external stimulation was used. CPVT CM presented a very accurate 1Hz stimulation value with a very small significant increase upon isoprenaline perfusion. However the observed rate for BT1 CM is significantly lower than the expected 1Hz. BT1 CM present a significantly lower rate compared with mutant cells in Tyrode's (figure 4.31A). After isoprenaline perfusion, BT1 CM presented a significant increase in peak regularity value, while no effect is seen in CPVT CM. Peak regularity was significantly smaller in CPVT CM comparing with BT1 Cm in basal conditions (figure 4.31C).*

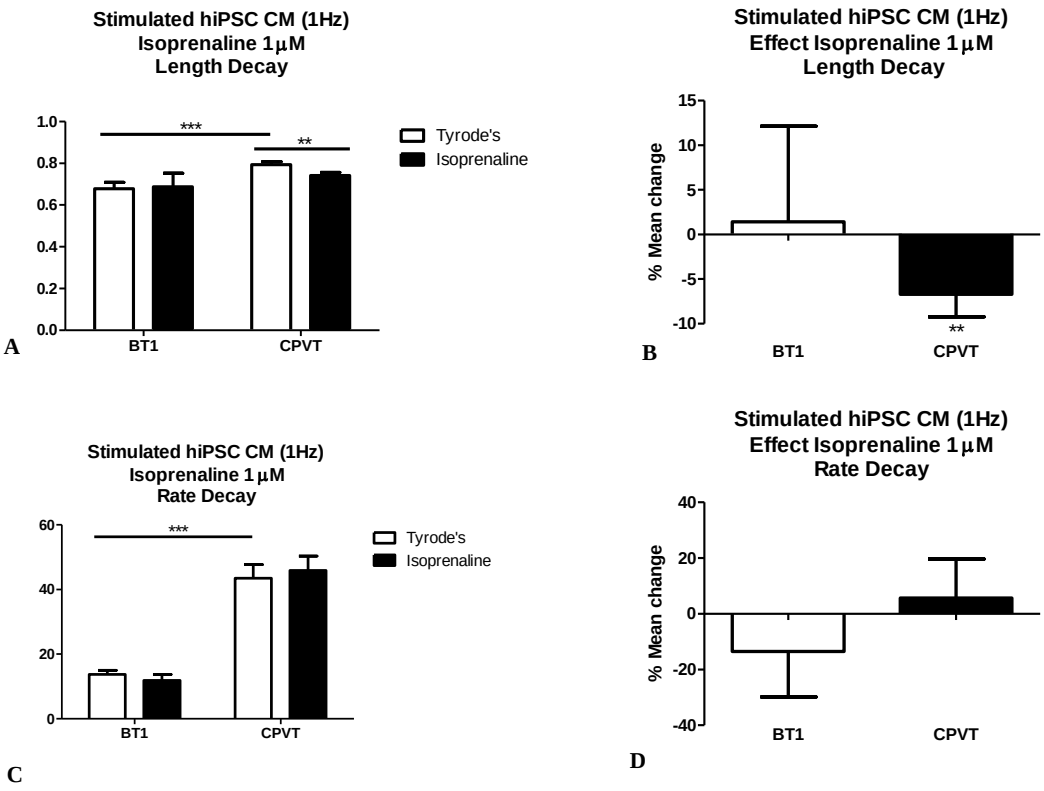

Figure 4.32 – Stimulated Ca^{2+} transient parameters (1Hz), Length decay (A) and Rate decay (C) *with respective isoprenaline (1µM) effect (B and D) in mean percentage change, for hiPSC BT1 CM (n=18) and hiPSC CPVT CM (n=40). A decrease in length decay was observed in CPVT CM cells upon isoprenaline perfusion. BT1 CM presented a significantly smaller legth decay value compared with CPVT CM in basal conditions (figure 4.32A). BT1 CM presents a significantly smaller value of rate decay compared with CPVT CM in Tyrode's (figure 4.32C).*

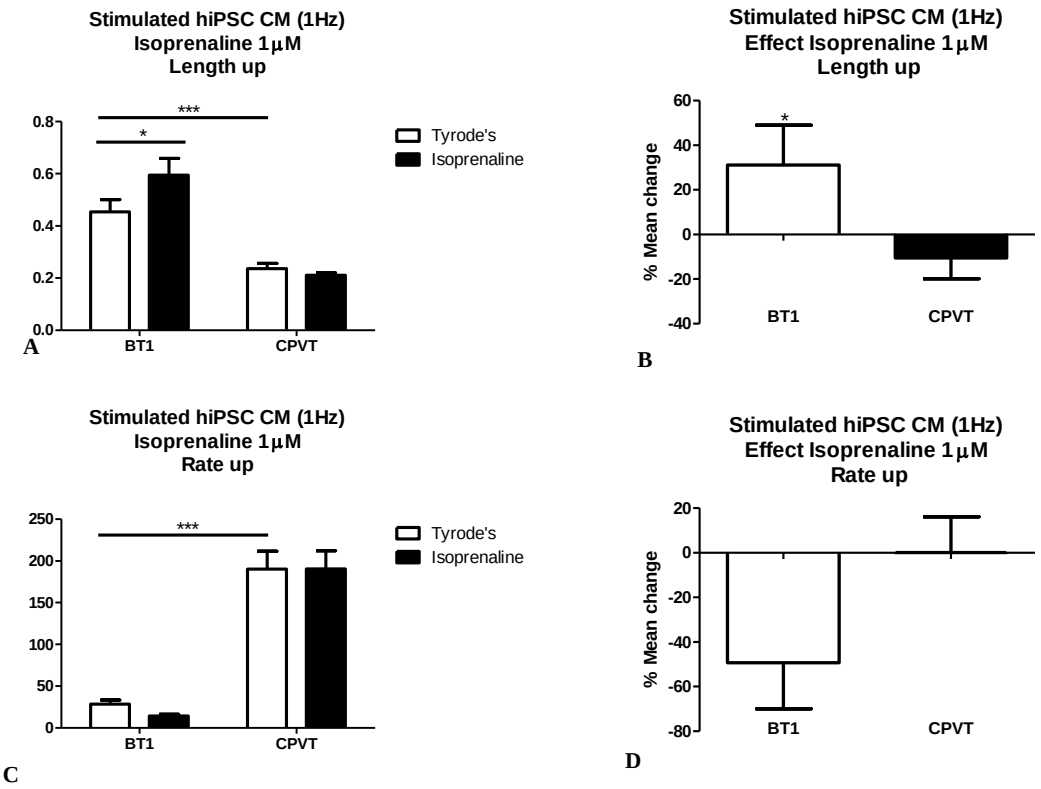

Figure 4.33 – Stimulated Ca^{2+} transient parameters (1Hz), Length up (A) and Rate up (C) *with respective isoprenaline (1µM) effect (B and D) in mean percentage change, for hiPSC BT1 CM (n=18) and hiPSC CPVT CM (n=40). An increase in length up in BT1 CM cells upon isoprenaline perfusion found. CPVT CM presents a significant smaller length up value compared with BT1 CM in Tyrode's (figure 4.33A). BT1 CM presented a very significant smaller rate up value compared with CPVT CM in basal conditions (figure 4.33C).*

4.6 Force-frequency study

A positive force-frequency relationship, evaluated by amplitude response to an increase in frequency of stimulation is an adult human cardiac characteristic (Pieske et al.,1999), but is not seen in rat and mice, in which a negative staircase response is present (Maier et al.,2000).

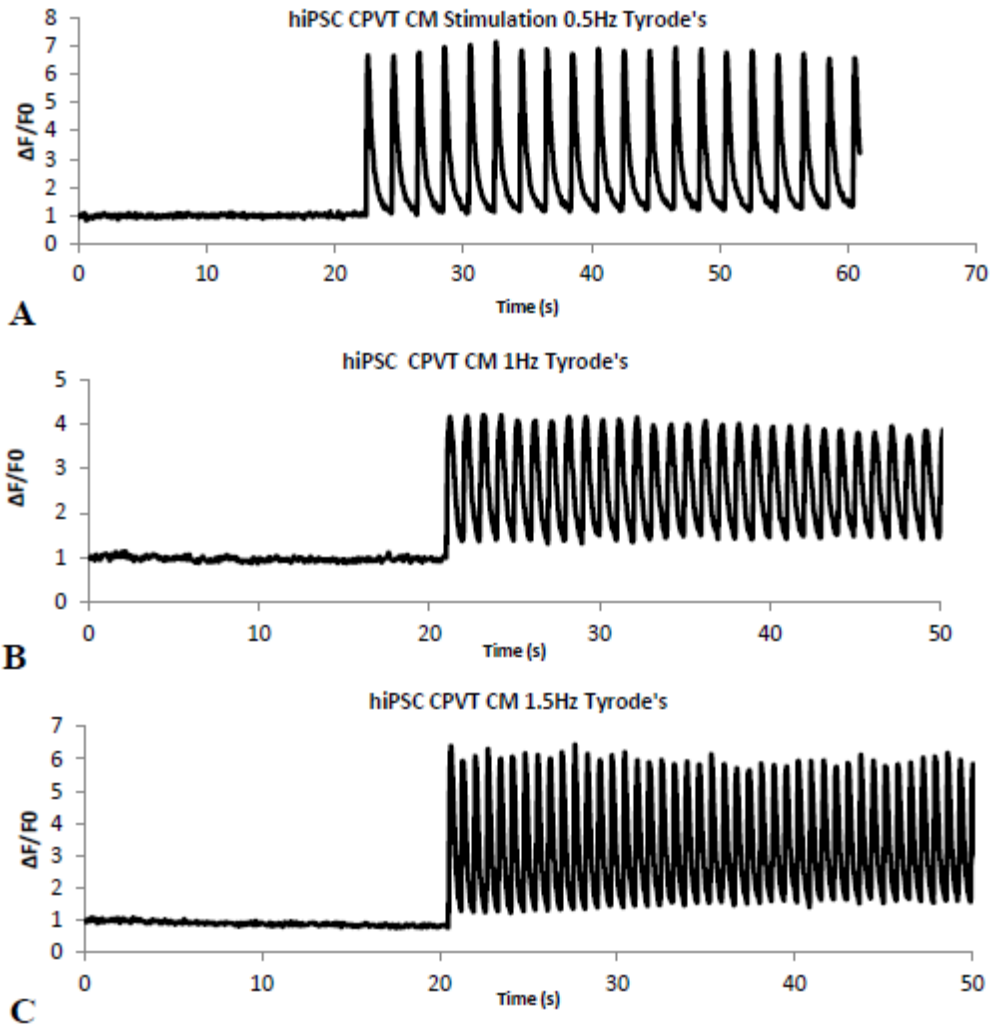

Figure 4.34 – Field stimulated example traces of Ca^{2+} transients *- traces from initially quiescent hiPSC CPVT CM at different stimulated frequencies (0.5Hz) (A), (1Hz) (B) and (1.5Hz) (C) in Tyrode's. Data for force-frequency study was obtained from similar traces for different pacing stimulation rates.*

Force of contraction is directly associated with a positive inotropic effect. Ca^{2+} transient amplitude increases with CM force of contraction in Newtons. A force-frequency study was performed in order to demonstrate if hiPSC CM have a positive force-frequency relationship. This positive response is a hallmark feature of mature human CM.

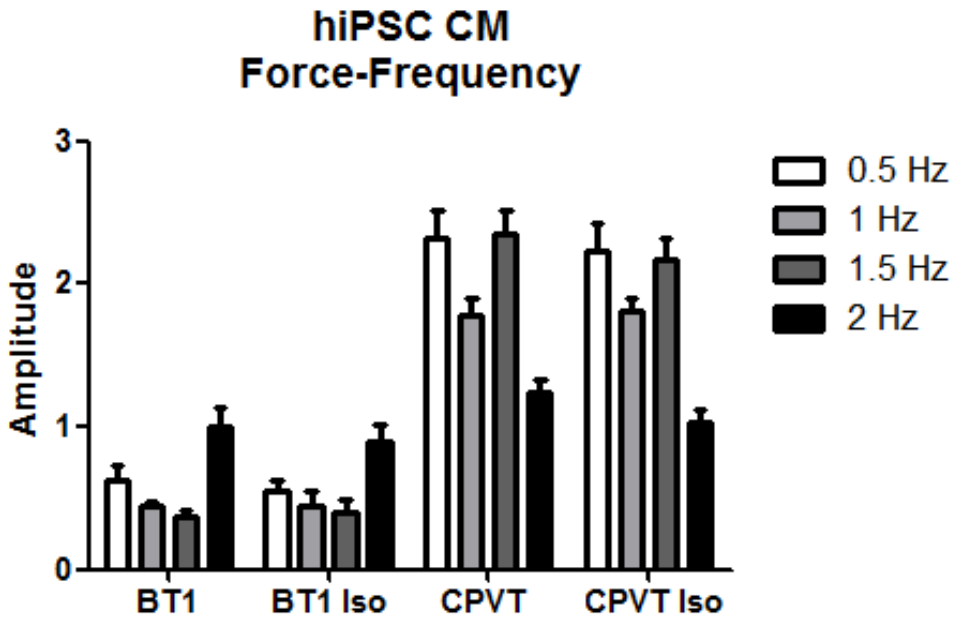

Figure 4.35 – Force-frequency relationship study in hiPSC CM *- data from paced (spontaneous and quiescent) BT1 CM (BT1 CM : 0.5Hz, n=18; 1Hz, n=18; 1.5Hz, n=18; 2Hz, n=16) and CPVT CM (CPVT CM : 0.5Hz, n=48; 1Hz, n=40; 1.5Hz, n=32; 2Hz, n=28), with and without isoprenaline (1μM) perfusion. No statistically significant positive force-frequency response is observed in figure 4.35, for any of the cell types either in the absence or presence of isoprenaline.*

4.7 CICR - Ca^{2+} Induced Ca^{2+} Release

In order to study Ca^{2+} handling in CM the response of cells to the application to specific drugs, with agonist or inhibition properties towards Ca^{2+} handling proteins, is needed.

Nifedipine is a specific L-type calcium channel (LTCC) blocker and as a consequence Ca^{2+} transients should have an amplitude reduction as less Ca^{2+} enters the cell during the AP. Ca^{2+} that enters the sarcoplasm via these ion channels opens RyR2 releasing more Ca^{2+} via CICR, so ryanodine that at 10µM inhibits the ability of RyR2 to open should also produce effective reduction or abolishment of calcium transients by affecting the amplitude or area under the curve by reducing available cytosolic Ca^{2+}.

The RyR2 is also sensitive to caffeine, and perfusion with this drug in the millimolar range should increase the probability of the channel opening and create a large Ca^{2+} transient due to Ca^{2+} release into the sarcoplasm. Using these drugs it's possible to determine if hiPSC derived CM have a functional CICR mechanism that is an intrinsic property of mammalian CM.

Evaluation of SERCA2A function using thapsigargin (a known SERCA inhibitor) was also planned, but due to time constraints these experiments could not be carried out.

4.7.1 Results

Nifedipine perfusion produced a Ca^{2+} transient amplitude significant decrease with both BT1 CM and CPVT CM. Washing out nifedipine with Tyrode's, did not reversed the nifedipine effect in CPVT CM (figure 4.36A). No effect was observed in Ca^{2+} transient amplitude upon ryanodine perfusion (figure 4.37). Caffeine perfusion did not presented a consistent and significant effect in either cell type (figure 4.39A).

In summary, no robust CICR profile was found for either cell type in these experiments.

4.7.2 L-type Ca^{2+} channels – Nifedipine

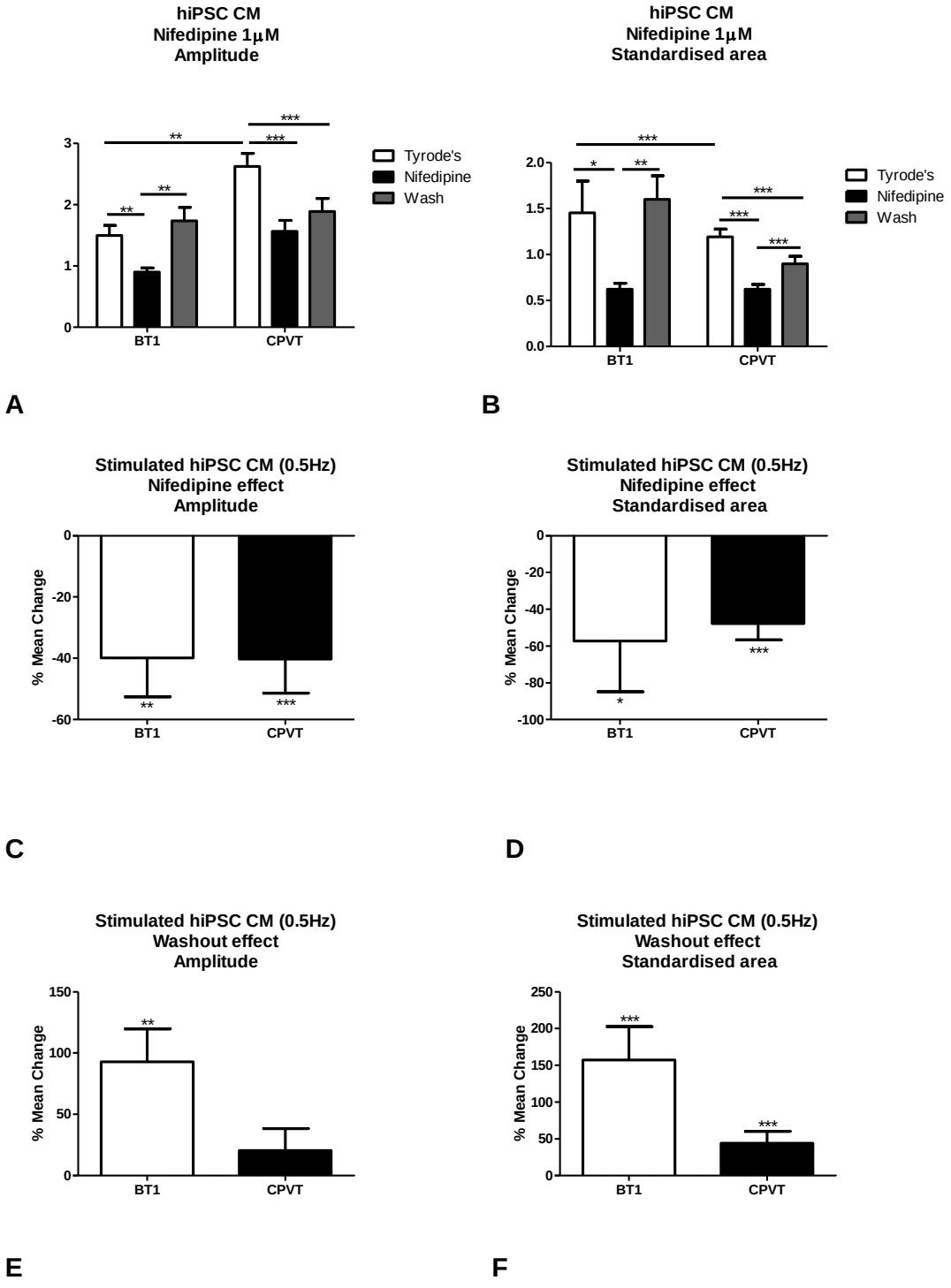

Figure 4.36 –Nifedipine (1µM) effect in stimulated (0.5Hz) *Ca^{2+} transient average, amplitude and standardised area for hiPSC BT1 CM (n=13) and hiPSC CPVT CM (n=23). Average Ca^{2+} transient amplitude presented a significant decrease with nifedipine (1µM) perfusion in both BT1 CM and CPVT CM (figure 4.36A). Washing out nifedipine with Tyrode's, caused a significant amplitude increase in control CM but*

not in CPVT CM. A significant decrease in standardised area after nifedipine perfusion, was observed in both cell types (figure 4.44 B). Nifedipine washout caused a significant increase in stardardised area for both cell types (figure 4.36 E). A significant higher amplitude value was observed in CPVT CM compared with BT1 CM in Tyrode's (figure 4.36A). BT1 CM presented a higher standardised area value compared with CPVT CM at basal conditions (figure 4.36B).

Perfusion with nifedipine at 1µM was used as reported by some authors as an optimal inhibitory concentration to LTCC (Harris et al.,2013; Dan et al.,2014). Initially it was planned to study the effect of nifedipine in both stimulated and spontaneous cells, but due to cell batch variability and time constraints, data are presented only from stimulated cells. Because the inhibition of LTCC by nifedipine is reversible, it was decided to washout this drug. This protocol established that its effect was reversible in these cells.

4.7.3 Ryanodine receptor RyR2– Ryanodine

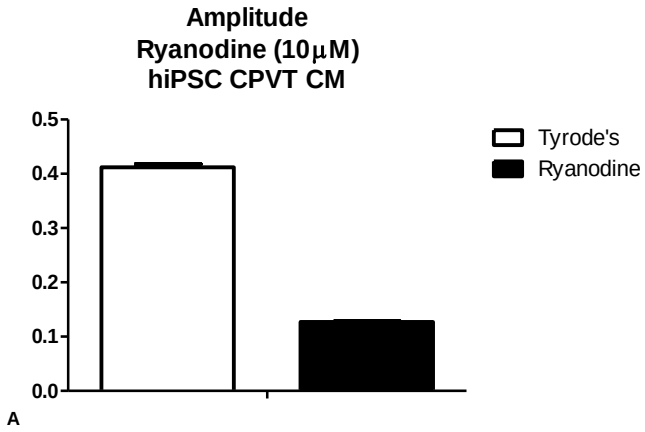

Figure 4.37 – Ryanodine perfusion in average transient amplitude *– data from spontaneous beating hiPSC CPVT CM (n=3) in Tyrode's and in Ryanodine (10µM). The presented differences did not show statistical significance.*

In order to evaluate if CPVT CM possessed functional RyR2, spontaneously beating cells were perfused with 10µM ryanodine (Meissner G.,1986; Satin et al.,2008) in Tyrode's for 5 minutes (figure 4.37A). The experiment could not be repeated in control CM due to time constraints and reduced cell availability.

4.7.4 Ryanodine receptor RyR2 - Caffeine

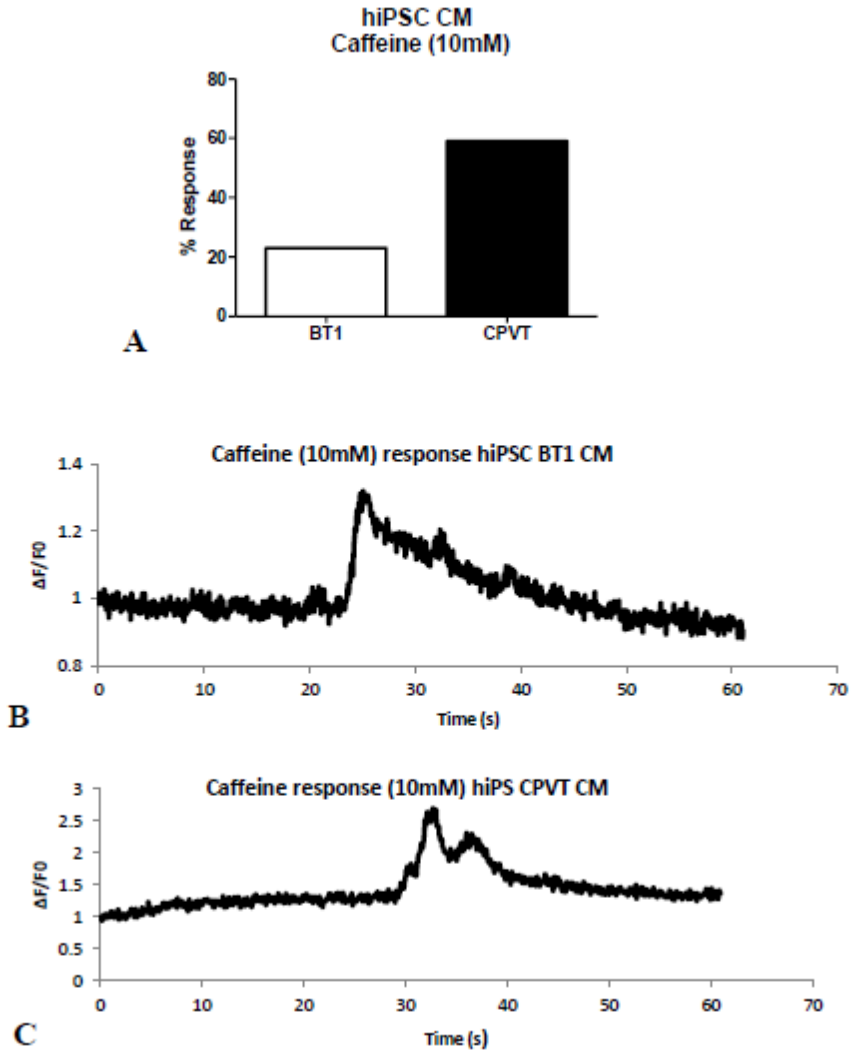

Figure 4.38 –Caffeine response and traces *– percentage of cells tested that produce a transient in response to 10mM caffeine stimulation. A Ca^{2+} wave response to caffeine was considered as being any transient resulting from caffeine perfusion in the absence of spontaneous transients. Spontaneous hiPSC BT1 CM (population of n=68) and hiPSC CPVT CM (population of n=63) (A). Example traces from a single cell caffeine response in hiPSC BT1 CM (B) and a hiPSC CPVT CM (C).*

Caffeine at 10mM (Kong et al.,2008; Satin et al.,2008) was perfused on single CM that presented initial spontaneous activity. Perfusion was only made at the end of each experiment. Example traces do not demonstrate spontaneous activity, as towards the end of the experiments there was a trend for lack of spontaneous activity. This way a confirmation of initial contractile activity was obtained.

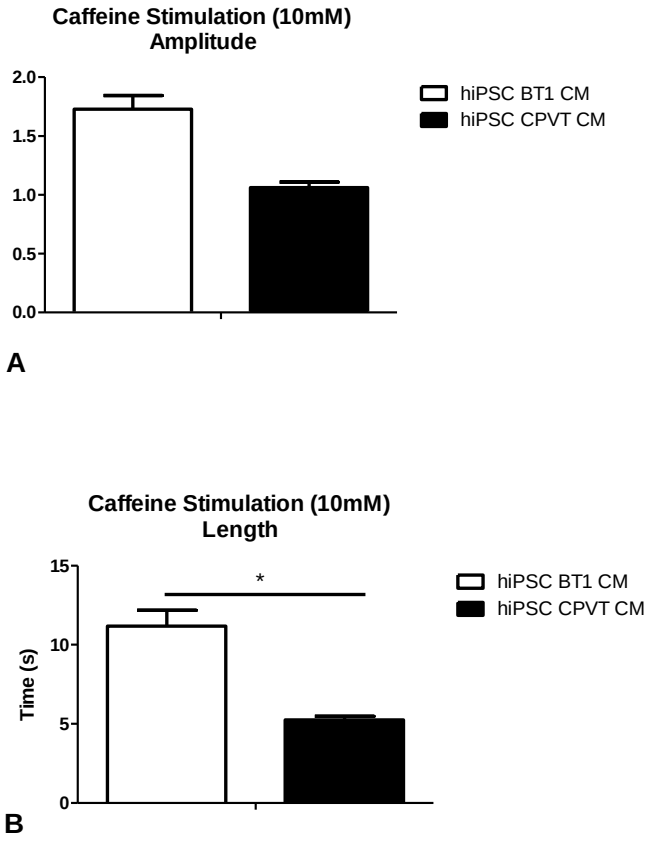

Figure 4.39 –Caffeine response - Mean average amplitude (A) and length (B) *of Ca^{2+} transient release in response to 10mM caffeine stimulation for spontaneous hiPSC BT1 CM (n=16) and hiPSC CPVT CM (n=37). A significantly longer length value was observed in BT1 CM when compared with CPVT CM (figure. 4.39B).*

4.8 Discussion of Ca^{2+} imaging characterisation

In this study an innovative and more detailed Ca^{2+} transient characterisation is presented for the first time in hiPSC derived CM. However, hiPSC BT1 and CPVT CM did not consistently demonstrated classical cardiac properties such as positive inotropy, lusitropy and chronotropy. A force-frequency relationship was also not confirmed by the obtained data. It was also not possible to establish a cardiac typical CICR protein handling profile. Both hiPSC CPVT and BT1 CM did not respond robustly to pharmacological study. A maturation study with hiPSC CM older than 3 months post-differentiation would be necessary to evaluate hiPSC CM cardiac characterisation.

4.9 Conclusion

Based on the data presented in this chapter it is clear that both CPVT and BT1 CM possess some basic cardiac physiological characteristics. However, when challenged, hiPSC CM do not always respond consistently. This will undoubtedly be a problem to overcome if hiPSC are to be used as *in vitro* models of disease. My data suggest that the electrophysiological features presented by these cells are not those of an adult CM. Lack of consistent positive inotropy and lusitropy are also features of foetal CM. Because for *in vitro* CPVT modelling, adult-like ventricular CM would be ideal, further efforts must be made to mature and select hiPSC CM sub-types. By increasing culture time, using selective factors or even transgenic technology, hiPSC CM should present a consistent, adult-like, ventricular profile to model CPVT in the near future.

Chapter 5

hiPSC derived CM *in vitro* CPVT1 model of disease

5.1 Introduction

The main objective of this project is to test the hypothesis that it is possible to recapitulate CPVT1 *in vitro*, using patient specific hiPSC derived CM. It is hypothesised that either pharmacological challenge with catecholamines, or increased pacing should elicit arrhythmic events (DADs, EADs). The use of anti-arrhythmic drugs (flecainide, propranolol, dantrolene, proprafenone), in the presence of such ß-agonist, should rescue or reduce any pro-arrhythmic presented behaviour.

The patch clamping technique was used to study spontaneous and evoked AP as well as CPVT hallmark arrhythmogenic events (DADs). AP parameter characterisation, under the effect of the drug in the presence of ß-agonist, was also made, (AP peak, amplitude, APD50 and APD90). Ca^{2+} fluorescent imaging was used to study Ca^{2+} handling and pro-arrhythmic Ca^{2+} transient behaviour.

To date, no similar studies have been published regarding hiPSC CPVT1 derived CM, containing the S2246L RyR2 mutation. Additionally, only a few publications (Jung et al.,2011; Fatima et al.,2011; Itzhaki et al.,2012; Kujala et al.,2012; Di Pasquale et al.,2013) have demonstrated the cardiac disease modelling potential of hiPSC CPVT CM with different mutations. If confirmed, CPVT1 *in vitro* recapitulation, could not only allow disease specific drug screening and discovery, but also open a new field in personalised therapy for this malignant inherited channelopathy.

There have been a number of publications describing different *in vitro* models of cardiac disease since 2011 (i.e.: Matsa et al., 2011; Novak et al., 2012; Terrenoire et al., 2013). However, due to the practical issues and cell culture complexity that creating and optimizing hiPSC culture bring, these publications focus mainly on CM production and the differentiation process. Although present in every publication, functional characterisation of patient specific hiPSC CM has been neglected over developmental studies. Reported functional studies frequently present a low number of studied cells or EBs (Novak et al.,2001; Itzhaki et al.,2012; E Di Pasquale et al.,2013).

Regarding electrophysiology studies to replicate disease *in vitro*, using the patch clamp technique, different approaches have been published. However arrhythmic endpoints and selected criteria are not well defined in the majority of publications and are often qualitative (Itzhaki et al.,2011; Kujala et al.,2012; E Di Pasquale et al.,2013). Despite the fact that most of these reports lack quantitative analysis of arrhythmic endpoints, the majority conclude that patient specific hiPSC CM are good *in vitro* models of disease.

5.2 Validation by patch-clamping

Functional electrophysiological characterisation and pharmacological challenge of CPVT hiPSC CM is essential to address the postulated hypothesis of recapitulating disease *in vitro*. Use of the patch-clamp technique in single cells is required to assess disease modelling potential. The classical arrhythmic hallmark of CPVT are DAD events which can only be detected by analysing the cell AP. However EADs events can also occur in CPVT, despite being more typical in LQT syndromes (Kujala et al., 2012). DADs can progress to full-triggered activity events (TA) which can be translated into extra-systoles.

One of the conventional explanations for DAD formation in CPVT1 is related to an intracellular Ca^{2+} overload, known as SOICR (Storage Overload Induced Calcium Release). SOICR can activate the Na-Ca exchanger (NCX). This membrane protein facilitates the exchange of these two ions (3 Na^{+} for 1 Ca^{2+}) so that when Ca^{2+} is in excess in the cytosol it can be extruded from the cell, creating at the same time an inward Na^{+} current, generating an inappropriate cell depolarization. This depolarization can then trigger a DAD or TA. A number of conditions can contribute to SOICR such as ß-adrenergic stimulation, digitalis toxicity, elevated extracellular Ca^{2+} concentration and fast pacing.

5.2.1 Electrophysiology and CPVT1 *in vitro* disease recapitulation

In the first publication regarding CPVT1 hiPSC derived CM, Fatima et al. (2011) observed that all analysed control derived CM (both hESC and hiPSC) presented positive chronotropy and no arrhythmic endpoints when perfused with isoprenaline, a ß-agonist. In contrast approximately 58% of CPVT hiPSC derived CM presented negative chronotropy and 34% presented after depolarization events. All of the electrophysiology experiments were conducted in cells with spontaneous activity and no evoked activity experiments were mentioned.

In 2012, Kujala et al. also published data on hiPSC CPVT1 CM with the RyR2 mutation P2328S. This group reported that these cells not only present DADs but also EADs as a pro-arrhythmic hallmark in the presence of ß-agonists. In this study the authors also defined DADs and EADs as events >3% of the previous AP, but no quantitative data were presented. For this endpoint the cells were all spontaneously beating and experiments conducted at 37ºC. Although the authors mention criteria to define EADs and DADs, it seems difficult to measure these events objectively based on the

percentage of the previous AP. This is particularly difficult in the case of EADs which occur during repolarization. DADs were observed in 42% of spontaneous contracting mutant cells while only 19% of control cells presented similar arrhythmogenic abnormalities. For this mutation of CPVT1 CM paced cells didn't present an increase in DADs compared with spontaneous activity.

5.2.1.2 Electrophysiology for drug screening

One of the potential uses of CPVT hiPSC derived CMs is personalised and disease specific drug screening.

Jung et al.,2012 took advantage of this use to study the effect of dantrolene in hiPSC CPVT derived CM carrying the N-terminal RyR2 single point mutation S406L. CM used in this study were matured for 3-4 months and the authors report a similar percentage of ventricular CM sub-type (70-80%) using not only the AP signature from patch clamp experiments, but also ICC labelling for ventricular myosin light chain (MLC2v). This time, only quiescent cells were selected for dantrolene patch clamp experiments, and no difference in resting membrane potential was observed in mutant and control cells. The authors mention that 56% of control cells didn't present after depolarizations after stopping 1Hz pacing (compared to 88% of CPVT cells). This means that presumably 44% of control ventricular cells did present arrhythmogenic behaviour, such as DADs and TA. Interestingly, dantrolene at 10µM apparently abolished arrhythmogenic activity in all CPVT investigated cells but the efficacy of this drug in control cells was unreported. The authors also reported that CPVT CM exhibited not only more DADs, but also a higher incidence of spontaneous activity after the end of pacing stimulation. The percentage or number of cells that responded to dantrolene perfusion is not reported and it is not clear whether in these experiments a ß-agonist was used to induce the CPVT phenotype. However, for the first time, some efficacy using dantrolene as an anti-arrhythmic agent is reported using hiPSC CPVT CM.

Another emergent drug used to treat some patients with CPVT is flecainide, an anti-arrhythmic class 1c that is also a $I_{(Na)}$ blocker. This drug apparently confirmed treatment potential using hiPSC derived CM, as demonstrated by Itzhaki et al.,2012. In this study approximately 69% of hiPSC CPVT CM presented DADs compared with 11% of control cell when perfused with 1µM isoprenaline.

The current literature concerning CPVT hiPSC CM, lacks consistent protocols for quantitative analysis of arrhythmic endpoints, namely DADs. Arrhythmic or abnormal Ca^{2+} handling reports using fluorescent Ca^{2+} imaging techniques also frequently lack report of quantitative endpoints (Jung et al.,2012;Itzhaki et al.,2012; Kujala et al.,2012). When reported, Ca^{2+} imaging endpoint quantification was confined to localised Ca^{2+} release events termed calcium "sparks" (Fatima et al.,2011; Jung et al.,2012).

Quantification of arrhythmic endpoints in hiPSC CPVT CM clearly needs to be addressed in order to validate any hiPSC CPVT CM model of disease. In this chapter, using patch clamp and Ca^{2+} fluorescent imaging techniques, a quantitative and qualitative approach is reported for hiPSC CPVT CM in the studied mutation. Qualitative analysis was also performed to compare global validation of hiPSC CPVT CM with quantitative analysis of arrhythmic endpoints. The main objective is to determine if hiPSC CPVT CM recapitulate disease *in vitro* by using an innovative approach regarding determination of quantitative arrhythmic endpoints.

5.3 Electrophysiology Methods

For more detailed methods for electrophysiology drug trials, please refer to section 2.3 of Chapter 2.

Whole single cell recordings in the current-clamp mode, using the rupture membrane modality, was used to study both spontaneous and evoked action potentials. Each trial started with one Gap-free mode protocol and then three current clamp protocols, with subsequent exposure to drugs. RMP was clamped at -80mV in the three current clamp protocols.

Spontaneous data was obtained from the initial Gap-free mode protocol and isoprenaline was perfused 1 minute after the Tyrode's only perfusion.

Protocol sequence for drug trial perfusion:

1 – Gap Free mode – Tyrode's,

2 – Current clamp – Tyrode's only,

3 – Current clamp – Tyrode's and isoprenaline (1μM),

4 – Current clamp - Tyrode's and isoprenaline + drug (10μM flecainide, 1μM propranolol, 10μM propafenone or 10 μM dantrolene).

Quantitative endpoints were DADs, defined as any inter AP event with amplitude ≥3mV. Events were analysed within the full length of the trace (the first 50 evoked or spontaneous APs). Evoked APs were obtained from quiescent and spontaneous beating cells.

5.4 Electrophysiology Results

5.4.1 Global quantitative analysis of electrophysiology arrhythmic endpoints

DADs are the primary arrhythmic event in CPVT. In order to test if hiPSC CPVT CM recapitulated the disease phenotype *in vitro*, a quantitative study was undertaken.The quantitative study of arrhythmic endpoints for CPVT, namely DADs, involves the measurement of these events for frequency (events per minute), amplitude (mV) and duration (milliseconds). Although DADs were selected as endpoints for arrhythmogenesis in this project, TA (triggered activity) is also an important arrhythmogenic event that can occur after a DAD. However, since these were very rarely present in these experiments, they weren't included in the quantitative analysis. This data set includes hiPSC CM from all the drug rescue experiments. Data from spontaneous and evoked AP paced at 0.5Hz and 1Hz are included.

No statistical significance was found in the data sets presented for spontaneous, evoked AP at 0.5Hz and evoked AP at 1Hz for DAD frequency, duration and amplitude.

Disease recapitulation could not be established using DADs as arrhythmic endpoint with the patch clamp technique for the current hiPSC CPVT CM model.

5.4.1.1 Spontaneous activity

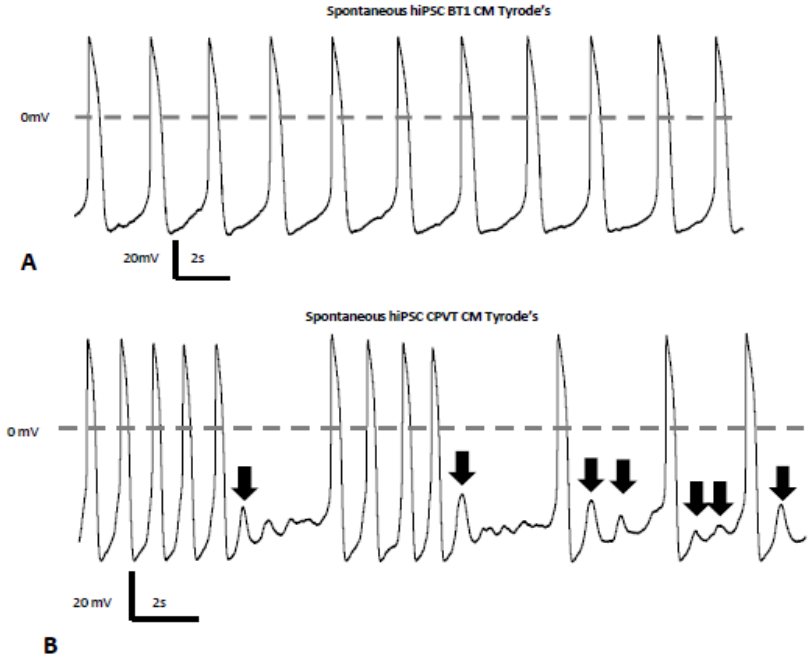

Figure 5.1 – Example traces of spontaneous AP *- hiPSC BT1 CM (A) and hiPSC CPVT CM (B) in Tyrode's. Recording obtained in Gap free mode. Irregular rhythm and DADs (black arrows) are present in mutant cells trace. Circa 40% hiPSC BT1 CM traces presented a DAD absent trace such as seen in figure 6.1A. 90% hiPSC CPVT CM traces presented DADs as seen in figure 5.1B. hiPSC CPVT CM (n=21) and hiPSC Control BT1 CM (n=10).*

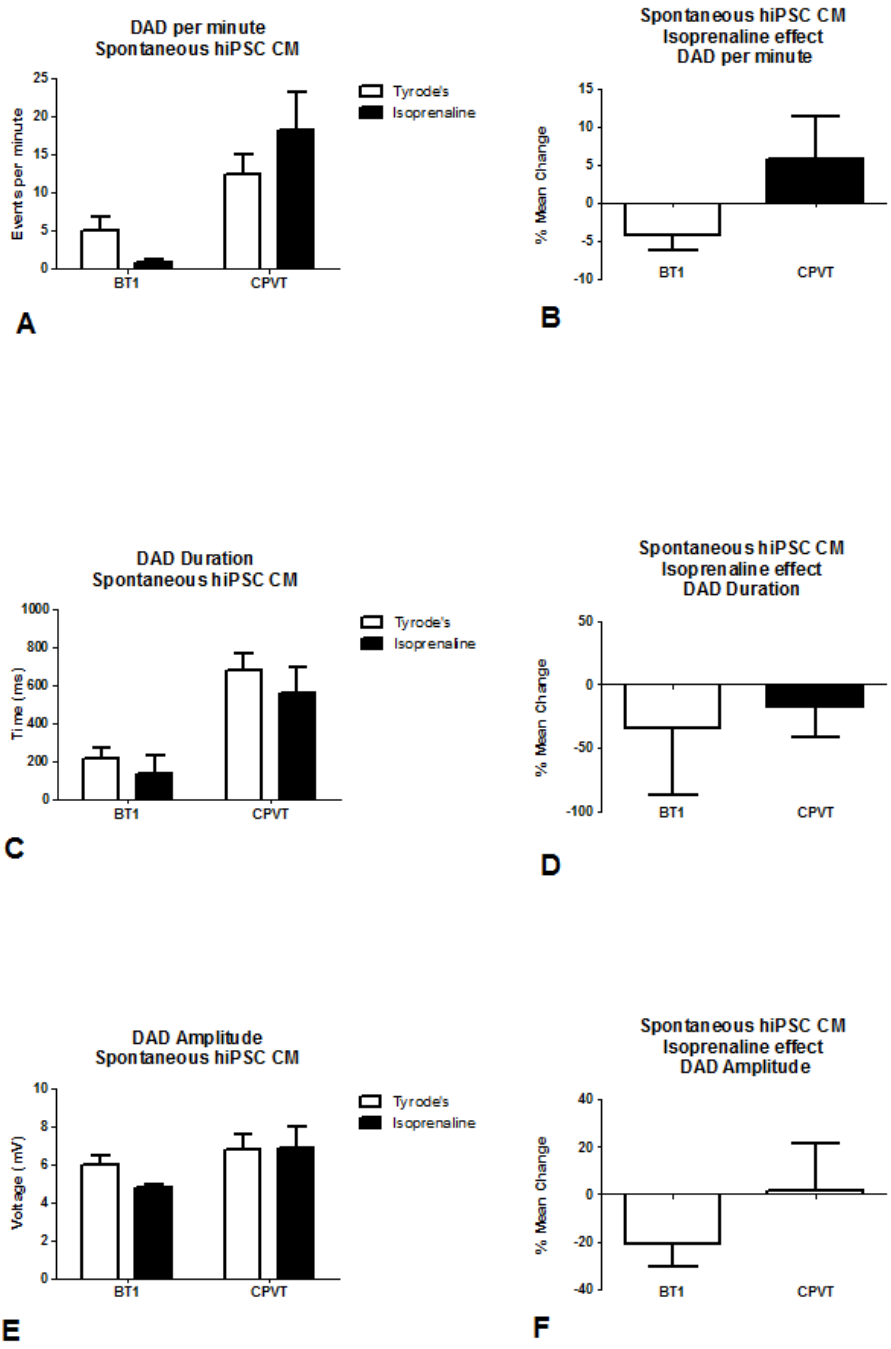

Figure 5.2 - Spontaneous beating hiPSC CM arrhythmic parameters *- DADs frequency - events per minute (A), average DAD duration (C) and average DAD amplitude (E) with respective mean percentage change (B, D, F) for hiPSC CPVT CM (n=21) and hiPSC Control BT1 CM (n=10). None of the differences reported in figure 6.2 were found to be statistically significant.*

5.4.1.2 Evoked activity

5.4.1.2.1 Induced AP 0.5Hz

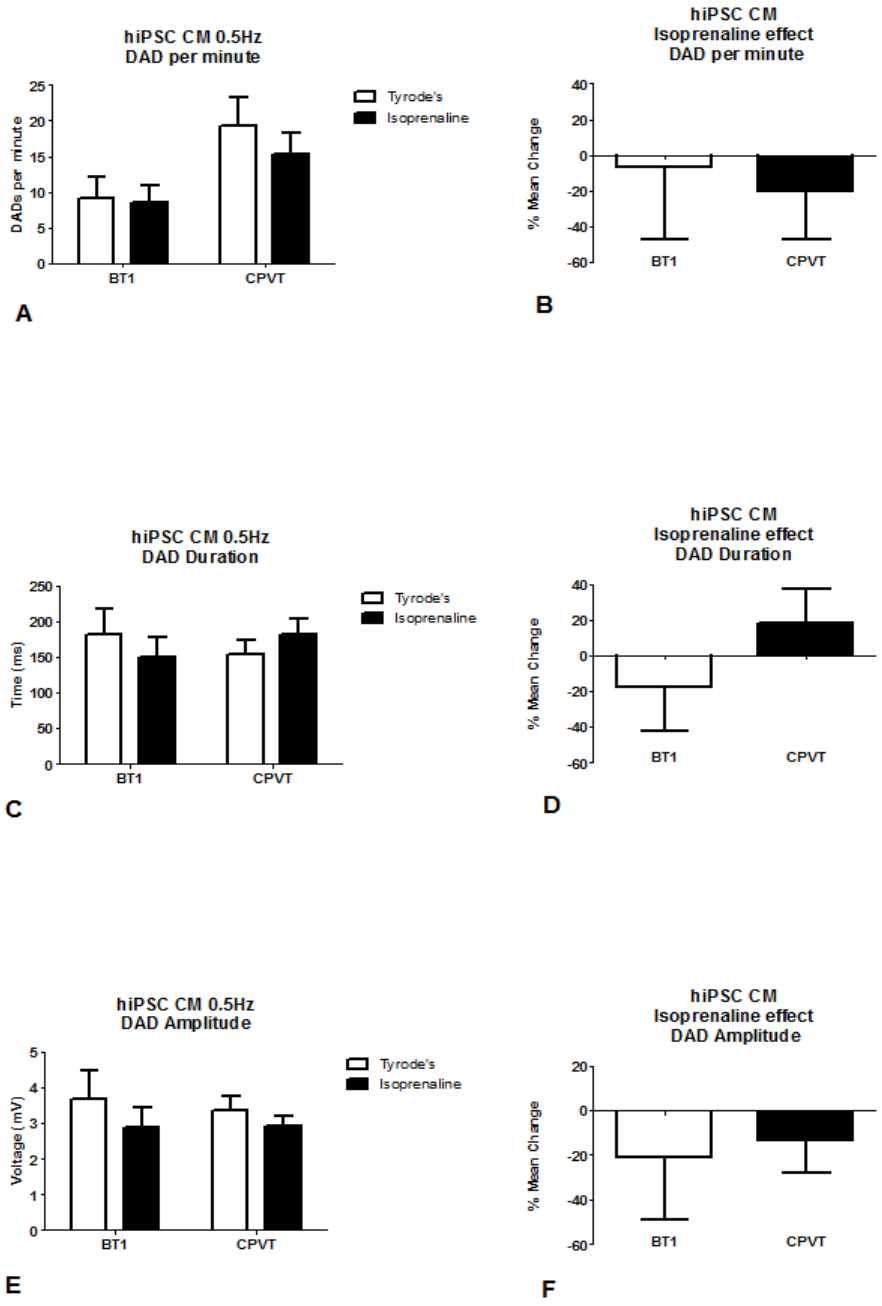

Figure 5.3 – Global arrhythmic endpoints for evoked AP 0.5Hz *- DADs frequency - events per minute (A), average DAD duration (C) and average DAD amplitude (E) with respective mean percentage change (B, D, F). hiPSC CPVT CM (n=58) and control hiPSC BT1 CM (n=27) , from evoked AP at 0.5Hz in Tyrode's and isoprenaline (1µM) perfusion. None of the differences reported in figure 5.3 were found to be statistically significant.*

5.4.1.2.2 Induced AP 1Hz

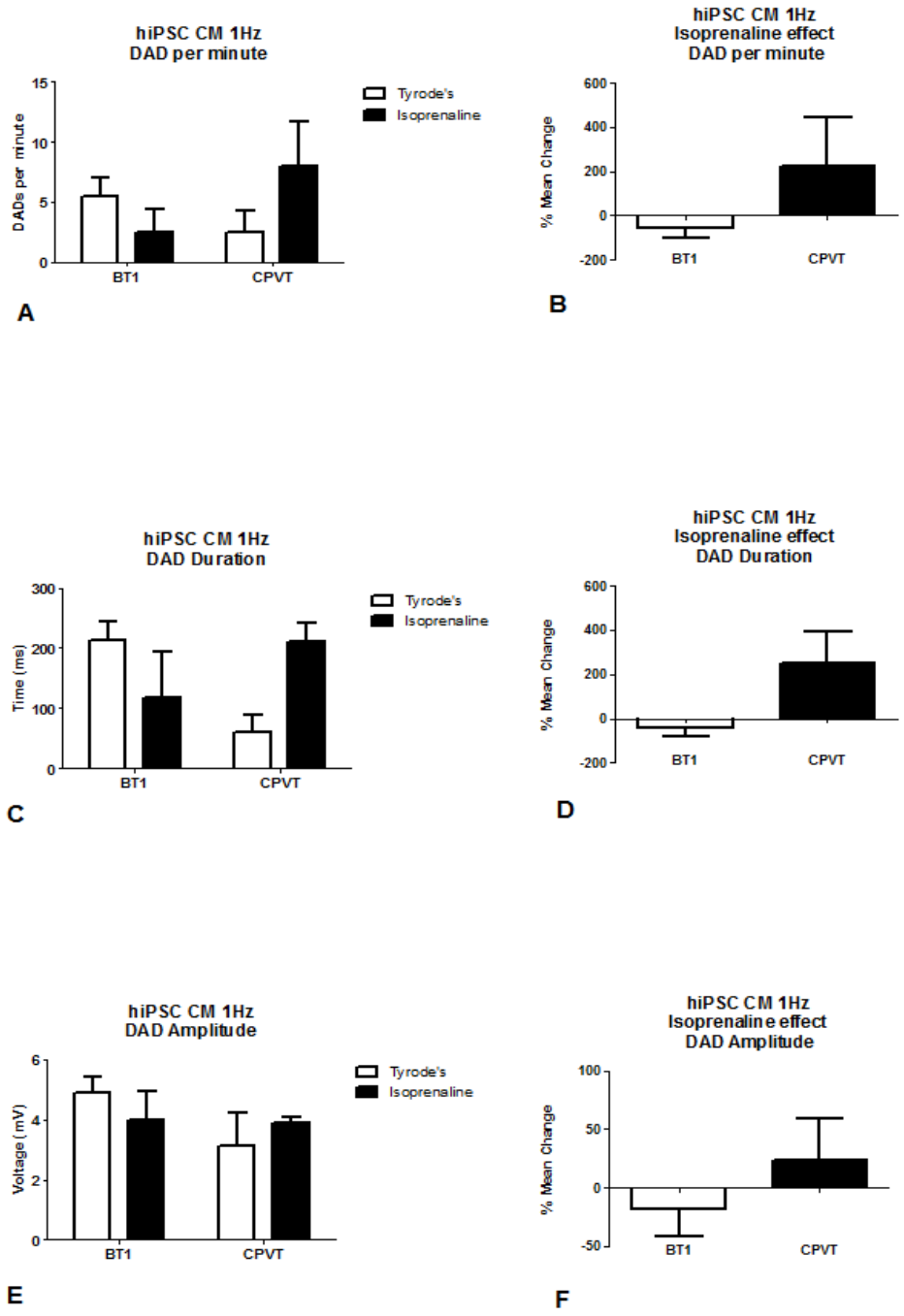

Figure 5.4 - Global arrhythmic endpoints for evoked AP 1Hz *- DADs frequency - events per minute (A), average DAD duration (C) and average DAD amplitude (E) with respective mean percentage change (B, D, F). hiPSC CPVT CM (n=10) and control hiPSC BT1 CM (n=8) , from evoked AP at 1Hz in Tyrode's and isoprenaline (1µM) perfusion. None of the differences reported in figure 5.4 were found to be statistically significant.*

5.4.2 AP pharmacological rescue

The main hypothesis for this project is that hiPSC CPVT CM are able to recapitulate the disease phenotype *in vitro*. To prove if this hypothesis is true, a ß-adrenergic challenge with a sequential anti-arrhythmic drug rescue in the presence of the ß-adrenergic agent was made. It was postulated that hiPSC CPVT CM would present an increase in pro-arrhythmic events (DADs) in the presence of a ß-agonist agent. When perfused with the selected anti-arrhythmic drug in the presence of isoprenaline (ß-agonist) it was expected that any arrhythmic events would be abolished or reduced in frequency, duration and/or amplitude. Other AP parameters were also analysed in order to evaluate any potential drug effects in AP shape (AP peak, amplitude, APD50 and APD90).

For the pharmacological rescue experiments all cells were paced at 0.5Hz and AP evoked with RMP clamped at -80mV. The chosen anti-arrhythmic drugs were flecainide 10µM (Itzhaki et al.,2012), propafenone 10µM (Caspi et al.,2009), propranolol 1µM (Matsa et al.,2011 and dantrolene 10µM (Jung et al.,2012).

Drugs such as flecainide and propafenone are already used in ventricular tachycardia management, despite some controversy, especially regarding the first drug. Flecainide use has been suggested in refractory cases as a joint therapy with verapamil and propranolol (Watanabe et al.,2009). Flecainide is also reported to have an anti-arrhythmic effect in hiPSC CPCT CM (Itzhaki et al.,2012). It was therefore important to assess if the same effect was observed when used to rescue pro-arrhythmic events in hiPSC CPVT CM for the mutation studied in the current project.

Propranolol is a ß-adrenergic blocker and since a catecholaminergic stimulus can trigger arrhythmia in CPVT, this is a drug of first line of treatment for clinical management of this channelopathy.

Dantrolene is a muscle relaxant that acts on RyR1 and is used in the treatment of malignant hyperthermia. Dantrolene has been suggested as a possible agent to treat CPVT1 based on results obtained from a hiPSC cardiac model of disease (Jung et al.,2012).

5.4.2.1 Quantitative analysis of arrhythmic endpoints

Arrhythmic endpoints from CPVT and BT1 CM stimulated at 0.5Hz are presented in this section as well as AP parameters during the perfusion sequence. Presented parameters are AP peak, amplitude, APD50 and APD90. Changes in these parameters may reflect drug effect or toxicity so a more detailed study is presented.

The perfusion sequence of three solutions for each cell was: Tyrode's only followed by isoprenaline in Tyrode's, followed by antiarrhythmic drug in the presence of isoprenaline in Tyrode's. A wash out period of 60 seconds in Tyrode's was made in between stimulation protocols and different perfused solutions. Arrhythmic endpoints were DAD frequency, DAD duration and DAD amplitude.

Due to lack of consistent statistical significance for data sets in all experiments using different arrhythmic drugs, AP parameter changes and DAD quantification study could not demonstrate pharmacological rescue of hiPSC CPVT CM. No significant changes were also seen in BT1 CM.

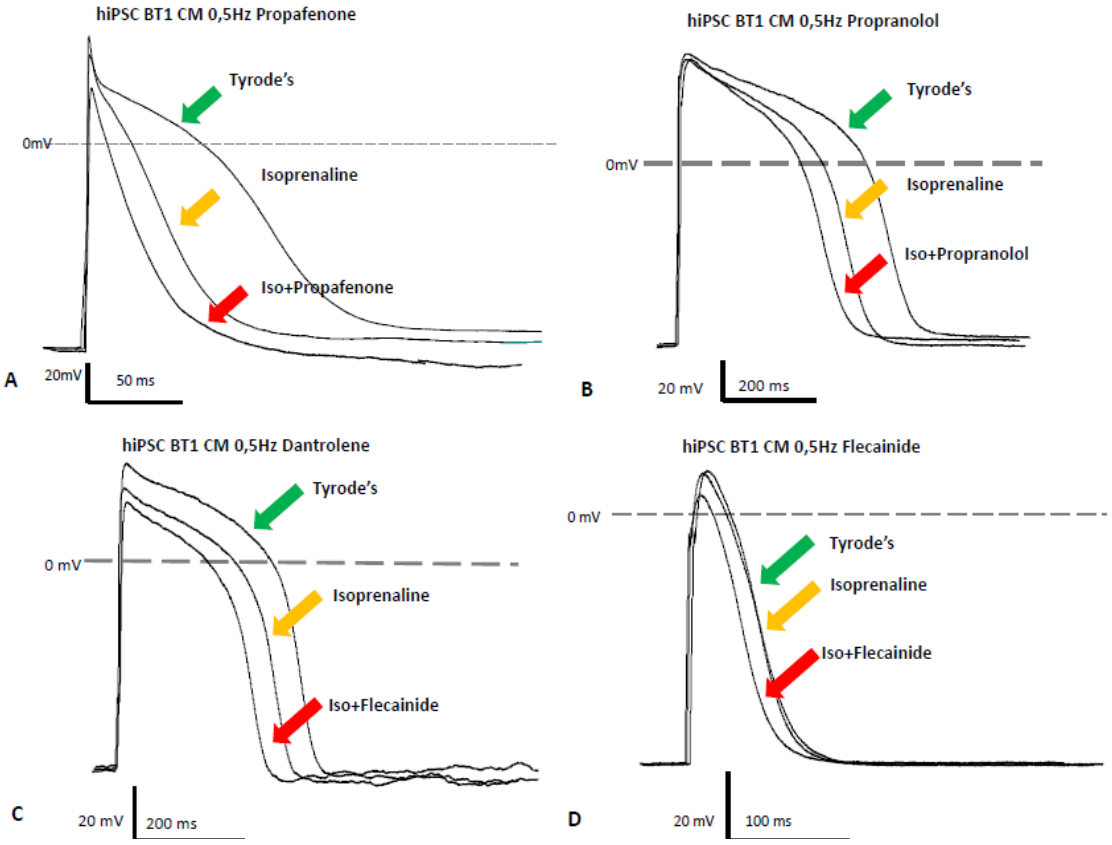

Figure 5.5 – Stimulated AP traces 0.5Hz from control BT1 CM - *example traces of evoked activity at 0.5Hz of hiPSC BT1 CM, perfused with Tyrode's (green arrow) with sequential isoprenaline (yellow arrow) and anti-arrhythmic drug in the presence of isoprenaline (red arrow).*

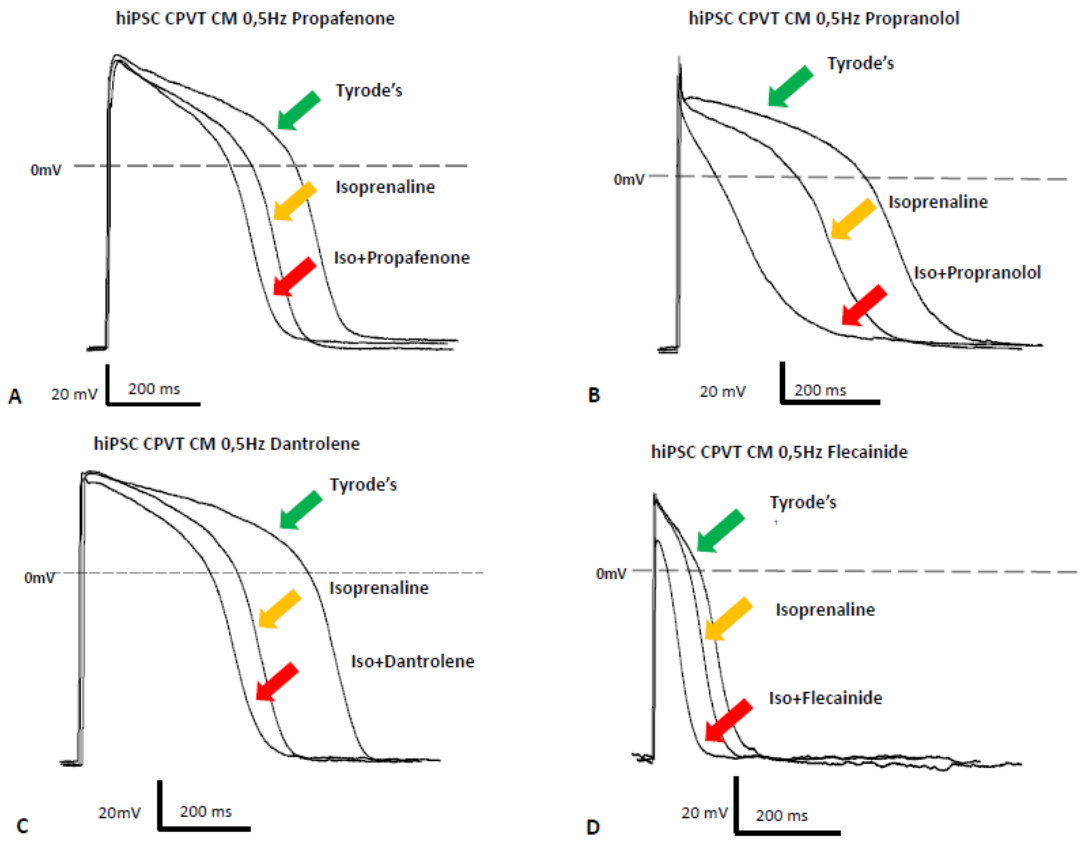

Figure 5.6 – Stimulated AP 0.5Hz traces from CPVT CM *–example traces of evoked activity at 0.5Hz of hiPSC CPVT CM, perfused with Tyrode's (green arrow) with sequential isoprenaline (yellow arrow) and anti-arrhythmic drug in the presence of isoprenaline (red arrow). Average APD in Tyrode's is longer in CPVT CM when compared with BT1 CM (figure 5.5). This observation is in accordance with cumulative data. Average amplitude is also similar between both cell types in Tyrode's.*

5.4.2.1.1 Flecainide

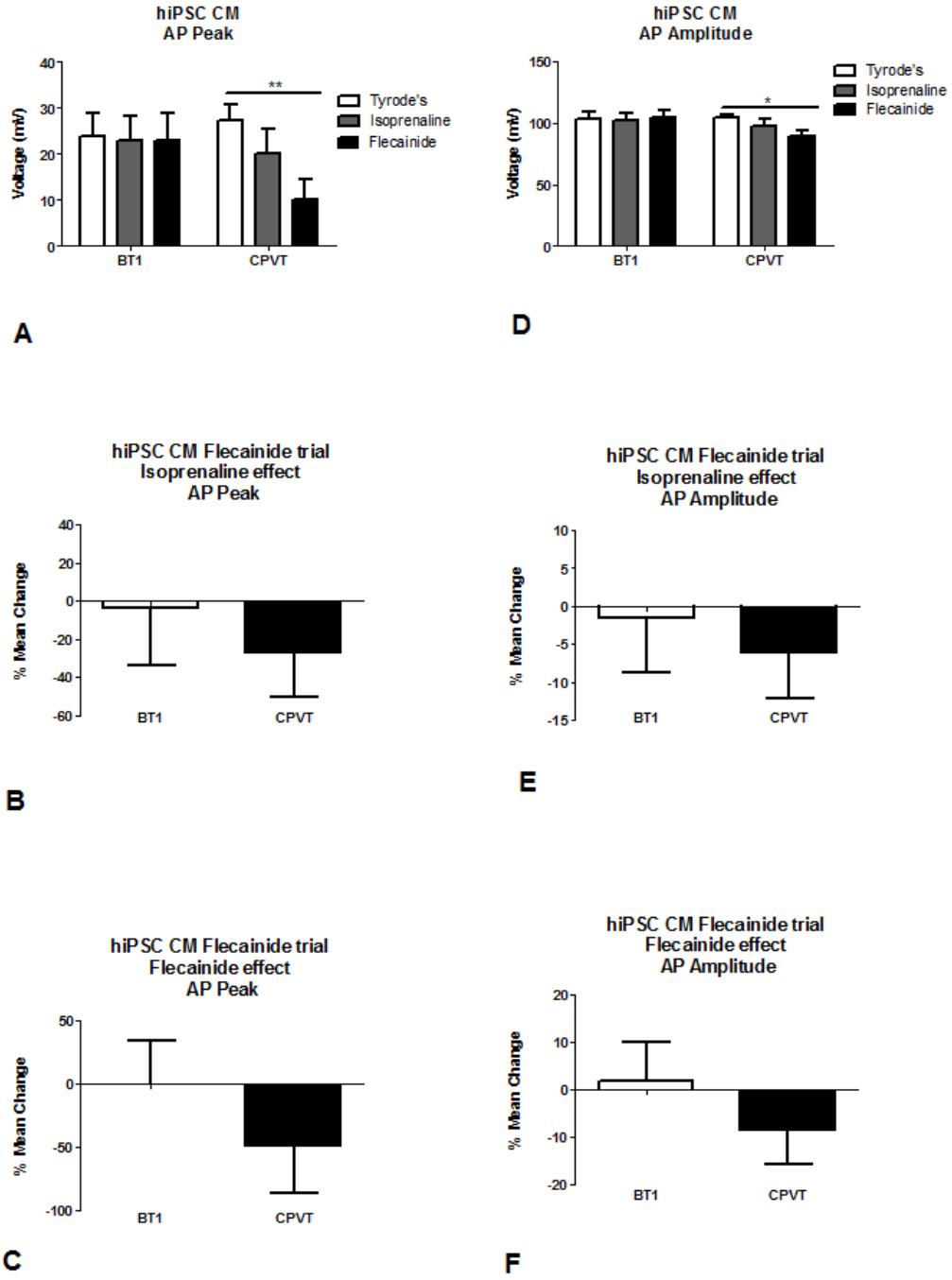

Figure 5.7 – Flecainide perfusion - AP peak and amplitude evoked AP 0.5Hz *- AP peak (A) and amplitude (D) with respective mean percentage change for isoprenaline (1µM) perfusion (B, E) and flecainide in the presence of isoprenaline (C, F). hiPSC BT1 CM (n=11) and hiPSC CPVT CM (n=20). Statistical significance in figure 5.7A and 5.7D was only seen in CPVT CM between Tyrode's and flecainide in the presence of isoprenaline. No statistical significance was found between other data columns.*

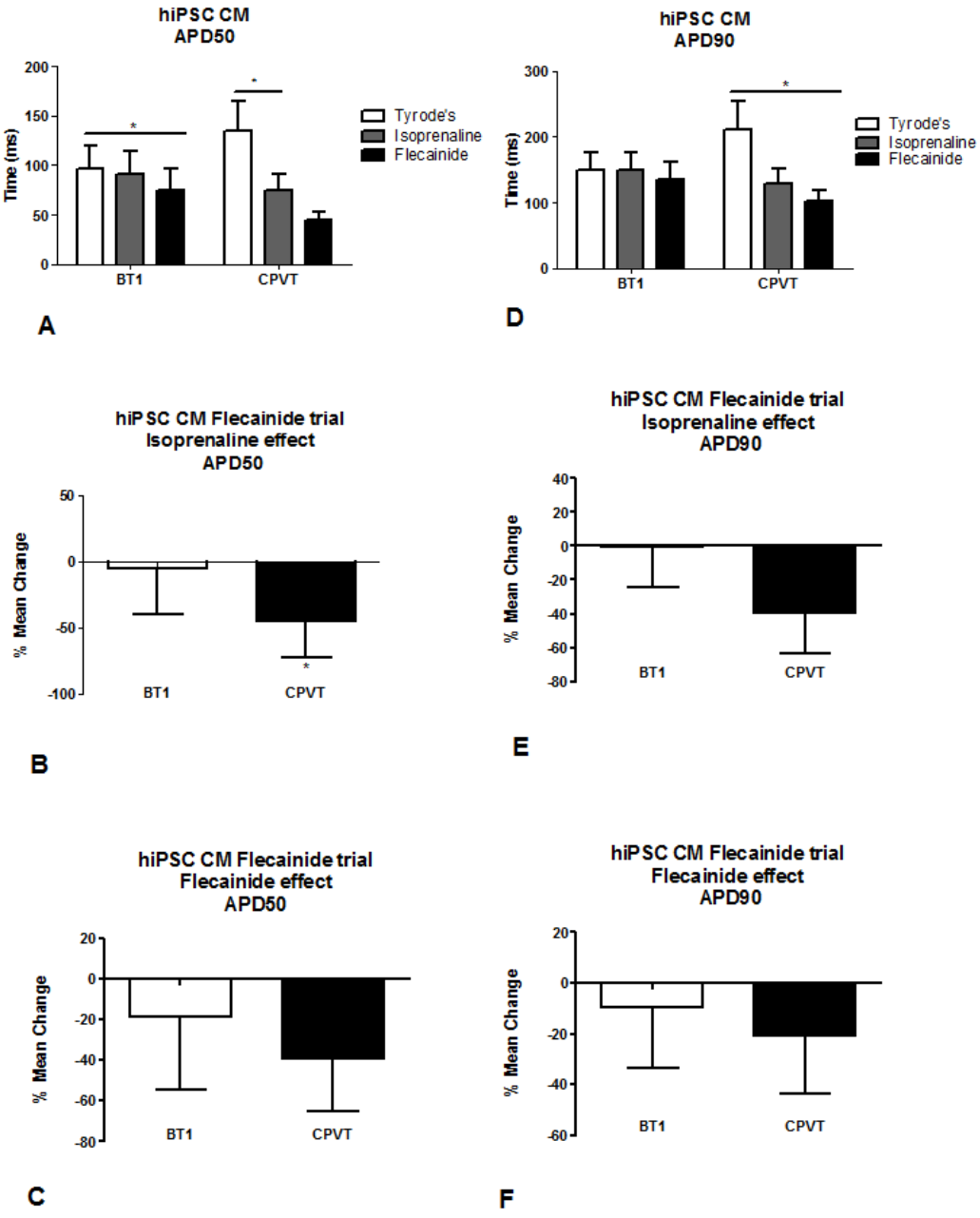

Figure 5.8 – Flecainide perfusion – APD50 and APD90 evoked AP 0.5Hz - *APD50 (A) and APD90 (D) with respective mean percentage change for isoprenaline (1µM) perfusion (B, E) and flecainide in the presence of isoprenaline (C, F). hiPSC BT1 CM (n=11) and hiPSC CPVT CM (n=20). Statistical significance in figure 5.8A for BT1 CM was only seen between Tyrode's and flecainide in the presence of isoprenaline columns as well in figure 5.8D for CPVT CM. In figure 5.8A CPVT CM statistical significance was found between Tyrode's and sequential isoprenaline perfusion.*

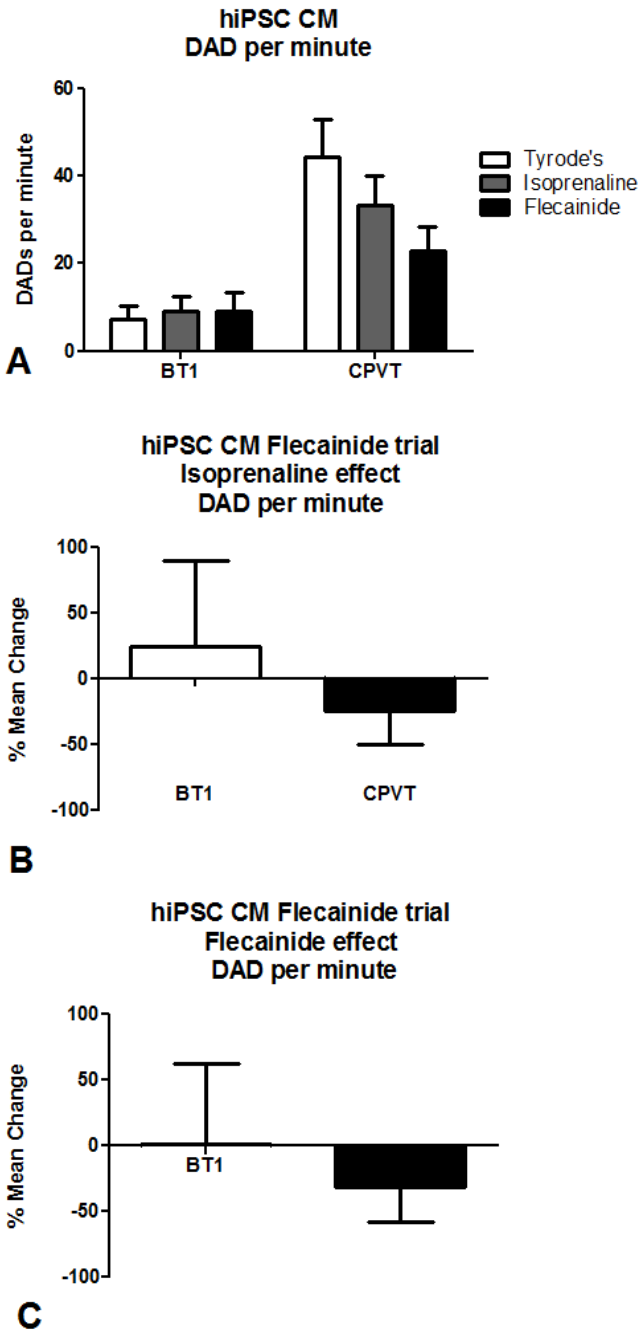

Figure 5.9 – Flecainide perfusion – DAD frequency, evoked AP 0.5Hz *- DAD frequency in events per minute (A), mean percentage change for isoprenaline (1µM) perfusion (B), and mean percentage change for flecainide in the presence of isoprenaline (C). hiPSC BT1 CM (n=11) and hiPSC CPVT CM (n=20). None of the differences reported in figure 5.9 were found to be statistically significant.*

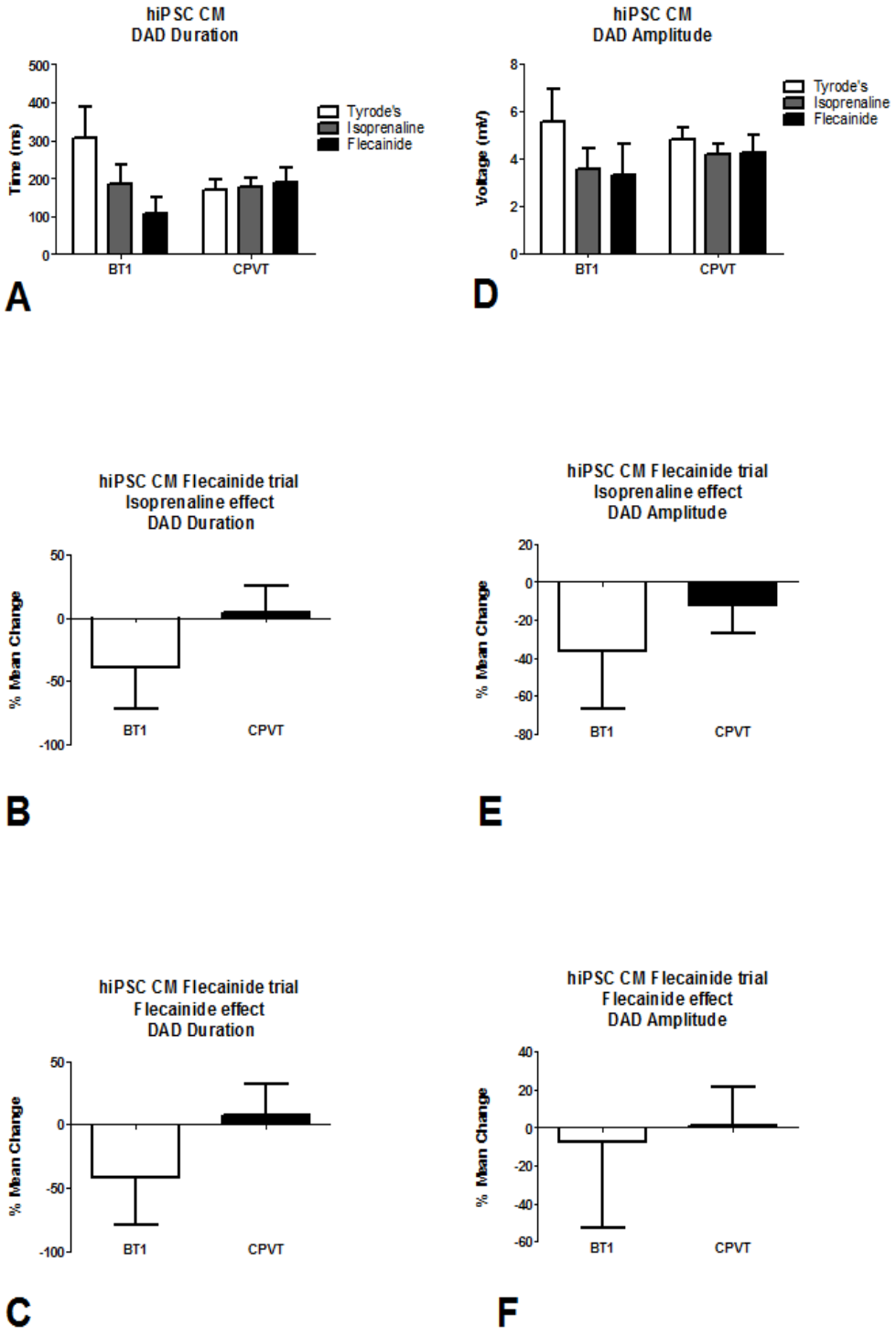

Figure 5.10 – Flecainide perfusion – DAD duration and amplitude, evoked AP 0.5Hz *- DAD duration (A) and DAD amplitude (D) with respective mean percentage change for isoprenaline (1µM) perfusion (B, E) and mean percentage change for flecainide in the presence of isoprenaline (C, F,). hiPSC BT1 CM (n=11) and hiPSC CPVT CM (n=20). None of the differences reported in figure 5.10 were found to be statistically significant*

5.4.2.1.2 Propafenone

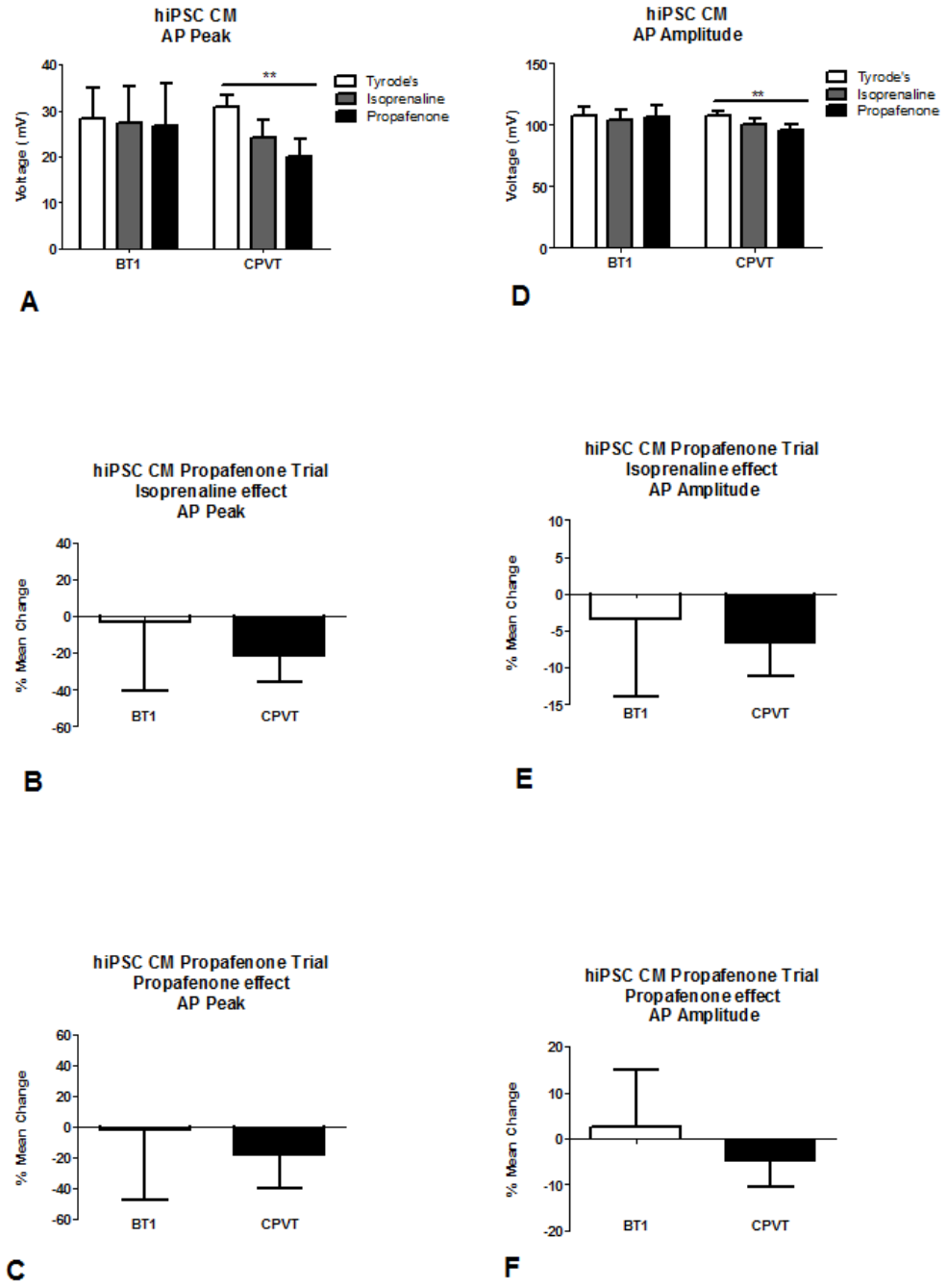

Figure 5.11 – Propafenone perfusion - AP peak and amplitude evoked AP 0.5Hz *- AP peak (A) and amplitude (D) with respective mean percentage change for isoprenaline (1µM) perfusion (B, E) and propafenone in the presence of isoprenaline (C, F). hiPSC BT1 CM (n=8) and hiPSC CPVT CM (n=10). Statistical significant decrease is present for CPVT CM (figure 5.11A and 5.11D, between Tyrode's and propafenone in the presence of isoprenaline. No significant effect was seen with isoprenaline perfusion alone.*

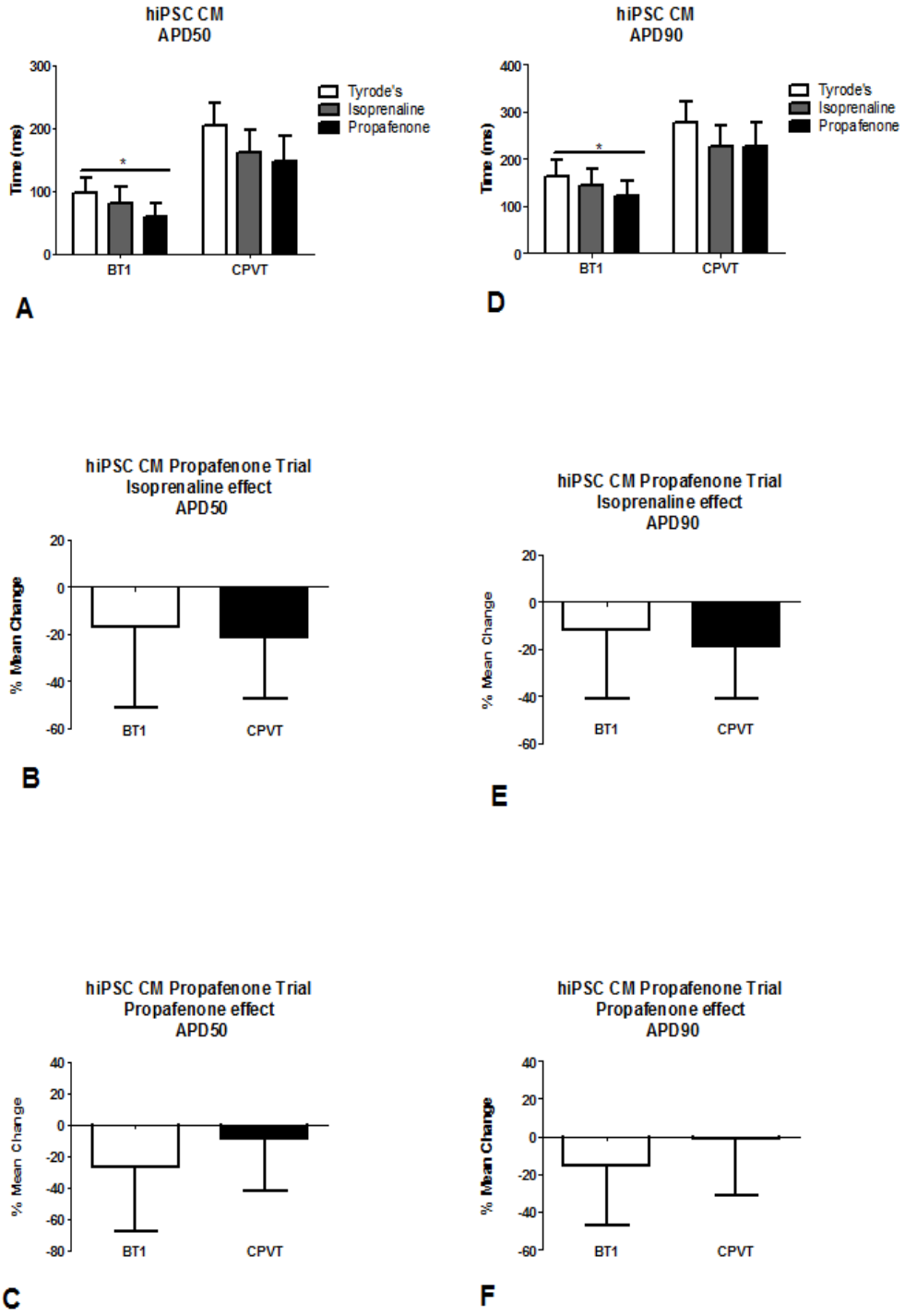

Figure 5.12 – Propafenone perfusion – APD50 and APD90 evoked AP 0.5Hz - *APD50 (A) and APD90 (D) with respective mean percentage change for isoprenaline (1µM) perfusion (B, E) and propafenone in the presence of isoprenaline (C, F). hiPSC BT1 CM (n=8) and hiPSC CPVT CM (n=10). Statistical significant decrease found only for BT1 CM (figure 5.12A and 5.12D) between Tyrode's and propafenone in the presence of isoprenaline. No effect was seen for isoprenaline perfusion alone.*

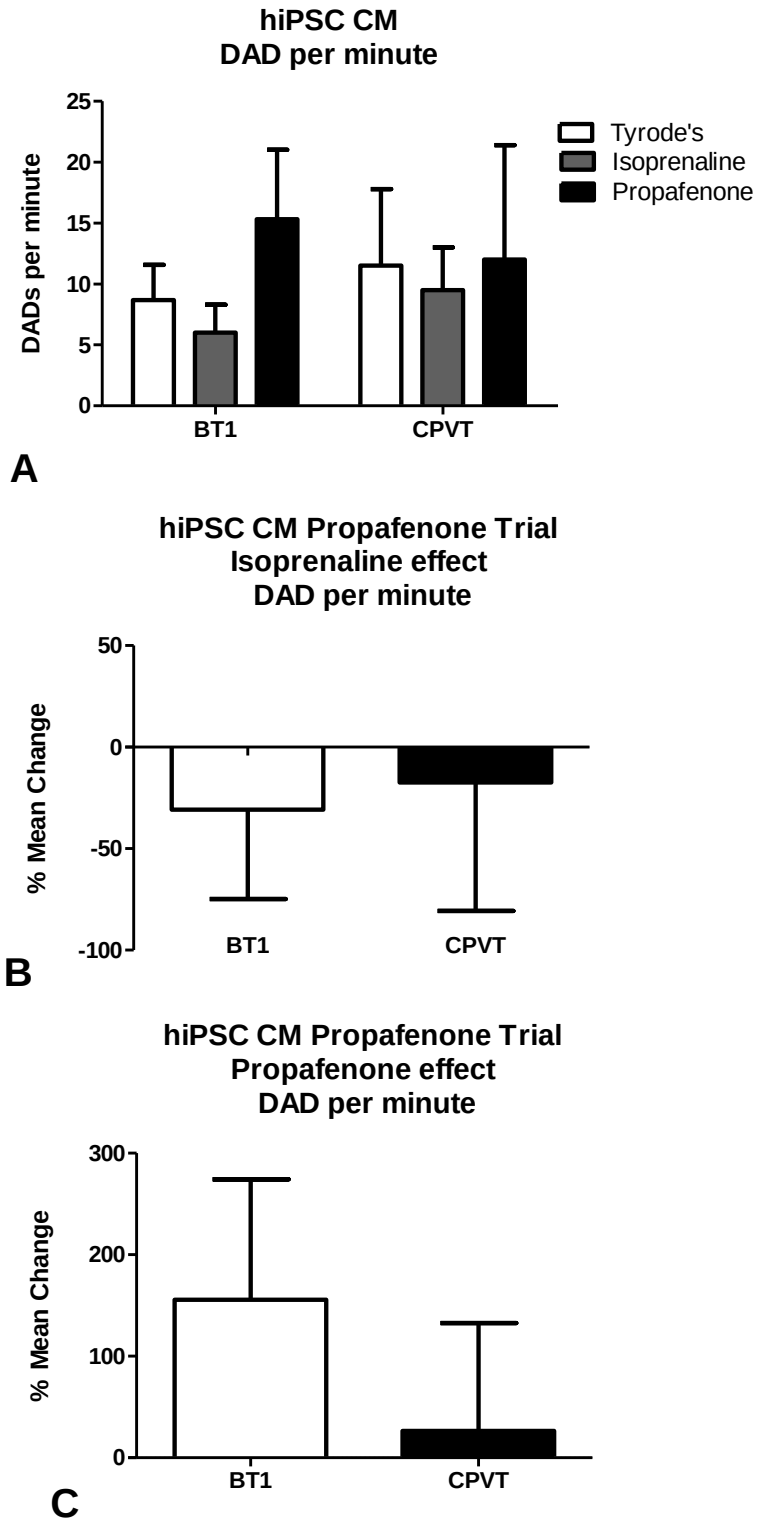

Figure 5.13 – Propafenone perfusion – DAD frequency, evoked AP 0.5Hz *- DAD frequency in events per minute (A), mean percentage change for isoprenaline (1µM) perfusion (B), and mean percentage change for propafenone in the presence of isoprenaline (C). hiPSC BT1 CM (n=8) and hiPSC CPVT CM (n=10). None of the differences reported in figure 5.13 were found to be statistically significant.*

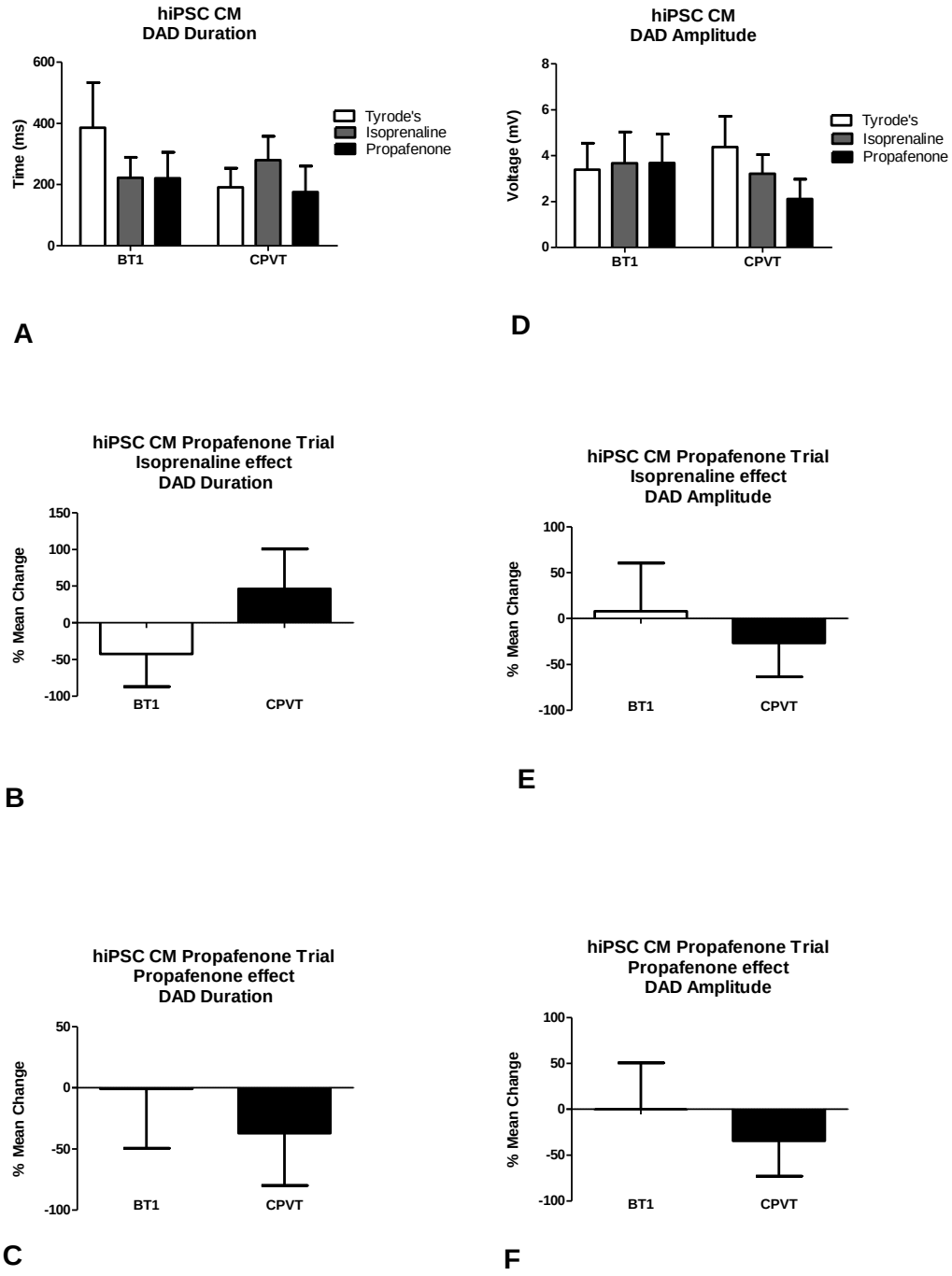

Figure 5.14 – Propafenone perfusion – DAD duration and amplitude, evoked AP 0.5Hz *- DAD duration (A) and DAD amplitude (D) with respective mean percentage change for isoprenaline (1µM) perfusion (B, E) and mean percentage change for propafenone in the presence of isoprenaline (C, F). hiPSC BT1 CM (n=8) and hiPSC CPVT CM (n=10). None of the differences reported in figure 5.14 were found to be statistically significant.*

5.4.2.1.3 Propranolol

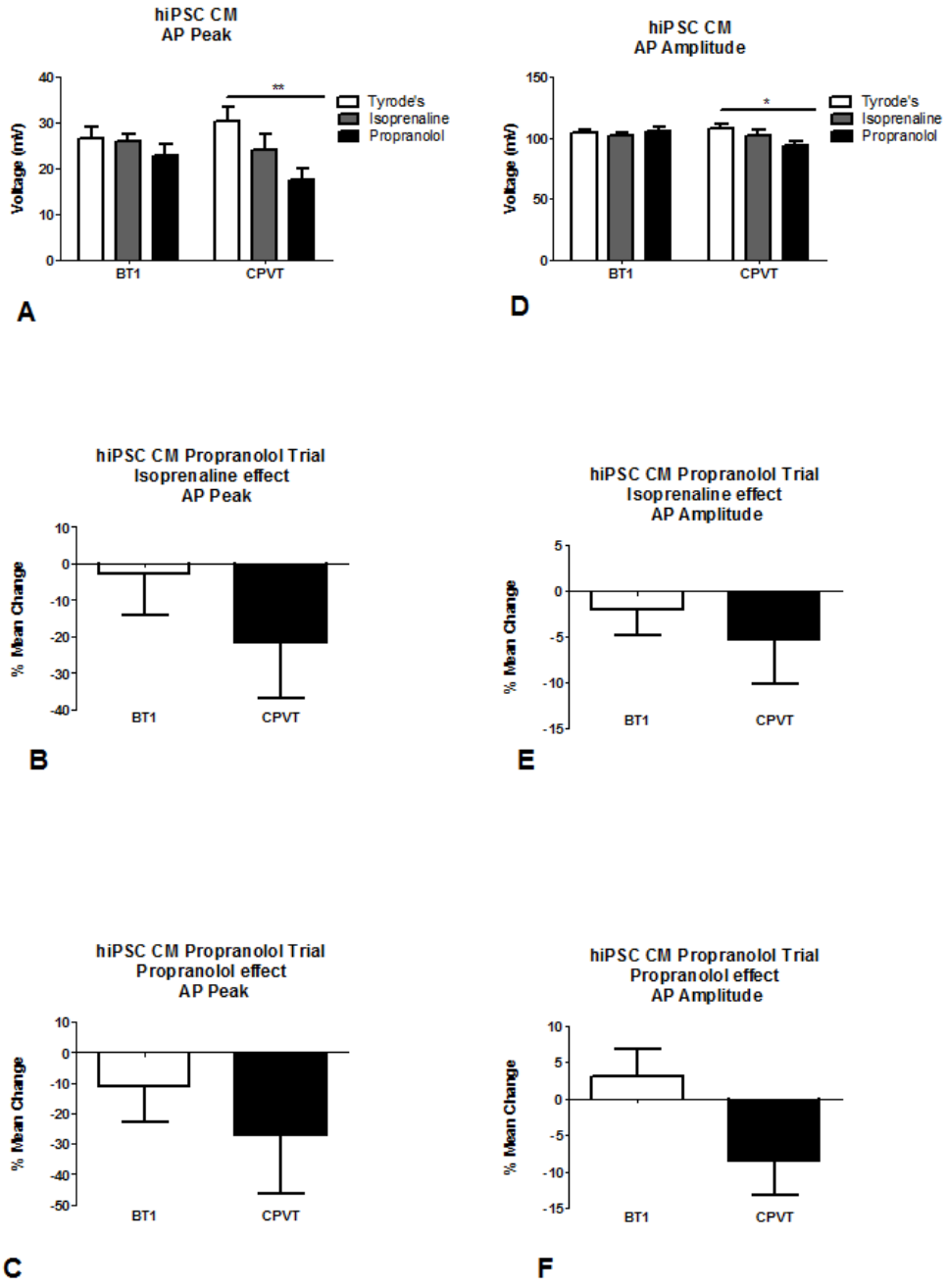

Figure 5.15 – Propranolol perfusion - AP peak and amplitude evoked AP 0.5Hz *- AP peak (A) and amplitude (D) with respective mean percentage change for isoprenaline (1µM) perfusion (B, E) and propranolol in the presence of isoprenaline (C, F). hiPSC BT1 CM (n=5) and hiPSC CPVT CM (n=16). Statistically significant decrease is present for CPVT CM (figure 5.15A and 5.15D), between Tyrode's and propranolol in the presence of isoprenaline. No statistically significant effect was seen with isoprenaline perfusion alone.*

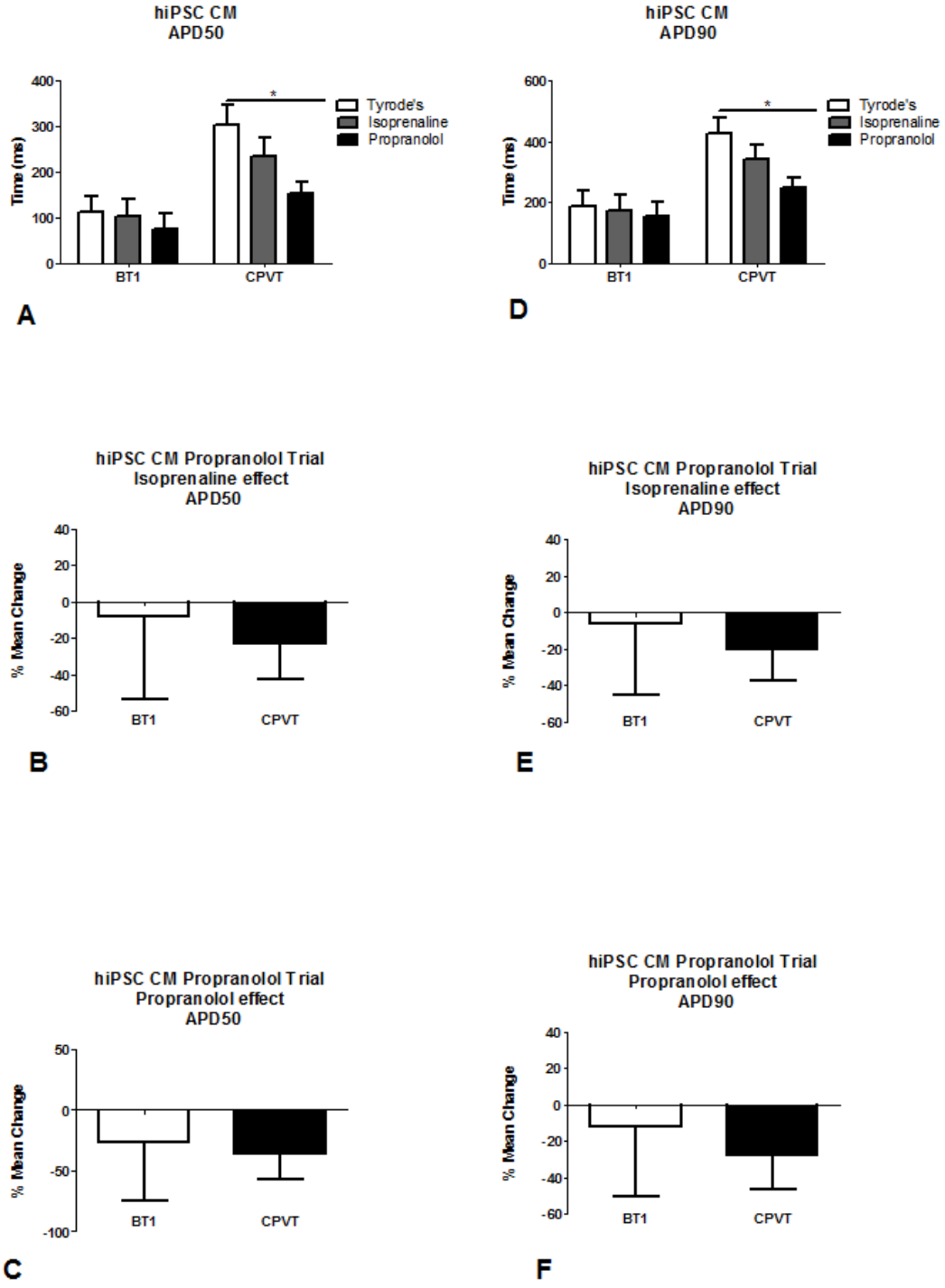

Figure 5.16 – Propranolol perfusion – APD50 and APD90 evoked AP 0.5Hz *- APD50 (A) and APD90 (D) with respective mean percentage change for isoprenaline (1µM) perfusion (B, E) and propranolol in the presence of isoprenaline (C, F). hiPSC BT1 CM (n=5) and hiPSC CPVT CM (n=16). Statistical significant decrease is present for CPVT CM (figure 5.16A and 5.16D), between Tyrode's and propranolol in the presence of isoprenaline. No statistically significant effect was seen with isoprenaline perfusion alone.*

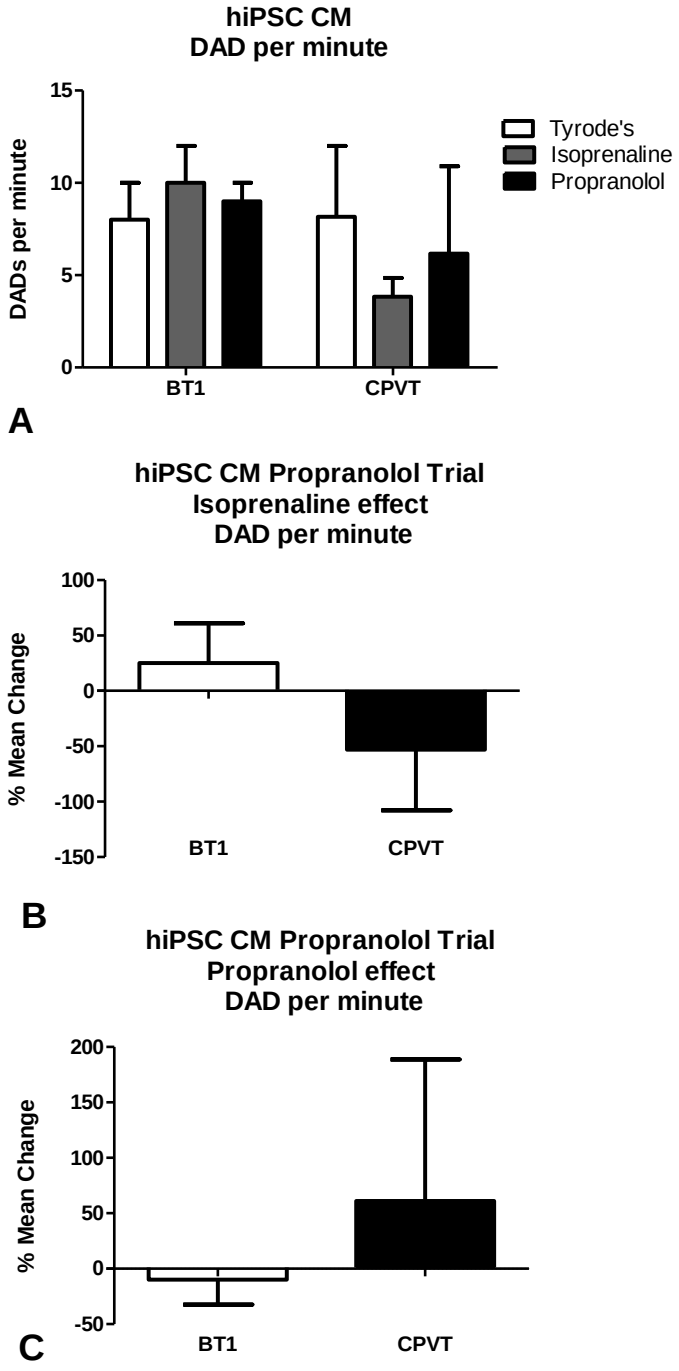

Figure 5.17 – Propranolol perfusion – DAD frequency, evoked AP 0.5Hz *- DAD frequency in events per minute (A), mean percentage change for isoprenaline (1µM) perfusion (B), and mean percentage change for propranolol in the presence of isoprenaline (C). hiPSC BT1 CM (n=5) and hiPSC CPVT CM (n=16). None of the differences reported in figure 5.17 were found to be statistically significant.*

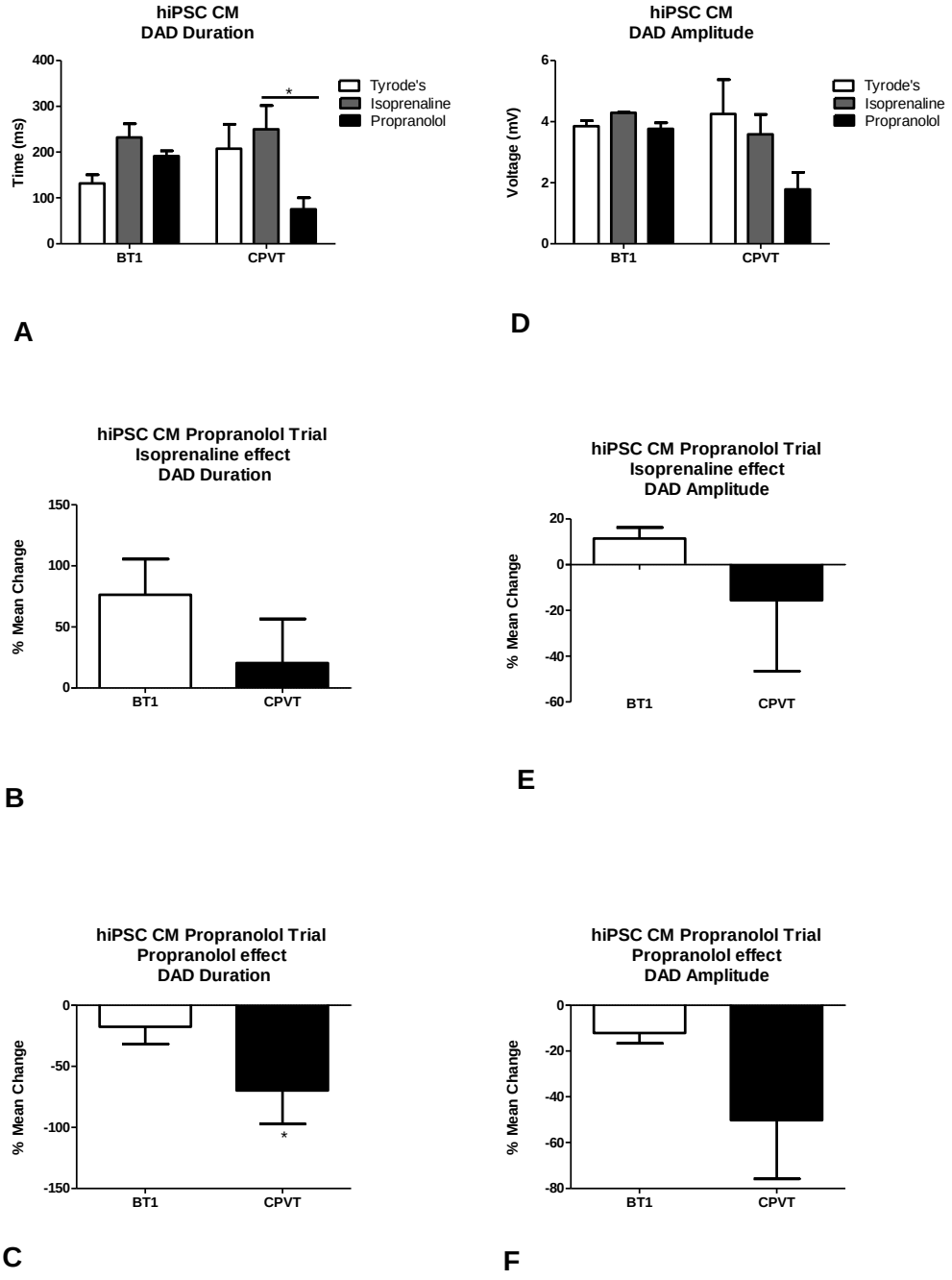

Figure 5.18 – Propranolol perfusion – DAD duration and amplitude, evoked AP 0.5Hz - *DAD duration (A) and DAD amplitude (D) with respective mean percentage change for isoprenaline (1µM) perfusion (B, E) and mean percentage change for propranolol in the presence of isoprenaline (C, F,). hiPSC BT1 CM (n=5) and hiPSC CPVT CM (n=16). A statistical significant 70% decrease is present in DAD duration when propranolol in the presence of isoprenaline is perfused after isoprenaline stimulation alone (figure 5.18A, 5.18C).*

5.4.2.1.4 Dantrolene

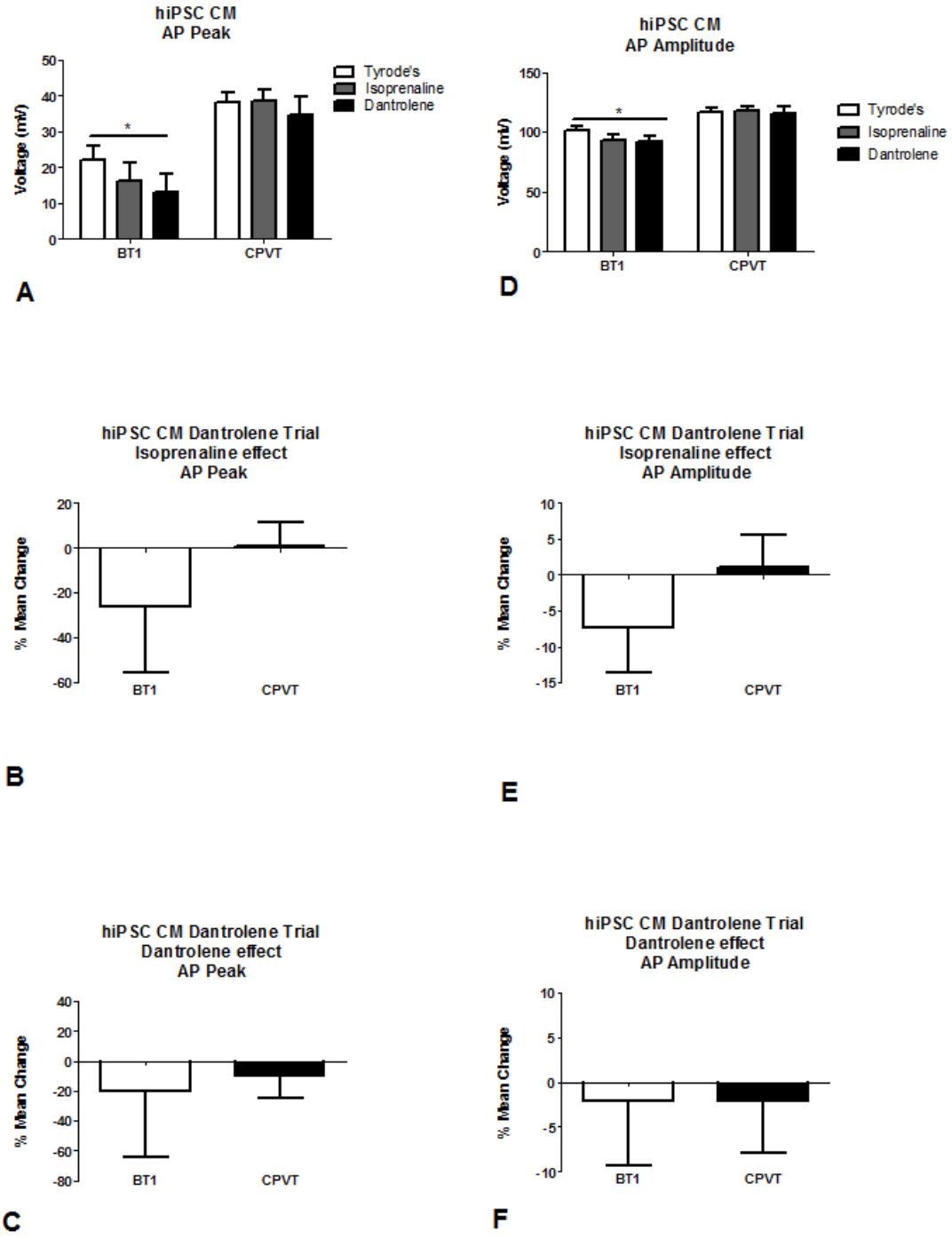

Figure 5.19 – Dantrolene perfusion - AP peak and amplitude evoked AP 0.5Hz *- AP peak (A) and amplitude (D) with respective mean percentage change for isoprenaline (1µM) perfusion (B, E) and dantrolene in the presence of isoprenaline (C, F). hiPSC BT1 CM (n=9) and hiPSC CPVT CM (n=10). Statistically significant decrease found only for BT1 CM (figure 5.19A and 5.19D) between Tyrode's and dantrolene in the presence of isoprenaline. No effect was seen for isoprenaline perfusion alone.*

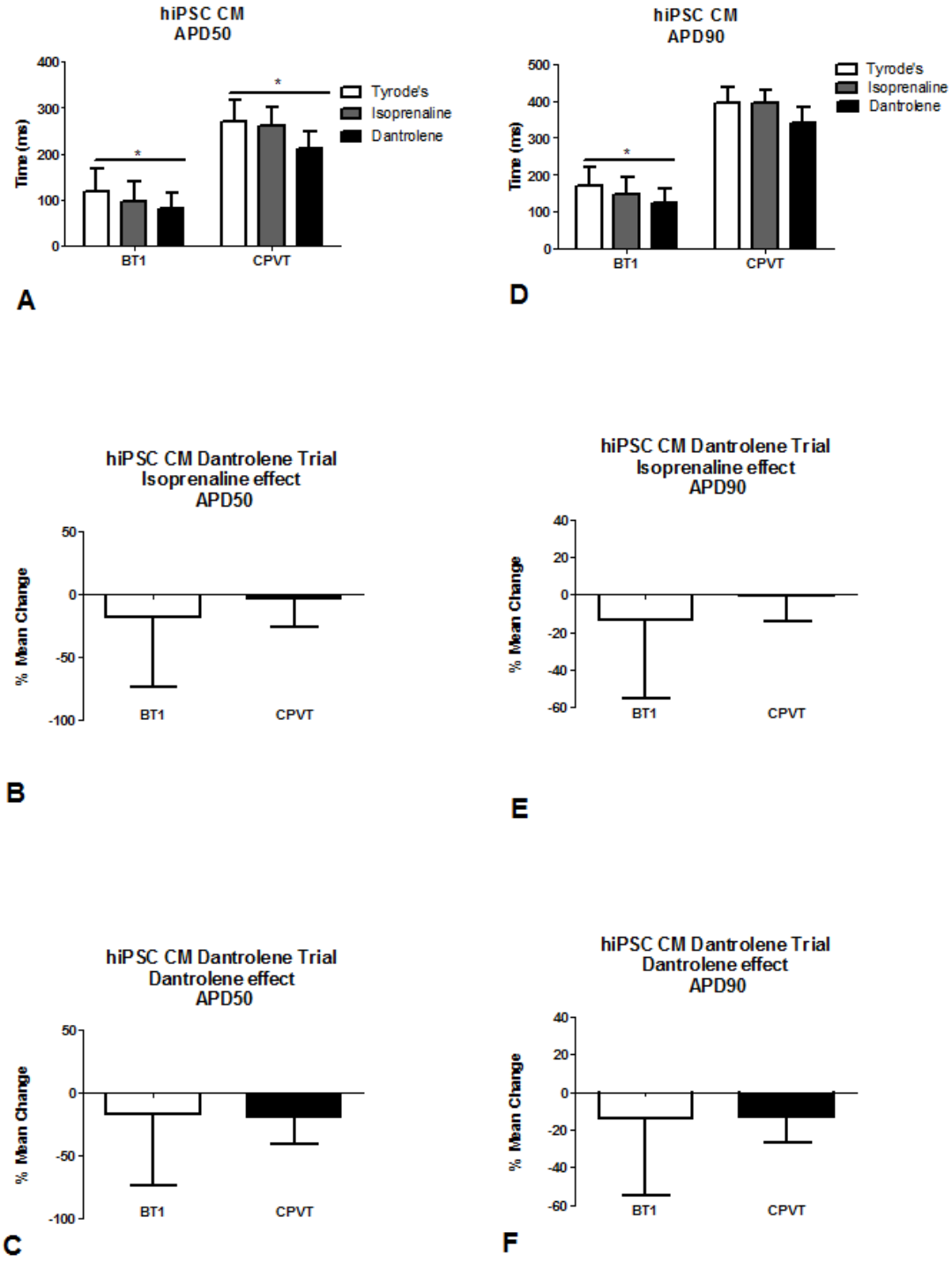

Figure 5.20 – Dantrolene perfusion – APD50 and APD90 evoked AP 0.5Hz *- APD50 (A) and APD90 (D) with respective mean percentage change for isoprenaline (1µM) perfusion (B, E) and dantrolene in the presence of isoprenaline (C, F). hiPSC BT1 CM (n=9) and hiPSC CPVT CM (n=10). Statistically significant decrease found for BT1 CM and CPVT CM between Tyrode's and dantrolene in the presence of isoprenaline (figure 5.20A). Figure 5.20D also presents a statistically significant decrease found for BT1 CM between Tyrode's and dantrolene in the presence of isoprenaline. No effect was seen for isoprenaline perfusion alone.*

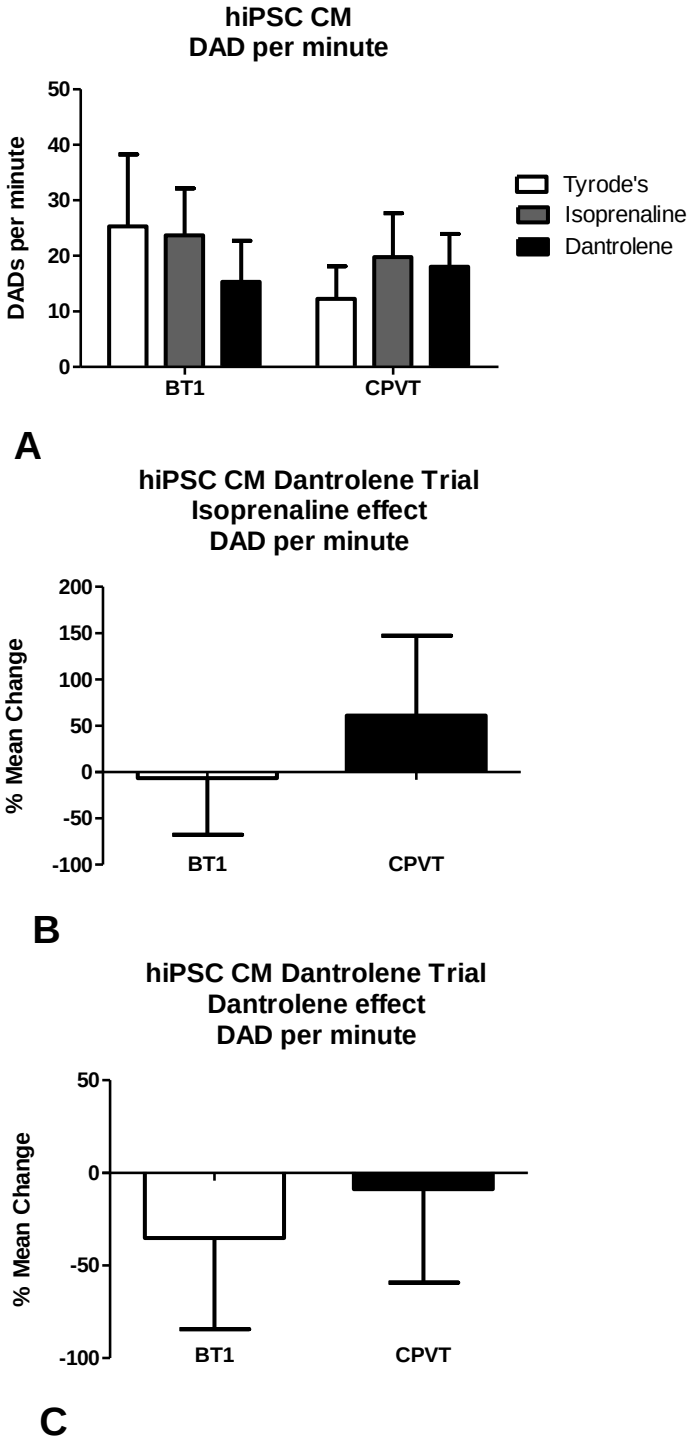

Figure 5.21 – Dantrolene perfusion – DAD frequency, evoked AP 0.5Hz *- DAD frequency in events per minute (A), mean percentage change for isoprenaline (1µM) perfusion (B), and mean percentage change for dantrolene in the presence of isoprenaline (C). hiPSC BT1 CM (n=9) and hiPSC CPVT CM (n=10). None of the differences reported in figure 5.21 were found to be statistically significant.*

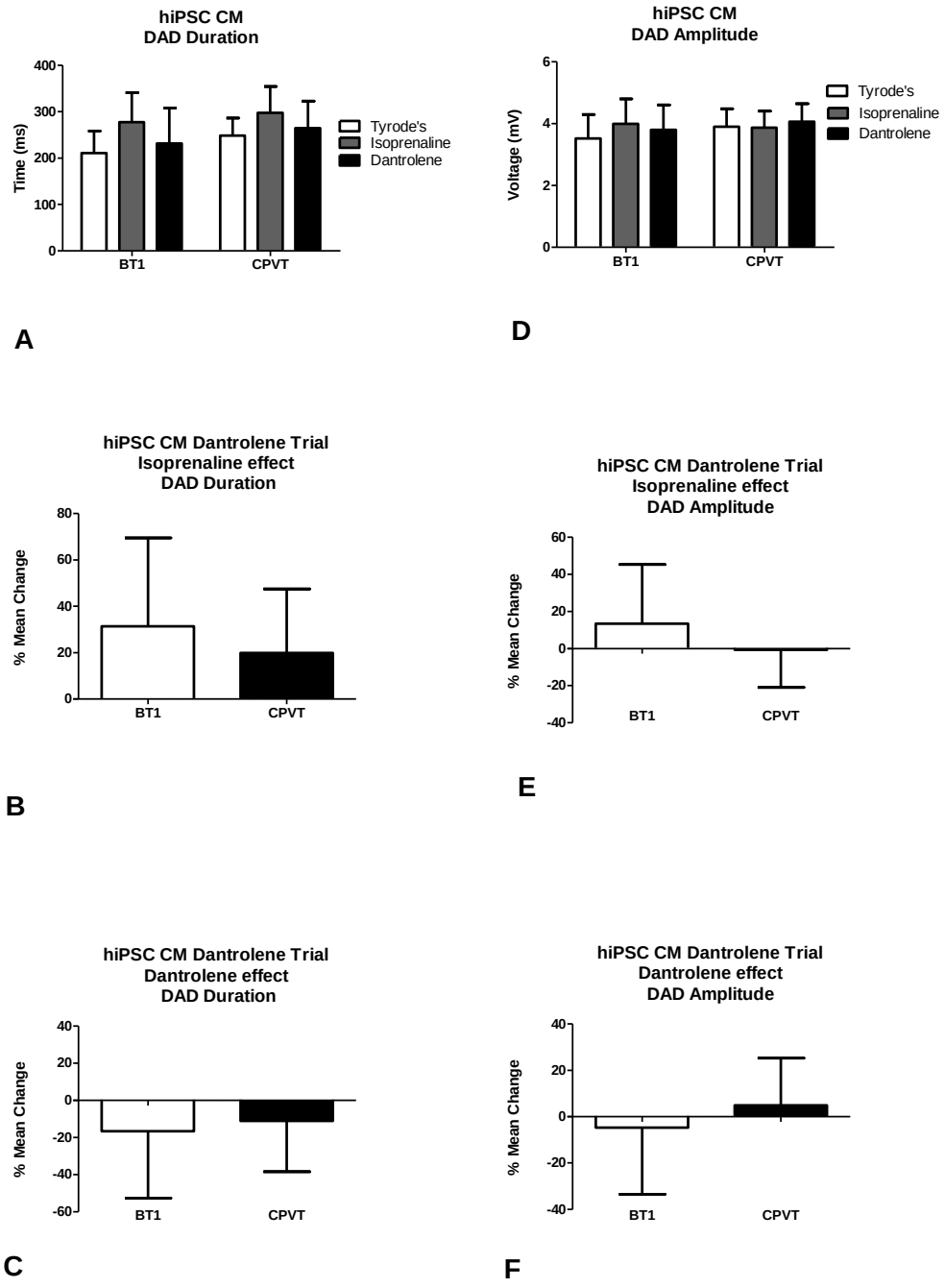

Figure 5.22 – Dantrolene perfusion – DAD duration and amplitude, evoked AP 0.5Hz *- DAD duration (A) and DAD amplitude (D) with respective mean percentage change for isoprenaline (1µM) perfusion (B, E) and mean percentage change for dantrolene in the presence of isoprenaline (C, F,). hiPSC BT1 CM (n=9) and hiPSC CPVT CM (n=10). None of the differences reported in figure 5.22 were found to be statistically significant.*

5.4.2.2 Qualitative analysis of arrhythmic endpoints

In this project, it was determined that, in order to study and eventually validate an *in vitro* model of a CPVT1, the selected endpoints (DADs) should be counted and measured while perfused with different pharmacological agents. However, this approach was largely absent in the published literature where a more or less qualitative evaluation was more frequently reported. A qualitative study analysis of obtained data is here presented.

DADs are the most typical arrhythmic endpoint in CPVT. However, the presence of EADs has also been documented in CPVT hiPSC CM (Kujala et al., 2012). EADs are not the most frequent hallmark for this disease but for comparative purposes with published data, these endpoints are also included in this qualitative analysis. Both spontaneous and evoked traces at 0.5Hz were analysed. In the case of spontaneous activity experiments no anti-arrhythmic drugs were perfused.The criteria used for the qualitative analysis was the presence of one event of each type per full trace. DADs and EADs were considered as any event with an amplitude $\geq$ 3mV, either between APs (DADs) or before reaching full repolarization (EADs). Each trace could therefore have a maximum of one DAD and one EAD (possibly both simultaneously) for this analysis. A normal trace did not present a single DAD or EAD.

No statistical significance was found in the presented qualitative endpoint arrhythmogenic study for mutant and control CM with spontaneous and evoked activity (0.5Hz and 1Hz).

5.4.2.2.1 Spontaneous activity

In this data set, normal traces were considered absent from any DAD or EAD (with amplitude ≥3 mV). Each arrhythmic trace may have a maximum of one DAD and one EAD simultaneously.

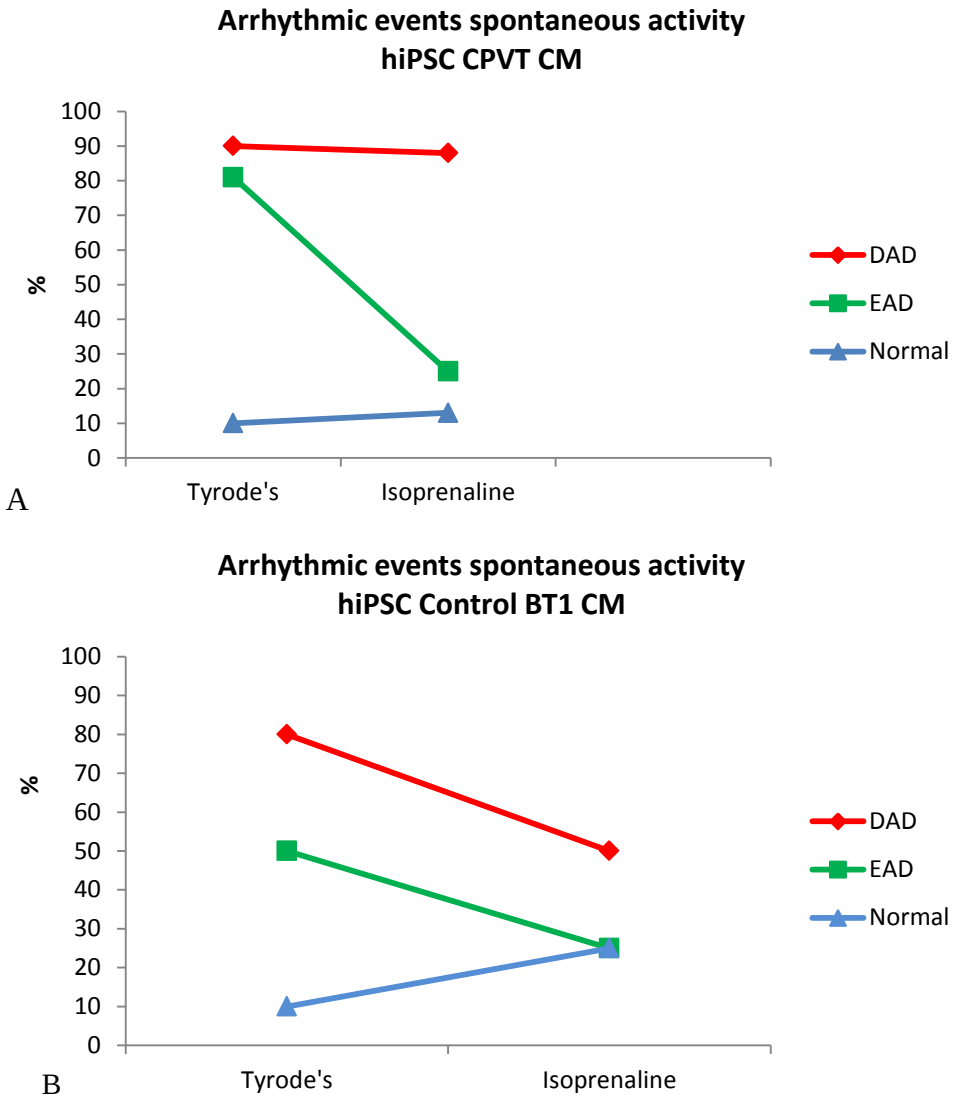

Figure 5.23 – Qualitative analysis of spontaneous hiPSC CM arrhythmic endpoints *- data from spontaneous activity traces for both hiPSC CPVT CM (A, n=21) and control hiPSC BT1 CM (B, n=10). None of the differences reported in figure 5.23 were found to be statistically significant.*

.

5.4.2.2.2 Evoked activity

For evoked activity experiments, analysed traces were the same as those analysed for quantitative data. Data were obtained with sequential perfusion protocol using Tyrode's only, isoprenaline and anti-arrhythmic drug in the presence of isoprenaline.

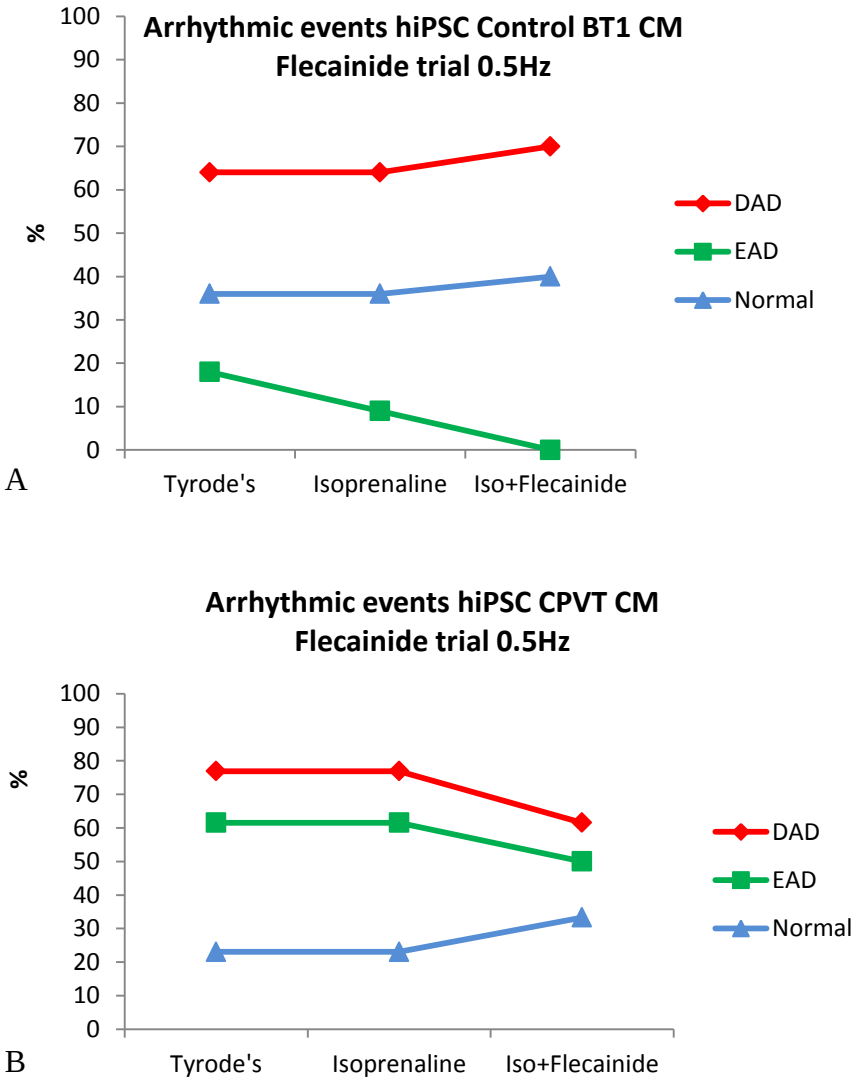

Figure 5.24 – Flecainide - Qualitative analysis of arrhythmic endpoints from evoked activity traces - *Evoked activity 0.5Hz, hiPSC BT-1 CM (A, n=20) and hiPSC CPVT CM (B, n=11) using flecainide (10µM) as anti- arrhythmic drug. None of the differences reported in figure 5.24 were found to be statistically significant.*

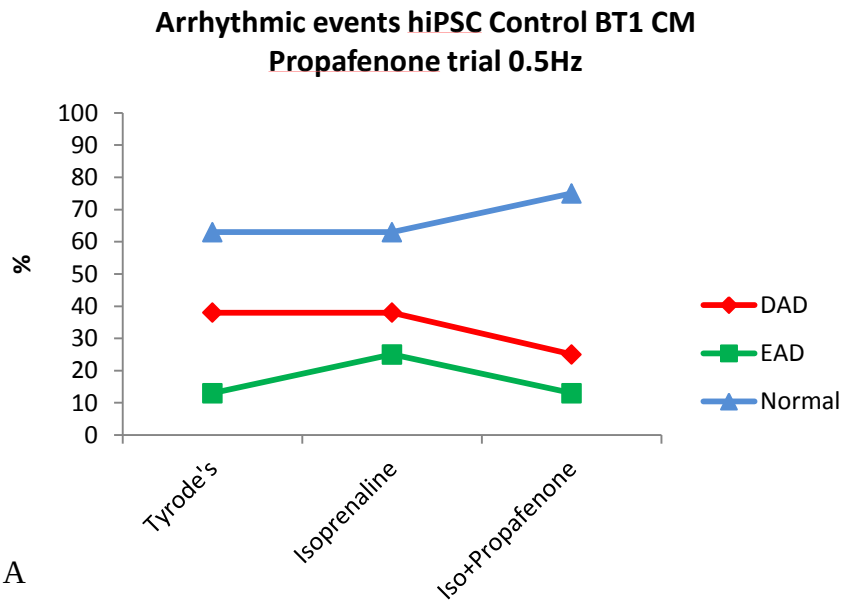

A

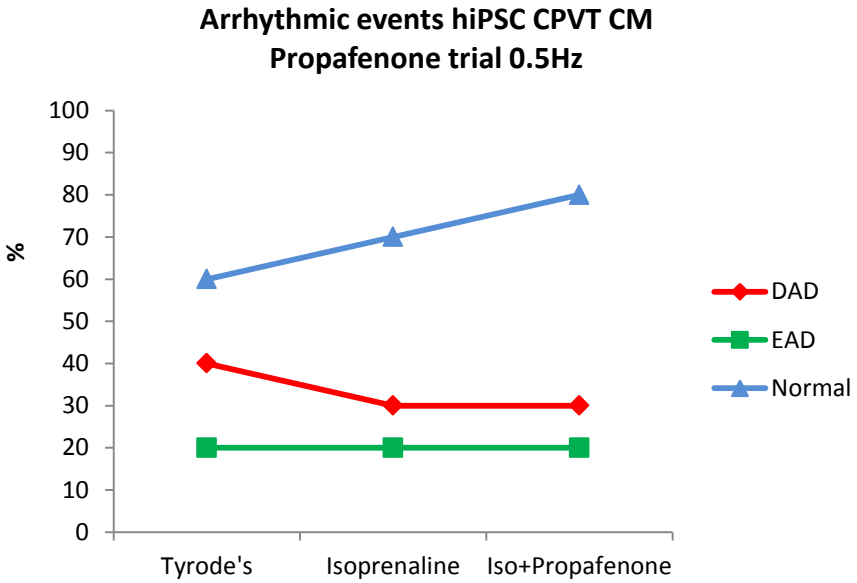

B

Figure 5.25 – Propafenone - Qualitative analysis of arrhythmic endpoints from evoked activity traces - *Evoked activity 0.5Hz, hiPSC BT-1 CM (A, n=8) and hiPSC CPVT CM (B, n=10) using propafenone (10µM) as anti-arrhythmic drug. None of the differences reported in figure 5.25 were found to be statistically significant.*

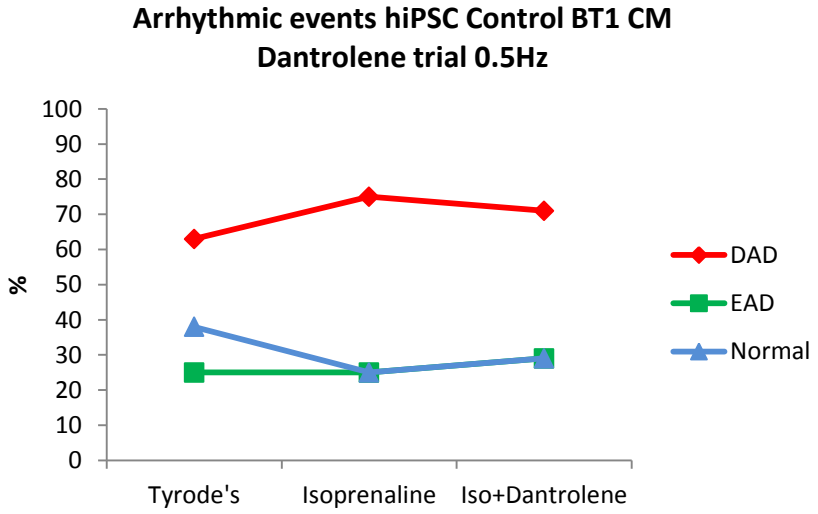

A

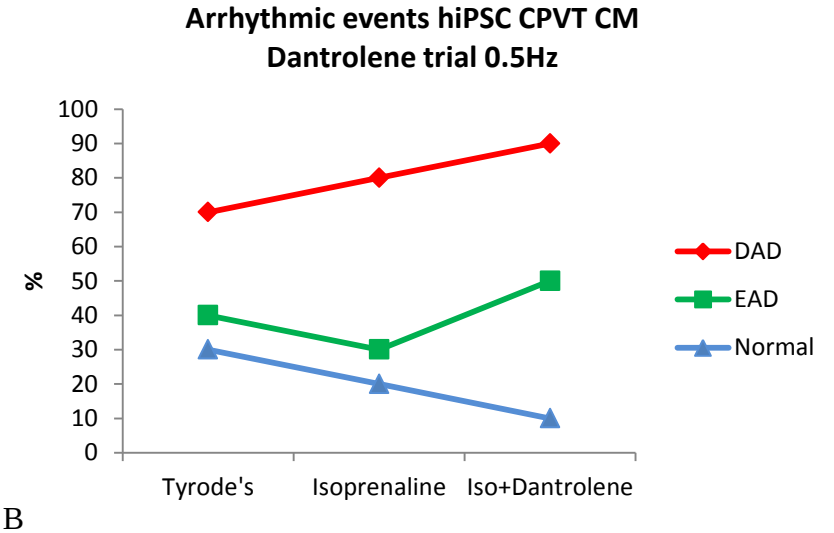

B

Figure 5.26 – Dantrolene - Qualitative analysis of arrhythmic endpoints from evoked activity traces - *Evoked activity 0.5Hz, hiPSC BT-1 CM (A, n=9) and hiPSC CPVT CM (B, n=10) using dantrolene (10μM) as anti-arrhythmic drug. None of the differences reported in figure 5.26 were found to be s statistically significant.*

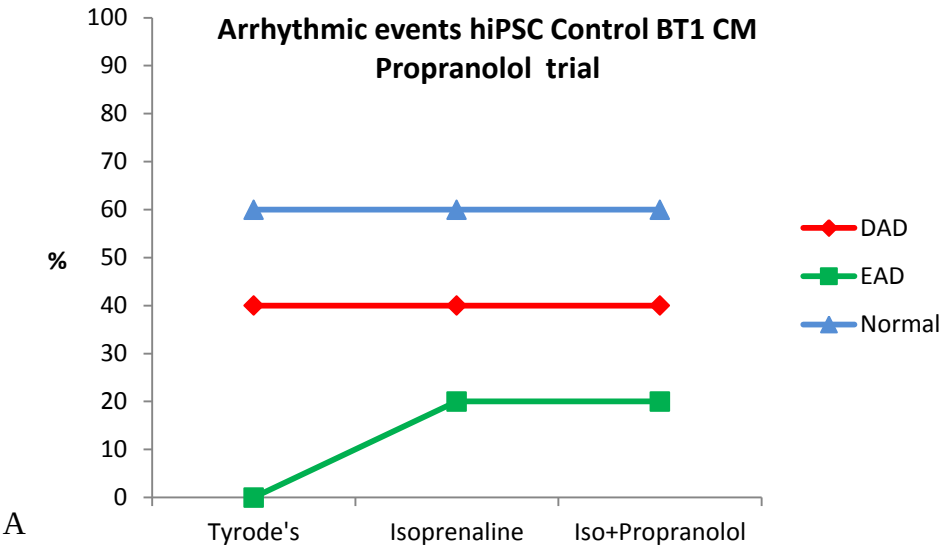

A

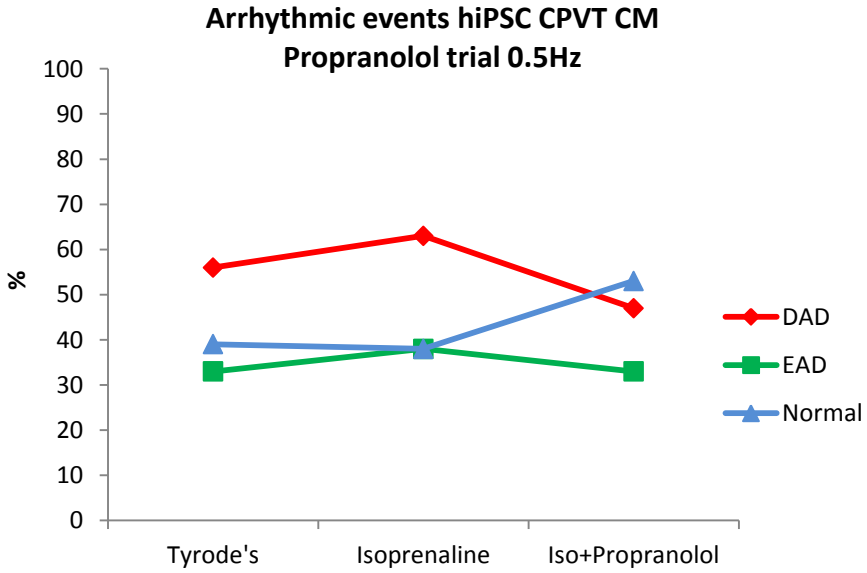

B

Figure 5.27 – Propranolol - Qualitative analysis of arrhythmic endpoints from evoked activity traces - *Evoked activity 0.5Hz, hiPSC BT-1 CM (A, n=5) and hiPSC CPVT CM (B, n=21) using propranolol (1µM) as anti-arrhythmic drug. None of the differences reported in figure 5.27 were found to be statistically significant.*

5.5 Discussion - Electrophysiology

A trial of a more rigorous electrophysiological quantitative analysis is reported for the first time regarding the use of hiPSC CPVT CM as an *in vitro* model of disease. No reports of this nature were found in the current literature, and hence this is also an innovative approach for *in vitro* CPVT disease modelling. A qualitative comparative analysis was also presented so that a comparison could be made with literature reports. If these cells are able to have any real potential to model disease and eventually be used for CPVT novel drug discovery and personalised treatment, quantification of arrhythmic endpoints seems to be essential to validate their predictive translational clinical value.

Although lower than the physiological range for the human adult heart rate (60 to 100bpm), 0.5Hz frequency was chosen for most of the experiments. Higher frequencies would not only bias the endpoint baseline, reducing the ability to measure any change, but would also shorten AP duration. This could eventually mask possible endogenous pro-arrhythmic behaviour, in the form of DADs and eventually EADs. Studied cells, would also last longer while being patched at 0.5Hz than at higher frequencies presenting stronger, more lasting patch clamp seals. However for comparison purposes, data obtained from 1Hz stimulation is also presented in this study.

5.5.1 Quantitative arrhythmic endpoint analysis

The expected response from a good *in vitro* model of CPVT should involve an increase in DAD frequency and amplitude when stimulated with a ß-agonist. In this study isoprenaline was used. This drug should also predispose to TA if a higher DAD threshold would be reached. DAD duration was expected to decrease with isoprenaline response as well an APD50 shortening.

5.5.1.1 Spontaneous activity

Spontaneous activity AP analysis tends to present more subjectivity than evoked activity APs. It is very difficult to start measurements systematically in the same point of origin and these cells are more prone to irregular rhythm when spontaneously beating than when APs are induced and therefore better controlled. One of the main factors that predisposes to increased native frequency of hiPSC CM is temperature. For this reason most recordings were made at 25ºC in order to reduce potential depolarizing events and to try to isolate the isoprenaline effect. Despite these limitations, several reports (Kujala et al., 2012; Itzhaki et al.,2012) studied arrhythmic events mainly in cells with spontaneous activity at 37 ºC.

In this study, no significant differences were found in DADs frequency, duration or amplitude for hiPSC CM with spontaneous activity. Due to the spontaneous nature of hiPSC CM, it was considered that evoked APs could give more certainty that observed events were not due to spontaneous beating.

5.5.1.2 Evoked activity

Data obtained from evoked activity at 0.5Hz and 1Hz showed no statistically significant differences. Measurement of DADs from evoked activity is less prone to bias than data obtained from hiPSC CM with spontaneous activity. Obtaining more data from a higher number of cells could help in determining if increasing pacing frequency could worsen the CPVT phenotype by increasing DAD and TA frequency. More mature cells may eventually display a more accurate CPVT phenotype. Using the procedures described here and based on present data, it was not possible to establish a correlation between CPVT severity and pacing rate.

5.5.1.2.1 Pharmacological rescue

The use of flecainide in the presence of isoprenaline did not demonstrate any significant effect on measured parameters of DADs. A significant AP peak and AP amplitude decrease in CPVT CM (Figure 6.7A and D respectively) can be explained by the $I_{(Na)}$ blocking properties of flecainide. Decreased APD50 with isoprenaline (Figure 6.8) was also expected, as a shortening of this parameter is typical for a ß-agonist effect. In contrast to what Itzhaki et al., (2012) demonstrated, flecainide efficacy in reducing arrhythmic endpoints, could not be observed in the current project. It is nonetheless surprising that these authors found significant results in a small number of analysed cells (n=6), since in the data reported in the present project, 20 hiPSC CPVT CM were analysed.

Similar to what was observed in the flecainide experiments, propafenone perfusion, significantly decreased AP peak and AP amplitude in CPVT CM. This can be explained with a similar mechanism of action to flecainide, by blocking $I_{(Na)}$ (Figure 6.11A and D respectively). A significant shortening of APD50 and APD90 in BT1 CM was also observed, possibly as a result of isoprenaline or propafenone effect. Since no response to isoprenaline alone was observed and no propafenone alone experiments were made, it is difficult to determine any clear drug effect over APD50.

The anti-arrhythmic agent propranolol caused a significant reduction in DAD duration in the presence of isoprenaline (Figure 6.18A,C). However, this seems to be an isolated finding since in no other experiment was this response repeated. From a disease recapitulation perspective it could have some importance if isoprenaline alone had previously caused a significant response.

Dantrolene efficacy in reducing pro-arrhythmic events has already been demonstrated in hiPSC CPVT CM (Jung et al.,2012). In the present study no significant effect was seen in the arrhythmic selected endpoints for this study, but no effect was seen with isoprenaline perfusion as well.

It was expected that isoprenaline would cause a significant increase in arrhythmic events. Since this response was absent, a correlation could not be established for the sequential pharmacological rescue with the chosen drugs.

In summary, using quantitative arrhythmic endpoints as DAD frequency, amplitude or duration, it was not possible to recapitulate CPVT *in vitro*.

5.5.2 Qualitative endpoint analysis

By analysing the same data sets using a qualitative approach, no statistical significant changes were found. Therefore these data could not be compared with other published results that report DAD and EAD percentage of events.

5.6 Validation by Ca^{2+} Imaging

In order to validate hiPSC CPVT CM as an *in vitro* model of disease, Ca^{2+} handling in these cells needed to be studied. Different Ca^{2+} fluorescence imaging experiments were performed and both qualitative and quantitative arrhythmogenic endpoints were defined to evaluate the effects of increased pacing (simulating intense exercise) and ß – agonist stimulation. The published literature contains only two reports using defined qualitative arrhythmic endpoints. These reports used stimulated activity in hiPSC CPVT CM to determine the percentage of pro-arrhythmogenic Ca^{2+} cycling abnormalities (Kujala et al.,2012; Jung et al.,2012). In both reports three types of pro-arrhythmic Ca^{2+} transient traces were defined as endpoints. Both hiPSC CPVT CM and control hiPSC CM were then challenged with ß-agonist perfusion and increased pacing.

For the current project three types of qualitative arrhythmic traces were defined, based on Ca^{2+} transient amplitude and rhythmicity: AR1 – transients with irregular amplitude and regular rhythm; AR2 – transients with regular amplitude and irregular rhythm and AR3 – transients with irregular amplitude and irregular rhythm. This last type of Ca^{2+} transient represents a more severe phenotype of Ca^{2+} cycling abnormality (figure 5.28C). A normal trace was considered to have regular amplitude and regular rhythm.

It was determined that a quantitative approach would also be necessary to evaluate the *in vitro* disease recapitulation potential of these cells. Selected Ca^{2+} imaging parameters were peak regularity, ITN (Inter Transient Noise), amplitude, standardised area, rate and rate of decay. Perfusion with anti-arrhythmic drugs in the presence of isoprenaline should rescue pro-arrhythmic behaviour, as reflected in these parameters. Decreases in ITN and peak regularity are good indicators of antiarrhythmic response. However, effects on amplitude, rate and rate decay are also important parameters to study in order to observe the actions of a drug on basic CM behaviour. These last three parameters are related to inotropy, chronotropy and lusitropy of the heart.

The main hypothesis tested in these experiments was that abnormal Ca^{2+} handling behaviour is more frequent and severe in CPVT CM compared with BT1 CM. It was also hypothesised that isoprenaline perfusion or increased pacing would produce a more severe arrhythmic phenotype. Perfusion with anti-arrhythmic drugs in the presence of isoprenaline should improve this phenotype by restoring endpoints close to baseline levels.

No reports were found in the literature that used quantitative pro-arrhythmic parameters from global Ca^{2+} transients. The current study hence presents an innovative approach to determine if hiPSC CPVT CM have the ability to recapitulate disease *in vitro.*

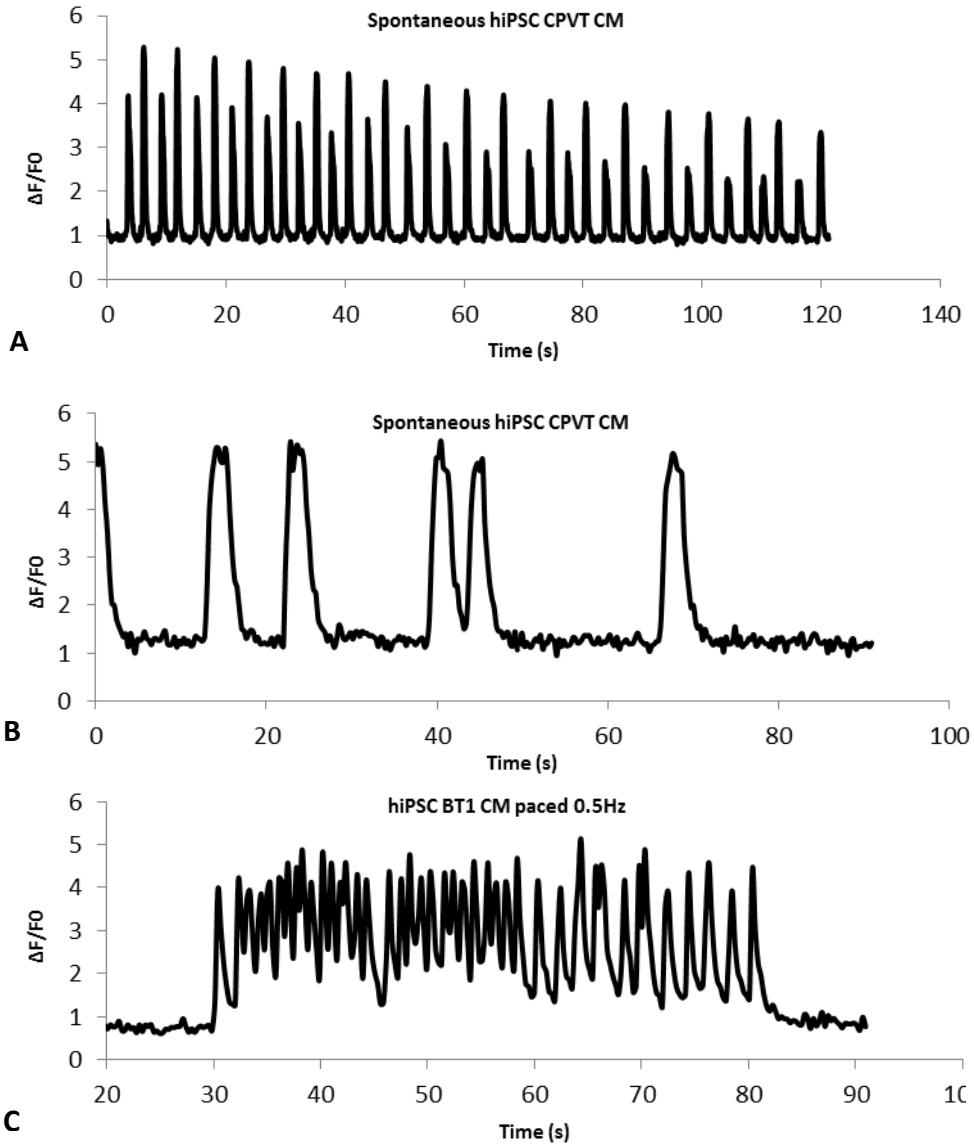

Figure 5.28 – Example traces of arrhythmic sub-types used in* Ca^{2+} *imaging qualitative assessment study. *(A) Arrhythmic sub-type AR1 with "calcium alternans"; (B) Arrythmic sub-type AR2, (C) Arrhythmic sub-type AR3.*

5.7 Ca^{2+} Imaging Methods

For more detailed information about Ca^{2+} Imaging Methods, please refer to section 2.4 of Chapter 2.

For the drug perfusion trial experiments, FLUO-4 AM® (fluo-4 acetoxymethyl) from Invitrogen was used as a Ca^{2+} sensitive fluorescent indicator (5µM). Local and global hiPSC CM Ca^{2+} signals, were recorded using laser scanning confocal microscopy, (SP5; Leica Microsystems).

Disaggregated single cells, in glass bottom Mattek dishes, were incubated for 20 minutes at room temperature in modified Tyrode's and FLUO-4 AM® (5µM). Ca^{2+} dependent signals were visualized with a 63x oil immersion objective, using argon laser excitation at 488nm. Experiments were conducted at 37 ºC and images recorded every 100ms at a 512x512 pixel resolution.

All recordings (90 seconds each) were made following a triple sequential protocol for each field of view. First perfusion on Tyrode's only, second perfusion withTyrode's and isoprenaline (1µM), and third with Tyrode's with a drug in the presence of isoprenaline (1µM). Drugs used were propranolol (1µM), flecainide (10µM) and dantrolene (10µM). A 60 seconds washout was performed with Tyrode's in between each protocol.

5.8 Ca^{2+} Imaging Results

Validation of hiPSC CPVT CM as an *in vitro* model of disease requires that the Ca^{2+} handling and arrhythmogenic profile these cells be determined. Both qualitative and quantitative arrhythmogenic endpoints were defined to evaluate the effects of ß– agonist stimulation (strong emotion and exercise).

It is the first time that a more detailed Ca^{2+} handling arrhythmogenic profile is investigated using hiPSC CPVT CM as a potential model of disease.

For the chosen quantitative Ca^{2+} handling arrhythmogenic endpoints, no consistent statistically response was found for the majority of the experiments.

Qualitative analysis of the chosen arrhythmic endpoints also did not show statistical significance.

From the presented Ca^{2+} handling arrhythmogenic profile data it was conclude that disease recapitulation is not consistent and therefore relevant for the CPVT CM model used in this project.

5.8.1 Quantitative analysis of arrhythmic endpoints

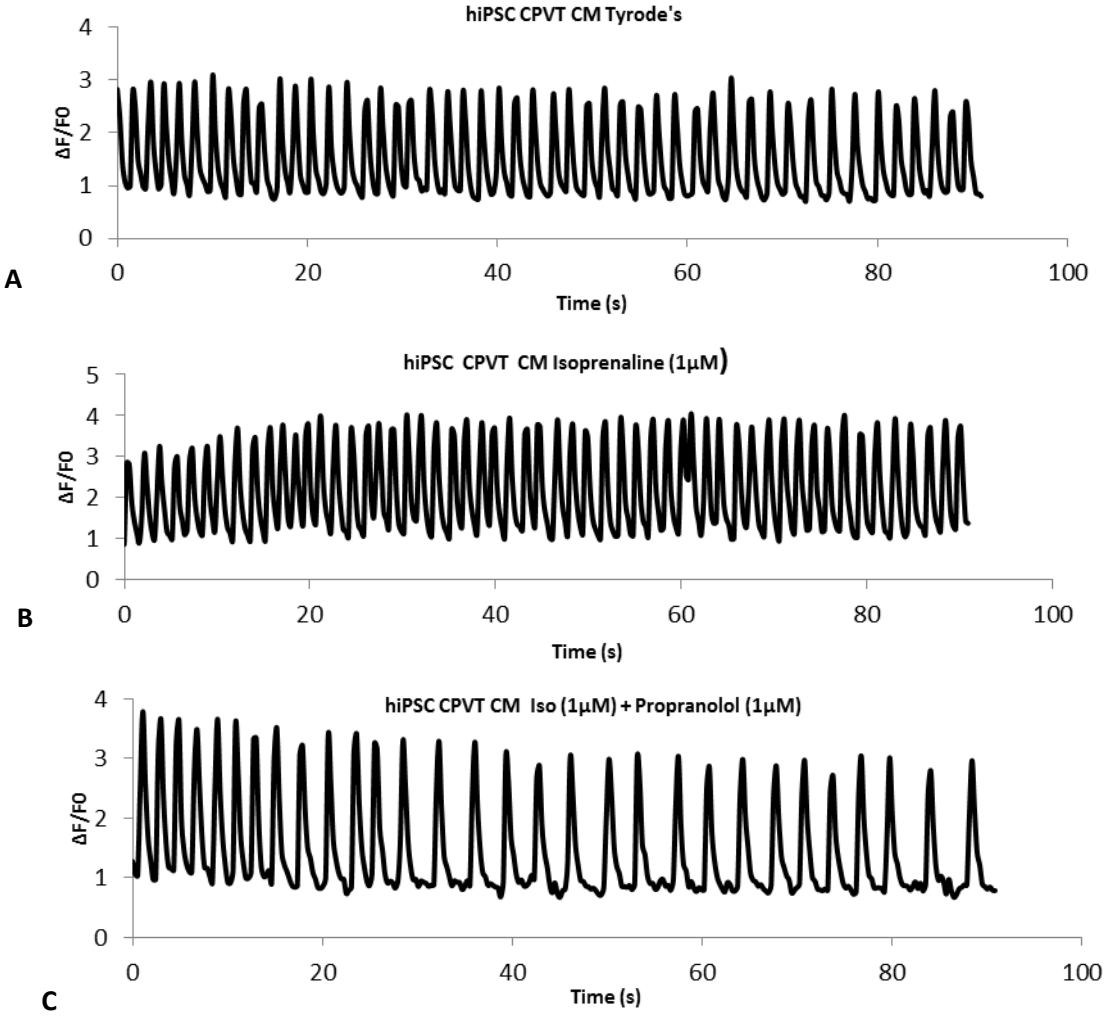

Figure 5.29 – Sequential example traces of Ca^{2+} imaging drug perfusion trial *- Ca^{2+} imaging of spontaneous beating hiPSC CPVT CM, in Tyrode's (A) isoprenaline 1µM (B) and propranolol 1µM in the presence of isoprenaline 1µM (C). Sequential traces from the same cell. Similar sequence of traces was obtained for dantrolene and flecainide.*

5.8.1.1 Flecainide

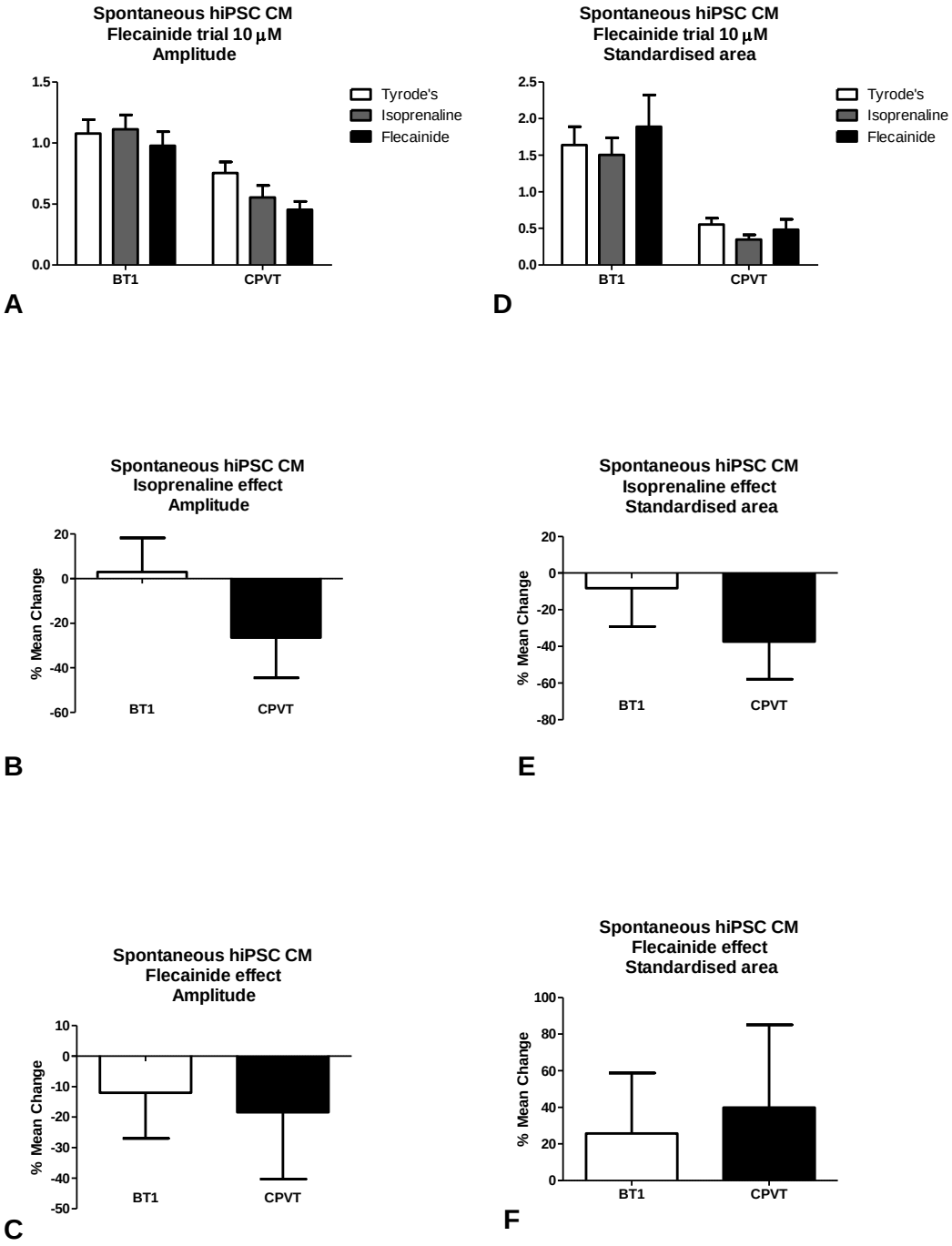

Figure 5.30 – Amplitude and standardised area of Ca^{2+} transients upon flecainide perfusion *- Mean percentage change presented for isoprenaline perfusion in amplitude and standardised area (B and E respectively) and flecainide in the presence of isoprenaline (C, F respectively). hiPSC CPVT CM (n=16) and control hiPSC BT1 CM (n=36). None of the differences reported in figure 5.30 were found to be statistically significant.*

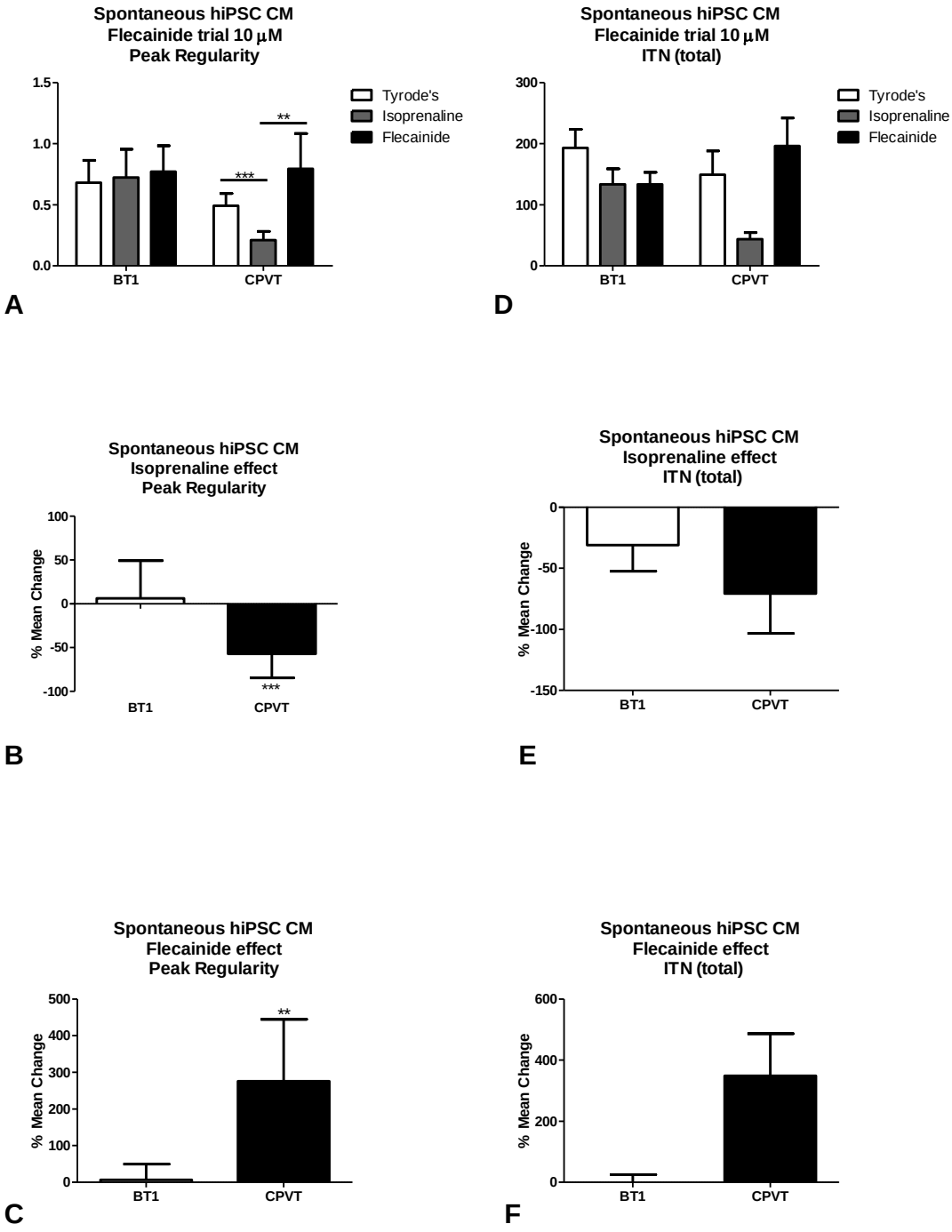

Figure 5.31 – Peak regularity and ITN of Ca^{2+} transients upon flecainide perfusion - *Mean percentage change presented for isoprenaline perfusion in peak regularity and ITN (B and E respectively) and flecainide in the presence of isoprenaline (C, F respectively). hiPSC CPVT CM (n=16) and control hiPSC BT1 CM (n=36). A significant 50% decrease in peak regularity was observed in CPVT CM upon isoprenaline perfusion (figure 5.31A, B). Flecainide in the presence of isoprenaline, presented a very significant increase of 300% in peak regularity (figure 5.31C) for CPVT CM. None of the differences reported in figure 5.31A were found to be statistically significant for BT1 CM.*

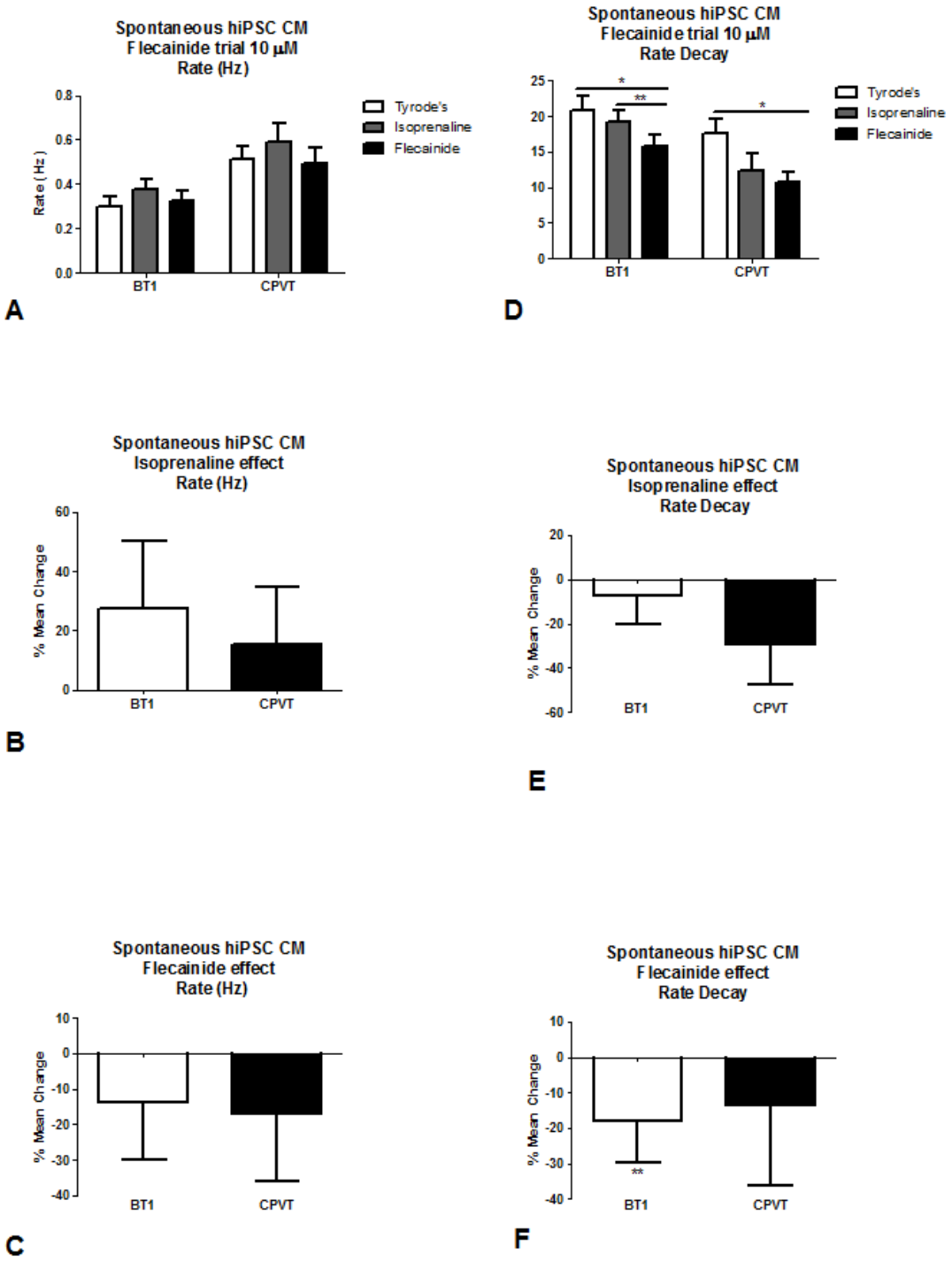

Figure 5.32 – Rate (Hz) and Rate decay of Ca^{2+} transients upon flecainide perfusion - *Mean percentage change presented for isoprenaline perfusion in rate (Hz) and rate decay (B and E respectively) and flecainide in the presence of isoprenaline (C, F respectively). hiPSC CPVT CM (n=16) and control hiPSC BT1 CM (n=36). Rate decay presented a significant decrease in BT1 CM upon flecainide perfusion in the presence of isoprenaline after isoprenaline alone (figure 5.32D, F). CPVT CM rate decay also presented a significant decrease when perfused with flecainide in the presence of isoprenaline, compared with the Tyrode's rate decay value (figure 5.32D). None of the differences reported for rate (Hz) (figure 5.32A) were found to be statistically significant for both cell types.*

5.8.1.2 Dantrolene

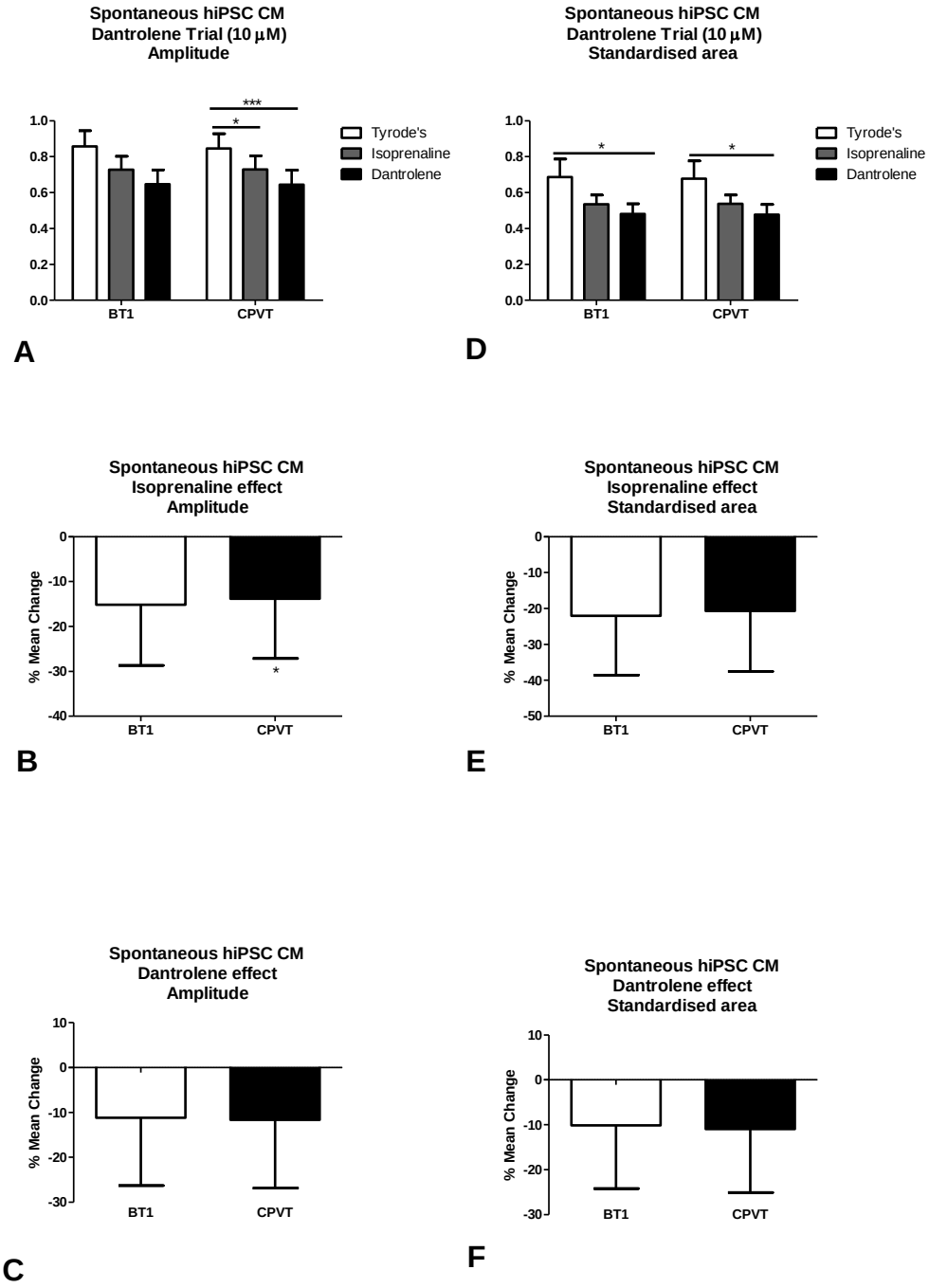

Figure 5.33 – Amplitude and standardised area of Ca^{2+} transients upon dantrolene perfusion *- Mean percentage change presented for isoprenaline perfusion in amplitude and standardised area (B and E respectively) and dantrolene in the presence of isoprenaline (C, F respectively). hiPSC CPVT CM (n=14) and control hiPSC BT1 CM (n=14). Amplitude in CPVT CM significantly decreased in the presence of isoprenaline compared with Tyrode's (figure 5.33A, B). A significant decrease was also observed in CPVT CM when perfused with dantrolene in the presence of isoprenaline when compared with the Tyrode's baseline values (figure 5.33A). A 20% decrease in standardised area was found to be significant for both BT1 CM and CPVT CM when perfused with dantrolene in the presence of isoprenaline and compared with the baseline Tyrode's values (figure 5.33D).*

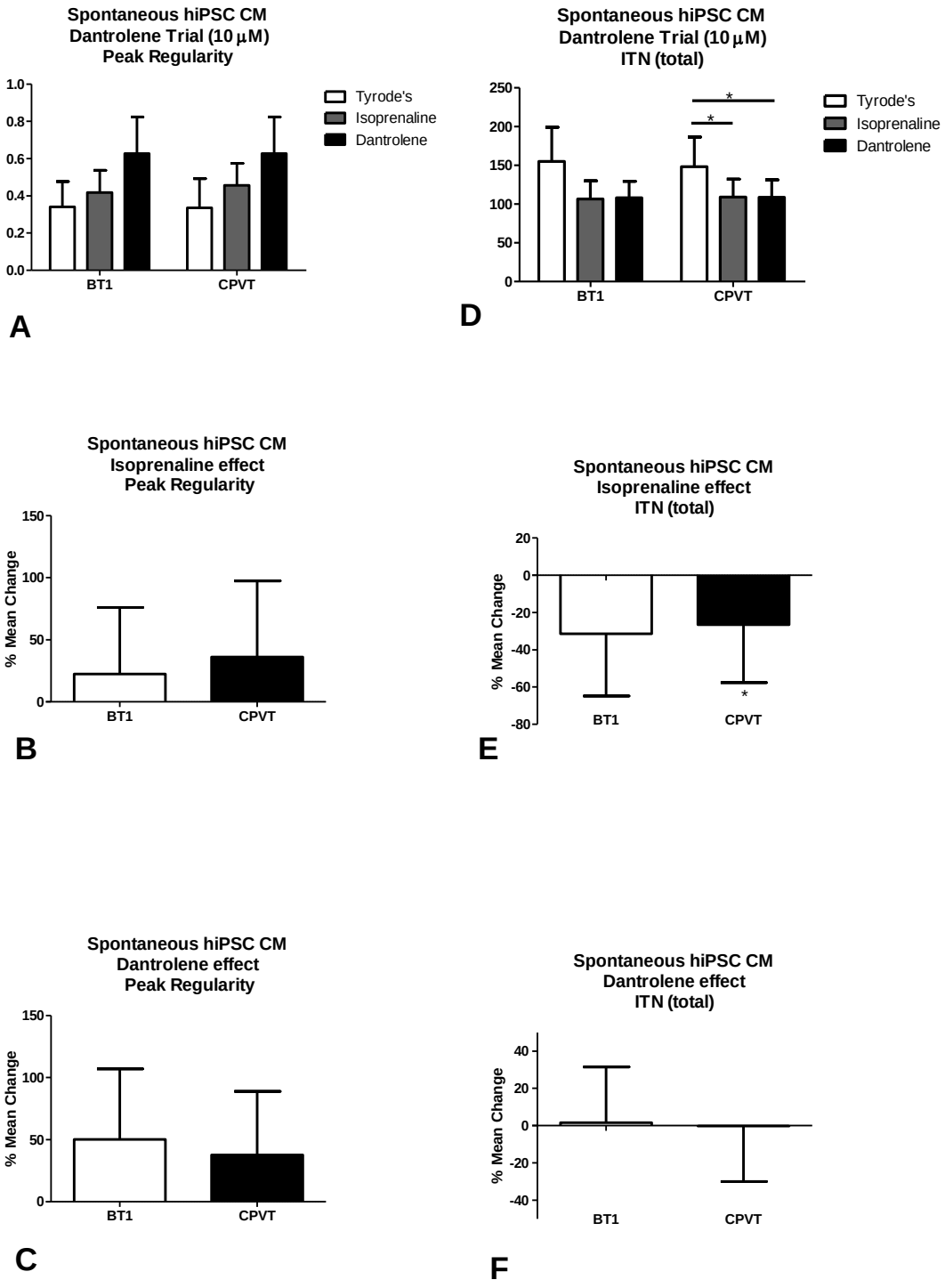

Figure 5.34 – Peak regularity and ITN of Ca^{2+} transients upon dantrolene perfusion *- Mean percentage change presented for isoprenaline perfusion in peak regularity and ITN (B and E respectively) and dantrolene in the presence of isoprenaline (C, F respectively). hiPSC CPVT CM (n=14) and control hiPSC BT1 CM (n=14). When perfused with isoprenaline alone, ITN showed a significant 20% decrease in CPVT CM when compared with Tyrode's (Figure 5.34 D, E). Perfusion of dantrolene in the presence of isoprenaline also produced a significant ITN decrease if compared with the baseline Tyrode's value (figure 5.34 D).*

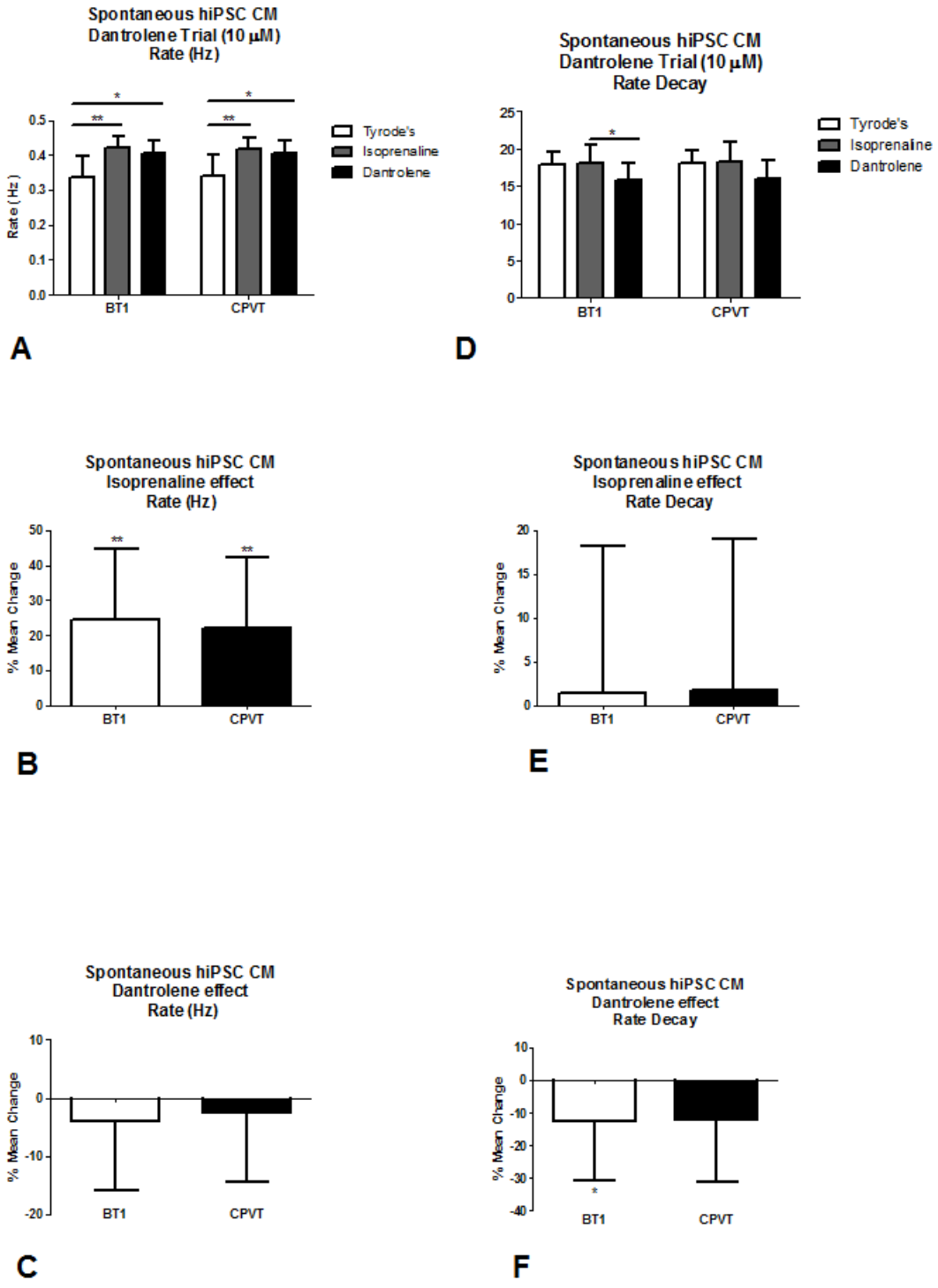

Figure 5.35 – Rate (Hz) and Rate decay of Ca^{2+} transients upon dantrolene perfusion *- Mean percentage change presented for isoprenaline perfusion in rate (Hz) and rate decay (B and E respectively) and dantrolene in the presence of isoprenaline (C, F respectively). hiPSC CPVT CM (n=14) and control hiPSC BT1 CM (n=14). A significant increase was seen in beating rate (Hz) in both control and mutant CM upon isoprenaline perfusion (figure 5.35A, B). Similarly, a rate increase was found to be significant when BT1 CM and CPVT CM were perfused with dantrolene in the presence of isoprenaline and compared with Tyrode's (figure 5.35A). In figure 5.35D and 5.35F a significant 10% decrease in rate decay was present in BT1 CM upon perfusion with dantrolene in the presence of isoprenaline.*

5.8.1.3 Propranolol

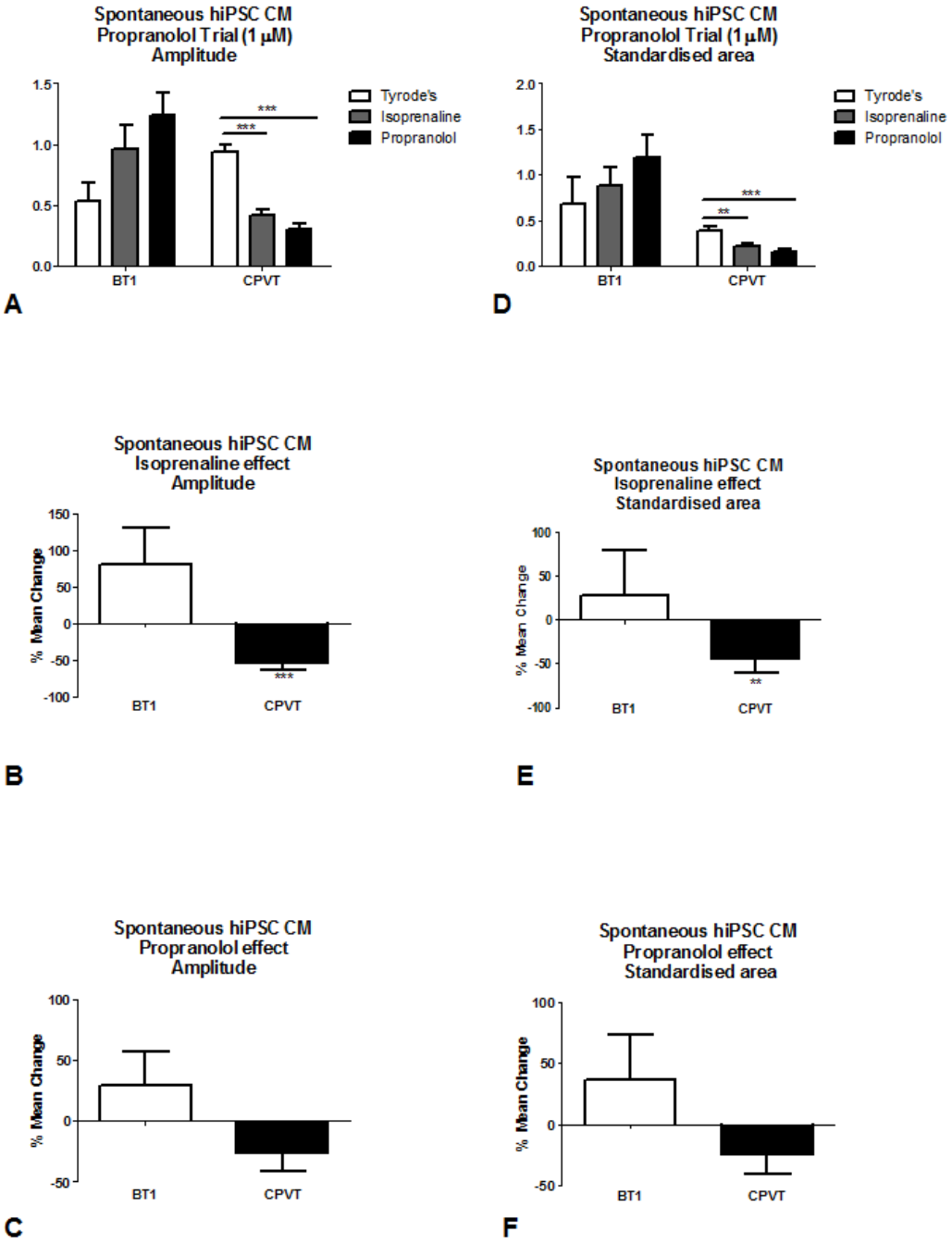

Figure 5.36 – Amplitude and standardised area of Ca^{2+} transients upon propranolol perfusion *- Mean percentage change presented for isoprenaline perfusion in amplitude and standardised area (B and E respectively) and propranolol in the presence of isoprenaline (C, F respectively). hiPSC CPVT CM (n=12) and control hiPSC BT1 CM (n=29). Average Ca^{2+} transient amplitude, significantly decreased by 50% in CPVT CM when perfused with isoprenaline (figure 5.36A,B). A significant decrease was also observed in amplitude when perfused with propranolol in the presence of isoprenaline when compared with Tyrode's alone (figure 5.36A). Standardised area value also presented a significant decrease in CPVT CM when perfused with isoprenaline (figure 5.36D, E). In the presence of propranolol and isoprenaline a significant decrease was also present when compared with Tyrode's alone (figure 5.36D).*

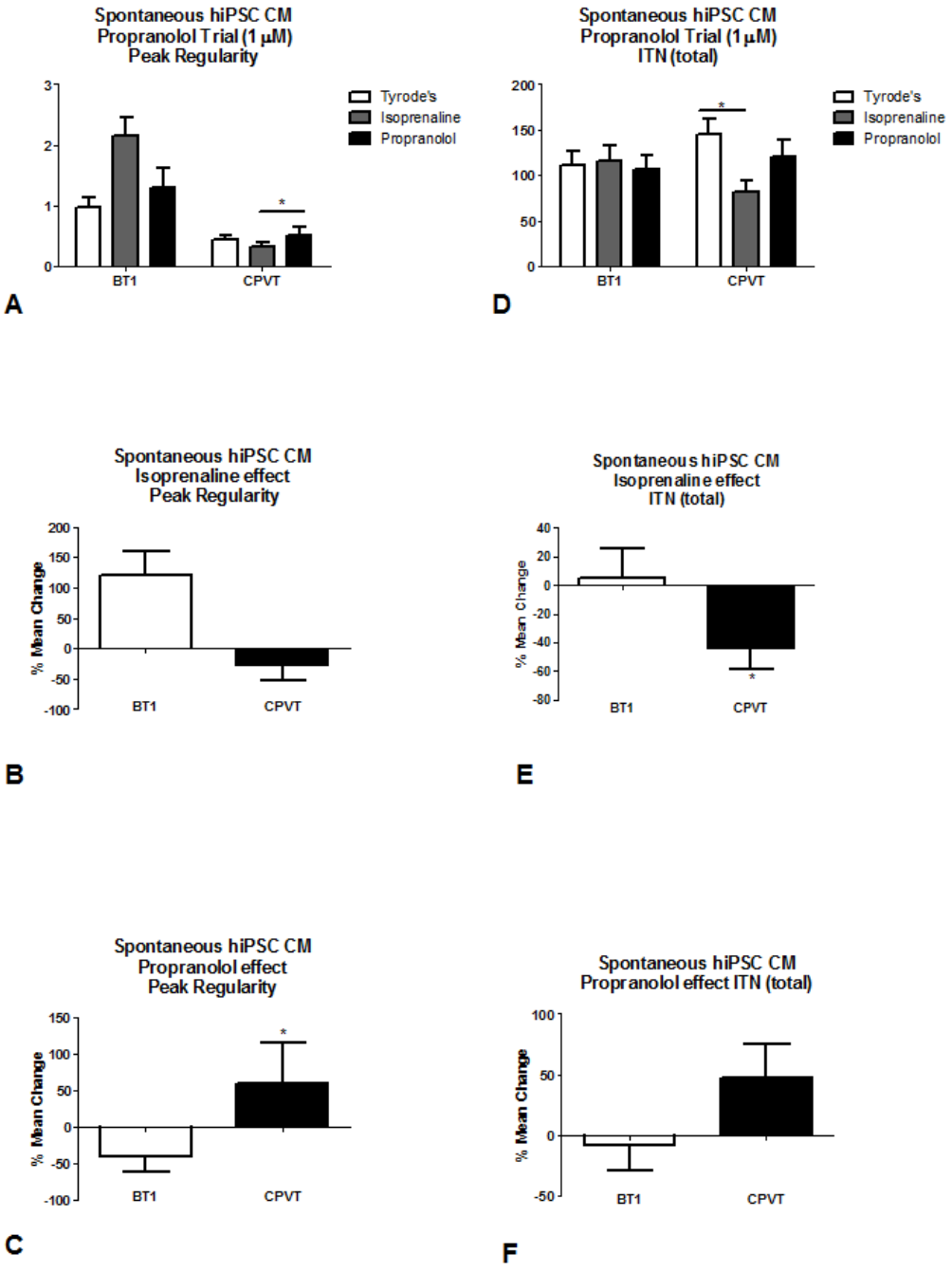

Figure 5.37 – Peak regularity and ITN of Ca^{2+} transients upon propranolol perfusion *- Mean percentage change presented for isoprenaline perfusion in peak regularity and ITN (B and E respectively) and propranolol in the presence of isoprenaline (C, F respectively). hiPSC CPVT CM (n=12) and control hiPSC BT1 CM (n=29). A significant increase of approximately 50% was observed in the peak regularity parameter for CPVT CM when perfused with propranolol in the presence of isoprenaline, compared with isoprenaline perfused alone (figure 5.37 A, C). Isoprenaline perfusion produced a significant 43% decrease in ITN in CPVT CM compared with baseline Tyrode's data (figure 5.37D, E).*

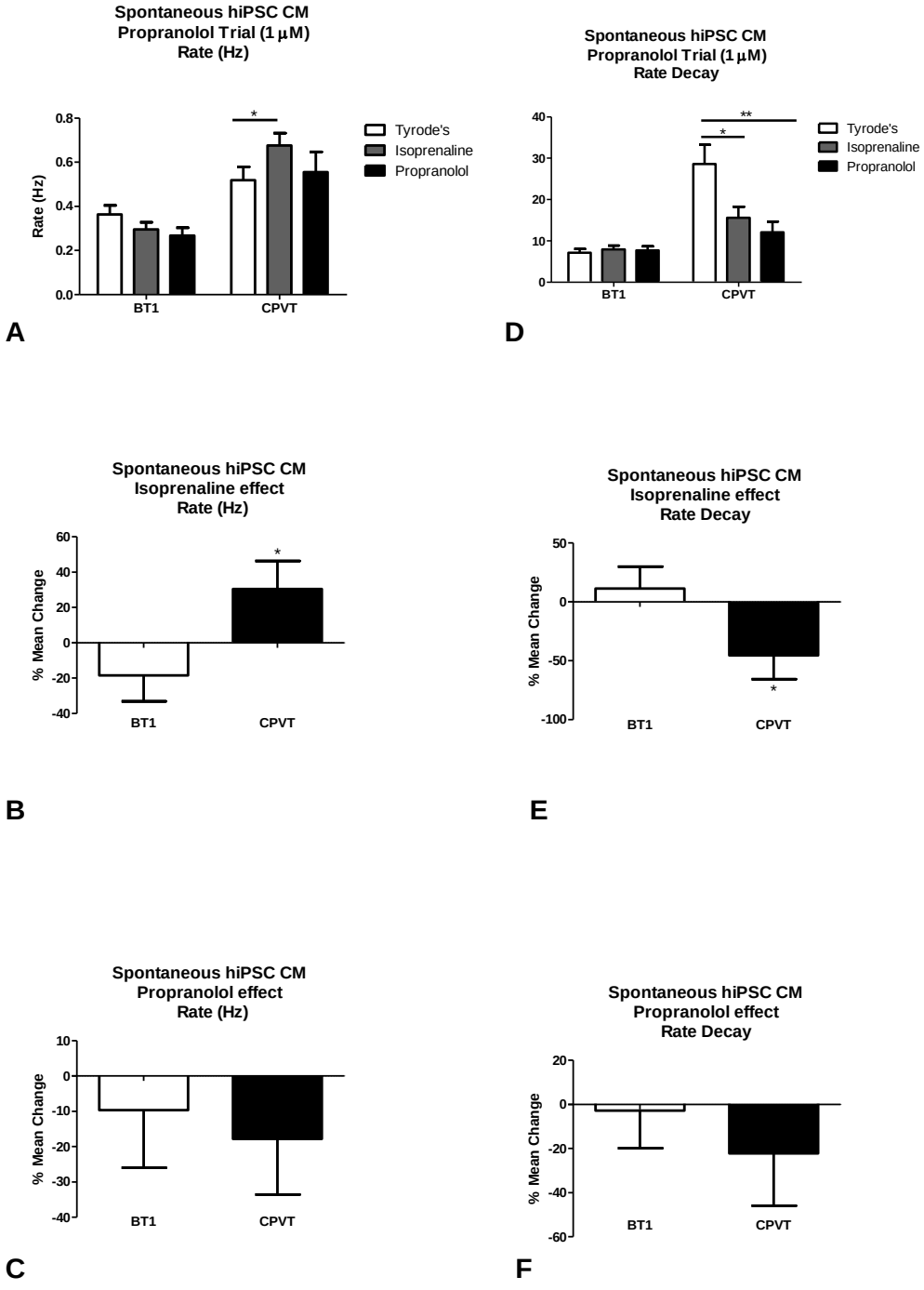

Figure 5.38 – Rate (Hz) and Rate decay of Ca^{2+} transients upon propranolol perfusion *- Mean percentage change presented for isoprenaline perfusion in rate (Hz) and rate decay (B and E respectively) and propranolol in the presence of isoprenaline (C, F respectively). hiPSC CPVT CM (n=12) and control hiPSC BT1 CM (n=29). A significant 30% increase in beating rate (Hz) was observed in CPVT when perfused with isoprenaline (figure 5.38A, B). Rate decay value significantly decreased 50% in CPVT CM with isoprenaline perfusion (figure 5.38D,E), demonstrating a positive lusitropic effect. A significant decrease was also observed with propranolol in the presence of isoprenaline when compared with Tyrode's (figure 5.38D).*

5.8.2 Qualitative analysis of arrhythmic endpoints

In this set of experiments, a qualitative study of arrhythmic endpoints is presented for hPSC CM with spontaneous activity. Traces used for this study were the same obtained for the quantitative drug perfusion trial presented in the previous section. A normal trace was defined as presenting normal rhythm and normal amplitude. AR1 – trace with irregular amplitude and regular rhythm, AR2 – trace with regular amplitude and irregular rhythm, AR3 – trace with irregular amplitude and irregular rhythm.

5.8.2.1 Spontaneous activity

5.8.2.1.1 Flecainide

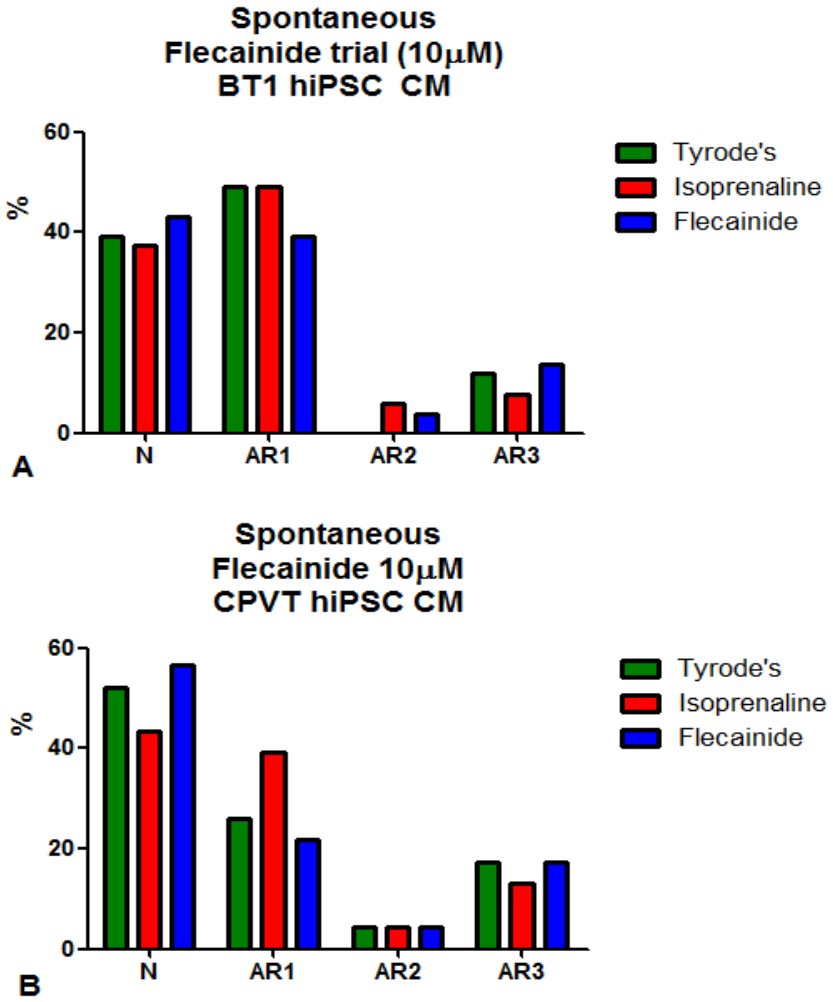

Figure 5.39 – Flecainide perfusion qualitative study *- Ca^{2+} imaging arrhythmic endpoints, on spontaneous beating hiPSC BT1 CM (n=36) and hiPSC CPVT CM (n=16). None of the differences reported in figure 5.39 were found to be statistically significant.*

5.8.2.1.2 Dantrolene

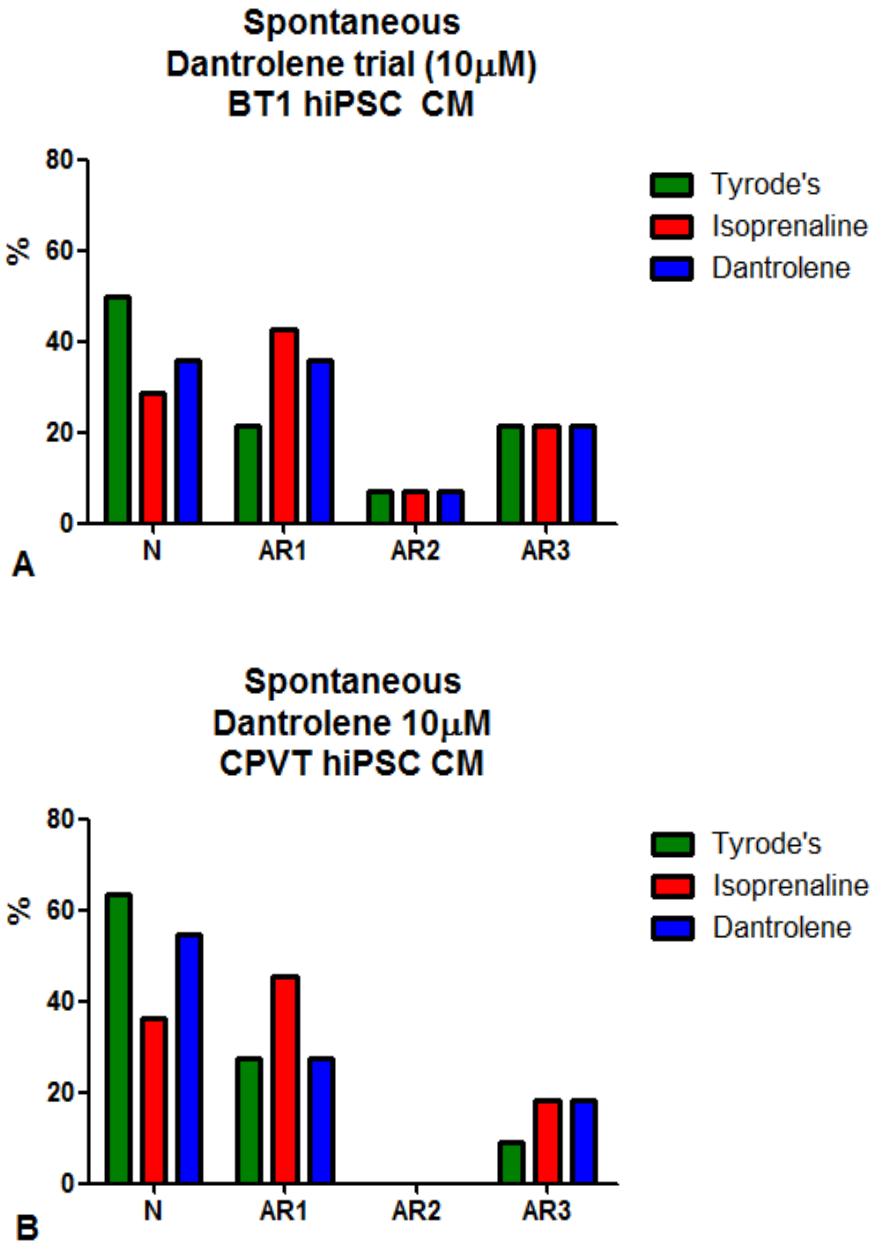

Figure 5.40 – Dantrolene perfusion qualitative study *- Ca^{2+} imaging arrhythmic endpoints, on spontaneous beating hiPSC BT1 CM (n=14) and hiPSC CPVT CM (n=14). None of the differences reported in figure 5.40 were found to be statistically significant.*

5.8.2.1.3 Propranolol

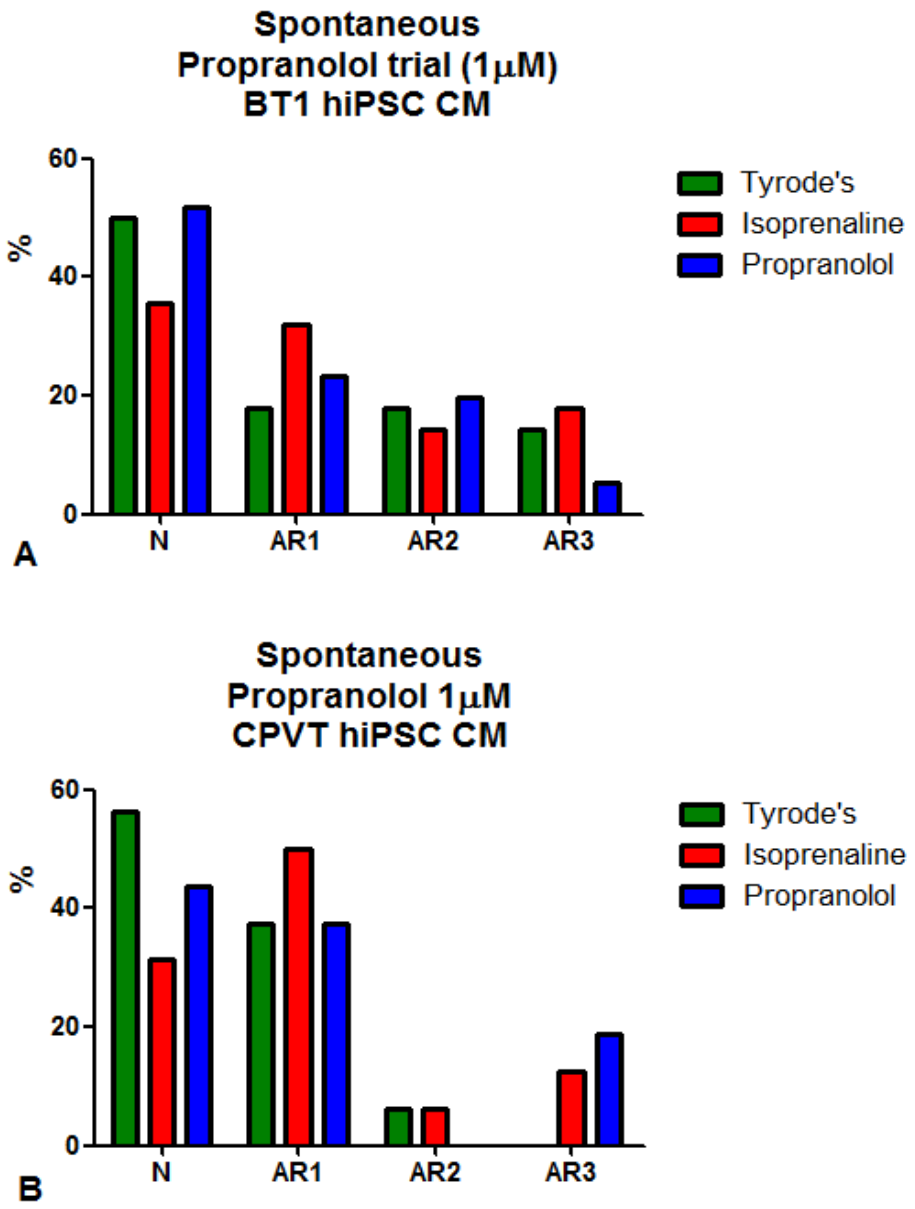

Figure 5.41 – Propranolol perfusion qualitative study *- Ca^{2+} imaging arrhythmic endpoints, on spontaneous beating hiPSC BT1 CM (n=29) and hiPSC CPVT CM (n=12). None of the differences reported in figure 5.41 were found to be statistically significant.*

5.8.2.2 Stimulated activity – Frequency study

The objective of doing an increased stimulated frequency study was to determine if the arrhythmic phenotype of CPVT CM would increase with frequency increase. It was expected for the number of normal traces to decrease with frequency increase. This could be a suggestion of disease recapitulation, simulating what violent exercise does in CPVT. Isoprenaline perfusion was expected to worsen the phenotype in each stimulated frequency.

5.8.2.2.1 – 0.5Hz

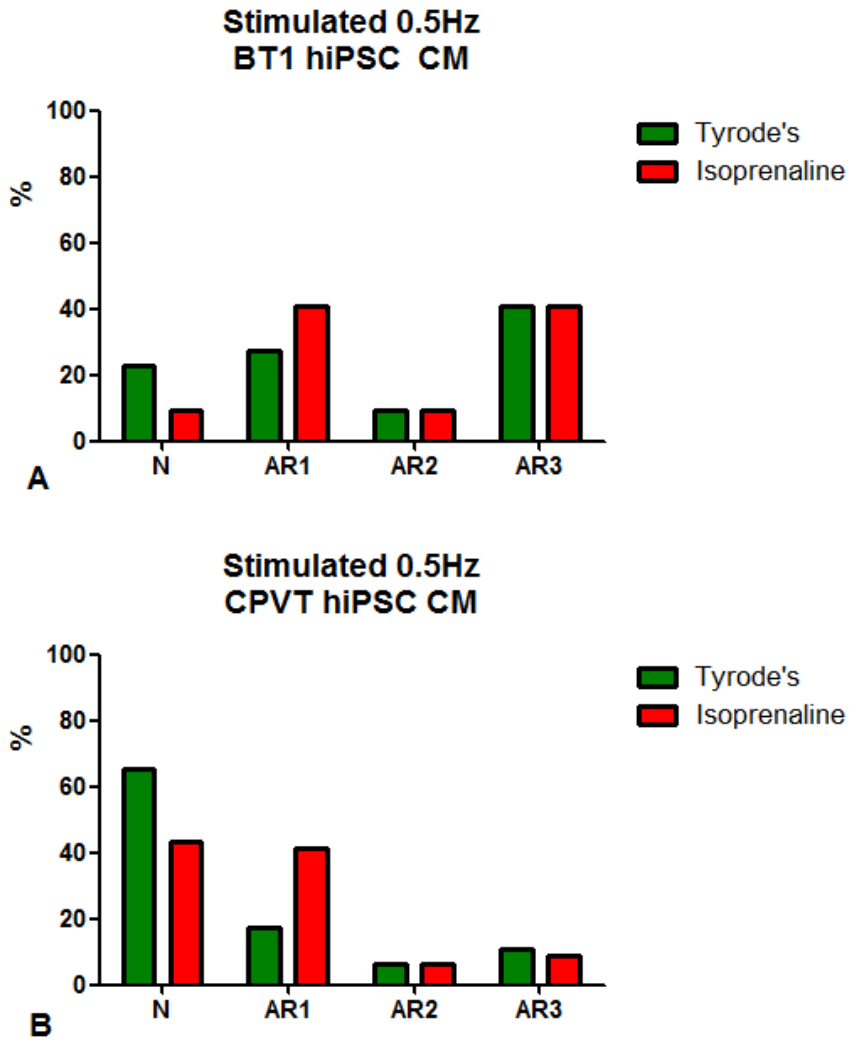

Figure 5.42 – Stimulation 0.5Hz qualitative study *- arrhythmic endpoints from Ca^{2+} imaging data in Tyrode's and isoprenaline perfusion (1μM). hiPSC BT1 CM (n=18) and hiPSC CPVT CM (n=48). None of the differences reported in figure 5.42 were found to be statistically significant.*

5.8.2.2.2 – 1Hz

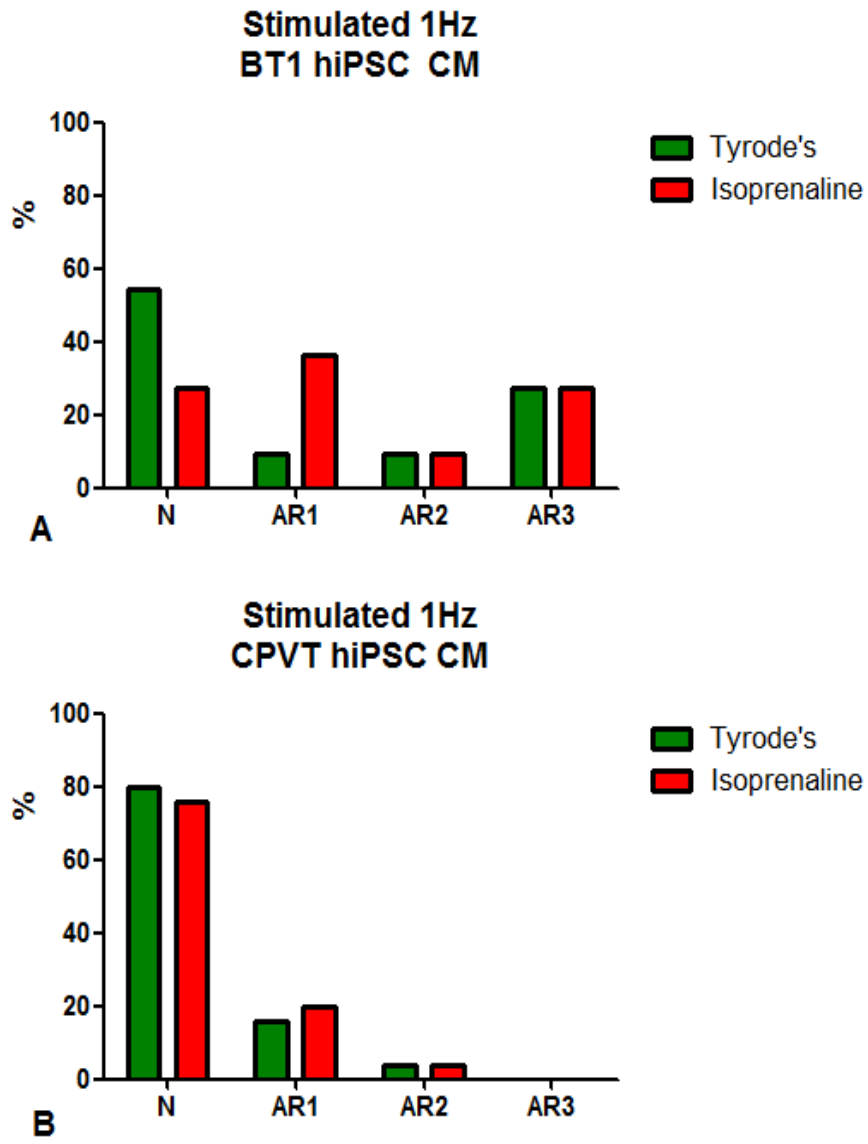

Figure 5.43 – Stimulation 1Hz qualitative study *- arrhythmic endpoints from Ca^{2+} imaging data in Tyrode's and isoprenaline perfusion (1µM). hiPSC BT1 CM (n=18) and hiPSC CPVT CM (n=40). None of the differences reported in figure 5.43 were found to be statistically significant.*

5.8.2.2.3 – 1.5Hz

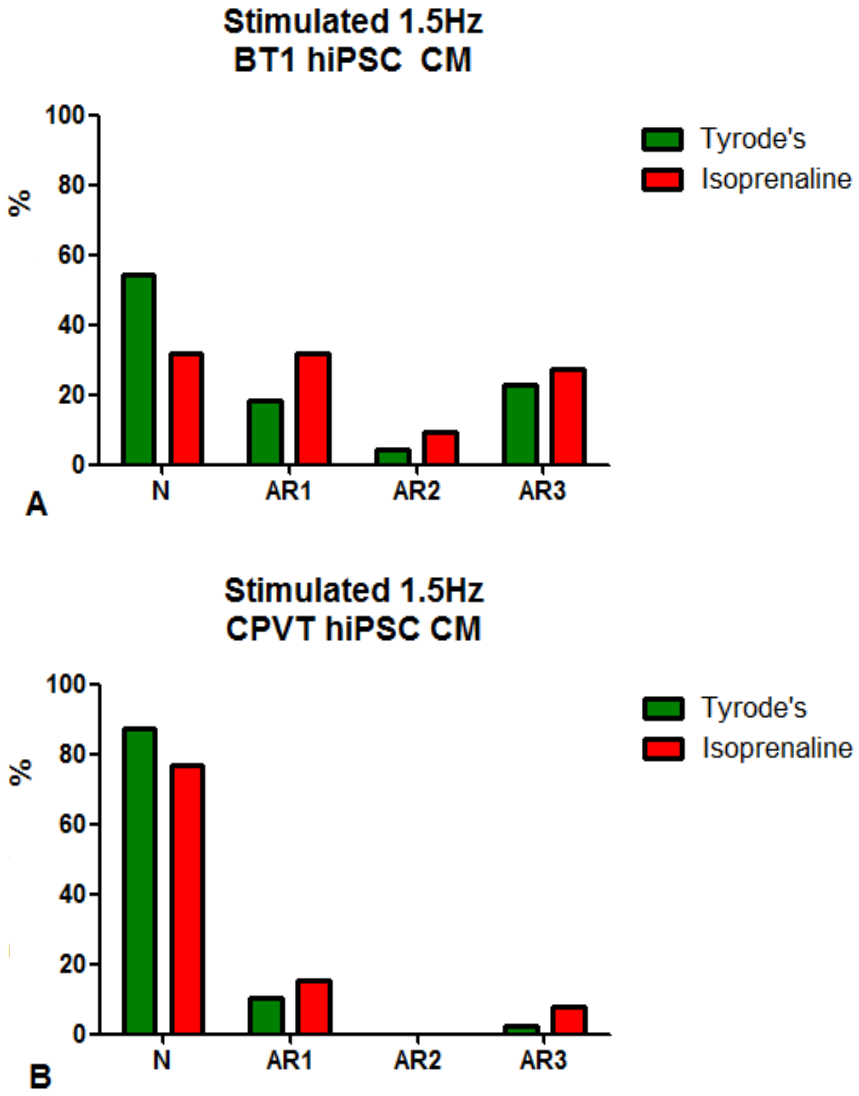

Figure 5.44 – Stimulation 1.5Hz qualitative study *- arrhythmic endpoints from Ca^{2+} imaging data in Tyrode's and isoprenaline perfusion (1μM). hiPSC BT1 CM (n=18) and hiPSC CPVT CM (n=32). None of the differences reported in figure 5.44 were found to be statistically significant.*

5.8.2.2.4 – 2Hz

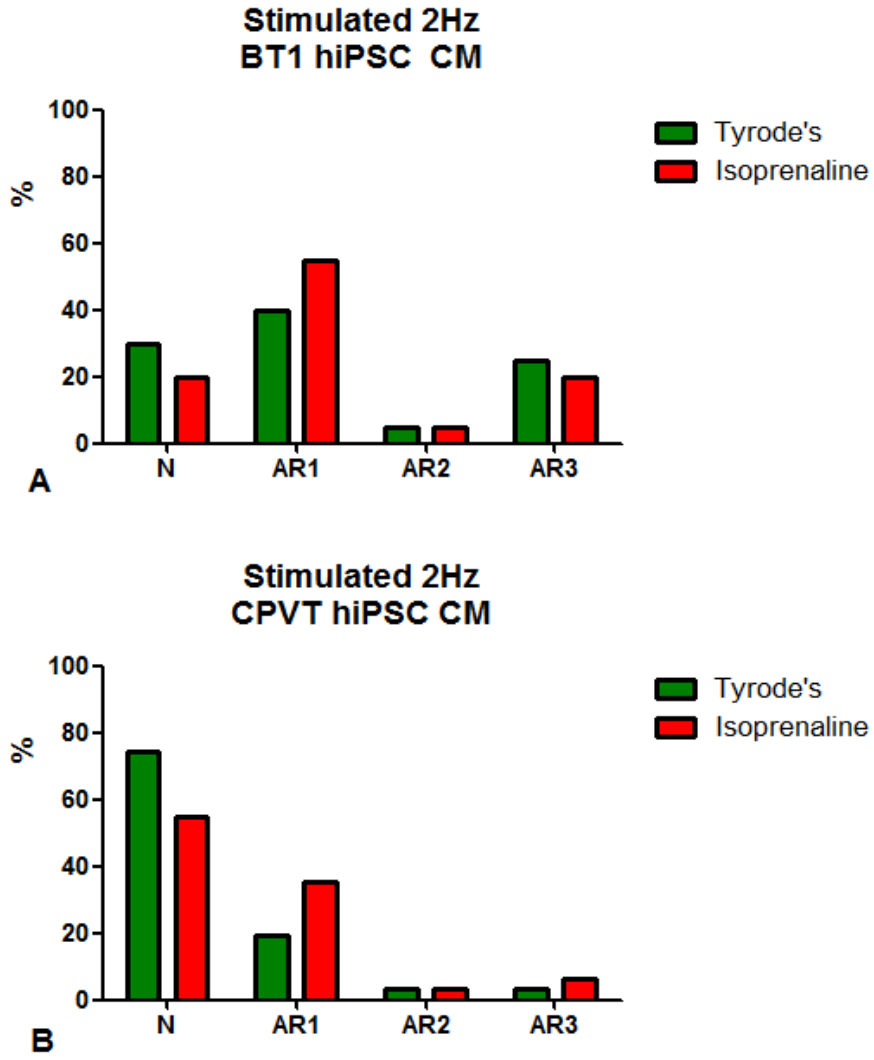

Figure 5.45 – Stimulation 2Hz qualitative study *- arrhythmic endpoints from Ca^{2+} imaging data in Tyrode's and isoprenaline perfusion (1μM). hiPSC BT1 CM (n=16) and hiPSC CPVT CM (n=28). None of the differences reported in figure 5.45 were found to be statistical significant.*

5.9 Discussion for Ca^{2+} imaging

5.9.1 Quantitative analysis

From Ca^{2+} imaging experiments presented in this chapter it was not possible to establish that the chosen endpoints recapitulate disease. Firstly, because no statistical significance was found for the majority of the data sets in both mutant and control cells. But when statistically significant differences are confirmed, expected response to isoprenaline perfusion, fails to recapitulate CPVT in most cases. A response to isoprenaline perfusion is pivotal to validate a CPVT model of *in vitro* disease. If this response does not clearly increase the average of arrhythmic endpoints drug rescue is not valid and hence results not trustworthy for any translational extrapolation.

5.9.2 Qualitative analysis

5.9.2.1 Drug trial

No statistical significance was found for the qualitative analysis of arrhythmic endpoints in the current report.

5.9.2.2 Frequency stimulation study

This study was designed to determine if an increase in pacing frequency would increase arrhythmogenic behaviour. It also aimed to determine if isoprenaline perfusion would increase different sub-types of arrhythmic behaviour in synergy with an increase in pacing rate. No statistical significance was found for qualitative analysis of arrhythmic endpoints in any of the frequency stimulation trials.

6.10 Conclusion

From the data reported in this chapter it is clear that hiPSC CPVT CM with the Ser2246Leu mutation did not recapitulate the disease *in vitro*. An electrophysiology study of DADs frequency, duration and amplitude did not present statistical significance and even failed to show a clear trend towards CPVT phenotype recapitulation. In Ca^{2+} imaging experiments, some parameters, in a limited number of trials, seem to recapitulate CPVT features, but statistical significance was not found in the majority of parameters. An increase in population sample of both CPVT CM and control CM could make a difference in statistical significance determination. More mature hiPSC CM may also display a more "adult-like" phenotype and eventually recapitulate disease more consistently. Despite this a high degree of variability in the behaviour of hiPSC CM between batches for the same protocols is obvious.

More studies using different mutations could assist in clarifying if hiPSC CPVT CM are able to recapitulate disease and if different mutations present a different severity of phenotype.

Chapter 6

Discussion

6.1 CPVT1 hiPSC *in vitro* models of disease

Inherited channelopathies such as CPVT are a major clinical challenge to modern medicine. The accurate diagnosis of this disease involves specific procedures that may include a stress test, with carries with it associated risks, and genetic testing. But one of the biggest problems may arise with treating this channelopathy as a number of patients may be refractory to medical treatment. In this case an ICD implantation is required, which will result in a great loss of quality of life for the affected patient. This becomes even more dramatic as the majority of CPVT patients are children (Liu et al.,2008).

Innovative hiPSC technology has allowed the creation of individual specific pluripotent cells that can be differentiated in CM. By maintaining a patient genotype, during the reprograming process, a specific individual cardiac model can be created. The possibility of replicating disease *in vitro* is incredible, presenting great potential in determining CPVT phenotype severity and in eventually optimising personalised treatment options. The potential that hiPSC CPVT CM may have, has already been presented as a reality by several authors (Fatima et al.,2011; Itzhaki et al.,2012; Kujala et al.,2012; Jung et al.,2012 and Di Pasquale et al; 2013).

However these publications seem to lack an objective measure of CPVT characteristic arrhythmic endpoints. Without a rigorous assessment of arrhythmic endpoints it appears premature to claim CPVT disease recapitulation using hiPSC CM. Another problem found in most publications is the absence of optimal control hiPSC CM that can be used to compare with mutant cells. Individual and batch heterogeneity is an accepted problem of hPSC CM, from hESC CM to hiPSC CM and different control lines have been used in different publications.

The ideal control hiPSC CM would be a hiPSC CPVT CM with a non functional expressed mutation. This could be achieved artificially with siRNA as demonstrated with success in a different channelopathy (Matsa et al.,2014).

In the current project it was not possible to use these ideal control hiPSC CPVT CM. Instead a “healthy” subject hiPSC derived CM cell line was used as control. The best protocol to recapitulate CPVT *in vitro* involves a ß-agonist perfusion to elicit cardiac arrhythmogenesis. In these experiments isoprenaline was chosen for this purpose.

Sequential perfusion with a target drug in the presence of isoprenaline may determine if disease phenotype can be rescued or reduced.

A characterisation of any cardiac *in vitro* model of disease is required before hiPSC derived CM can be used as a potential translational clinical instrument.

In the current project, a hiPSC CM characterisation was made in order to study if these cells present cardiac physiological features. Positive inotropy, lusitropy and chronotry should be consistently present before determining that these cells recapitulate disease *in vitro*. If the studied cells failed to demonstrate that they behave like adult CM, then drug rescue experiments will have limited value.

Another unresolved problem that hiPSC CPVT CM present is that the majority of these cells are spontaneously active. CPVT is mainly a ventricular disease so spontaneous activity is not desirable for an ideal model. For this reason, in the current project both spontaneous and stimulated experiments were used to compare results. Arrhythmic endpoints are more standardised and less biased by using evoked or stimulated activity.

The final validation of the hiPSC CPVT CM used in this study was the sequential perfusion of cells with Tyrode's, isoprenaline and an antiarrhythmic drug in the presence of isoprenaline. The objective of this sequence was to recreate a physiological response that was similar to what happens in a human CPVT heart. Another arrhythmic factor is pacing rate. To account for this, experiments were performed at different pacing rates, both with patch clamp and Ca^{2+} imaging.

Recapitulation of CPVT *in vitro* using hiPSC derived CM is a complex process that involves multiple factors. And while an ideal method may not be possible, a more rigorous attempt to produce such a model is reported in the current project.

6.2 Functional characterisation of hiPSC CPVT CM

The following hypotheses were formulated in an attempt to establish if hiPSC CPVT CM are representative of adult cardiac cells.

1 – hiPSC CPVT CM and hiPSC control CM BT-1 express basic CM markers (Troponin C) and Ca^{2+} handling proteins (RyR2, CASQ2, PLB, SERCA2A).

From WB experiments (Chapter 4) it was not possible to confirm expression of basic cardiac Ca^{2+} handling proteins (RyR2, CASQ, PLB and SERCA2A). Troponin C was found to be present in control BT1 CM with ICC but could not be found in CPVT CM. Other authors have confirmed expression of CASQ and PLB (Jung et al.,2012) and RyR2 (Di Pasquale et al.,2013) in CPVT CM. These reports mention the use of more mature cells, from 1 to 3 months post differentiation. This factor may be very relevant to the negative expression found for the CM marker proteins in this project. A more prolonged maturation study could clarify if hiPSC CPVT CM used in this project do not express a CM typical protein profile or if just more time is needed for them to do so.

2 - hiPSC CPVT CM and hiPSC Control CM BT-1 possess a typical CM AP and that the three CM sub-types are present in a cell population.

In this report, typical cardiac AP were obtained both from BT1 CM and CPVT CM. Typical AP traces were obtained from both spontaneous (figure 4.6) and evoked AP (figure 4.8). The three different sub-types of AP were present in both cell types for evoked activity (figure 4.17). Differences in sub-type percentages are seen in the literature, and these can change from batch to batch, as do the criteria used to classify them. Di Pasquale et al., 2013 and Zhu et al., 2010 classified hPSC CM in two subtypes, nodal (i.e. cells from the AV node) and working like (i.e. atrial and ventricular chamber). The fact that hPSC can produce the three main cardiac AP sub-types suggests that these cells have the potential to behave like CM.

3- hiPSC CPVT CM and hiPSC control CM BT-1 present basic CM physiological and pharmacological response; namely the ß- adrenergic response (to isoprenaline and propranolol) demonstrated by the expected inotropic, lusitropic and chronotropic properties.

A good cardiac model is expected to present positive inotropy, lusitropy and chronotropy. In this project no consistent response was seen across different experiments for ß-adrenergic stimulation. Lack of statistical significance for observed positive differences in most isoprenaline perfusion experiments and significant negative responses in some cases make it impossible to confirm the expected responses to isoprenaline and propranolol. These findings demonstrate a high degree of variability in individual cells and cell batches.

4 - hiPSC CPVT CM and hiPSC Control CM (BT-1) present a basic cardiomyocyte Ca^{2+} handling pharmacological response, namely to caffeine, ryanodine and nifedipine.

Both hiPSC CPVT and BT1 CM responded as expected to nifedipine perfusion, with a decrease of Ca^{2+} transient average amplitude or standardised area. This suggests that both cell types have functional LTCC (figure 4.36). Caffeine perfusion experiments suggest a functional RyR2 with 20% BT1 CM and 60% CPVT CM response to this drug (figure 4.38). Ryanodine was only perfused in a low number of CPVT cells so it was not possible to determine the effect of this drug effect on RyR2 expressed in these cells. Overall, it was not possible to establish that the CPVT CM and BT1 CM used in this project have a fully functional CICR protein profile.

6.3 Validation of hiPSC CPVT CM as *in vitro* model of disease

An increase in arrhythmic endpoints upon isoprenaline perfusion was expected from both a quantitative and a qualitative analysis. To validate these hiPSC CPVT CM as a good *in vitro* model of disease these arrhythmogenic endpoints should decrease or return to baseline when perfused with an antiarrhythmic drug. Although several authors have presented data that they interpret as demonstrating disease recapitulation, no systematic methodology has been reported to determine quantitative response of DADs (using patch clamp) or other objective parameters for Ca^{2+} imaging (ITN, peak regularity, rate decay) in these cells.

In order to validate the cells used in this project, the following hypotheses were formulated:

1 – hiPSC CPVT CM will present a higher qualitative and quantitative arrhythmic response (with higher AP DADs incidence as a hallmark) than hiPSC control CM BT-1 when stimulated by increased pacing or ß-agonist stimulation.

Using the patch clamp technique to measure DAD frequency, duration and amplitude, no statistically significant changes were observed for these parameters as the result of isoprenaline perfusion in both control and mutant cells. The same observation was made in qualitative data analysis. Although this systematic approach was carefully designed to evaluate DADs with an innovative and previously unreported methodology, disease recapitulation could not be confirmed. No consistent and significant increase in arrhythmic endpoints was observed upon ß-agonist stimulation.

2 – hiPSC CPVT CM will have both a qualitative and quantitative higher incidence of abnormal calcium transients (indicating enhanced arrhythmic behaviour) than hiPSC control BT-1 CM when stimulated by increased pacing or ß-agonist stimulation.

In agreement with data collected using the patch clamp technique, Ca^{2+} imaging revealed that ß-agonist stimulation did not caused a statistically significant increase in arrhythmogenic endpoints in CPVT CM. Qualitative analysis demonstrated a trend that could be interpreted as an indication of disease recapitulation, but no statistically significant differences were observed.

A quantitative reduction in ITN peak regularity was expected with isoprenaline perfusion, but across different experiments, this response was not statistically significant and therefore the hypothesis was rejected.

3 - hiPSC CPVT CM arrhythmic behaviour (namely DADs frequency, amplitude and duration) can be rescued or improved when treated with anti-arrhythmic drugs in the presence of isoprenaline.

4 – hiPSC CPVT CM arrhythmic behaviour (abnormal Ca^{2+} transients and respective parameters) can be rescued or improved when treated with anti-arrhythmic drugs in the presence of isoprenaline.

Hypotheses 3 and 4 were also rejected, since they can only be tested following an increase in arrhythmogenic endpoints upon ß-agonist stimulation. As this initial response was not confirmed, pharmacological rescue of an arrhythmic phenotype could not be considered relevant or significant.

6.4 Conclusion remarks

Disease modelling using patient specific CPVT hiPSC derived CM is still a relatively new research area that has emerged in the past four years. The need to develop human CPVT cardiac models to study mechanisms of disease and for new drug discovery has generated some advances concerning the disease modelling potential of these cells. However, a systematic and quantitative approach, that is necessary to determine how accurate a model of patient specific disease these cells are, is absent from the literature. By using an innovative more accurate quantitative approach the present report demonstrates that these cells do not always recapitulate CPVT *in vitro*.

There are nonetheless some factors that can be relevant to this conclusion. The immature nature of these hiPSC derived CM may contribute to a lack of consistent response of disease modelling. Different AP sub-types may also contribute to a more heterogeneous response and different mutations may also present different specific phenotypes.

Despite these factors, it is clear from the work presented in this thesis, that, contrary to several reports in the literature (Fatima et al.,2011; Jung et al,2012; Itzhaki et al.,2012, Kujala et al.,2012), disease recapitulation is not always easily attainable using CPVT hiPSC derived CM. The potential of hiPSC CPVT CM as an *in vitro* model of disease therefore requires further investigations using more quantitative methods, as used here, to measure arrhythmic endpoints.

6.5 Future work

In order to better understand the hiPSC CPVT CM potential as an *in vitro* model of disease future work is necessary. Some of the adaptations that could be done to the methodology reported in this thesis could be:

- Use of more mature hiPSC CM with 3-4 months post differentiation.
- Control hiPSC CM derived from CPVT CM with corrected mutation (possibly with siRNA).
- Dose- response curve for isoprenaline perfusion.
- Selective analysis of ventricular-like CM with flow cytometry.
- Comparison analysis of quiescent ventricular-like CM with spontaneous ventricular-like CM.
- Comparison of single cell results with results from monolayers or small clumps of cells.
- Use of a different mutation and cell line of hiPSC CPVT CM in order to compare results.

By incorporating these changes into the study of hiPSC CPVT CM, new and more accurate insights in to the cells real potential for *in vitro* disease modelling will be obtained.

References

Reference List:

http://www.fsm.it/cardmoc - Cardiac mutations

SALVO User Manual, (2012) Version 3.7

A.M. BROWN (2004) Drugs, hERG and sudden death. *Cell Calcium* ; 35, 543–547

ALTSCHAFL BA, et al., (2011) Dual role of junctin in the regulation of ryanodine receptors and calcium release in cardiac ventricular myocytes. *J Physiol.* ;589 (Pt 24):6063-80.

ANTZELEVITCH, C. *et al.* (2005). Brugada syndrome: report of the second consensus conference: endorsed by the Heart Rhythm Society and the European Heart Rhythm Association. *Circulation* 111, 659–670

ARNESTAD M, et al. (2007) Prevalence of long-QT syndrome gene variants in sudden infant death syndrome. *Circulation*;115:361e7.

ASP J, STEEL D, JONSSON M, AMÉEN C, DAHLENBORG K, JEPPSSON A, LINDAHL A, SARTIPY P. (2010) Cardiomyocyte clusters derived from human embryonic stem cells share similarities with human heart tissue. *J Mol Cell Biol.* ;2(5):276-83.

ASSMUS B, ROLF A, ERBS S (2010) Clinical outcome 2 years after intracoronary administration of bone marrow-derived progenitor cells in acute myocardial infarctation. *Circulation Heart Failure*; 3: 2978-84.

BAI Y, JONES PP, GUO J, ZHONG X, CLARK RB, ZHOU Q, WANG R, VALLMITJANA A, BENITEZ R, HOVE-MADSEN L, SEMENIUK L, GUO A, SONG LS, DUFF HJ, CHEN SR.(2013) Phospholamban knockout breaks arrhythmogenic Ca^{2+} waves and suppresses catecholaminergic polymorphic ventricular tachycardia in mice. *Circ Res.* ;113(5):517-26.

BANNISTER ML, THOMAS NL, SIKKEL MB, MUKHERJEE S, MAXWELL C, MACLEOD KT, GEORGE CH, WILLIAMS AJ (2015) The mechanism of flecainide action in CPVT does not involve a direct effect on RyR2 *Circ Res.* ;116(8):1324-35

BAUCE B, RAMPAZZO A, BASSO C, BAGATTIN A, DALIENTO L, TISO N, TURRINI P, THIENE G, DANIELI GA, NAVA A (2002) Screening for ryanodine receptor type 2 mutations in families with effort-induced polymorphic ventricular arrhythmias and sudden death: early diagnosis of asymptomatic carriers. *J Am Coll Cardiol*. 40:341–349.

BEHR ER, DALAGEORGOU C, CHRISTIANSEN M, SYRRIS P, HUGHES S, TOME ESTEBAN MT, ROWLAND E, JEFFERY S, MCKENNA WJ. (2008) Sudden arrhythmic death syndrome: familial evaluation identifies inheritable heart disease in the majority of families. *Eur Heart J.* ;29(13):1670-80.

BEHR ER, et al. (2007) Sudden arrhythmic death syndrome: a national survey of sudden unexplained cardiac death. *Heart* 93:601e5.

BEHR ER, et al. (2003) Cardiological assessment of first-degree relatives in sudden arrhythmic death syndrome. *The Lancet* 362:1457e9.

BELTRAMI AP, BARLUCCHI L, TORELLA D, BAKER M, LIMANA F, CHIMENTI S, KASAHARA H, ROTA M, MUSSO E, URBANEK K, LERI A, KAJSTURA J, NADAL-GINARD B & ANVERSA P. (2003) Adult cardiac stem cells are multipotent and support myocardial regeneration. *Cell*. ;114(6):763-76

BELTRAN M, BULL R, DONOSO P, HIDALGO C. (1996) Ca2+ and pH-dependent halothane stimulation of Ca2+ release in sarcoplasmic reticulum from frog muscle. *Am J Physiol* 271: C540–6.

BERNSTEIN D, BURRIDGE P. (2014) Patient-Specific Pluripotent Stem Cells in Doxorubicin Cardiotoxicity: A New Window Into Personalized Medicine. *Progress in Pediatric Cardiology* . 1;37(1-2):23-27.

BERS, D.M. (2004). Macromolecular complexes regulating cardiac ryanodine receptor function. J. *Mol. Cell. Cardiol*. 37:417–429

BERS DM. (2002) Cardiac excitation-contraction coupling. *Nature*. 415:198–205.

BERS DM. (2000) Calcium fluxes involved in control of cardiac myocyte contraction. *Circ Res* 87: 275–281

BESCH HR, SHAO CH, BIDASEE KR. (2005) Ryanoids, receptor affinity and RyR channel subconductance. In: Wehrens XH, Marks AR, editors. *Ryanodine receptors: structure, function and dysfunction in clinical disease.* New York: Springer; p 179–89.

BIERNACKA EK, HOFFMAN P. (2010) Efficacy of flecainide in a patient with catecholaminergic ventricular polymorphic tachycardia. *Europace* 13:129-30

BINAH, O et al., (2007) Functional and developmental properties of human embryonic stem cells-derived cardiomyocytes. *Journal of electrocardiology*,.40(6 Suppl): p.S192-6.

BLAZESKI A, ZHU R, HUNTER DW, WEINBERG SH, BOHELER KR, ZAMBIDIS ET, TUNG L. (2012) Electrophysiological and contractile function of cardiomyocytes derived from human embryonic stem cells *Prog Biophys Mol Biol*. 110(2-3):178-95

BOYETT MR, HART G, LEVI AJ, ROBERTS A. (1987) Effects of repetitive activity on developed force and intracellular sodium in isolated sheep and dog Purkinje fibres. *J Physiol.* ;388:295-322

BRAAM SR, TERTOOLEN L, VAN DE STOLPE A, MEYER T, PASSIER R, MUMMERY CL. (2010) Prediction of drug-induced cardiotoxicity using human embryonic stem cell-derived cardiomyocytes. *Stem Cell Research* 4, 107–116

BRIGGS, R. AND KING, T.J. (1952) Transplantation of living nuclei from blastula cells into enucleated frogs' eggs. *Proc. Natl. Acad. Sci. USA* 38 (5), 455–463.

BRILLANTES AB, et al. (1994) Stabilization of calcium release channel (ryanodine receptor) function by FK506-binding protein. *Cell* 77(4):513–523.

BRUGADA R, et al., (2004) Sudden Death Associated With Short-QT Syndrome Linked to Mutations in HERG *Circulation.* 109:30-35

BURRIDGE, P.W., et al., (2011) A universal system for highly efficient cardiac differentiation of human induced pluripotent stem cells that eliminates interline variability. *PloS one,* 6(4): p. e18293.

BURRIDGE PW, KELLER G, GOLD JD, WU JC. (2012) Production of de novo cardiomyocytes: human pluripotent stem cell differentiation and direct reprogramming. *Cell Stem Cell.* ;10(1):16-28.

BURRIDGE PW, METZLER SA, NAKAYAMA KH, ABILEZ OJ, SIMMONS CS, BRUCE MA, MATSUURA Y, KIM P, WU JC, BUTTE M, HUANG NF, YANG PC (2014) Multi-cellular interactions sustain long-term contractility of human pluripotent stem cell-derived cardiomyocytes *Am J Transl Res.* 22;6(6):724-35.

CARLSSON L, ALMGREN O & DUKER G. (1990) QTU-prolongation and torsades de pointes induced by putative class III antiarrhythmic agents in the rabbit: etiology and interventions. *J Cardiovasc Pharmacol* ;16(2):276-85

CARLSSON L. (2006) In vitro and in vivo models for testing arrhythmogenesis in drugs. *Journal of Internal Medicine* ;259(1):70-80

CARVAJAL-VERGARA X. et al., (2010) Patient-specifi c inducedpluripotent stemcell-derived models of LEOPARD syndrome. *Nature* 465,808–812

CASPI O ET AL (2009) In Vitro Electrophysiological Drug Testing Using Human, Embryonic Stem Cell Derived Cardiomyocytes, *Stem cells and development*, Volume 18, Number 1,

CERRONE M, et al. (2005) Bidirectional ventricular tachycardia and fibrillation elicited in a knock-in mouse model carrier of a mutation in the cardiac ryanodine receptor. *Circ Res*. 96(10): e77–e82.

CERRONE M, et al., (2004) Clinical and molecular characterization of a large cohort of patients affected with catecholaminergic polymorphic ventricular tachycardia. *Circulation* 110:552, (Suppl II).

CHARPENTIER F, DEMOLOMBE S, ESCANDE D. (2004) Cardiac channelopathies: from men to mice. *Ann Med*. 36 Suppl 1:28-34.

CHEN JX , KRANE M, DEUTCH MA, (2012) Inefficient reprogramming of fibroblasts into cardiomyocytes using Gata4, Mef2c and Tbx5. *Circulation Research*; 111: 50-5.

CHEN FM, YAMAMURA HI, ROESKE WR. (1979) Ontogeny of mammalian myocardial beta-adrenergic receptors. *Eur J Pharmacol.* ;58(3):255-64.

CHÉZALVIEL-GUILBERT F, DAVY J-M, POIRIER J-M, WEISSENBURGER J. (1995) Mexiletine antagonizes effects of sotalol on QT interval duration and its proarrhythmic effects in a canine model of torsade de pointes. *J Am Coll Cardiol*. ;26(3):787-92

CHING LL, WILLIAMS AJ, SITSAPESAN R. (2000) Evidence for Ca(2+) activation and inactivation sites on the luminal side of the cardiac ryanodine receptor complex. *Circ Res*. 87:201–206.

CHRISTOFFELS VM, BURCH JB, MOORMAN AF (2004) Architectural plan for the heart: early patterning and delineation of the chambers and the nodes. *Trends Cardiovasc Med. 14(8):301-7.*

CLAYCOMB W, LANSON JR N, STALLWORTH B, EGELAND D, DELCARPIO J, BAHINSKI A & IZZO JR N. (1998) HL-1 cells: a cardiac muscle cell line that contracts and retains phenotypic characteristics of the adult cardiomyocyte. *Proc Natl Acad Sci USA* ;95(6):2979-84

CLEMENTS J.A., HASSON K. AND SMITH G. (1980) Effects of ascorbic acid and disodium edetate on the degradation of isoprenaline *Journal of Pharmacy and Pharmacology* Volume 32, Issue S1, page 50P

COBALEDA C., JOCHUM W., BUSSLINGER M. (2007) Conversion of mature B cells into T cells by dedifferentiation to uncommitted progenitors. *Nature* 449 (7161), 473–477.

CONNELLY TJ, CORONADO R. (1994) Activation of the Ca2+ release channel of cardiac sarcoplasmic reticulum by volatile anesthetics. *Anesthesiology;* 81: 459–69.

COPELLO JA, et al. (1997) Heterogeneity of Ca2+ gating of skeletal muscle and cardiac ryanodine receptors. Biophysical Journal;73(1):141–156.

COUMEL P, FIDELLE J, LUCET V, ATTUEL P, BOUVRAIN Y. (1978) Catecholaminergic-induced severe ventricular arrhythmias with Adams-Stokes syndrome in children: report of four cases. *Br Heart J*.; 40:28–37.

DAN P, ZENG Z, LI Y, QU Y, HOVE-MADSEN L, TIBBITS GF (2014) Phenotype-dependent role of the L-type calcium current in embryonic stem cell derived cardiomyocytes. *Am J Stem Cells*. 13;3(1):37-45.

DAVIS RP, et al. (2011) Pluripotent stem cell models of cardiac disease and their implication for drug discovery and development. *Trends Mol Med.* 17:475–84.

DAVIS, R.L., WEINTRAUB, H. AND LASSAR, A.B. (1987) Expression of a single transfected cDNA converts fibroblasts to myoblasts. *Cell* 51 (6), 987–1000.

DE FERRARI GM, DUSI V, SPAZZOLINI C, BOS JM, ABRAMS DJ, BERUL CI, CROTTI L, DAVIS AM, ELDAR M, KHARLAP M, KHOURY A, KRAHN AD, LEENHARDT A,MOIR CR, ODERO A, OLDE NORDKAMP L, PAUL T, ROSÉS I NOGUER F, SHKOLNIKOVA M, TILL J, WILDE AA, ACKERMAN MJ, SCHWARTZ PJ (2015) Clinical Management of Catecholaminergic Polymorphic Ventricular Tachycardia: The Role of Left Cardiac Sympathetic Denervation; *Circulation*.;131(25):2185-93.

DENEGRI M, BONGIANINO R, LODOLA F, BONCOMPAGNI S, DE GIUSTI VC, AVELINO-CRUZ JE, LIU N, PERSAMPIERI S, CURCIO A, ESPOSITO F, PIETRANGELO L,MARTY I, VILLANI L, MOYAHO A, BAIARDI P, AURICCHIO A, PROTASI F, NAPOLITANO C, PRIORI SG (2014) Single delivery of an adeno-associated viral construct to transfer the CASQ2 gene to knock-in mice affected bycatecholaminergic polymorphic ventricular tachycardia is able to cure the disease from birth to advanced age. *Circulation* ;129(25):2673-81.

DI PASQUALE, E., et al., (2013) CaMKII inhibition rectifies arrhythmic phenotype in a patient-specific model of catecholaminergic polymorphic ventricular tachycardia. *Cell death & disease*, 2013. 4: p. e843.

DIAZ ME, Trafford AW, O'Neill SC, EISNER DA. (1997) Measurement of sarcoplasmic reticulum Ca2+ content and sarcolemmal Ca2+ fluxes in isolated rat ventricular myocytes during spontaneous Ca2+ release. *J Physiol*. 501, 3–16.

DOLNIKOV K, SHILKRUT M, ZEEVI-LEVIN N, DANON A, GERECHT-NIR S, ITSKOVITZ-ELDOR J, BINAH O. (2005) Functional properties of human embryonic stem cell-derived cardiomyocytes. *Ann N Y Acad Sci*. ;1047:66-75.

DOLNIKOV, K., et al., (2006) Functional properties of human embryonic stem cell-derived cardiomyocytes: intracellular Ca2+ handling and the role of sarcoplasmic reticulum in the contraction. *Stem cells* 24(2): p. 236-45.

DU DT et al., (2015) Action potential morphology of human induced pluripotent stem cell derived cardiomyocytes does not predict cardiac chamber specificity and is dependent on cell density *Biophys J*. 6108(1):1-4.

DU GG, GUO X, KHANNA VK, MACLENNAN DH (2001) Ryanodine sensitizes the cardiac Ca(2+) release channel (ryanodine receptor isoform 2) to Ca(2+) activation and dissociates as the channel is closed by Ca(2+) depletion. *Proc Natl Acad Sci USA*. 98:13625–13630.

EULALIO A, et al; (2012) Functional screening identifies miRNAs inducing cardiac regeneration; *Nature*; Vol 492: 376-381

EVANS MJ, KAUFMAN MH. (1981) Establishment in culture of pluripotential cells from mouse embryos. *Nature*. ;292(5819):154-6.

FABIATO A. (1992) Two kinds of calcium-induced release of calcium from the sarcoplasmic reticulum of skinned cardiac cells. *Adv Exp Med Biol.* 311:245–262.

FABIATO A. (1983) Calcium-induced release of calcium from the cardiac sarcoplasmic reticulum. *Am J Physiol*. 245(1):C1-14.

FATIMA A. et al., (2011) In vitro modeling of ryanodine receptor 2 dysfunction using human induced pluripotent stem cells. *Cell Physiol Biochem*. ;28(4):579-92

FILL M & COPELLO JA. (2002) Ryanodine receptor calcium release channels. *Physiol Rev.* Oct;82(4):893-922.

FLEISCHER S. et al. (1985). Localization of Ca2+ Release Channels with Ryanodine in Junctional Terminal Cisternae of Sarcoplasmic Reticulum of Fast Skeletal Muscle. *Proceedings of the National Academy of Sciences of the United States of America* 82(21): 7256-7259.

FU, J.D., et al., (2010) Na+/Ca2+ exchanger is a determinant of excitation-contraction coupling in human embryonic stem cell-derived ventricular cardiomyocytes. *Stem cells and development*, 19(6): p. 773-82.

MIRAMS GR, et al., (2011) Simulation of multiple ion channel block provides improved early prediction of compounds' clinical torsadogenic risk; *Cardiovascular Research* 91, 53–61

GEORGE CH, HIGGS GV, LAI FA. (2003) Ryanodine Receptor Mutations Associated With Stress-Induced Ventricular Tachycardia Mediate Increased Calcium Release in Stimulated Cardiomyocytes. *Circulation Research.* 93:531–540.

GILBERT, S.F. (2010) *Developmental Biology*. 9th ed. Sinauer Associates, Inc., Sunderland.

GNECCHI M, ZHANG Z, NI A (2008) Paracrine mechanisms in adult stem cell aignaling and therapy. *Circulation Res*; 103:1204-19.

GUPTA, M.K., et al., (2010) Global transcriptional profiles of beating clusters derived from human induced pluripotent stem cells and embryonic stem cells are highly similar. *BMC developmental biology*, 10: p. 98.

GURDON, J.B. (1962) The developmental capacity of nuclei taken from intestinal epithelium cells of feeding tadpoles. *J. Embryol. Exp. Morphol*. 10, 622–640.

GYORKE S, TERENTYEV D. (2008) Modulation of ryanodine receptor by luminal calcium and accessory proteins in health and cardiac disease. *Cardiovascular Research* 77(2):245–255.

HANOUZ JL, et al. (2000) In vitro effects of desflurane, sevoflurane, isoflurane, and halothane in isolated human right atria. *Anesthesiology* 92: 116–24.

HARRIS K, AYLOTT M, CUI Y, LOUTTIT JB, MCMAHON NC, SRIDHAR A. (2013) Comparison of electrophysiological data from human-induced pluripotent stem cell-derived cardiomyocytes to functional preclinical safety assays, *Toxicol Sci.* 134(2):412-26.

HAYASHI M, DENJOY I, EXTRAMIANA F, MALTRET A, BUISSON NR, LUPOGLAZOFF JM, KLUG D, TAKATSUKI S, VILLAIN E, KAMBLOCK J, MESSALI A, GUICHENEY P, LUNARDI J, LEENHARDT A. (2009) Incidence and risk factors of arrhythmic events in catecholaminergic polymorphic ventricular tachycardia. *Circulation*.119:2426–2434.

HE JQ, MA Y, LEE Y, THOMSON JA, KAMP TJ. (2003) Human embryonic stem cells develop into multiple types of cardiac myocytes: action potential characterization. *Circ Res*. ;93(1):32-9.

HEDLEY PL, et al. (2009) The genetic basis of long QT and short QT syndromes: A mutation update. *Hum Mutat* 30:1486e511.

HERRMANN-FRANK A, RICHTER M, SARKOZI S, MOHR U, LEHMANNHORN F. (1996) 4-Chloro-m-cresol, a potent and specific activator of the skeletal muscle ryanodine receptor. *Biochim Biophys Acta* 1289: 31–40.

HICK A, et al. (2013) Neurons and cardiomyocytes derived from induced pluripotent stem cells as a model for mitochondrial defects in Friedreich's ataxia. *Dis Model Mech*; 6: 608 – 621.

HILL AP, KINGSTON O, SITSAPESAN R. (2004) Functional regulation of the cardiac ryanodine receptor by suramin and calmodulin involves multiple binding sites. *Mol Pharmacol* 65: 1258–68.

HILLIARD FA, STEELE DS, LAVER D, YANG Z, LE MARCHAND SJ, CHOPRA N, PISTON DW, HUKE S, KNOLLMANN BC. (2010) Flecainide inhibits arrhythmogenic Ca2+ waves by open state block of ryanodine receptor Ca2+ release channels and reduction of Ca2+ spark mass. *J Mol Cell Cardiol*.;48:293– 301.

HOEKER GS, KATRA RP, WILSON LD, PLUMMER BN, LAURITA KR. (2009) Spontaneous calcium release in tissue from the failing canine heart. *Am J Physiol Heart Circ Physiol.* 297:H1235–1242.

HOEKSTRA M., et al., (2012) Induced pluripotent stem cell derived cardiomyocytes as models for cardiac arrhythmias. *Frontiers in physiology* 3: p. 346.

HONDA M, KIYOKAWA J, TABO M, INOUE T. (2011) Electrophysiological characterization of cardiomyocytes derived from human induced pluripotent stem cells. *J Pharmacol Sci*. ;117(3):149-59. 5.

HUANG HP, et al. (2011) Human Pompe disease-induced pluripotent stem cells for pathogenesis modeling, drug testing and disease marker identification. *Hum Mol Genet* ; 20: 4851 – 4864.

HUANGFU, D., OSAFUNE, K., MAEHR, R., GUO, W., EIJKELENBOOM, A., CHEN, S., MUHLESTEIN, W. AND MELTON, D.A. (2008) Induction of pluripotent stem cells from primary human fibroblasts with only oct4 and sox2. *Nat. Biotechnol.* 26 (11), 1269– 1275.

HUKE S, BERS DM. (2008) Ryanodine receptor phosphorylation at Serine 2030, 2808 and 2814 in rat cardiomyocytes. *Biochem Biophys Res Commun*.376:80–85.

HWANG HS, KRYSHTAL DO, FEASTER TK, SÁNCHEZ-FREIRE V, ZHANG J, KAMP TJ, HONG CC, WU JC, KNOLLMANN BC.(2015) Comparable calcium handling of human iPSC-derived cardiomyocytes generated by multiple laboratories. *J Mol Cell Cardiol*. 85:79-88.

IEDA M, FU JD, DELGADO-OLGUIN P (2010) Direct reprogramming of fibroblasts into functional cardiomyocytes by defined factors. *Cell*; 142: 375-86.

IKEMOTO N, YAMAMOTO T. (2000) Postulated role of inter-domain interaction within the ryanodine receptor in Ca(2+) channel regulation. *Trends Cardiovasc Med.* 10:310–316.

ITZHAKI, I., et al. (2012) Modeling of Catecholaminergic Polymorphic Ventricular Tachycardia With Patient-Specific Human-Induced Pluripotent Stem Cells. *Journal of the American College of Cardiology*, 60(11): p. 990-1000.

ITZHAKI, I., et al., (2011) Modelling the long QT syndrome with induced pluripotent stem cells. *Nature* 471(7337): p. 225-9.

JAYAWARDENA TM, EGEMNAZAROV B, FINCH EA (2012) MicroRNA-mediated in vitro and in vivo direct reprogramming of cardiac fibroblasts to cardiomyocytes. *Circulation Research* 110:1465-73

JEZEK K, PUCELIK P, SAUER J, BARTAK (1982) F. Basic electrophysiological parameters and frequency sensitivity of the ventricular myocardium of human embryos.*Physiol Bohemoslov.* 31: 11–19.

JIA ZHANG, JINGKUN QU, JIANSHENG WANG (2014) Patch clamp apply in cardiomyocytes derived from patient's iPS cells for individual anticancer therapy. *Int J Clin Exp Med*;7(11):4475-4478

JIANG D, XIAO B, ZHANG L, CHEN SR (2002) Enhanced basal activity of a cardiac Ca2+ release channel (ryanodine receptor) mutant associated with ventricular tachycardia and sudden death. *Circ Res* ;91:218–25.

JIANG D, XIAO B, YANG D, WANG R, CHOI P, ZHANG L, CHENG H, CHEN SR. (2004) RyR2 mutations linkedto ventricular tachycardia and sudden death reduce the threshold for store-overload-induced Ca2+ release (SOICR). *Proc.Natl.Acad Sci U.S.A.*; 101:13062–13067.

JIANG D, WANG R, XIAO B, KONG H, HUNT DJ, CHOI P, ZHANG L, CHEN SR. (2005) Enhanced store overloadinduced Ca2+ release and channel sensitivity to luminal Ca2+ activation are common defects of RyR2 mutations linked to ventricular tachycardia and sudden death. *Circ Res.* 97:1173– 1181.

JIANG Y. et al., (2014) An induced pluripotent stem cell model of hypoplastic left heart syndrome (HLHS) reveals multiple expression and functional differences in HLHS-derived cardiac myocytes. *Stem Cells Translational Medicine*, 3(4):416-23

JOSHUA T. MAXWELL, TIMOTHY L. DOMEIER, AND LOTHAR A. BLATTER: (2012) Dantrolene prevents arrhythmogenic Ca2+ release in heart failure; *Am J Physiol Heart Circ Physiol* 302: H953–H963

JUNG G, BERNSTEIN D. (2014) hiPSC Modeling of Inherited Cardiomyopathies. *Curr Treat Options Cardiovasc Med*. ;16(7):320.

JUNG CB et al., (2012) Dantrolene rescues arrhythmogenic RYR2 defect in a patient-specific stem cell model of catecholaminergic polymorphic ventricular tachycardia. *EMBO Mol Med*. ;4(3):180-91..

KAFTAN E, MARKS AR, EHRLICH BE. (1996) Effects of rapamycin on ryanodine receptor/Ca2+ release channels from cardiac muscle. *Circ Res* 78: 990–7.

KANNANKERIL PJ et al., (2006) Mice with the R176Q cardiac ryanodine receptor mutation exhibit catecholamine-induced ventricular tachycardia and cardiomyopathy. *Proc Natl Acad Sci USA*;103:12179–84.

KANNEL WB, CUPPLES LA, D'AGOSTINO RB. (1987) Sudden death risk in overt coronary heart disease: the Framingham Study. *Am Heart J.* ;113(3):799-804.

KAPPLINGER JD, et al (2010) An international compendium of mutations in the SCN5A-encoded cardiac sodium channel in patients referred for Brugada syndrome genetic testing. *Heart Rhythm* 7:33e46.

KAUFERSTEIN S, KIEHNE N, JENEWEIN T, BIEL S, KOPP M, KÖNIG R, ERKAPIC D, ROTHSCHILD M, NEUMANN T. (2013) Genetic analysis of sudden unexplained death: a multidisciplinary approach. *Forensic Sci Int*. ;229(1-3):122-7.

KAZEMIAN P, GOLLOB MH, PANTANO A, OUDIT GY. (2011) A novel mutation in the RYR2 gene leading to catecholaminergic polymorphic ventricular tachycardia and paroxysmal atrial fibrillation: dose-dependent arrhythmia-event suppression by ß-blocker therapy. *Can J Cardiol*.27:870. e7–870. e10.

KEHAT I, et al., (2001) Human embryonic stem cells can differentiate into myocytes with structural and functional properties of cardiomyocytes. *Journal of Clinical Investigation*, 108(3): p. 407-414.

KIM C, et al., (2013) Studying arrhythmogenic right ventricular dysplasia with patient specific iPSCs. *Nature* 494, 105–110 (2013).

KIMBERLEY J. LEWIS, NICOLE C. SILVESTER, STEVEN BARBERINI-JAMMAERS, SAMMY A. MASON, SARAH A. MARSH, MAGDALENA LIPKA, CHRISTOPHER H. GEORGE (2015). A New System for Profiling Drug-Induced Calcium Signal Perturbation in Human Embryonic Stem Cell–Derived Cardiomyocytes. *J Biomol Screen*. 20(3): 330–340.

KIMES B & BRANDT B. (1976) Properties of a clonal muscle cell line from rat heart. *Exp Cell Res* : 98(2):367-81

KNOLLMANN BC, et al. (2006) Casq2 deletion causes sarcoplasmic reticulum volume increase, premature Ca2+ release, and catecholaminergic polymorphic ventricular tachycardia. *J Clin Invest* 116:2510–20.

KOBAYASHI S. et al. (2010) Dantrolene, a therapeutic agent for malignant hyperthermia, Inhibits catecholaminergic polymorphic ventricular tachycardia: insights from a RyR2 R2474S/+ knock-in mouse model. *Circulation* 116:II–654.

KONG H , JONES PP., A KOOP A, ZHANG L, DUFF H. J. , CHEN S. R. W . (2008) Caffeine Induces Ca^{2+} Release by Reducing The Threshold for Luminal Ca^{2+} Activation of the Ryanodine Receptor. *Biochem J.* 15; 414(3): 441–452.

KUJALA K, et al., (2012) Cell model of catecholaminergic polymorphic ventricular tachycardia reveals early and delayed afterdepolarizations. *PLoS One*. ;7(9):e44660.

LAIOSA, C.V., STADTFELD, M., XIE, H., DE ANDRES- AGUAYO, L. AND GRAF, T. (2006) Reprogramming of committed T cell progenitors to macrophages and dendritic cells by C/EBP alpha and PU.1 transcription factors. *Immunity* 25 (5), 731–744.

LAITINEN PJ, et al., (2001) Mutations of the cardiac ryanodine receptor (RyR2) gene in familial polymorphic ventricular tachycardia. *Circulation*. ;103(4):485-90.

LAKATTA EG. (1992) Functional implications of spontaneous sarcoplasmic reticulum Ca2+ release in the heart. *Cardiovasc Res.* 26:193–214.

LAKATTA EG, GUARNIERI T. (1993) Spontaneous myocardial calcium oscillations: are they linked to ventricular fibrillation? *J Cardiovasc Electrophysiol*. 4:473–489.

LAN F. et al., (2013) Abnormal calcium handling properties underlie familial hypertrophic cardiomyopathy pathology in patient-specific induced pluripotent stem cells. *Cell Stem Cell* 12, 101–113

LASLETT LJ, ALAGONA P JR, CLARK BA 3RD, DROZDA JP JR, SALDIVAR F, WILSON SR, POE C, HART M. (2012) The worldwide environment of cardiovascular disease: prevalence, diagnosis, therapy, and policy issues: a report from the American College of Cardiology. *J Am Coll Cardiol.* 25;60(25 Suppl):S1-49

LEE YK, et al., (2011) Calcium homeostasis in human induced pluripotent stem cell-derived cardiomyocytes. *Stem cell reviews*, 7(4): p. 976-86.

LEENHARDT A, LUCET V, DENJOY I, GRAU F, NGOC DD, COUMEL P (1995) Catecholaminergic polymorphic ventricular tachycardia in children. A 7-year follow-up of 21 patients. *Circulation.* ;91(5):1512-9.

LEHNART SE et al., (2008) Leaky Ca2+ release channel/ryanodine receptor 2 causes seizures and sudden cardiac death in mice. *J Clin Invest* 118(6):2230-45.

LEISTNER DM, FISHER-RASOKAT U, HONOLD J; (2011) Transplantation of progenitor cells and regeneration enhancement in acute myocardial infarctation (TOPCARE-AMI): final 5-year result suggests long-term safety and efficacy. *Clinical Res Cardiology* ;100:925-34.

LI QIAN, YU HUANG, C. IAN SPENCER, AMY FOLEY, VASANTH VEDANTHAM, LEI LIU, SIMON J. CONWAY, JI-DONG FU, AND DEEPAK SRIVASTAVA (2012) *In vivo* reprogramming of murine cardiac fibroblasts into induced cardiomyocytes . *Nature* ; 485(7400): 593–598.

LI X, ZHANG F, SONG G (2013) Intramyocardial injection of pig pluripotent stem cells improves left ventricular function and perfusion: a study in porcine model of acute myocardial infarctation. *PLoS One* 8: e66688.

LIANG P., LAN F., LEE A. S., GONG T., SANCHEZ-FREIRE V., WANG Y., DIECKE S., SALLAM K., KNOWLES J. W., WANG P. J., NGUYEN P. K., BERS D. M., ROBBINS R. C., WU J. C. (2013) Drug screening using a library of human induced pluripotent stem cell-derived cardiomyocytes reveals disease-specifi c patterns of cardiotoxicity. *Circulation* 127, 1677–1691

LINDSAY AR, TINKER A, WILLIAMS AJ. (1994) How does ryanodine modify ion handling in the sheep cardiac sarcoplasmic reticulum Ca(2+)-release channel? *J Gen Physiol*. ; 104:425–447

LIU N, et al. (2006) Arrhythmogenesis in catecholaminergic polymorphic ventricular tachycardia: insights from a RyR2 R4496C knock-in mouse model. *Circ Res*. 99(3): 292–298.

LIU J. et al., (2007) Functional sarcoplasmic reticulum for calcium handling of human embryonic stem cell-derived cardiomyocytes: insights for driven maturation. *Stem cells*, 25(12): p. 3038-44.

LIU, N., Y. RUAN, AND S.G. PRIORI, (2008) Catecholaminergic polymorphic ventricular tachycardia. *Progress in cardiovascular diseases*, 51(1): p. 23-30.

LIU N, RIZZI N, BOVERI L, PRIORI SG. (2009) Ryanodine receptor and calsequestrin in arrhythmogenesis: what we have learnt from genetic diseases and transgenic mice. *J Mol Cell Cardiol*. 46(2):149-59.

LIU N, et al. (2010) Sodium channel blockers prevent triggered activity but not abnormal Ca2+ release in a knock-in mouse model with ryanodine receptor mutation R4496C. *Circulation*. 122(21):A13707.

LIU Y., et al., (2013) The CPVT-associated RyR2 mutation G230C enhances store overloadinduced Ca2+ release and destabilizes the N-terminal domains. *The Biochemical Journal* 454(1): p. 123-31.

LOKUTA AJ, et al. Modulation of cardiac ryanodine receptors by sorcin (1997) *The Journal of Biological Chemistry* 272(40):25333–25338.

MA D, et al. (2013) Generation of patient-specific induced pluripotent stem cell-derived cardiomyocytes as a cellular model of arrhythmogenic right ventricular cardiomyopathy. *Eur Heart J*; 34: 1122 – 1133.

MA D. et al., (2013) Modeling type 3 long QT syndrome with cardiomyocytes derived from patient-specific induced pluripotent stem cells. *Int.J. Cardiol.* 168, 5277–5286

MA J. (1993) Block by ruthenium red of the ryanodine-activated calcium release channel of skeletal muscle. *J Gen Physiol* 102: 1031–56.

MA J, HAYEK SM, BHAT MB (2004) Membrane topology and membrane retention of the ryanodine receptor calcium release channel. *Cell Biochem Biophys*. 40:207–224.

MA J, GUO L, FIENE SJ, ANSON BD, THOMSON JA, KAMP TJ, KOLAJA KL, SWANSON BJ, JANUARY CT. (2011) High purity human-induced pluripotent stem cell-derived cardiomyocytes: electrophysiological properties of action potentials and ionic currents. *Am J Physiol Heart Circ Physiol*. ;301(5):H2006-17.

MAIER LS, BERS DM, PIESKE B (2000) Differences in Ca^{2+} handling and sarcolplasmic reticulum Ca^{2+} content in isolated rat and rabbit myocardium. *J Mol Cell Cardiol*. 32:2249-2258.

MALAN D, FRIEDRICHS S, FLEISCHMANN BK, SASSE P. (2011) Cardiomyocytes obtained from induced pluripotent stem cells with long-QT syndrome 3 recapitulate typical disease-specific features in vitro. *Circ Res.* 30;109(8):841-7.

MALI, P., CHOU, B.K., YEN, J., YE, Z., ZOU, J., DOWEY, S., BRODSKY, R.A., OHM, J.E., YU, W., BAYLIN, S.B., YUSA, K., BRADLEY, A., MEYERS, D.J., MUKHERJEE, C., COLE, P.A. AND CHENG, L. (2010) Butyrate greatly enhances derivation of human induced pluripotent stem cells by promoting epigenetic remodeling and the expression of pluripotency-associated genes. *Stem Cells* 28 (4), 713–720.

MALTSEV VA, WOBUS AM, ROHWEDEL J, BADER M, HESCHELER J. (1994) Cardiomyocytes differentiated in vitro from embryonic stem cells developmentally express cardiac-specific genes and ionic currents. *Circ Res*. ;75(2):233-44.

MARBAN E, ROBINSON SW, WIER WG. (1986) Mechanisms of arrhythmogenic delayed and early afterdepolarizations in ferret ventricular muscle. *J Clin Invest*. 78:1185–1192.

MARJAMAA A, LAITINEN-FORSBLOM P, WRONSKA A, TOIVONEN L, KONTULA K, SWAN H. (2011) Ryanodine receptor (RyR2) mutations in sudden cardiac death: studies in extended pedigrees and phenotypic characterization in vitro. *Int J Cardiol*. ;147(2):246-52.

MARX SO, et al. (2000) PKA phosphorylation dissociates FKBP12.6 from the calcium release channel (ryanodine receptor): Defective regulation in failing hearts. *Cell* 101(4):365– 376.

MARX SO, REIKEN S, HISAMATSU Y, JAYARAMAN T, BURKHOFF D, ROSEMBLIT N, MARKS AR. (2000) PKA phosphorylation dissociates FKBP12.6 from the calcium release channel (ryanodine receptor): defective regulation in failing hearts. *Cell* 101:365–376.

MASUMIYA H, LI P, ZHANG L, CHEN SR. (2001) Ryanodine sensitizes the Ca(2+) release channel (ryanodine receptor) to Ca(2+) activation. *J Biol Chem.* 276:39727–39735.

MATSA E, RAJAMOHAN D, DICK E, YOUNG L, MELLOR I, STANIFORTH A, DENNING C. (2011) Drug evaluation in cardiomyocytes derived from human induced pluripotent stem cells carrying a long QT syndrome type 2 mutation. *Eur Heart J.* ;32(8):952-62.

MATSA E., DENNING C. (2012) In vitro uses of human pluripotent stem cell-derived cardiomyocytes. *J. Cardiovasc. Transl. Res*. 5, 581–592

MATSA E, DIXON JE, MEDWAY C, GEORGIOU O, PATEL MJ, MORGAN K, KEMP PJ, STANIFORTH A, MELLOR I, DENNING C. (2014) Allele-specific RNA interference rescues the long-QT syndrome phenotype in human-induced pluripotency stem cell cardiomyocytes. *Eur Heart J.* ;35(16):1078-87.

MCGARRY SJ, WILLIAMS AJ. (1993) Digoxin activates sarcoplasmic reticulum Ca(2+)-release channels: a possible role in cardiac inotropy. *Br J Pharmacol* 108: 1043–50.

MEDEIROS-DOMINGO A, BHUIYAN ZA, TESTER DJ, HOFMAN N, BIKKER H, VAN TINTELEN JP, MANNENS MM, WILDE AA, ACKERMAN MJ. (2009) The RyR2- encoded ryanodine receptor/calcium release channel in patients diagnosed previously with either catecholaminergic polymorphic ventricular tachycardia or genotype negative, exercise-induced long QT syndrome: a comprehensive open reading frame mutational analysis. *J Am Coll Cardiol*. 54:2065–2074.

MEISSNER G, HENDERSON JS. (1987) Rapid calcium release from cardiac sarcoplasmic reticulum vesicles is dependent on Ca2+ and is modulated by Mg2+, adenine nucleotide, and calmodulin. *The Journal of Biological Chemistry* ;262(7):3065–3073.

MEISSNER G. (1984) Adenine nucleotide stimulation of Ca^{2+} - induced Ca^{2+} release in sarcoplasmic reticulum. *J Biol Chem* 259: 2365-74

MEISSNER G. (1986) Ryanodine activation and inhibition ofthe Ca2+release channel of sarcoplasmic reticulum. *J Biol Chem*, 261:6300–6306.

MESSINA E, DE ANGELIS L, FRATI G, MORRONE S, CHIMENTI S, FIORDALISO F, SALIO M, BATTAGLIA M, LATRONICO MV, COLETTA M, VIVARELLI E, FRATI L, COSSU G & GIACOMELLO A. (2004) Isolation and expansion of adult cardiac stem cells from human and murine heart. *Circ Res*. ;95(9):911-21

MEYER T, LEISGEN C, GONSER B, GUNTHER E (2004) QT-screen: high-throughput cardiac safety pharmacology by extracellular electrophysiology on primary cardiac myocytes. *Assay Drug Dev Technol*. 2:507–14.

MEYER GP,WOLLERT KC, LOTZ J (2009) Intracoronary bone marrow cell transfer after myocardial infarction: 5 year follw up from the randomized-controlled BOOST trial. *European Heart Journal*; 30: 2978-84.

MIHIC A. et al., (2014) The effect of cyclic stretch on maturation and 3D tissue formation of human embryonic stem cell-derived cardiomyocytes. *Biomaterials* 35, 2798–2808

MIKKELSEN T.S., HANNA, J., ZHANG, X., KU, M., WERNIG, M., SCHORDERET, P., BERNSTEIN, B.E., JAENISCH, R., LANDER, E.S. AND MEISSNER, A. (2008) Dissecting direct reprogramming through integrative genomic analysis. *Nature* 454 (7205), 794.

MOHAMED U, NAPOLITANO C, PRIORI SG. (2007) Molecular and electrophysiological bases of catecholaminergic polymorphic ventricular tachycardia. *J Cardiovasc Electrophysiol.* 18:791–797.

MOHLER PJ, et al. (2004) A cardiac arrhythmia syndrome caused by loss of ankyrin-B function. *Proc Natl Acad Sci U S A.* 101(24):9137–9142.

MORETTI A. et al., (2010) Patient-specific induced pluripotent stem-cell models for long-QT syndrome. *N. Engl. J. Med.* 363, 1397–1409

MORITA H, WU J, ZIPES DP. (2008) The QT syndromes: long and short. *Lancet* 30;372(9640):750-63.

MUKHERJEE S, THOMAS NL, WILLIAMS AJ. (2012) A mechanistic description of gating of the human cardiac ryanodine receptor in a regulated minimal environment. *J Gen Physiol*.; 140:139–158.

MUMMERY, C., et al., (2003) Differentiation of human embryonic stem cells to cardiomyocytes: role of coculture with visceral endoderm-like cells. *Circulation* 107(21): p. 2733-40.

MUMMERY C., et al., (2012) Differentiation of human embryonic stem cells and induced pluripotent stem cells to cardiomyocytes: a methods overview. *Circulation research*, 111(3): p. 344-58.

NADEMANEE K, et al. (2011) Prevention of ventricular fibrillation episodes in Brugada syndrome by catheter ablation over the anterior right ventricular outflow tract epicardium. *Circulation* 123:1270e9.

NAGASAKI K, FLEISCHER S. (1988) Ryanodine sensitivity of the calcium release channel of sarcoplasmic reticulum. *Cell Calcium* 9: 1–7.

NAKAGAWA, M., KOYANAGI, M., TANABE, K., TAKAHASHI, K., ICHISAKA, T., AOI, T., OKITA, K., MOCHIDUKI, Y., TAKIZAWA, N. AND YAMANAKA, S.(2008) Generation of induced pluripotent stem cells without c-Myc from mouse and human fibroblasts. *Nat. Biotechnol.* 26 (1), 101–106.

NAKAI J et al., (1990) Primary structure and functional expression from cDNA of the cardiac ryanodine receptor/calcium release channel. *FEBS Letters* ;271(1–2):169–177.
NELSON TJ, MARTINEZ-FERNANDEZ A, YAMADA S (2009) Repair of acute myocardial infarctation by human stemness factors induced pluripotent stem cells. *Circulation* ; 120:408-16.

NOVAK, A., et al., (2012) Cardiomyocytes generated from CPVTD307H patients are arrhythmogenic in response to beta-adrenergic stimulation. *Journal of cellular and molecular medicine,* 16(3): p. 468-82.

NOVAK A, LORBER A, ITSKOVITZ-ELDOR J, BINAH O. (2012) Modeling Catecholaminergic Polymorphic Ventricular Tachycardia using Induced Pluripotent Stem Cell-derived Cardiomyocytes. *Rambam Maimonides Med J.* 31;3(3):e0015.

NOVAK A, BARAD L, LORBER A, GHERGHICEANU M, REITER I, EISEN B, ELDOR L, ITSKOVITZ-ELDOR J, ELDAR M, ARAD M, BINAH O (2015) Functional abnormalities in iPSC-derived cardiomyocytes generated from CPVT1 and CPVT2 patients carrying ryanodine or calsequestrin mutations. *J Cell Mol Med*. 19(8):2006-18.

NUSSBAUM J, MINAMI E, LAFLAMME MA, VIRAG JA, WARE CB, MASINO A, MUSKHELI V, PABON L, REINECKE H, MURRY CE. (2007) Transplantation of undifferentiated murine embryonic stem cells in the heart: teratoma formation and immune response. *FASEB J.* ;21(7):1345-57.

OHGO T, OKAMURA H, NODA T, et al. (2007) Acute and chronic management in patients with Brugada syndrome associated with electrical storm of ventricular fibrillation. *Heart Rhythm* 4:695e700.

OKITA, K., ICHISAKA, T. AND YAMANAKA, S. (2007) Generation of germ-line competent induced pluripotent stem cells. *Nature* 448, 313–317.

OKUDAIRA N, KUWAHARA M, HIRATA Y, OKU Y, NISHIO H (2014) A knock-in mouse model of N-terminal R420W mutation of cardiac ryanodine receptor exhibits arrhythmogenesis with abnormal calcium dynamics in cardiomyocytes. *Biochem Biophys Res Commun.* 26;452(3):665-8

OTSU K et al. (1990) Molecular cloning of cDNA encoding the Ca2+ release channel (ryanodine receptor) of rabbit cardiac muscle sarcoplasmic reticulum. *The Journal of Biological Chemistry* ;265(23):13472–13483.
OVEREND CL, EISNER DA, O'NEILL SC. (1997) The effect of tetracaine on spontaneous Ca2+ release and sarcoplasmic reticulum calcium content in rat ventricular myocytes. *J Physiol* 502: 471–9

PAPADAKIS M, SHARMA S, COX S, et al. (2009) The magnitude of sudden cardiac death in the young: a death certificate-based review in England and Wales. *Europace*; 11:1353e8.

PARNESS J. (2005) The dantrolene binding site on RyR1. In: Wehrens XH, Marks AR, editors. *Ryanodine receptors: structure, function and dysfunction in clinical disease.* New York: Springer; p 243–51.

PAUL-PLETZER K., YAMAMOTO T., BHAT M., MA J., IKEMOTO N., JIMENEZ L., MORIMOTO H., WILLIAMS P., PARNESS J. (2002) Identification of the dantrolene binding sequence of the skeletal muscle ryanodine receptor. *J. Biol. Chem*. 277:34918–34923.

PAUL-PLETZER K., YAMAMOTO T., IKEMOTO N., JIMENEZ L., MORIMOTO H., WILLIAMS P., MA J., PARNESS J. (2005) Probing a putative dantrolene-binding site on the cardiac ryanodine receptor. *Biochem. J*. 387:905–909.

PENG S et al., (2010) The action potential and comparative pharmacology of stem cell-derived human cardiomyocytes. *Journal of pharmacological and toxicological methods* ; 61(3): p. 277-86.

PIESKE B, MAIER LS, BERS DM, HASENFUSS G. (1999) Ca^{2+} handling and sarcolplasmic reticulum Ca^{2+} content in isolated failing and nonfailing human myocardium. *Circ Res*. 83:38-46,

PIGNIER C, ROUGIER JS, VIÉ B, CULIÉ C, VERSCHEURE Y, VACHER B, ABRIEL H, LE GRAND B. (2010) Selective inhibition of persistent sodium current by F15845 prevents ischaemia-induced arrhythmias. *British Journal of Pharmacology* 161(1):79-91

POSTMA AV, BHUIYAN ZA, SHKOLNIKOVA M, et al. (2002) Involvement of the Kir2 gene family in catecholaminergic polymorphic ventricular tachycardia; analysis for mutations and identification of numerous pseudogenes. *Eur Heart J*. 25:66.

POTT C, DECHERING DG, REINKE F, MUSZYNSKI A, ZELLERHOFF S, BITTNER A, KÖBE J, WASMER K, SCHULZE-BAHR E, MÖNNIG G, KOTTHOFF S, ECKARDT L. (2011) Successful treatment of catecholaminergic polymorphic ventricular tachycardia with flecainide: a case report and review of the current literature *Europace* 13(6):897-901

POWELL T, TWIST VW (1976) A rapid technique for the isolation and purification of adult cardiac muscle cells having respiratory control and a tolerance to calcium. *Biochem Biophys Res Commun.* 7;72(1):327-33.

PRIORI, S.G. & S.R. CHEN (2001), Inherited dysfunction of sarcoplasmic reticulum Ca2+ handling and arrhythmogenesis. *Circulation research* . 108(7): p. 871-83.

PRIORI, S.G., (2002) Clinical and Molecular Characterization of Patients With Catecholaminergic Polymorphic Ventricular Tachycardia. *Circulation*, 106(1): p. 69-74.

QUIGLEY EM. (2011) Cisapride: what can we learn from the rise and fall of a prokinetic. J *Dig Dis.* 12:147–56

RAJAMOHAN D., MATSA E., KALRA S., CRUTCHLEY J., PATEL A.,.GEORGE V, DENNING C. (2013) Current status of drug screening and disease modelling in human pluripotent stem cells. *Bioessays* 35, 281–298

REID DS, TYNAN M, BRAIDWOOD L, Fitzgerald GR. (1975) Bidirectional tachycardia in a child. A study using His bundle electrography. *Br Heart J* 37:339-344

RIZZI N. et al., (2008) Unexpected structural and functional consequences of the R33Q homozygous mutation in cardiac calsequestrin: a complex arrhythmogenic cascade in a knock in mouse model. *Circ Res* 103:298–306.

RODEN DM. (1993) Torsade de pointes. *Clin Cardiol* 16:683e6.

ROSSO R,KALMAN JM, ROGOWSKI O,et al. (2007) Calcium channel blockers and beta-blockers versus beta-blockers alone for preventing exercise-induced arrhythmias in catecholaminergic polymorphic ventricular tachycardia. *Heart Rhythm* 4:1149-1154

SATIN, J., et al., (2008) Calcium handling in human embryonic stem cell-derived cardiomyocytes. *Stem cells* 26(8): p. 1961-72.

SCHLOTTHAUER K, BERS DM. (2000) Sarcoplasmic reticulum Ca(2+) release causes myocyte depolarization.Underlying mechanism and threshold for triggered action potentials. *Circ Res*. 87:774–780.

SEDEJ S, HEINZEL FR, WALTHER S, (2010) et al. Na+-dependent SR Ca2+ overload induces arrhythmogenic events in mouse cardiomyocytes with a human CPVT mutation. *Cardiovasc Res*. 87(1):50–59.

SEIDEL M, LAI FA, ZISSIMOPOULOS S (2015): Structural and functional interactions within ryanodine receptor*; Biochemical Society Transactions* 43 (3) 377-383.

SETTE C, CONTI M (1996) Phosphorylation and activation of a cAMP-specific phosphodiesterase by the cAMP-dependent protein kinase. Involvement of serine 54 in the enzyme activation *J Biol Chem*. ;271(28):16526-34.

SIKKEL, M.B., et al., (2013) Flecainide reduces Ca(2+) spark and wave frequency via inhibition of the sarcolemmal sodium current. *Cardiovascular research* 98(2): p. 286-96.

SMITH JS, CORONADO R, MEISSNER G. (1985) Sarcoplasmic reticulum contains adenine nucleotide-activated calcium channels. *Nature* 316: 446–9

SONG L et al., (2007) Calsequestrin 2 (CASQ2) mutations increase expression of calreticulin and ryanodine receptors, causing catecholaminergic polymorphic ventricular tachycardia. *J Clin Invest* ;117:1814–23.

SOUFI, A., DONAHUE, G. AND ZARET, K.S. (2012) Facilitators and impediments of the pluripotency reprogramming factors' initial engagement with the genome. *Cell* 151 (5), 994–1004.

STOTZ S, et al., (2000) Fast Inactivation of Voltage-dependent Calcium Channels *The journal of biological chemistry* Vol. 275, No. 32 pp. 24575–24582

STRAUER BE, STEINHOFF G. (2011) 10 years of intracoronary and intramyocardial bone marrow stem cell therapy of the heart: from the methodological origin to clinical practice. *Journal of American College of Cardiology*; 58: 1095-104.

SUN N., et al., (2012) Patient-specific induced pluripotent stem cells as a model for familial dilated cardiomyopathy. *Sci. Transl. Med*. 4, 130.

SWAN H, PIIPPO K, VIITASALO M, HEIKKILÄ P, PAAVONEN T, KAINULAINEN K, KERE J, KETO P, KONTULA K, TOIVONEN L.(1999) Arrhythmic disorder mapped to chromosome 1q42-q43 causes malignant polymorphic ventricular tachycardia in structurally normal hearts. *J Am Coll Cardiol*.; 34(7):2035-42.

TACHIBANA M, et al. (2013) Human embryonic stem cells derived by somatic cell nuclear transfer. *Cell* 153.6 1228-1238.

TAKAHASHI, K. AND YAMANAKA, S. (2006) Induction of pluripotent stem cells from mouse embryonic and adult fibroblast cultures by defined factors. *Cell* 126 (4), 663–676.

TAKAHASHI, K., TANABE, K., OHNUKI, M., NARITA, M., ICHISAKA, T., TOMODA, K. AND YAMANAKA, S. (2007) Induction of pluripotent stem cells from adult human fibroblasts by defined factors. *Cell* 131 (5), 861–872.

TAN HL, et al. (2005) Sudden unexplained death: heritability and diagnostic yield of cardiological and genetic examination in surviving relatives. *Circulation* 112:207e13.

TANABE, K., NAKAMURA, M., NARITA, M., TAKAHASHI, K. AND YAMANAKA, S. (2013) Maturation, not initiation, is the major roadblock during reprogramming toward pluripotency from human fibroblasts. *Proc. Natl. Acad. Sci. USA* 110 (30), 12172–12179.

TATEISHI H, YANO M, MOCHIZUKI M, SUETOMI T, ONO M, XU X, UCHINOUMI H, OKUDA S, ODA T, KOBAYASHI S, YAMAMOTO T, IKEDA Y, OHKUSA T, IKEMOTO N, MATSUZAKI M. (2009) Defective domaindomain interactions within the ryanodine receptor as a critical cause of diastolic Ca2+ leak in failing hearts. *Cardiovasc Res.* 81:536–545.

TERRENOIRE C, WANG K, TUNG KW, CHUNG WK, PASS RH, LU JT, JEAN JC, OMARI A, SAMPSON KJ, KOTTON DN, KELLER G, KASS RS (2013) Induced pluripotent stem cells used to reveal drug actions in a long QT syndrome family with complex genetics. *J Gen Physiol*. 141(1):61-72.

TERRENOIRE, C., et al., (2013) Induced pluripotent stem cells used to reveal drug actions in a long QT syndrome family with complex genetics. *The Journal of general physiology*, 141(1): p. 61-72.

TESTER DJ, WILL ML, ACKERMAN MJ. (2006) Mutation detection in congenital long QT syndrome: cardiac channel gene screen using PCR, dHPLC, and direct DNA sequencing. *Methods Mol Med*. ;128:181-207.

THOMAS, N.L., et al., (2010) Ryanodine receptor mutations in arrhythmia: The continuing mystery of channel dysfunction. *FEBS letters*, 584(10): p. 2153-60.

THOMSEN MB, MATZ J, VOLDERS PGA & VOS MA. (2006) Assessing the proarrhythmic potential of drugs: Current status of models and surrogate parameters of torsades de pointes arrhythmias. *Pharmacol Ther*. ;112(1):150-70.

THOMSON JA, ITSKOVITZ-ELDOR J, SHAPIRO SS, WAKNITZ MA, et al. (1998) Embryonic stem cell lines derived from human blastocysts. *Science* 1998; 282:1145–7

TINKER A, WILLIAMS AJ (1993) Using large organic cations to probe the nature of ryanodine modification in the sheep cardiac sarcoplasmic reticulum calcium release channel. *Biophys J*.; 65:1678–1683.

TRAFFORD AW, SIBBRING GC, DIAZ ME, EISNER DA. (2000) The effects of low concentrations of caffeine on spontaneous Ca release in isolated rat ventricular myocytes. *Cell Calcium.* 28:269–276.

TRIPATHY A, MEISSNER G. (1996) Sarcoplasmic reticulum luminal Ca2+ has access to cytosolic activation and inactivation sites of skeletal muscle Ca2+ release channel. *Biophys J.* 70:2600–2615.

UCHINOUMI H, YANO M, OHNO M, XU X, TATEISHI H, KOBAYASHI S, et al. (2007) Enhanced sensitivity of the cardiac ryanodine receptor to activation by luminal Ca2+ as a primary cause of catecholaminergic polymorphic ventricular tachycardia. *Circulation* 116:II–153.

VALDIVIA HH, KIRBY MS, LEDERER WJ, CORONADO R. (1992) Scorpion toxins targeted against the sarcoplasmic reticulum Ca2+-release channel of skeletal and cardiac muscle. *Proc Natl Acad Sci USA* 89: 12185–9.

VALDIVIA HH, KAPLAN JH, ELLIS-DAVIES GC, et al.(1995) Rapid adaptation of cardiac ryanodine receptors: Modulation by Mg2+ and phosphorylation. *Science* 267(5206):1997–2000.

VISKIN S, WILDE AAM, TAN HL, et al. (2009) Empiric quinidine therapy for asymptomatic Brugada syndrome: Time for a prospective registry. *Heart Rhythm* 6:401e4.

VOLDERS PG, VOS MA, SZABO B, SIPIDO KR, DE GROOT SH, GORGELS AP, WELLENS HJ, LAZZARA R.(2000) Progress in the understanding of cardiac early afterdepolarizations and torsades de pointes: time to revise current concepts. *Cardiovasc Res.* 46:376–392.

WATANABE H, CHOPRA N, LAVER D, HWANG HS, DAVIES SS, ROACH DE, DUFF HJ, RODEN DM, WILDE AA, KNOLLMANN BC.(2009) Flecainide prevents catecholaminergic polymorphic ventricular tachycardia in mice and humans. *Nat Med.* 15:380–383.

WEHRENS XH, LEHNART SE, HUANG F, VEST JA, REIKEN SR, MOHLER PJ, SUN J, GUATIMOSIM S, SONG LS, ROSEMBLIT N, D'ARMIENTO JM, NAPOLITANO C, MEMMI M, PRIORI SG, LEDERER WJ, MARKS AR. (2003) FKBP12.6 deficiency and defective calcium release channel (ryanodine receptor) function linked to exercise-induced sudden cardiac death. *Cell.* 113:829–840.

WEST, D. J., SMITH, E., & WILLIAMS, A. J. (2002). A novel and rapid approach to isolating functional ryanodine receptors. *Biochemical and Biophysical Research Communications*, *294*, 402–407.

WEST, D. J., & WILLIAMS, A. J. (2007). Pharmacological regulators of intracellular calcium release channels. *Current Pharmaceutical Design*, *13*(24), 2428–2442.

WILDE AA, BHUIYAN ZA, CROTTI L, FACCHINI M, DE FERRARI GM, PAUL T, FERRANDI C, KOOLBERGEN DR, ODERO A, SCHWARTZ PJ. (2008) Left cardiac sympathetic denervation for catecholaminergic polymorphic ventricular tachycardia. *N Engl J Med*. 358:2024–2029.

WILMUT, I., SCHNIEKE, A.E., MCWHIR, J., KIND, A.J. AND CAMPBELL, K.H. (1997) Viable offspring derived from foetal and adult mammalian cells. *Nature* 385 (6619), 810–813.

WORRINGER, K.A., RAND, T.A., HAYASHI, Y., SAMI, S., TAKAHASHI, K., TANABE, K., NARITA, M., SRIVASTAVA, D. AND YAMANAKA, S. (2014) The let- 7/LIN-41 pathway regulates reprogramming to human induced pluripotent stem cells by controlling expression of prodifferentiation genes. *Cell Stem Cell* 14 (1), 40–52.

XIN HB, SENBONMATSU T, CHENG DS, et al. (2002) Oestrogen protects FKBP12.6 null mice from cardiac hypertrophy. *Nature* 416(6878):334–338.

XU L, JONES R, MEISSNER G. (1993) Effects of local anesthetics on single channel behavior of skeletal muscle calcium release channel. *J Gen Physiol* 101: 207–33.

YAMAGUCHI N, TAKAHASHI N, XU L, et al. (2007) Early cardiac hypertrophy in mice with impaired calmodulin regulation of cardiac muscle Ca release channel. *The Journal of Clinical Investigation* 117(5):1344–1353.

YAMAGUCHI N et al. (2003) Molecular basis of calmodulin binding to cardiac muscle Ca(2+) release channel (ryanodine receptor. *The Journal of Biological Chemistry* 278(26):23480– 23486.

YAN Z et al., (2015) Structure of the rabbit ryanodine receptor RyR1 at near-atomic resolution. *Nature*. ;517(7532):50-5.

YANG X, PABON L, MURRY C. E. (2014) Engineering adolescence: Maturation of human pluripotent stem cell-derived cardiomyocytes. *Circ. Res*. 114, 511–523.

YANO, M. (2008). Ryanodine Receptor as a New Therapeutic Target of Heart Failure and Lethal Arrhythmia. *Circulation* 72: 509-514.

YAZAWA M., et al., (2011) Using induced pluripotentstem cells to investigate cardiac phenotypes in Timothy syndrome. *Nature* 471, 230–234.

YU, J., VODYANIK, M.A., SMUGA-OTTO, K., ANTOSIEWICZ-BOURGET, J., FRANE, J.L., TIAN, S., NIE, J., JONSDOTTIR, G.A., RUOTTI, V., STEWART, R., SLUKVIN, I.I. AND THOMSON, J.A. (2007) Induced pluripotent stem cell lines derived from human somatic cells. *Science* 318 (5858), 1917–1920.

YUNLONG B. et al., (2013) Phospholamban Knockout Breaks Arrhythmogenic Ca2+ Waves and Suppresses Catecholaminergic Polymorphic Ventricular Tachycardia in Mice; *Circ Res*. 113(5).

ZAMUDIO FZ, CONDE R, AREVALO C, BECERRIL B, MARTIN BM, VALDIVIA HH, et al. (1997) The mechanism of inhibition of ryanodine receptor channels by imperatoxin I, a heterodimeric protein from the scorpion Pandinus imperator. *J Biol Chem* 272: 11886– 94.

ZHANG D. et al (2013) Tissue-engineered cardiac patch for advanced functional maturation of human ESC-derived cardiomyocytes. *Biomaterials* 34, 5813–5820.

ZHANG, J., et al., (2009) Functional cardiomyocytes derived from human induced pluripotent stem cells. *Circulation research*, 104(4): p. e30-41.

ZHANG, L. et al., (1997) Complex Formation between Junctin, Triadin, Calsequestrin, and the RyanodineReceptor. Proteins of the cardiac junctional sarcoplasmic reticulum membrane. *Journal of Biological Chemistry,*. 272(37): p. 23389-23397.

ZHANG, X.H., et al., (2013) Ca2+ signaling in human induced pluripotent stem cell-derived cardiomyocytes (iPS-CM) from normal and catecholaminergic polymorphic ventricular tachycardia (CPVT)-afflicted subjects. *Cell calcium*, 54(2): p. 57-70.

ZHAO YT et al.,(2015) Arrhythmogenesis in a catecholaminergic polymorphic ventriculat tachycardia mutation that depresses ryanodine receptor function. *Proc Natl Acad Sci USA* ;112(13):E1669-77.

ZIPES DP, et al. (2006) ACC/AHA/ESC 2006 Guidelines for Management of Patients With Ventricular Arrhythmias and the Prevention of Sudden Cardiac Death: a report of the American College of Cardiology/American Heart Association Task Force and the European Society of Cardiology Committee for Practice Guidelines (writing committee to develop Guidelines for Management of Patients With Ventricular Arrhythmias and the Prevention of Sudden Cardiac Death): developed in collaboration with the European Heart Rhythm Association and the Heart Rhythm Society. *Circulation.* 5;114(10):e385-484.

Appendix

Appendix I

In this section, the hiPSC CPVT characterisation data is presented. Procedures were, performed at University of Nottingham, by Prof. Chris Denning's group at the Wolfson Centre for Stem Cells. The control cell line BT1 CM was also characterised by the same group using the same methods (data not shown).

The adult fibroblasts reprogrammed into hiPSC for this project were obtained from a patient that had undergone cardiac surgery for implantation of an ICD. This 5 year old patient presented a RyR2 genotyped mutation, c.6737C>T (Ser2246Leu) and the resultant ryanodine receptor malfunction is known to cause a classical bidirectional ventricular tachycardia, leading to arrhythmia. The patient presented clinical symptoms and because no response was obtained to antiarrhythmic medical treatment an ICD was placed to prevent arrhythmia and potentially syncope and death.

RyR2 mutation detection - c.6737C>T (Ser2246Leu)

Normal
6721 - GAT GTG GCT GCA GCT TCG GTG ATG GAT AAT AAT GAA CTA GCA TTA GCT CTG CGT GAG CCG - 6780

2241 - D V A A A S V M D N N E L A L A L R E P - 2260

Mutant
6721 – GAT GTG GCT GCA GCT TTG GTG ATG GAT AAT AAT GAA CTA GCA TTA GCT CTG CGT GAG CCG - 6780

2241 – D V A A A L V M D N N E L A L A L R E P – 2260

A

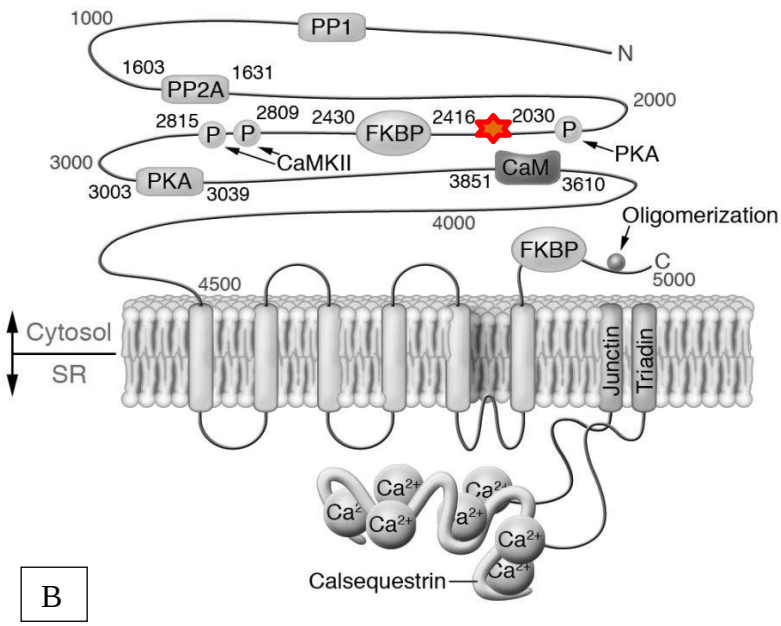

B

Patient mutation

Figure 1a - Current study CPVT1 patient single point mutation at the RyR2 *- aminoacid sequence from normal and mutant RyR2 (A). Location of the mutation in the RyR2 predicted structure and domains (B). Adapted from (Bers,2004) Journal of Molecular and Cellular Cardiology.*

CPVT1 patient fibroblast culture and reprogramming

Dermal fibroblasts were isolated from a skin biopsy obtained from a CPVT1 clinically and genetically diagnosed patient, after informed consent was given by the patient. Skin samples were cleaned from adipose and epidermal tissue and were reduced to 1mm pieces. They were then digested with 2.5% trypsin (Invitrogen) for 15min, and 1mg/ml Collegenase IV (Invitrogen) for 90 minutes, both at 37^{o}C. Digested cells were plated in Chang's-D medium (Metachem) supplemented with 2mM L-glutamine (Invitrogen) and 100mM HEPES (SIGMA). Cells were then grown for 2-3 weeks until fibroblast populations emerged. Fibroblasts were grown in DMEM medium (Invitrogen), supplemented with 10% FBS, 0.1mM non-essential amino acids (Invitrogen) and 2mM L-glutamine. Fibroblast culture for 10-15 passages was completed before exposure to reprogramming factors. Generation of hiPSCs clones was obtained by lentiviral delivery of human OCT4, SOX2, NANOG, and LIN28 (Matsa et al.,2011) into patient fibroblasts between passage 15 and 20. Fibroblast cells were seeded in tissue culture-treated 6 well plates (NUNC) at a density of 100,000 cells/well and left to adhere to the plastic for 4h. Lentiviral particles encoding human *OCT4*, *SOX2*, *LIN28* and *NANOG* were produced using the HEK293 cell line. Viral supernatants were precipitated *via* incubation in 60mM $CaCl_2$ at 37 °C for 30-40 minutes and then purified by conjugation to streptavidin paramagnetic beads (Promega), for 3-5h at room temperature on a rolling platform. Viral particles were finally re-suspended in DMEM with 10% FBS, and were used to transduce fibroblasts.

A medium change with fibroblast culture medium was performed 24h post transduction (PTD), and 48h PTD the cells were transferred to 90mm dishes where they were cultured onto mitomycin C inactivated MEFs ($3.6x10^6$ cells/plate) in hiPSC culture medium (DMEM-F12 supplemented with 15% KSR, 100μM β-mercaptoethanol, 10ng/ml bFGF (Sigma-Aldrich), 2mM GlutaMAX™-1 (Invitrogen), and 0.1mM non-essential amino acids). The medium was changed daily with hiPSC culture medium for 1 week, and with MEF conditioned medium supplemented with 10ng/ml bFGF.

At 18-23 days PTD, reprogrammed hiPSCs were isolated by TRA-1-81 based positive selection over a magnetic column (Miltenyi Biotec), as described previously (Matsa et al.,2011). hiPSCs were then transferred to feeder-free conditions on Matrigel-coated flasks and cultured in MEF conditioned medium supplemented with 10ng/ml bFGF.

Mutation identification

To confirm the presence of the CPVT mutation in patients specific fibroblasts and derived CPVT hiPSCs, genomic DNA was extracted from frozen cell pellets (QIAGEN DNeasy Blood and Tissue kit). Polymerase chain reaction (PCR) was performed using 25 mL reaction mixture, which comprised Hotstar Taq polymerase (0.125 mL; QIAGEN), 5 mM forward and reverse primers (Invitrogen), 10× buffer (2.5 mL; QIAGEN), 2.5 mM dNTPs (2.5 mL; Invitrogen) and 1 mL of genomic DNA diluted to 100 ng/mL. The PCR conditions were 958C for 15 min, then 35 cycles (958C, 1 min; 558C, 30 s; 728C, 1 min) and a final extension step at 728C for 5 min. Polymerase chain reaction products were electrophoresed on a 1.5% agarose gel, purified (QIAGEN QIAquick Gel Extraction kit), and sequenced using the reverse primer.

Pluripotency markers

Pluripotency and differentiation markers were detected by ICC and flow cytometry.

Primary antibody	Supplier	Dilution	Secondary antibody	Supplier	Dilution
OCT4	Santa Cruz; SC-5279	1:200	goat anti-mouse AlexaFluor® 633	Invitrogen; A21052	1:400
SSEA4	Millipore; MAB4304	1:50			
SSEA1	Millipore; MAB117P	1:50			
TRA-1-81	Millipore; MAB4381	1:50			
P4HB	Abcam; ab44971	1:50			
c-MYC	Abcam; ab32	1:250			
α-actinin	SIGMA; A7811	1:800			
β-III-tubulin	COVANCE; MMS-435P	1:1000			
AFP	Sigma; A8452	1:1000			
LIN28	Abcam; ab462020	1:1500	goat anti-rabbit AlexaFluor® 633	Invitrogen; A21071	1:400
REX1	Abcam; ab50828	1:50			1:200
Troponin-I	Spectral Diagnostics; PA-1010	1:1000			
SOX2	R&D Systems; AF2018	1:200	rabbit anti-goat AlexaFluor® 568	Invitrogen; A11079	1:400
NANOG	R&D Systems; AF1997	1:50			
DNMT3B	Santa Cruz; SC-10236	1:250			
KLF4	R&D Systems; AF3640	1:100			1:200

Table 1a - Antibodies list used for CPVT hiPSC immunofluorescence staining and flow cytometry *- used for pluripotency characterisation at Nottingham University – Wolfson Centre for Stem Cells.*

ICC

For CPVT hiPSC immunofluorescence experiments, cells were grown to confluence in 8-chamber glass slides (NUNC) and then fixed in 4% PFA. Cells were permeabilised with 0.1% Triton-X-100 (Sigma-Aldrich), and blocked with 8% goat or rabbit serum (Sigma-Aldrich) in PBS, as appropriate. Primary antibody incubations were performed overnight at 4°C and secondary antibodies at room temperature for 1h (antibody dilutions shown in table 3.1). Cells were imaged using a Nikon Eclipse 90i fluorescence microscope and images were analysed using Volovity software (Improvision).

Flow cytometry

For flow cytometry analysis, CPVT hiPSC were harvested and fixed in 4% paraformaldehyde (PFA, Sigma-Aldrich), then re-suspended in 2% FBS in PBS. Cells were incubated in the dark with PE-conjugated antibodies, or relevant isotype controls, for 20min at room temperature, washed in 2% FBS and analysed in a flow cytometer (FC500, BD Biociences).

Growth kinetics

Population doublings (PDs) at each passage were calculated using the formula [log10 (total cell counts/cells seeded)/ log10 (2)], where the cell number seeded was $1.2x10^6$ cells/t25 flask. Proliferation rates were calculated by total hours in test culture/ cumulative PDs.

Results

CPVT hiPSC line was genotyped for mutation RyR2 6737 C>T (figure 1a, 2a) and presented a normal karyotype (data not shown). CPVT hiPSC displayed population doubling rates similar to hESCs (figure 6a).

Flow cytometry (figure 3a) and ICC showed that hiPSCs had reactivated marker SSEA1 and the pluripotency markers TRA-1-81 and SSEA4 (figure 4a). NANOG, SOX2, OCT4, cMYC were also activated (figure 5a) as well LIN28, DNMT3B, REX1 and KLF4, (data not shown).

Regulatory regions within the OCT4 and NANOG promoters acquired a hypomethylated state in hiPSCs, relative to the originating fibroblasts and hiPSC differentiated progeny (data not shown). EB differentiation from hiPSCs showed contribution to the three embryonic germ layers; endoderm, ectoderm, and mesoderm via expression of the markers b-III-tubulin, a-fetoprotein, and cardiac a-actinin (data not shown).
These experiments confirmed that hiPSC lines were pluripotent and ready to be used for differentiation protocols.

CPVT1 mutation confirmation

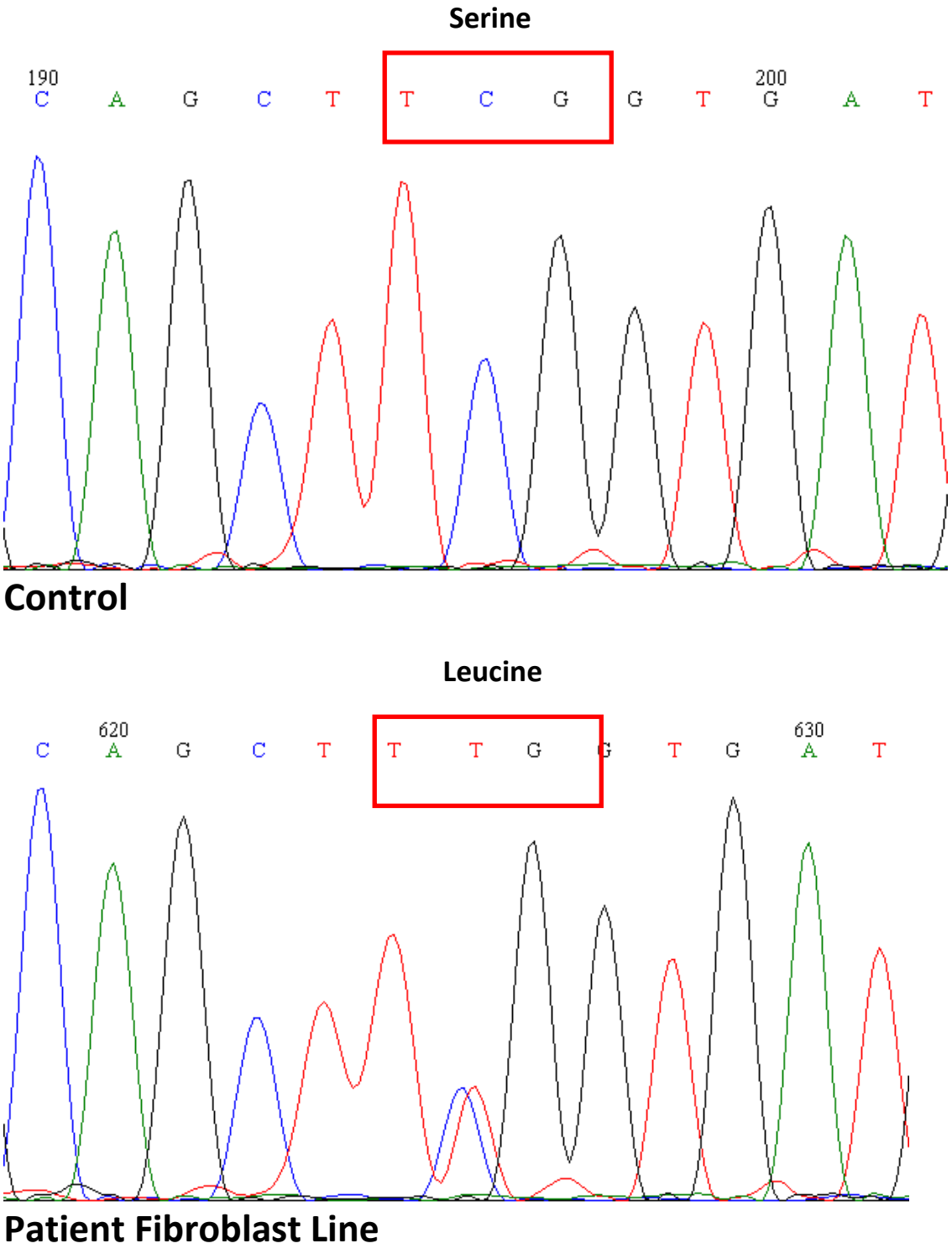

Figure 2a - Confirmation of patient genotype - *RyR2 6737 C>T . Chromatograms from control BT1 hiPSC cells and CPVT fibroblasts. Single point mutation in RyR2 identified in patient fibroblast line (mutant cells).*

Flow cytometry

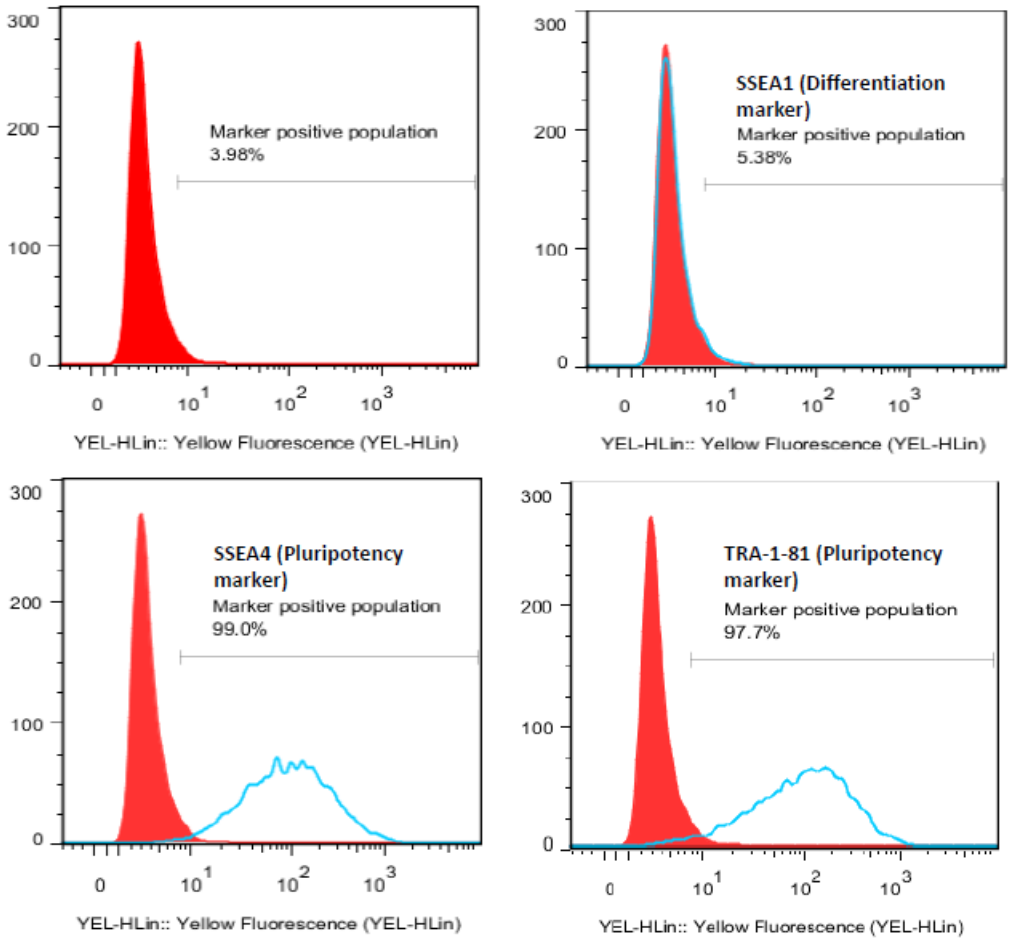

Figure 3a - Flow cytometry for differentiation marker and pluripotency markers confirmation *- SSEA1 and SSEA4 and TRA-1-81.*

ICC

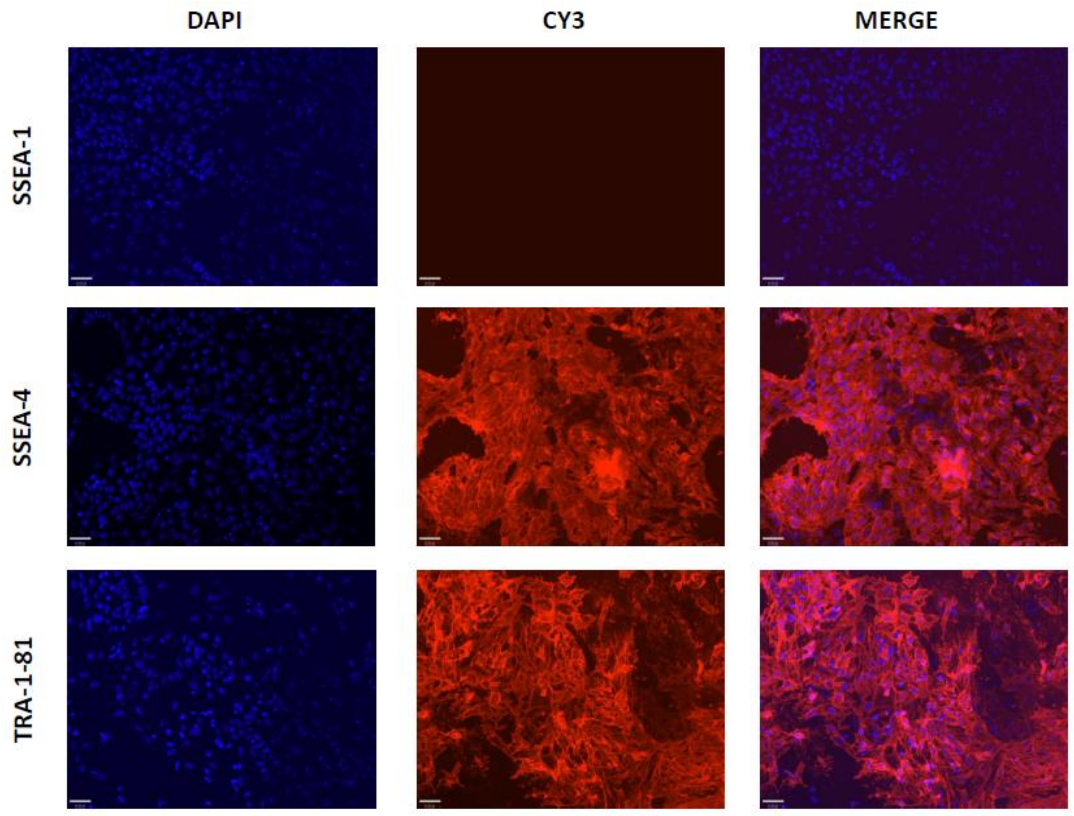

Figure 4a - ICC panel for differentiation and pluripotency markers - SSEA1 (differentiation marker) SSEA4 and TRA-1-81 *(pluripotency markers) – immunostaining for CPVT hiPSC cell line.*

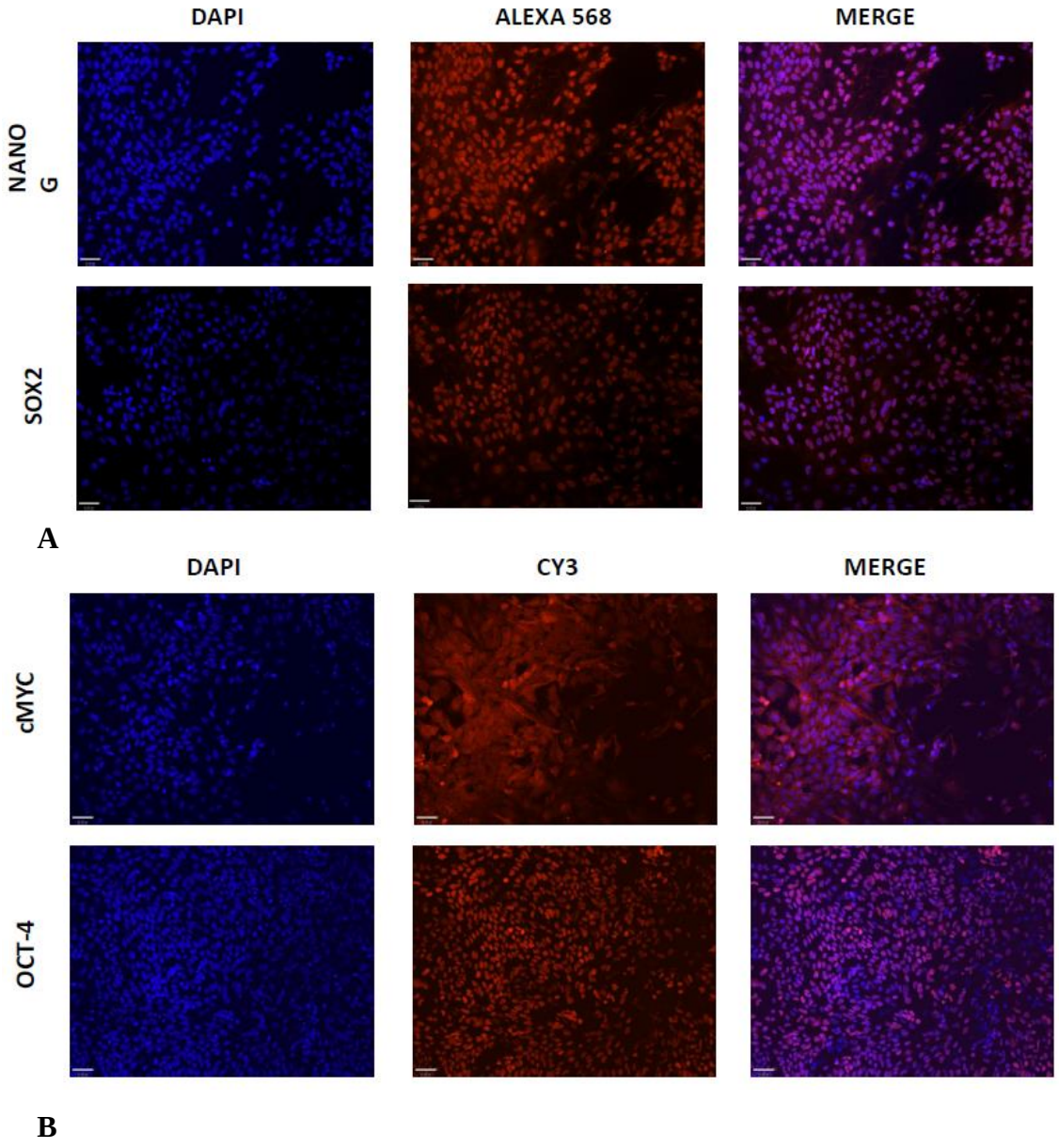

Figure 5a - ICC panel for pluripotency inducing reprogramming factors *- NANOG and SOX2 (A) and OCT4 and c-MYC (B) – immunostaining for CPVT hiPSC cell line.*

Growth kinetics

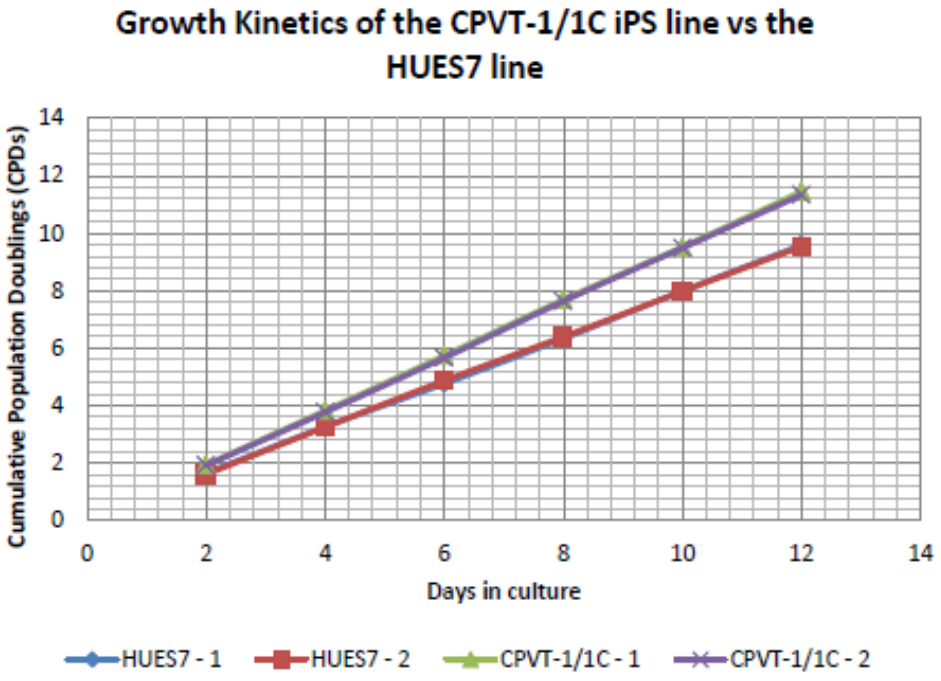

	Population Doubling (hours)				
Cell Line	Flask 1	Flask 2	Average	SDEV	SE
HUES7	30.03	30.19	30.11	0.113137	0.08
CPVT-1/1C	25.15	25.4	25.275	0.176777	0.125

Figure 6a - Growth kinetics of CPVT1 hiPSC line and HUES7 *– (hESC) cell line used as control.*